Synthesis and Characterisation of Indigo-Containing Conjugated Polymers

Dissertation

zur Erlangung des akademischen Grades
"Doktor der Naturwissenschaften"
(Dr. rer. nat.)

eingereicht in der Fakultät 4 - Mathematik und Naturwissenschaften der Bergischen Universität Wuppertal

von Anika Eckert
aus Schwerin

Wuppertal, März 2017

Die Dissertation kann wie folgt zitiert werden:

urn:nbn:de:hbz:468-20170628-095822-0
[http://nbn-resolving.de/urn/resolver.pl?urn=urn%3Anbn%3Ade%3Ahbz%3A468-20170628-095822-0]

Meiner Familie in Dankbarkeit

Life is like a cup of tea,

it's all in how you make it.

- ***Irish proverb***

Mistakes are the portals of discovery.

- ***James Joyce***

Die vorliegende Arbeit wurde im Zeitraum von Juni 2013 bis März 2017 am Institut für Makromolekulare Chemie der Fakultät 4 - Mathematik und Naturwissenschaften der Bergischen Universität Wuppertal unter Anleitung von Prof. Dr. U. Scherf durchgeführt.

1. Gutachter: Prof. Dr. Ullrich Scherf (Bergische Universität Wuppertal, De)
2. Gutachter: Prof. PhD João Sérgio Seixas de Melo (Universidade de Coimbra, Pt)
Dissertation eingereicht am: 22.03.2017

Zusammenfassung

Die in dieser Thesis vorgestellten Indigo- und „bay“-annelierten Indigo- haltigen Polymere wurden über Stille- oder Suzuki- Kreuzkupplungen synthetisiert. Durch die Verwendung von Modellverbindungen, in denen Indigo von Donor-Einheiten umschlossen ist, konnten weitere Rückschlüsse über die photophysikalischen Eigenschaften der Polymere gezogen werden. Die synthetisierten Polymere wurden mit spektroskopischen Methoden, wie unter anderem UV/Vis Spektroskopie, auf ihre optischen Eigenschaften hin untersucht und miteinander verglichen.

Weiterführende Untersuchungen der Polymere konzentrierten sich auf die Verbesserung der Löslichkeit. Dafür wurden unter anderem *tert*-Butyloxycarbonyl (Boc) Indigo-Derivate hergestellt und mit entsprechenden Donor-Comonomeren gekuppelt. Des Weiteren wurde im Vergleich zwischen einem BAI-CPDT Copolymer („bay“-annelierten Indigo-Cyclopentadithiophen) und einem BAI-CPDT Copolymer mit zusätzlichen Dodecyl-Thiophen-Einheiten der löslichkeitsvermittelnde Einfluss der Dodecyl-Thiophen-Bausteine auf die Polymereigenschaften untersucht.

Ein Vergleich der Reaktivitäten der Indigo-haltigen Polymere mit denen von Indigo erfolgte durch polymeranaloge Reaktionen. Hierfür wurde die Boc-Gruppe säurekatalytisch, beziehungsweise thermisch abgespalten, um die entschützten Polymere zu erhalten. Die Möglichkeit, Indigo zu reduzieren und zu oxidieren, ist die Grundlage des Indigo-Färbeprozesses, beruhend auf der Wasserlöslichkeit von reduziertem Indigo. Diese Reduktions- und Oxidations- Prozesse wurden an den Indigo-haltigen Polymeren getestet.

Die Polymere wurden für die Verwendung in organischen elektronischen Bauteilen, wie organischen Solarzellen oder Feldeffekttransistoren, getestet.

Abstract

In this thesis, indigo- and “bay”-annulated indigo-containing polymers were synthesised either by Stille or Suzuki cross-coupling. To draw conclusions about the photophysical properties model compounds were synthesised, in which indigo is sandwiched between two donor units. The optical properties of the polymers were recorded and compared with those of the model compounds.

Further investigations focused on the improvement of solubility. Hence, a *tert*-butyloxycarbonyl (boc) indigo derivate was synthesised and coupled with suited donor co-monomers. The influence of additional dodecylthiophene spacers on the polymer solubility were investigated by coupling cyclopentadithiophene (CPDT) and “bay”-annulated indigo (BAI) monomers.

Polymer-analogous reactions were used to compare the similar properties of indigo-containing polymers and indigo. For this, the boc-protected indigo polymers were cleaved under thermal or acid exposure under formation of deprotected indigo units. During the dying process, indigo as dye is reduced and re-oxidised, whereas the reduced form is soluble in water. These reduction and oxidation processes were also investigated for the indigo-containing polymers.

The polymers were also tested for applications in organic electronics like organic solar cells or transistors.

Outline

1. Introduction 1

1.1. History of Dyes and Natural Indigo 1
1.2. Synthesis of the First Synthetic Dyes and Indigo 3
1.3. Dying with Indigo 5
1.4. Photophysical Properties of Indigo and Indigo Derivatives 6
1.5. Indigoids 8
1.6. Isoindigo and Isoindigo-Based Polymers 9
1.7. Indigo-Based Polymers 10
1.8. Aim and Scope 12

2. Indigo-Containing Polymers 15

2.1. Monomer Synthesis 15
2.1.1. Indigo Synthesis 15
2.1.2. Fluorene Synthesis 21
2.1.3. Bithiophene Synthesis 23
2.1.4. CPDT Synthesis 28
2.2. Model Compounds and Polymers Containing the Indigo Building Block 32
2.2.1. Synthesis of the CPDT Model Compound 32
2.2.2. Synthesis of the Fluorene Model Compound 35
2.2.3. Synthesis of Indigo-CPDT and Indigo-Bithiophene Polymers 37
2.2.4. Synthesis of Indigo-Fluorene Polymers 38
2.2.5. Characterisation of Indigo-CPDT Polymers 39
2.2.6. Characterisation of Indigo-Bithiophene Polymers 41
2.2.7. Characterisation of Indigo-Fluorene Polymers 43
2.3. Optical Properties 44
2.3.1. Absorption Properties 44
2.3.2. Molar Extinction Coefficient 48
2.3.3. Photophysical Properties of PIC-1 and PIF-1 49
2.3.4. Energy Levels 52
2.4. Polymer-Analogous Reactions 54
2.4.1. Cleaving the Boc–Protecting Group 54
2.4.2. Oxidation and Reduction Experiments 59

2.5. Summary Indigo-Containing Polymers 60
3. BAI-Containing Polymers 65
3.1. Monomer Synthesis 65
3.1.1. BAI Synthesis 65
3.1.2. Benzodithiophene Synthesis 70
3.2. Polymers Containing the BAI Building Block 75
3.2.1. Synthesis 75
3.2.2. Characterisation 76
3.3. Optical properties 79
3.3.1. Absorption Properties 79
3.3.2. Molar Extinction Coefficient 81
3.3.3. Energy Levels 81
3.4. Summary BAI-Containing Polymers 82
4. Applications 85
4.1. Solar Cell Investigations 85
4.2. Organic Field Effect Transitor Investigations 88
5. Summary and Outlook 91
5.1. Summary 91
5.2. Outlook 92
6. Experimental Part 95
6.1. General Information 95
6.1.1. Materials 95
6.1.2. Instrumentation 95
6.2. Monomer Synthesis 98
6.3. Model Compounds and Polymer Synthesis 123
6.4. Polymer-Analogous Reactions 136
Directories 139
List of Figures 139
List of Schemes 142
List of Tables 144

References 145
Acknowledgements 153

1. Introduction

1.1. History of Dyes and Natural Indigo

Indigo, madder, and saffron are the first known dyes and were used in India since 2500 BC (Figure 1). These dyes were extracted either from plants, animals or minerals.[1] For blue colour, indigo was used and extracted from woad or indigo plants. Kermes, madder root plants, and brazilwood are natural sources for red colours. The yellow colours were extracted from weld, Persian berries, saffron, and dyers broom. Combinations of these three colours lead to the colours green, brown, and violet.[2]

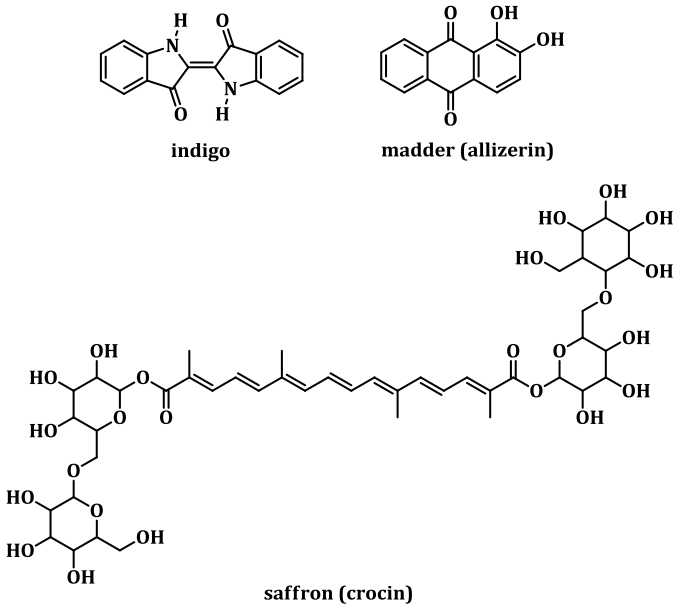

Figure 1: Chemical structures of the chromophores of indigo, madder, and saffron[1,3]

Maya blue is just one example for expressions of the unique indigo dye. It was used to decorate pottery, statues, and wall paintings by the Maya civilisation and was used since 800 AD in Mexico. Maya blue is an organic/inorganic hybrid consisting of indigo and clay, which was later discovered by Van Olphen.[4] Mayas called this clay 'White Earth'. The range of colour varies between light turquoises to dark greenish blue, depending on the amount of 'White Earth' which is mixed with indigo. Maya blue is known to be stable against base, oxidation and reducing agents, diluted mineral acids, heat, and biodegradation. This stability is proposed to result from heating the dye/clay mixture up to 100°C.[4–12]

Shellfish purple, Tyrian purple, and Royal purple are displaying the value of the indigo derivate 6,6'-dibromoindigo (Figure 2). These names already give an indication on the purple colour of the indigo derivate, which will be explained later in this chapter. Royal purple was a status symbol during the Roman and Byzantine Empire and was reserved for the wealthiest and most powerful people. The dye was extracted from the mollusc *Murex trunculus.* To extract 1 g of the dye, 10,000 molluscs had to be extracted. This demonstrates the rareness of this dye.[11,13]

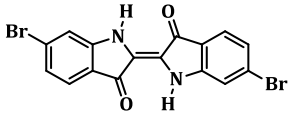

Tyrian purple

Figure 2 left: Chemical structure of 6,6'-dibromoindigo (Tyrian purple); right: *Murex trunculus*, also known as *Hexaplex trunculus* © Hans Hillewaert

Indigo is versatile. It was not only used as dye, but also as medicine by the Aztecs. The yellow leuco form of indigo can be extracted from *Isatis tinctoria* and *Indigofera tinctoria*. Afterwards, leucoindigo is oxidised by oxygen to the blue keto form. *Isatis tinctoria* or the so-called woad is a flowering plant from Northern Europe. *Indigofera tinctoria* belongs to the bean family plants and grows in Asia.[13] Indigo can be extracted from the bean family plants by fermentation process. Therefore, the leaves are washed by using a wool mill, which crushes the leaves. A pulp is kneaded and drained by hand to form a so-called woad ball. This woad ball has to be dried for one to four weeks. The balls are broken up and piled into layers, two to three feet deep and sprinkled with water. The fermentation takes over nine weeks, which smells badly and the remaining dark residue has to be dried.[13]

Scheme 1 shows the chemistry behind the indigo extraction. Isatan B and indican are extracted from the leaves during the washing process in the wool mill. The hydrolysis to indol-3-ol is initiated by the activity of β-glucosidase. Indoxyl is the keto form resulting from the keto-enol tautomerism. Indoxyl undergoes a spontaneous oxidation reaction which results in indigo. It has been shown, that the yield of indigo is increased in a low

oxygen medium, caused by microbial respiration. The side reaction is induced by a high oxygen amount. Isatin is the product of an oxygenase action and reacts with indoxyl to indirubin.[13,14]

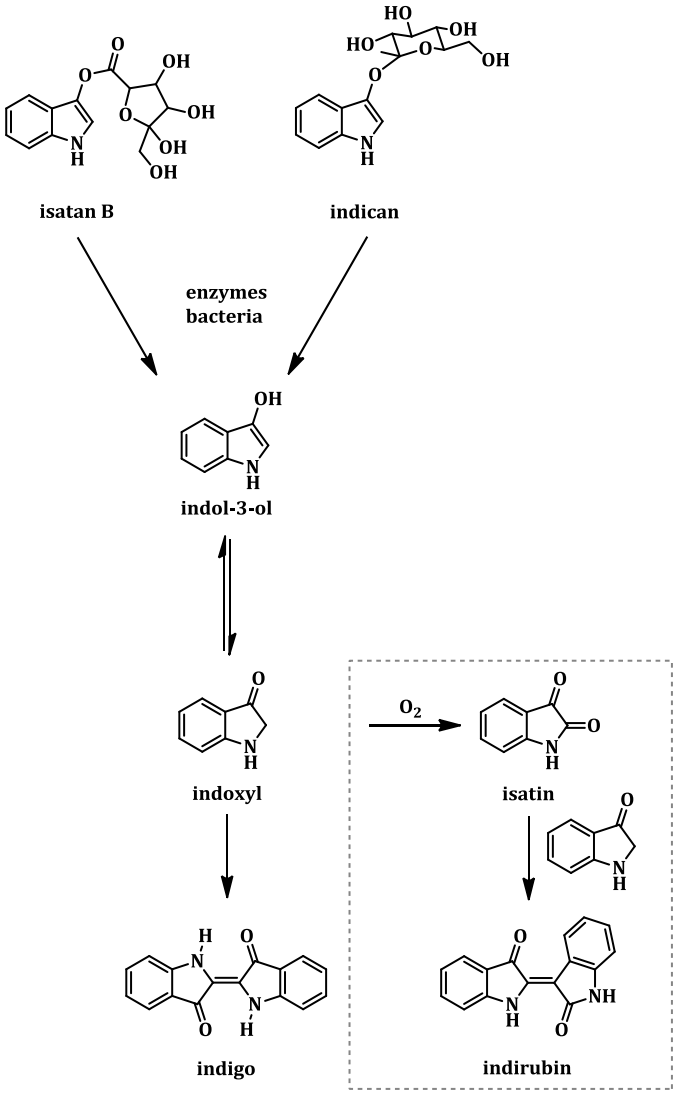

Scheme 1: Chemistry behind the indigo extraction, the dashed square demonstrates the side reaction[14,15]

Indirubin (3,2'-bisindole) is used as pharmacologically active ingredient against leukaemia, inflammation, psoriasis, and skin rashes.[14] Chinese people are using indirubin in curative medicine.[16]

1.2. Synthesis of the First Synthetic Dyes and Indigo

In 1856, at an early age of 18, W. H. Perkin synthesised the first synthetic dye and named it mauveine. The blue-violet solid was synthesised by oxidation of aniline (from

crude coal tar) and extracted from the reaction mixture in 5% yield. The chemical formula was proposed to be $C_{27}H_{24}N_4$.[17] In 1994, Meth-Cohn *et al.* investigated the structure of mauveine and observed, that it is a mixture of at least two different compounds (Figure 3).[18]

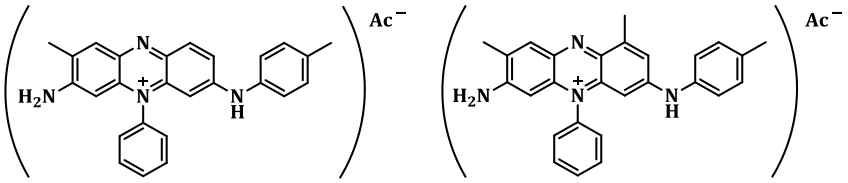

Figure 3: Structure of mauveine with acetate as counter ions, investigated by Meth-Cohn *et al.*[18]

Adolf von Baeyer determined the structure of 2,2'-bis(2,3-dihydro-3-oxoindolyliden) (indigo) in 1869. Thirteen years later he presented, together with Viggo Drewsen, the synthesis of indigo (Scheme 2).[19] They discovered the aldol-condensation of *o*-nitrobenzaldehyde with acetone in an alkaline medium. In the English speaking world, the reaction is known as Baeyer-Drewson reaction, it is not clear how the misspelling was achieved. In 1905, the work of Drewsen and Baeyer was rewarded with the Nobel Prize in Chemistry.[20,21]

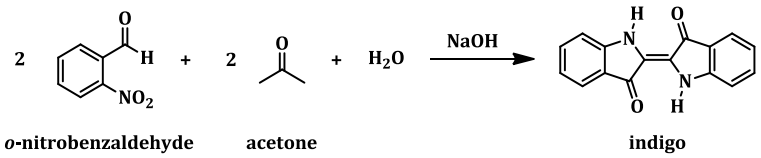

Scheme 2: Synthesis of indigo investigated by Adolf von Baeyer and Viggo Drewsen

In 1897, Heumann introduced another way to synthesise indigo from phenylglycine-*o*-carboxylic acid. The intramolecular cyclisation is performed in absence of oxygen with sodium hydroxide at 200°C. Indoxyl-2-carboxylic acid easily decarboxylates and dimerises under oxidation to indigo. Only four years later, Pfleger published a new way to synthesise indigo (Scheme 3). In the sense of atom economy, phenylglycine is a preferred starting material for the synthesis of indigo. An alkaline melt of sodium hydroxide and potassium hydroxide in the presence of sodium amide is used to form indoxyl from phenylglycine, which undergoes spontaneous oxidative dimerisation to indigo. The synthesis of Pfleger is still used. The reaction can be scaled up and phenylglycine can be obtained by condensation of aniline and chloroacetic acid.[7]

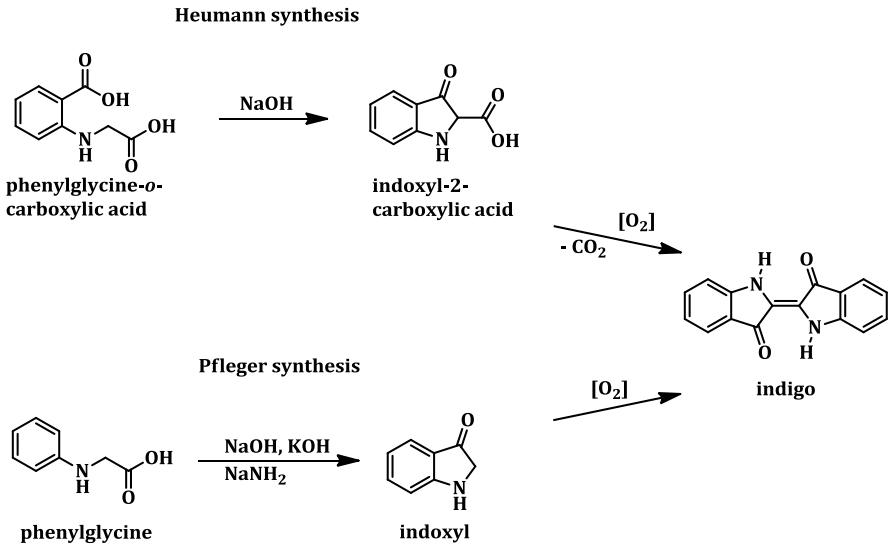

Scheme 3: Synthesis of indigo by Heumann (top) and Pfleger (bottom)[7]

1.3. Dying with Indigo

The indigo dying process was developed independently in Egypt, Asia, and America.[20] Indigo is a vat dye. The name is remaining from the historical process of dying, where indigo was placed in a vat (wooden barrel). Vat dyes are normally insoluble in organic solvents as well as in water. For the dying process, keto indigo has to be reduced with sodium dithionite into leucoindigo (Scheme 4).

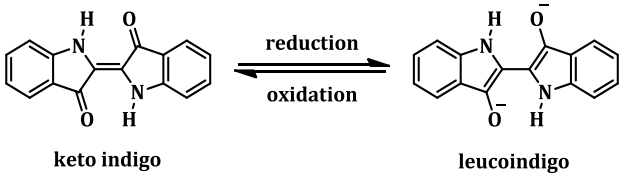

Scheme 4: Keto and leuco form of indigo

The yellow leucoindigo is soluble in water and deposits on the fibre, followed by oxidation by oxygen. Indigo is not chemically bonded to fibres. Therefore, the microscopic particles are suitable to dye all kind of fibres. Due to the low affinity to the fibres, the dying process has to be repeated several times. The sulphate emission (as by-product) has to be scaled down due to environmental regulations. Hence, processes with electrochemical reduction or catalytic hydrogenation are successful alternatives which are already used in dying processes.[1,11,22–24]

1.4. Photophysical Properties of Indigo and Indigo Derivatives

Baeyer postulated that the configuration of indigo is Z (*cis*).[25] In 1926, Posner[7] and in 1928 Reis and Schneider[26] proved the E-(*trans*) configuration by using X-ray crystal structure analysis. The solid state of indigo is highly aggregated due to intermolecular hydrogen bonding of up to four other indigo molecules. These hydrogen bonds cause the low solubility and relatively high melting point (390-392°C).[7] In vapour phase indigo is red due to the monomolecular state. When dissolved in non-polar solvents, it is violet, whereas it is blue in polar solvents, that means a pronounced positive solvatochromism.[27]

The remarkable photostability of indigo is resulting from the intramolecular hydrogen bonds between the carbonyl and secondary amine groups. For this reason, a photoinduced *trans-cis* isomerisation is not observed for indigo. Indigoid systems, which are not secondary amines and do not have intramolecular hydrogen bonds, show photoinduced isomerisations.[28–32]

In general, dyes consist of so-called chromophores and auxochromes. Herein, the chromophore is known as the electron accepting group and the auxochrome as the electron donating group. Both groups are linked by a conjugated system.[7,25,33]

Indigo is an H-chromophore, as shown in Figure 4. The two electron donating (N-H) and two electron accepting (C=O) groups are 'cross-conjugated' through an ethylene bridge, which causes the low energy absorption.[28,34–36]

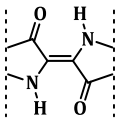

Figure 4: H-chromophore unit of indigo[7]

The small energy gap between the ground state and excited state causes the absorbance of indigo at low energy levels.[37] The H-chromophore theory can be confirmed by *ab initio* calculations, whereas the HOMO->LUMO (Highest Occupied Molecular Orbital -> Lowest Unoccupied Molecular Orbital) transition corresponds with the lowest energy optical absorption band. Jacquemin *et al*. investigated the π-character of the frontier orbitals. The excitation corresponds to a π->π* transition of conjugated organic molecules. The HOMO is located at the nitrogen atom and the central C=C bond whereas the LUMO is located in the central C-C bond and the carbonyls.[29]

Calculations of the first excited state of indigo demonstrate the transfer of electron density from the amine groups to the carbonyl groups, which leads to a higher acidity of the amine and a higher basicity of the carbonyl. The result of this discovery is that either a single or double proton transfer could occur, as shown in Figure 5. This excited-state keto-enol tautomerism is already initiated at low excitation energies resulting in an absorption maximum band of indigo above 600 nm.[38] It is known, that indigo does not show phosphorescence emission due to the rapid and efficient deactivation.[39]

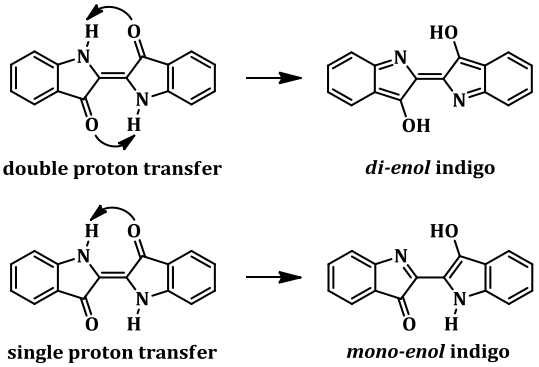

Figure 5: Excited state of indigo by either single or double proton transfer[38]

The electron density transfer from the amine to the carbonyl group of indigo in the first excited state can explain the influence of electron releasing or electron withdrawing substituents at the phenylene group (Table 1). Electron releasing groups in position five and seven are simplifying the electron density transfer, resulting in a bathochromic absorption shift, because less energy is necessary for the excitation. Electron withdrawing groups in these positions would furthermore exacerbate the transfer of electron density. Therefore, more energy is needed for the excitation resulting in a hypsochromic absorption shift. This assumption corroborates with MO (Molecular Orbital) calculations.[7,38]

Table 1: Absorption maxima of indigo and derivatives recorded in 1,2-dichloroethane; taken from ref.[7]

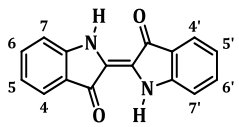

substituent	5,5'-isomer	6,6'-isomer
H	620 nm	620 nm
NO_2	580 nm	635 nm
OCH_3	645 nm	570 nm

1.5. Indigoids

Indigoid compounds are structurally related to indigo as shown in Figure 6. Either the secondary amine group is replaced by other heteroatoms, or the phenylene group is substituted. One example is Tyrian purple, which was already mentioned before. Another example is indigo carmine, in which the hydrogens of positions 5,5' are substituted by sulfonates. Due to the ionic group, this derivate is soluble in water. The absorption maximum is bathochromically shifted (8 nm) compared with the absorption maximum of indigo, in dimethylformamide.[40] Indigo carmine is used as food colorant and for determination of ozone in aqueous solutions.

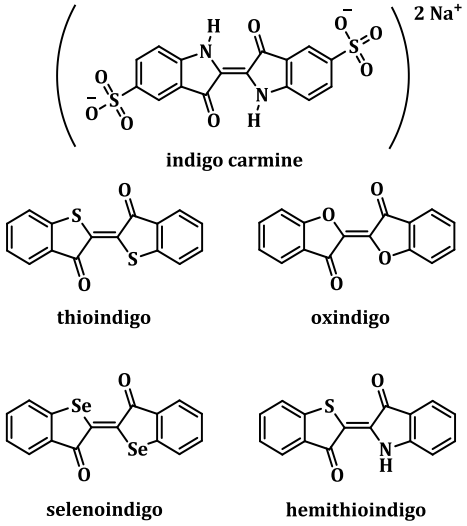

Figure 6: Selection of five indigoids based on the indigo core

The synthesis of thioindigo was first published by Fierz-David and Blangey in 1924.[41] In comparison to indigo, thioindigo shows an intense fluorescence emission when excited at its absorption maximum of 543 nm (in dimethylformamide).[25,42,43] Due to the absence of hydrogen bonds, a photoinduced *trans-cis* isomerisation is possible.

The remaining three indigoids shown are oxindigo, in which the amine groups are substituted by oxygen, selenoindigo, in which the amine groups are substituted by selenium, and hemithioindigo in which only one amine group is substituted by sulphur. Oxindigo shows an absorption maximum at 413 nm in *trans*-configuration and an absorption maximum at 396 nm in *cis*-configuration. The *cis*-conformation is thermally unstable and therefore *trans*-configuration is formed at 100°C.[44] Selenoindigo shows an absorption maximum in *trans*-configuration at 562 nm. As already quoted for the other

indigoids, the *cis*-configuration needs more energy to be excited. The corresponding absorption maximum in hexane is observed at 458 nm.[45]

Figure 7 shows two other indigoids related to indigo. Epindolidione (on the left) is a tetracene-analogous indigo. Epindolidione is known to be one of the best organic field effect transistor materials regarding charge carrier mobility (~2 cm^2/Vs) and stability. It was first mentioned by Ainley and Robinson in 1934. It is yellow in colour and shows intense fluorescence emission.[38,46]

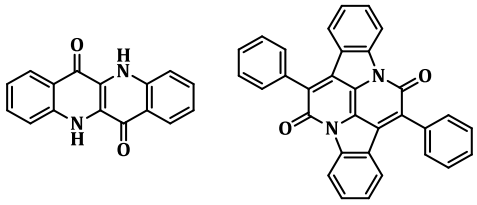

Figure 7: Selection of two indigoids related to indigo

The synthesis of cibalackrot was first published by Engi and Froehlich in 1914 and was performed by reacting indigo with phenylacetyl chloride.[47] Cibalackrot is a "bay"-annulated indigo (BAI) derivate. Compared to indigo, more energy is needed to excite cibalackrot, which is related to the missing proton transfer in the first excited state. The red fluorescence emission of 567 nm is caused by excitation at 544 nm in dioxane solution. Due to the fully conjugated system and the remarkable fluorescence, the suitability for organic electronics was investigated by Bronstein and co-workers.[48]

1.6. Isoindigo and Isoindigo-Based Polymers

The solubility of isoindigo is well-known in comparison to indigo due to weaker hydrogen bonds. In 2009, the group of Reynolds and co-workers described the synthesis of isoindigo oligomers which were applied in bulk heterojunction solar cells. Scheme 5 shows the acid induced coupling of 6-bromo-isatin and oxindole for the synthesis of functionalised isoindigo derivatives and the isoindigo-based oligomer by Reynolds.[49] The bulk heterojunction solar cell using this donor-acceptor-donor oligomer as donor and $PC_{61}BM$ as acceptor showed power conversion efficiencies (PCEs) of up to 1.8%.

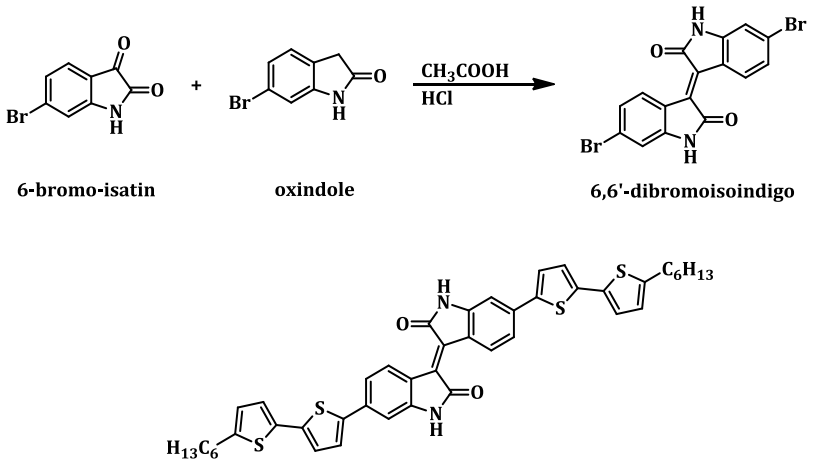

Scheme 5: Synthesis of 6,6'-dibromoisoindigo and (*E*)-6,6'-bis(5'-hexyl-[2,2'-bithiophene]-5-yl)-[3,3'-biindolinylidene]-2,2'-dione[49]

Andersson and co-workers published two years later an isoindigo-containing polymer (**PA-1**), in which the imide nitrogens are substituted by branched alkyl chains to increase the solubility (Figure 8). **PA-1** as donor showed PCEs in organic solar cells of up to 4.2% when using $PC_{61}BM$ as acceptor component.[50] Further investigations by Andersson resulted in PCEs of up to 6.3% when using $PC_{71}BM$ as acceptor (**PA-2** as donor).[51]

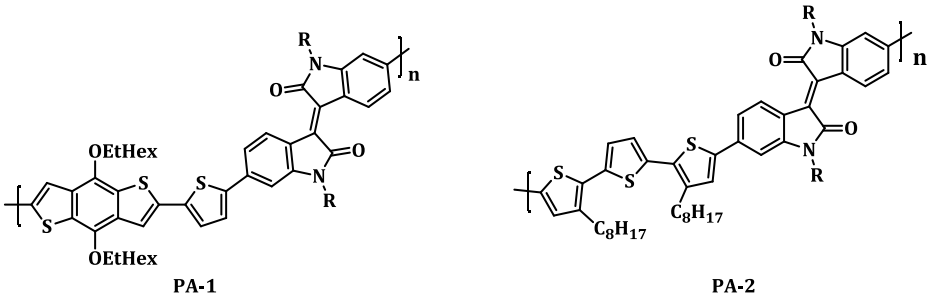

Figure 8: Copolymer synthesised by Andersson and co-workers, R=hexyldecyl[50,51]

1.7. Indigo-Based Polymers

The remarkable properties of indigo and indigoid systems are studied since decades and were already mentioned. Polymeric indigo is known since 1990 and was first prepared by Tanaka *et al.*.[52] The polymer consists of indigo units connected by methylene bridges. This polymer is insoluble due to missing solubilising groups. One

way to synthesise a soluble indigo-containing polymer was investigated by Voss *et al.* and is shown in Figure 9. To avoid the strong hydrogen bonds between amine and carbonyl groups, they used indoxyl and indolone co-monomers for the coupling with indigo. The obtained polymers **PV-1** and **PV-2** are soluble in dimethylformamide and form aggregates in concentrated solution, mainly by dimerisation of polymer chains. The absorption maximum of **PV-1** is at 660 nm and a hypsochromic shift of 18 nm is observed for **PV-2**.[53]

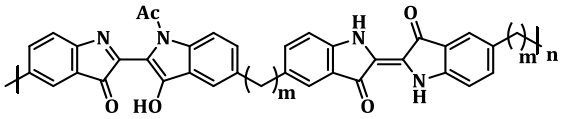

m=0, PV-1
m=1, PV-2

Figure 9: Indigo-containing polymers synthesised by Voss *et al.*, m=0-1[53]

Other ways to synthesise soluble indigo-based polymers were carried out by Sariciftci and co-workers[54] (2014), as well as Li and co-workers[55] (2015) (Figure 10). Both indigo-containing polymers are protected by *tert*-butyloxycarbonyl groups (boc-protecting group), which can be cleaved under thermal or acidic conditions.

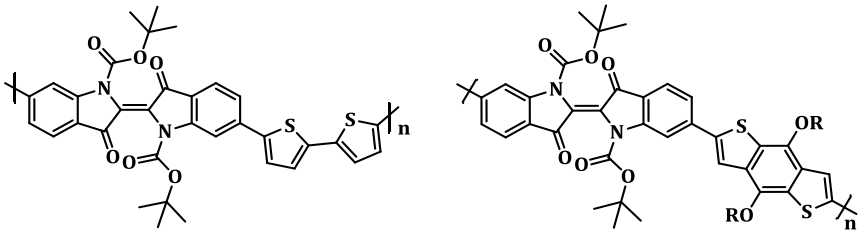

PS-1 **PL-1**

Figure 10 left: Polymer by Sariciftci (PS-1)[54]; right: Polymer by Li (PL-1)[55], R=2-decyltetradecyl

The electropolymerisation of **PS-1** performed by Sariciftci is followed by heating the thin layer film to observe the unprotected indigo-containing polymer. **PS-1** has an absorption maximum at 398 nm which is shifted to 632 nm by cleaving the boc-protecting group for 5 minutes at 150°C. Li and co-workers synthesised **PL-1** by Stille cross-coupling. The prepared thin films were heated to cleave the boc-protecting group which results in either bad solubility or insolubility. **PL-1** shows an absorption maximum at 585 nm and the maximum is shifted to 641 nm by cleaving the boc-protecting group at 200°C for 1 hour.

1.8. Aim and Scope

The absorption behaviour of indigo as a small molecule makes it attractive for application in organic solar cells. However, the poor solubility of indigo itself makes the design of solar cells challenging. Hence, indigo as acceptor compound is coupled with solubilising donor groups to synthesise indigo-containing polymers. In this thesis, conjugated polymers will be designed with fluorene, cyclopentadithiophene, and bithiophene as connecting units (Figure 11). The resulting photophysical properties of the indigo-containing polymers are explored in detail. Also model compounds, in which indigo is sandwiched by two donor units, are synthesised for comparison. These investigations will allow conclusions about energy transfer processes in the excited state. Another way to synthesise soluble and processible indigo-containing polymers is the introduction of a solubilising group at the indigo unit. Hence, *tert*-butyloxycarbonyl (boc) protected indigo monomers will be synthesised and coupled with suited connector units. The polymers will be characterised by absorption spectroscopy, and a determination of the HOMO- and LUMO-energy levels. Finally, solar cell investigations are planned.

The indigo-containing polymers will be further investigated for polymer-analogous reactions in which the indigo unit is reduced according to the indigo-based dying process. Moreover, the cleavage of the boc-protecting groups under formation of unprotected indigo units will be studied.

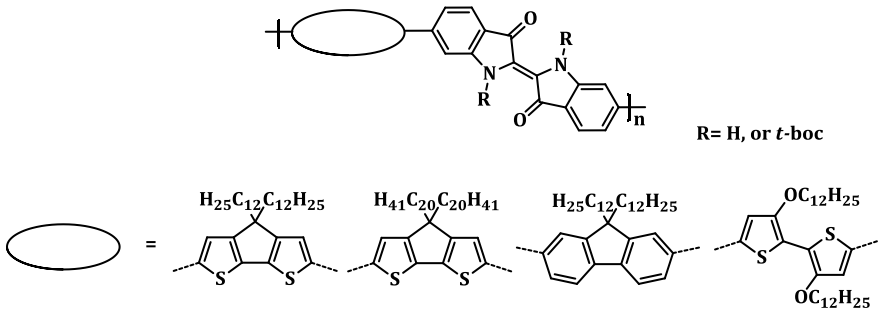

Figure 11: Target structures of indigo-containing polymers

"Bay"-annulated indigo (BAI) is nearly unexplored due to the limited solubility although it shows interesting absorption behaviour. Therefore, BAI-containing polymers with increased solubility will be designed by coupling BAI with different connector (donor) units, including BAI-containing polymers (BAI-CPDT copolymers) with

additional dodecylthiophene spacers (Figure 12). Benzodithiophene derivatives with branched alkyl chains in position four and eight are known to increase the solubility of donor-acceptor copolymers. Hence, BAI will be coupled with such benzodithiophene monomers. BAI-containing copolymers will be studied for potential applications in organic solar cells and organic field effect transistors.

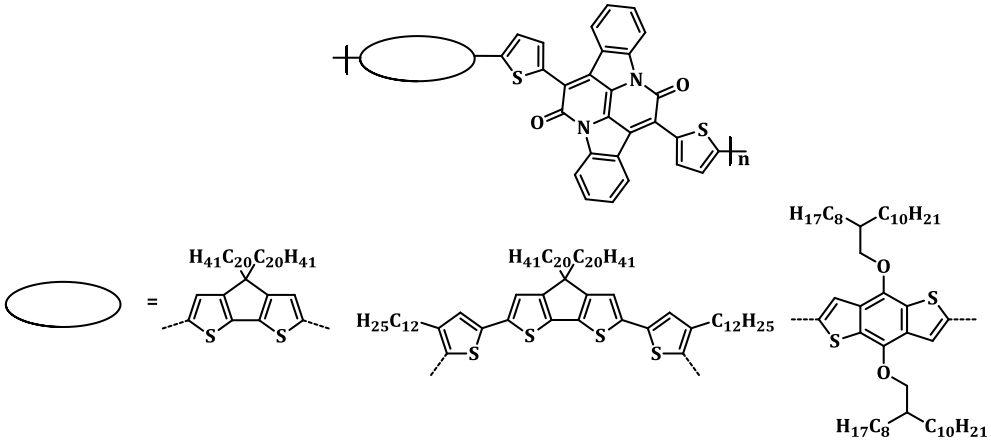

Figure 12: Target structures of BAI-containing polymers

2. Indigo-Containing Polymers

2.1. Monomer Synthesis

2.1.1. Indigo Synthesis

In 2006, Imming *et al.* published a suitable synthetic route of (*E*)-6,6'-dibromo-[2,2'-biindolinylidene]-3,3'-dione (6,6'-dibromoindigo, **I5**).[56] Scheme 6 depicts a related synthetic route. The distinctions will be discussed with the appropriate synthesis steps.

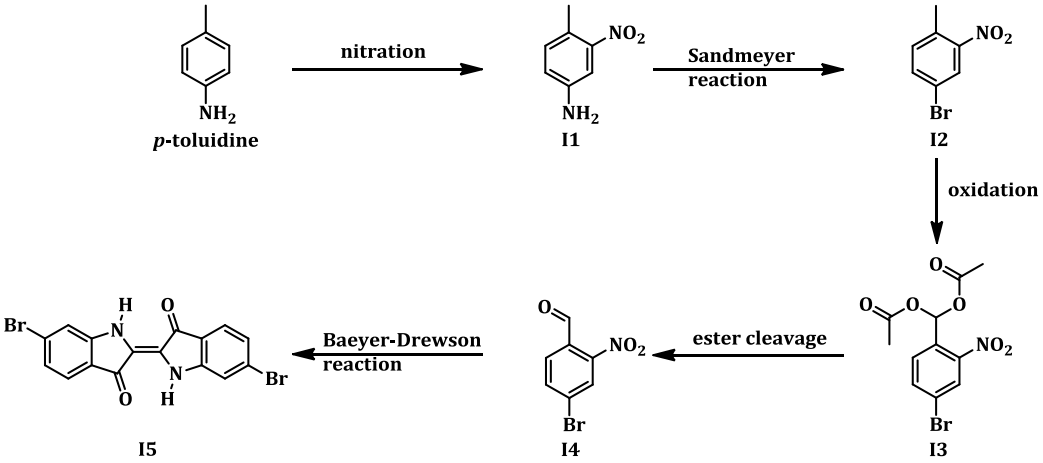

Scheme 6: Synthesis plan of 6,6'-dibromoindigo[56]

The nitration of *p*-toluidine results in 4-methyl-3-nitroaniline (**I1**) and is followed by a Sandmeyer reaction to substitute the amine function by a bromide group. 4-Bromo-2-nitromethylbenzene (**I2**) undergoes an oxidation reaction which affords 4-bromo-2-nitrobenzylidene diacetate (**I3**). A basic ester cleavage of diacetate **I3** results in 4-bromo-2-nitrobenzaldehyde (**I4**). The monomer 6,6'-dibromoindigo (**I5**) is afforded in a Baeyer-Drewson reaction.

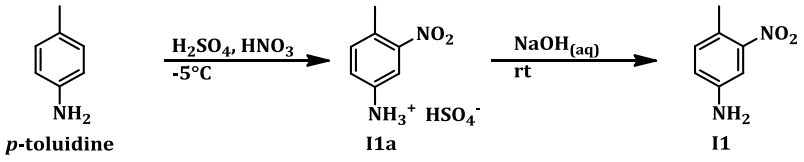

Scheme 7: Synthesis of 4-methyl-3-nitroaniline (I1), *via* I1a

Imming *et al.* synthesised the 3-nitro-4-methylphenylammonium hydrogensulphate (**I1a**) salt and used it for the Sandmeyer reaction.[56] In this work, the nitration reaction is followed by deprotonation with base, one of the enhancement steps compared to the

literature (Scheme 7).[56] The solubility in organic solvents is increased by deprotonation and within that, recrystallization from ethanol is possible. During the nitration reaction with nitric acid and sulphuric acid, the temperature must be kept stable below -5°C, to avoid double nitration. The reaction solution was poured into iced water and the precipitate was filtered off. By treating the solid with sodium hydroxide solution, the salt **I1a** is transformed into nitroaniline **I1**. The ^{1}H NMR spectrum shows the three aromatic protons as a doublet, a doublet of doublets, and a singlet signal at δ = 7.17, 7.02, and 6.74 ppm, respectively. The two amine protons show a singlet signal at δ = 3.79 ppm. The protons of the methyl group show a singlet signal at δ = 2.36 ppm. In the ^{13}C NMR spectrum, six aromatic signals (δ = 150-110 ppm) including the amine substituted carbon (δ = 145.6 ppm) can be observed. The methyl carbon exhibits a signal at δ = 19.8 ppm. The GC-MS measurement with an m/z = 152.0 is in accordance to the proposed structure.

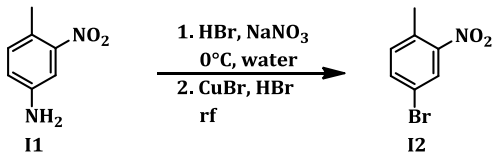

Scheme 8: Synthesis of 4-bromo-2-nitromethylbenzene (I2)

For the Sandmeyer reaction, the formation of a diazonium salt of **I1** is performed with sodium nitrite and hydrobromic acid at 0°C (Scheme 8). This aryl diazonium salt undergoes reduction by treatment with a boiling catalyst solution, in this case copper bromide, and leads to a diazo radical. Elimination of elemental nitrogen leads to a highly reactive aryl radical, which reacts with the nucleophilic bromide. After an aqueous workup and column chromatography, the yellow product **I2** was afforded with an m/z = 217.0 (GC-MS). Compared to the ^{1}H NMR spectrum of **I1**, the signals of the aromatic protons of **I2** are shifted downfield due to the electron withdrawing bromo-substituent. Moreover, the successful diazotisation can be proved by the absence of the proton signals caused by the amine group. The protons of the methyl group show a singlet signal at δ = 2.54 ppm. The ^{13}C NMR spectrum shows downfield shifts for all carbons. Clearly, the signal at δ = 119.6 ppm represents the bromo-substituted carbon.

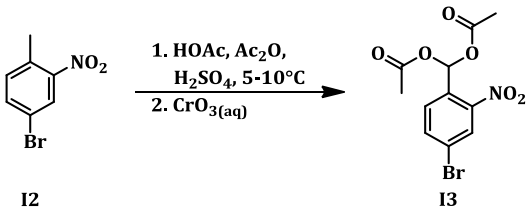

I2 I3

Scheme 9: Synthesis of 4-bromo-2-nitrobenzylidene diacetate (I3)

The oxidation of the methyl group of **I2** to the aldehyde **I4** is done in two steps. First of all, ester **I3** is synthesised followed by cleavage of the ester to afford the aldehyde **I4** (Scheme 9). During the reaction, aldehyde **I4** occurs as an intermediate but due to the excess of acetic anhydride the acetate **I3** is formed immediately. The oxidation with chromium trioxide in the absence of acetic anhydride would lead to the corresponding carboxylic acid, as well as higher temperatures. Hence, the reaction solution was cooled to avoid the formation of the carboxylic acid as a side product. Flash column chromatography afforded the pure diacetate **I3**. The LC-MS analysis shows an m/z = 354.0 according to the molecular weight. In the ^{1}H NMR spectrum, the signals at δ = 8.09, 7.77, and 7.54 ppm represent the protons of the phenyl ring as a doublet, a doublet of doublets, and another doublet signal. An additional singlet signal at δ = 8.01 ppm is dedicated to the α-proton of the ester function. The methyl groups protons show a singlet signal at δ = 2.06 ppm. In the ^{13}C NMR spectrum, the signal of the carbonyl carbons is observed at δ = 168.8 ppm. The peaks between δ = 148.2 and 124.4 ppm represent the six aromatic carbons of the phenyl group. A signal at δ = 85.6 ppm reveals the tertiary carbon of the ester. The singlet signal of the methyl groups occurs at δ = 20.9 ppm.

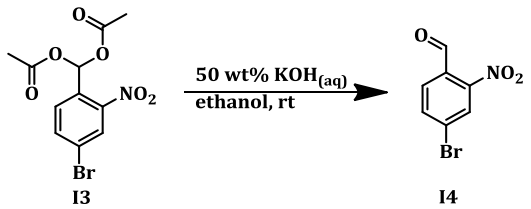

I3 I4

Scheme 10: Synthesis of 4-bromo-2-nitrobenzaldehyde (I4)

Instead of following Immings *et al.* procedure,[56] the ester cleavage is carried out by base (Scheme 10). The milder reaction conditions reduce the amount of side products compared to the acid induced cleavage. Therefore, acetate **I3** was dissolved in ethanol and treated with potassium hydroxide solution. Purification by column chromatography

yielded in the desired product with an m/z = 227.2 (LC-MS). In the ^{1}H NMR spectrum, the aldehyde proton shows a singlet signal at δ = 10.25 ppm. The peaks between δ = 8.16 and 7.73 ppm represent the protons of the phenyl group as a doublet, a doublet of doublets, and another doublet signal. In the ^{13}C NMR spectrum, the signal of the carbonyl carbon of the aldehyde **I4** is observed at δ = 187.6 ppm. The signals of the phenyl ring are recorded between δ = 149.9 and 127.9 ppm.

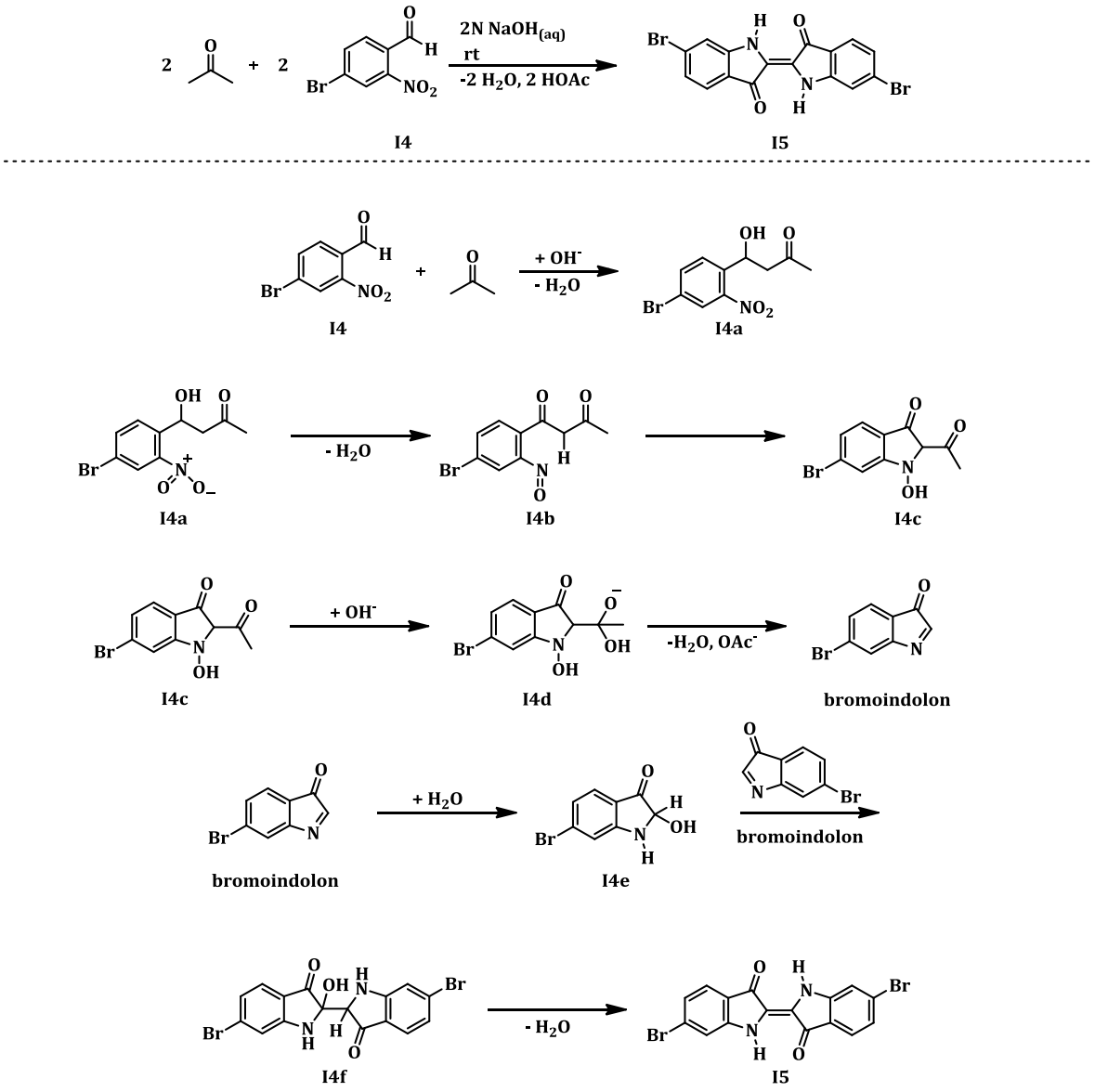

Scheme 11 top: Synthesis of dibromoindigo I5; bottom: Baeyer-Drewson reaction mechanism[19,57]

In a Baeyer-Drewson reaction,[19,57] **I4** is used to synthesise dibromoindigo **I5** (Scheme 11). As a first step, the acidic protons of acetone are removed by treating with hydroxide anions. The aldol addition of the resulting nucleophile derived from acetone

and aldehyde **I4** results in **I4a**. In an intramolecular redox reaction under elimination of water **I4b** is formed. Another abstraction of an acidic proton initiates an intramolecular cyclisation to **I4c**. A nucleophilic addition of a hydroxide anion to **I4c** leads to the intermediate **I4d**. Elimination of an acetate group and water results in bromoindolon. The strong nucleophile **I4e** results from the addition of water to bromoindolon. Condensation of **I4e** and bromoindolon affords **I4f**. As a final step, cleavage of water results in dibromoindigo **I5**. The pH was adjusted to 10 which leads to an immediately change of colour from yellow over orange to red brown. Red brown is the mixed colour of the purple dibromoindigo **I5** and the unreacted orange bromoindolon. After four days, the precipitate was filtered off and washed with water. Due to the limited solubility, solid state carbon NMR spectra of dibromoindigo **I5** and indigo werw recorded. In Figure 13 the resulted spectra are compared; the blue line for indigo and the purple one for **I5**. Both carbonyl groups show a signal at δ = 187.1 ppm. The peaks at δ = 151.4 ppm are quaternary carbons of indigo and **I5**. In the spectrum of indigo, a tertiary carbon signal at δ = 134.9 ppm is recorded, which is not observed for **I5** due to the bromo-substitution. The broad signal group between δ = 130.9 and 105.7 ppm represents the remaining carbon signals of **I5**. The peaks appearing between δ = 127.1 and 110.9 ppm in the indigo spectrum (blue) represent the remaining tertiary and quaternary carbons.

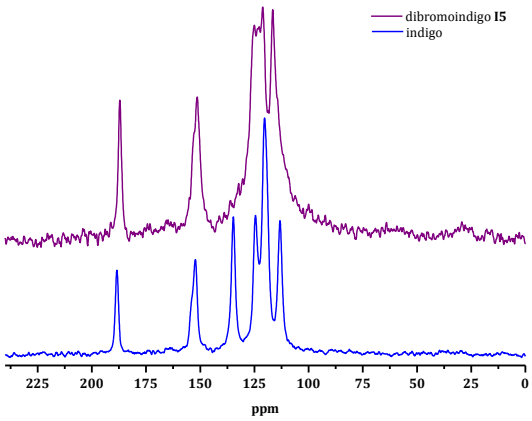

Figure 13: Solid ^{13}C NMR spectrum of indigo and dibromoindigo I5

Figure 14 shows the IR spectrum of dibromoindigo **I5**. The characteristic N-H stretching vibrations show a sharp peak at υ = 3381 cm^{-1}. At υ = 3080 cm^{-1} the aromatic C-H stretching vibrations are recorded. A sharp peak around υ = 1630 cm^{-1} represents

the C=O stretching vibrations. The N-H deformation vibrations show a peak at υ = 1575 cm^{-1}. The framework vibrations of C-Br show a peak at υ = 1080 cm^{-1}.

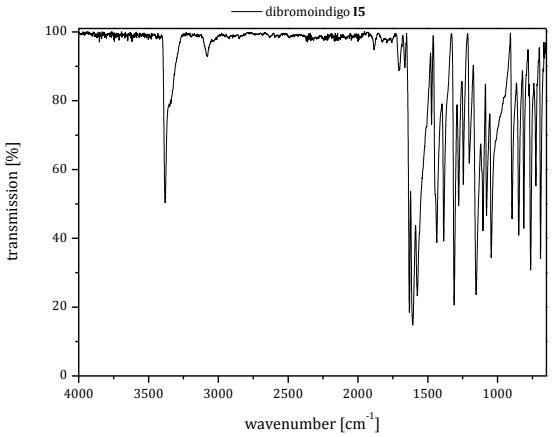

Figure 14: IR spectrum of dibromoindigo I5

The results of the solid ^{13}C NMR and IR spectroscopy, combined with an m/z = 419.0 (MALDI-MS) prove the successful synthesis of dibromoindigo **I5**.

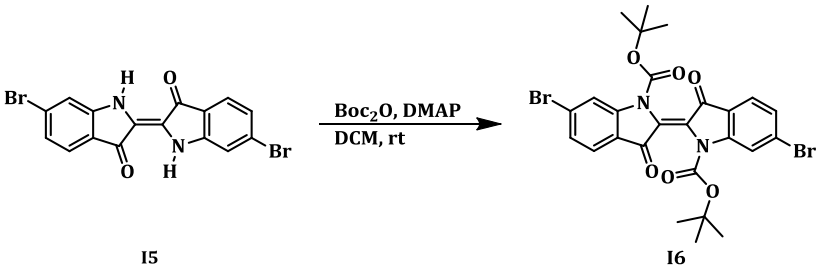

Scheme 12: Synthesis of (*E*)-6,6'-dibromo-3,3'-dioxo-[2,2'-biindolinylidene]-1,1-dicarboxylate (I6)

Due to the low solubility of indigo, a boc-protected dibromoindigo derivate was synthesised (Scheme 12). This derivate is soluble in common organic solvents and the solubilising group can be cleaved after polymerisation.[58] Hereby, the thermal and acid cleavable *tert*-butyloxycarbonyl (boc) group was used. The desired product was isolated after flash column chromatography and several recrystallizations from ethyl acetate. The ^{1}H NMR spectrum shows the aromatic protons at δ = 8.26, 7.61, and 7.36 ppm as a singlet, a doublet, and a doublet of doublets signals. The protons of the methyl groups give a singlet at δ = 1.61 ppm. In the ^{13}C NMR spectrum, the signal at δ = 182.5 ppm belongs to the carbonyl carbons of the indigo core. The peaks between δ = 149.6 and 120.4 ppm represent the aromatic carbons including the carbonyl carbons of the boc-protecting groups. For the tertiary carbons of the *tert*-butyl group, a signal at

δ = 85.4 ppm is recorded. The spectrum shows the signal of the methyl carbons at δ = 28.2 ppm. A mass analysis by APCI leads to an m/z = 621.0, which is in accordance to the desired structure.

The IR spectrum of the boc-substituted dibromoindigo **I6** is shown in Figure 15. Clearly, the sharp stretching and deformation vibrations of N-H are no longer recorded. The peaks between υ = 3124 and 2804 cm^{-1} represent the aromatic C-H and CH_3 stretching vibrations. An additional band at υ = 1739 cm^{-1} results from the C=O stretching vibrations of the alkoxycarbonyl. The spectrum also demonstrates the C=O stretching vibrations of the indigo core at υ = 1674 cm^{-1}. The framework vibrations of C-Br are recorded at υ = 1083 cm^{-1}.

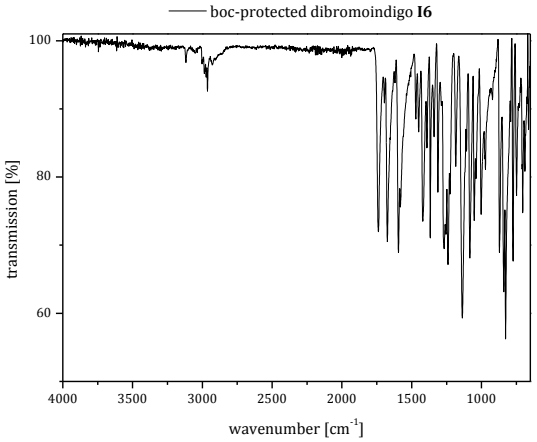

Figure 15: IR spectrum of the boc-substituted dibromoindigo I6

2.1.2. Fluorene Synthesis

In 1867, Berthelot discovered an amount of 2% fluorene in coal tar.[59] Commercially available 2,7-dibromo-9*H*-fluorene undergoes base-induced alkylation reaction in 9-position. In this thesis 2,7-dibromo-9,9-didodecyl-9*H*-fluorene (**F1**) is used in a Miyaura cross-coupling reaction to synthesise 2,2'-(9,9-didodecyl-9*H*-fluorene-2,7-diyl)-bis(4,4,5,5-tetramethyl-1,3,2-dioxaborolane) (**F2**) (Scheme 13).[60]

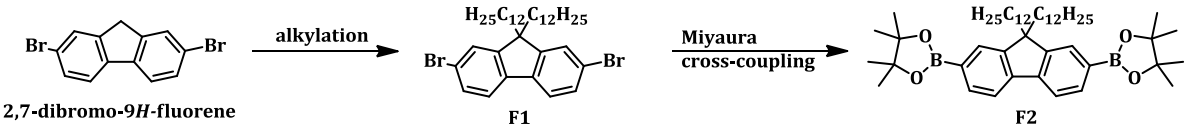

Scheme 13: Synthesis plan of 2,2'-(9,9-didodecyl-9*H*-fluorene-2,7-diyl)bis(4,4,5,5-tetramethyl-1,3,2-dioxaborolane) (F2) *via* 2,7-dibromo-9,9-didodecyl-9*H*-fluorene (F1)[a]

This reaction route can also be used to synthesise mono-brominated and mono-dioxaborolated fluorenes which will be discussed below (Scheme 14).

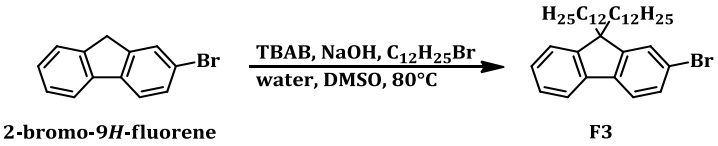

Scheme 14: Synthesis of 2-bromo-9,9-didodecyl-9*H*-fluorene (F3)

Hereby, 2-bromo-9*H*-fluorene, sodium hydroxide as base, and dodecyl bromide were heated in a two phase mixture of dimethyl sulfoxide and water. **F3** is characterised by NMR spectroscopy and APCI-MS, with an m/z = 582.4, as expected. The ^{1}H NMR spectrum shows the aromatic proton signals as three multiplet and one doublet signals, whereby the doublet signal is recorded at δ = 7.48 ppm and the multiplet signals at δ = 7.61-7.57, 7.42-7.36, and 7.28-7.22 ppm. Moreover, the signals of the seven aromatic carbons are recorded between δ = 153-120 ppm beside the bromo-substituted carbon at δ = 121.1 ppm. The aliphatic signals of the protons and carbons are in accordance to the proposed structure.

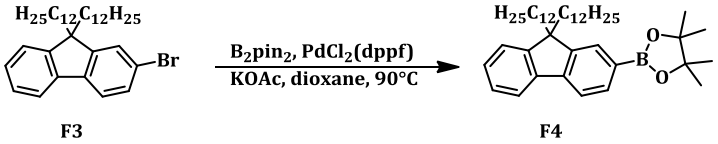

Scheme 15: Synthesis of 2-(9,9-didodecyl-9*H*-fluoren-2-yl)-4,4,5,5-tetramethyl-1,3,2-dioxaborolane (F4)

The Miyaura cross-coupling reaction is used to synthesise 2-(9,9-didodecyl-9*H*-fluoren-2-yl)-4,4,5,5-tetramethyl-1,3,2-dioxaborolane (**F4**), as shown in Scheme 15. Therefore, [1,1'-bis(diphenylphosphino)ferrocene]dichloropalladium(II) as catalyst and **F3** were suspended in dioxane and heated. The crude product was purified by silica gel

[a] F1 and F2 were synthesised by Dr. Nils Fröhlich.

column chromatography and recrystallization. The aromatic proton signals are shifted downfield compared to **F3**. The signal at δ = 1.29 ppm represents the methyl groups of the pinacolato group. In the ^{13}C NMR spectrum, an additional carbon signal at δ = 128.0 ppm occurs and the bromo-substituted carbon signal is no longer observed. The quaternary carbons of the pinacolato group show a signal at δ = 83.9 ppm. A signal at δ = 25.3 ppm is dedicated to the carbons of the methyl group from the pinacolato group. The proton and carbon signals of the dodecyl chains, as well as the m/z = 628.5 (APCI-MS) are as expected.

2.1.3. Bithiophene Synthesis

In 2008, Guo *et al.* published a four step synthesis route of 3,3'-bis(dodecyloxy)-5,5'-bis(tributylstannyl)-2,2'-bithiophene (**B4**).[61]

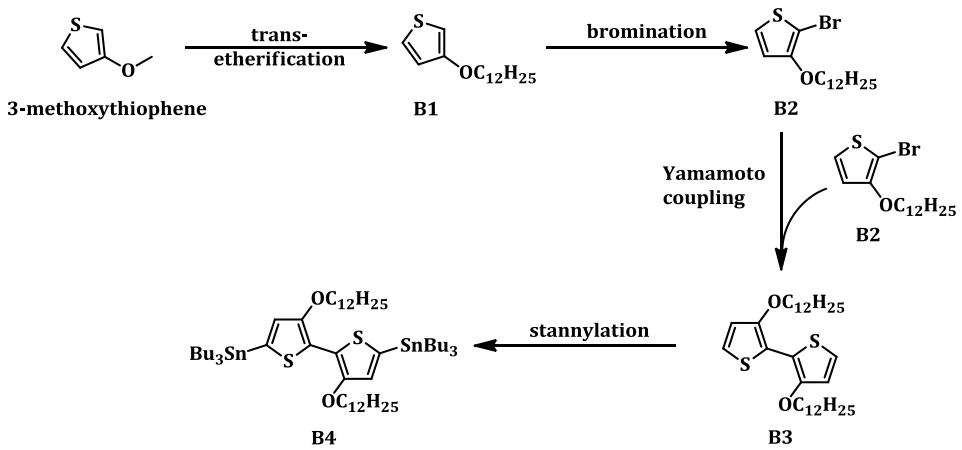

Scheme 16: Synthesis plan of 3,3'-bis(dodecyloxy)-5,5'-bis(tributylstannyl)-2,2'-bithiophene (B4)

Thereby, 3-methoxythiophene undergoes a transetherification reaction which results in 3-dodecyloxythiophene (**B1**), followed by bromination to afford 2-bromo-3-dodecyloxythiophene (**B2**). As a matter of fact, **B2** is highly reactive which will be discussed later in the chapter. **B2** is dimerised under Yamamoto-type conditions yielding 3,3'-bis(dodecyloxy)-2,2'-bithiophene (**B3**) which is then stannylated to afford the monomer **B4** (Scheme 16).

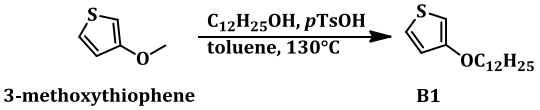

Scheme 17: Synthesis of 3-dodecyloxythiophene (B1)

Scheme 17 illustrates the formation of 3-dodecyloxythiophene (**B1**). The nucleophilic substitution reaction is initiated by *p*-toluenesulfonic acid in refluxing toluene. After an aqueous workup and column chromatography the product was characterised by NMR spectroscopy and APCI-MS, with an expected m/z = 269.2. In the ^{1}H NMR spectrum, three doublet signals are detected for the three aromatic protons at δ = 7.17, 6.76, and 6.23 ppm. The triplet signal of the methylene group adjacent to oxygen is recorded at δ = 3.94 ppm. The remaining alkyl signals are recorded between δ = 1.84-0.89 ppm. In the ^{13}C NMR spectrum, the quaternary carbon of the thiophene ring shows a signal at δ = 158.2 ppm. The tertiary aromatic carbon signals are detected at δ = 124.6, 119.7, and 97.1 ppm, whereas the last signal belongs to the carbon in position two. The methylene group adjacent to the oxygen shows a signal at δ = 70.4 ppm. In a range of δ = 32.1-14.3 ppm the remaining carbon signals of the alkyl chain are recorded.

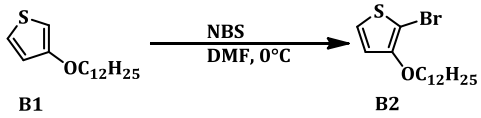

Scheme 18: Synthesis of 2-bromo-3-dodecyloxythiophene (B2)

During subsequent bromination, bromine is directed to position 2 due to the dodecyloxy substituent at the thiophene. To avoid a second bromination in position 5 only one equivalent of 1-bromopyrrolidine-2,5-dione is used. Hence, **B1** was dissolved in dimethylformamide cooled and treated with 1-bromopyrrolidine-2,5-dione (Scheme 18). A quick aqueous workup and a flash column chromatography afforded the desired product. **B2** is highly reactive and slightly dried for the NMR spectroscopy. The two doublet signals at δ = 7.18 and 6.74 ppm represent the aromatic protons in the ^{1}H NMR spectrum. Clearly, no additional aromatic proton signal is recorded. Due to the bromo-substituent, a slight shift for the alkyl chain protons to the downfield is observed. In the ^{13}C NMR spectrum, the bromo-substituted carbon shows a signal at δ = 97.8 ppm. The signal at δ = 72.4 ppm represents the methylene group adjacent to the oxygen. All

signals are in accordance to the proposed structure as well as an m/z = 348.1 measured by APCI-MS.

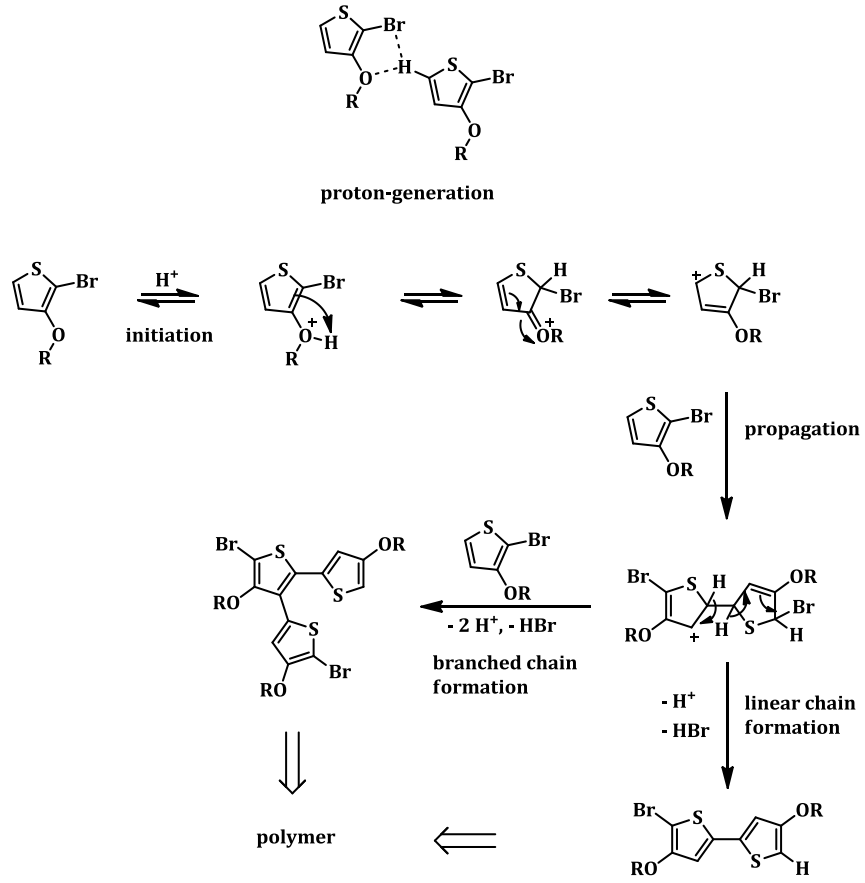

Scheme 19: Proposed mechanism of the autopolymerisation[62]

B2 is proposed to undergo an autopolymerisation in solid state. This reaction was examined by Officer and co-workers.[62] Hydrogen bromide gas was evolving and a black insoluble solid remained. The observations of Officer are in accordance to our observations for **B2**. The proposed mechanism of the autopolymerisation is initiated by an acidic proton and is shown in Scheme 19. The proton is probably added to an oxygen atom of the alkoxy group leading to a positive charge at the oxygen. Due to the conjugated π-system, a rearrangement of the electrons takes place. A nucleophilic attack by another bromoalkoxythiophene can occur in position five. The dimer is probably formed by re-aromatisation and cleavage of hydrogen bromide. In following propagation reactions linear or branched chains are formed.[62]

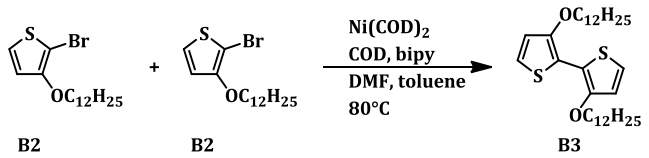

Scheme 20: Synthesis of 3,3'-bis(dodecyloxy)-2,2'-bithiophene (B3)

B2 was used without drying for the Yamamoto-type coupling (Scheme 20).[63],[64] Yamamoto-type couplings are initiated by a ligand exchange of the catalyst bis(1,5-cyclooctadiene)nickel(0) [Ni(COD)$_2$] by bipyridine [bipy] in dimethylformamide. The activated nickel complex [bipy-Ni-COD] and **B2** undergo an oxidative addition to form [bipy-Ni-**B2**], followed by coordination of a second oxidised molecule [(bipy-Ni-**B2**)$_2$]. This complex is disproportionated into a nickel compound with two bromo-substituents and one bipyridine [bipy-Ni-Br$_2$] and into a nickel compound with two thiophene rings [bipy-Ni-**B1**$_2$]. The following reductive elimination results in 3,3'-bis(dodecyloxy)-2,2'-bithiophene (**B3**). An aqueous workup and column chromatography results in pure **B3**. An m/z = 535.4 measured by APCI-MS correlates with the proposed structure. The ^{1}H NMR spectrum of **B3** shows two doublet signals for the four aromatic protons at δ = 7.08 and 6.84 ppm. Due to the positive mesomeric effect of the ether substituent, the methylene groups adjacent to the oxygen show a triplet at δ = 4.10 ppm. The peaks between δ = 1.88-1.28 ppm represent the remaining methylene groups. A triplet signal at δ = 0.90 ppm demonstrates the methyl groups. The quaternary peak at δ = 114.3 ppm, in the ^{13}C NMR spectrum, resulting from position two, indicates the successful dimerisation. All remaining carbon signals are in accordance to the proposed structure.

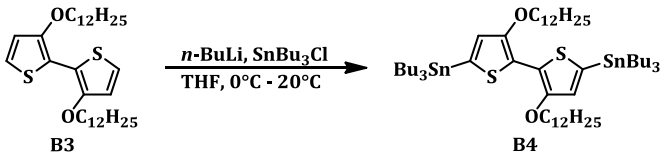

Scheme 21: Synthesis of 3,3'-bis(dodecyloxy)-5,5'-bis(tributylstannyl)-2,2'-bithiophene (B4)

As a matter of fact, stannylated compounds are unstable against acid and sensitive to base, the latter called protiodestannylation. Walton and co-workers discussed the protiodestannylation in 1971,[65] so did Guo *et al.* in 2008.[61] The protiodestannylation explains the cleavage of the organotin compound from the carbon under basic conditions. Electron donating groups like ether functions assist the electrophilic attack of the stannyl substituted carbon. The stannyl itself is attacked by a hydroxyl group. The

remaining proton of the cleaved compound is transferred by the solvent.[65] Therefore, after the double lithiation and following transmetalation by tributylstannyl chloride, the reaction solution was poured into highly diluted sodium hydroxide solution to remove inorganic salts (Scheme 21). Flash column chromatography yielded the pure stannylated **B4**. The product was used directly for the polymerisation. The m/z = 1111.9 is expected for the proposed compound and was measured by FD-MS. An immediately recorded ^{1}H NMR spectrum shows the aromatic protons at δ = 6.85 ppm as a singlet signal. The triplet of the methylene groups adjacent to the oxygen is barely shifted to δ = 4.12 ppm. The peaks between δ = 1.94-0.83 ppm represent the remaining alkyl protons of the ether and the alkyl protons of the tributylstannyl group. Three quaternary carbons are recorded in the ^{13}C NMR spectrum. A signal at δ = 153.9 ppm represents the oxygen substituted carbons, the signal at δ = 132.7 ppm the stannyl substituted carbons, and at δ = 120.5 ppm the carbons connecting the thiophene rings. The peak at δ = 124.0 ppm shows the tertiary carbons. A signal at δ = 72.1 ppm represents the oxygen substituted aliphatic carbons. The remaining alkyl carbons signals are recorded between δ = 32.1-10.9 ppm. A ^{119}Sn NMR spectrum shows a singlet signal at δ = -38.5 ppm.

2.1.4. CPDT Synthesis

The five step synthesis of 4*H*-cyclopenta[1,2-*b*:5,4-*b*']dithiophene (CPDT core, **C5**) is known since 1986 and was evolved by Kraak *et al.*.[66]

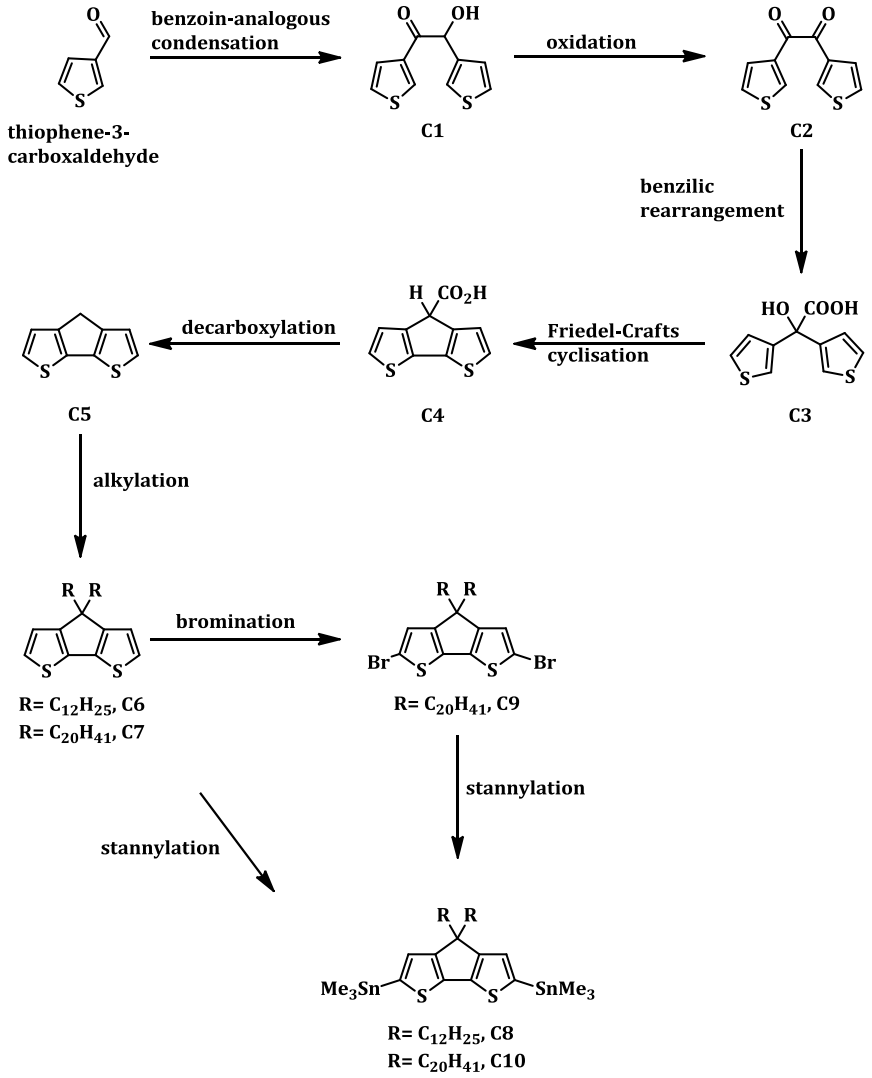

Scheme 22: Synthesis plan of CPDT; $C_{20}H_{41}$= octyldodecyl side chain

The benzoin-analogous condensation reaction of thiophene-3-carboxaldehyde results in 2-hydroxy-1,2-di(thiophen-3-yl)ethanone (**C1**). An oxidation of **C1** leads to 1,2-di(thiophen-2-yl)ethane-1,2-dione (**C2**). The following benzilic acid-analogous rearrangement affords 2-hydroxy-2,2-di(thiophen-2-yl)acetic acid (**C3**). 4*H*-Cyclopenta[1,2-*b*:5,4-*b*´]dithiophene-4-carboxyclic acid (**C4**) was synthesised by Friedel-Crafts type intramolecular cyclisation. The decarboxylation reaction affords the 4*H*-cyclopenta[1,2-b:5,4-b´]dithiophene (**C5**). Bisalkylation yields either 4,4-didodecyl-4*H*-cyclopenta[1,2-*b*:5,4-*b*']dithiophene (**C6**) or 4,4-bis(2-octyldodecyl)-4*H*-cyclopenta[1,2-

b:5,4-*b*']dithiophene (**C7**). **C6** is directly stannylated to 4,4-didodecyl-2,6-bis(trimethylstannyl)-4*H*-cyclopenta[1,2-*b*:5,4-*b*']dithiophene (**C8**) whereas **C7** is first brominated to afford 2,6-dibromo-4,4-bis(2-octyldodecyl)-4*H*-cyclopenta[1,2-*b*:5,4-*b*']dithiophene (**C9**). The reason for this will be explained later. The stannylation of **C9** results in 4,4-bis(2-octyldodecyl)-2,6-bis(trimethylstannyl)-4*H*-cyclopenta[1,2-*b*:5,4-*b*']dithiophene-2,6-diyl (**C10**) (Scheme 22).[67]

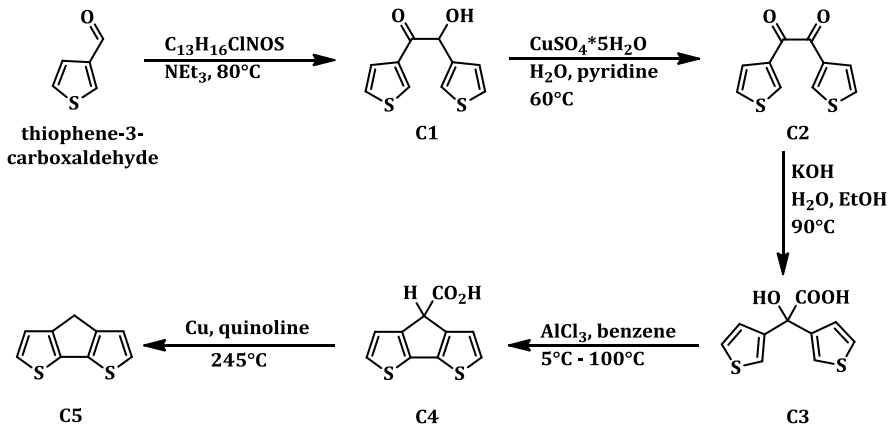

Scheme 23: Synthetic route to the CPDT core[68]

Scheme 23 shows a modified synthetic route by Asawapirom *et al.* which was used to synthesise the CPDT core.[68] The results of the NMR and mass analyses are in accordance to the proposed structures and presented in chapter 6.2.

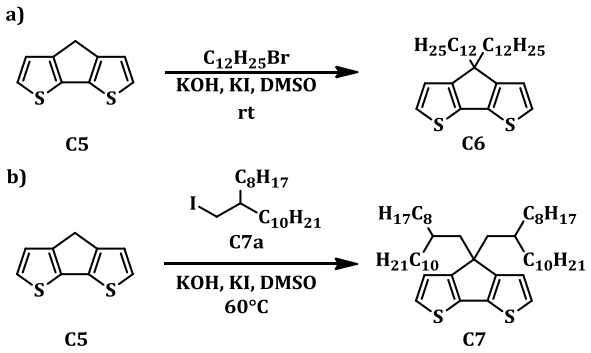

Scheme 24: Alkylation of CPDT; a: Using a bromide alkyl chain;[67] b: Using an iodide alkyl chain[69],[70]

The alkylation of the methylene bridge carbon was carried out by a nucleophilic substitution to receive **C6** (dodecyl) and **C7** (octyldodecyl). Due to the different steric requirements of the alkyl chains, the reaction conditions are slightly different as shown in Scheme 24. The linear 1-bromododecane shows a higher reactivity than the branched

9-(iodomethyl)nonadecane. To increase the reactivity of the branched alkyl group, the bromide was replaced by the corresponding iodide to establish a better leaving group. Moreover, the temperature and reaction time for the branched alkyl group was increased. **C6** was purified by column chromatography using hexane as eluent. The two doublet signals in the ^{1}H NMR spectrum at δ = 7.14 and 6.93 ppm are dedicated to the aromatic protons. In the ^{13}C NMR spectrum, the quaternary carbons are recorded at δ = 158.8, 137.0, and 53.3 ppm. Two tertiary proton signals are recorded at δ = 124.8 and 122.0 ppm. The remaining signals of the ^{1}H NMR and ^{13}C NMR spectra and the GC-MS analysis with an m/z = 515.4 correlates with the proposed structure. When introducing the branched alkyl chain, the solubility of the desired polymer ought to be increased. Due to the fact of higher solubility, the purification of **C7** needs to be done with a column chromatography on silica gel using hexane as eluent followed by RP18-silica gel flash chromatography using a solvent mixture of tetrahydrofuran and water. The ^{1}H NMR spectrum illustrates the two aromatic protons at δ = 7.03 and 6.85 ppm as doublet signals. In the ^{13}C NMR spectrum, the quaternary carbons show signals at δ = 157.9, 136.9, and 53.3 ppm, whereas the last one belongs to the bridged methylene carbon. The signals at δ = 124.3 and 122.7 ppm are dedicated to the two tertiary carbons. In addition, the signals of the aliphatic protons and carbons in the ^{1}H and ^{13}C NMR spectra are in accordance to the desired structure as well as the m/z = 739.3, measured by FD-MS.

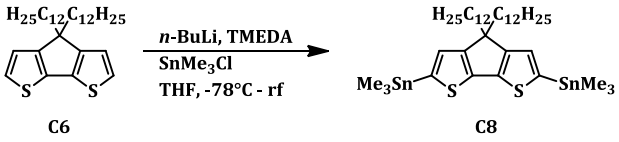

Scheme 25: Stannylation of the didodecyl-CPDT[71]

As mentioned before, the reactivity of the alkyl halides were different, the same hold for the resulting alkylated CPDT **C6** and **C7** when stannylated. While the stannylation of **C6** could be performed directly, the stannylation of **C7** needs an additional bromination step.

The double lithiation of **C6** was accomplished by *N,N,N',N'*-tetramethylmethanediamine as a complexation reactant to keep the intermediate Li-complex in solution (Scheme 25). After the transmetallation, the excess of trimethyltin chloride was removed, followed by column chromatography on deactivated aluminium

oxide, using hexane with 3% triethylamine as eluent. A mixture of 80.5% 4,4-didodecyl-2,6-bis(trimethylstannyl)-4*H*-cyclopenta[1,2-*b*:5,4-*b*']dithiophene (**C8**), 18% 4,4-didodecyl-2-(trimethylstannyl)-4*H*-cyclopenta[1,2-*b*:5,4-*b*']dithiophene and 1.5% 4,4-didodecyl-4*H*-cyclopenta[1,2-*b*:5,4-*b*']dithiophene (**C6**) was obtained. A further separation was not possible with the available instrumentations and chromatographic techniques. The ratio was calculated from the ^{1}H NMR spectrum and will be explained in chapter 6.2. The ratio of the three compounds is needed to calculate the stoichiometry ratio for the polymerisation reaction.

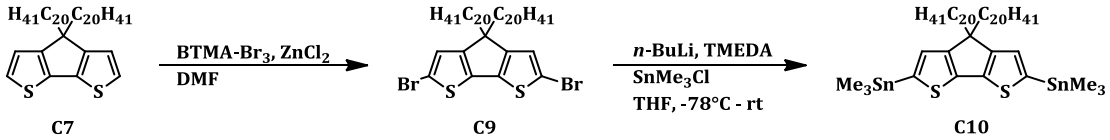

Scheme 26: Synthesis of the di-stannylated C10[72],[73]

First, the synthesis of 2,6-dibromo-4,4-bis(2-octyldodecyl)-4*H*-cyclopenta[1,2-*b*:5,4-*b*']dithiophene (**C9**) was carried out by a bromination reaction of CPDT **C7** with benzyltrimethylammonium tribromide for activating position two and six (Scheme 26). The aromatic protons are assigned to a singlet signal at δ = 6.88 ppm in the ^{1}H NMR spectrum. In the ^{13}C NMR spectrum, the bromo-substituted carbons show a signal at δ = 110.9 ppm. The remaining NMR signals and the m/z = 896.5, measured by APCI-MS, are as expected.

The stannylation reaction of **C9** leads to the monomer **C10** and was performed with four equivalents of *n*-butyl lithium and trimethyltin chloride (Scheme 26). In the ^{1}H NMR spectrum, the singlet signal of the aromatic protons shows a downshift to δ = 6.94 ppm compared to the precursor **C9**. The stannylated carbons show a signal at δ = 142.8 ppm in the ^{13}C NMR spectrum. In the ^{119}Sn NMR spectrum, a signal for tin is recorded at δ = -28.5 ppm. An m/z = 1064.8 was measured by FD-MS and is another proof of the successful synthesis.

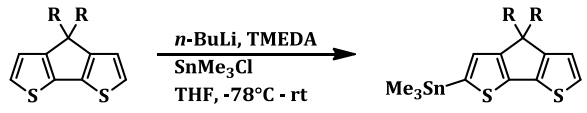

Scheme 27: Synthesis of the mono-stannylated C11 and C12[74]

For the synthesis of the model compounds, 4,4-didodecyl-2-(trimethylstannyl)-4*H*-cyclopenta[1,2-*b*:5,4-*b*']dithiophene (**C11**) and 4,4-bis(2-octyldodecyl)-2-(trimethylstannyl)-4*H*-cyclopenta[1,2-*b*:5,4-*b*']dithiophene (**C12**) were needed. Scheme 27 shows the reaction to the mono-stannylated **C11** and **C12**. In general it is to mention, that *n*-butyl lithium and trimethyltin chloride has to be added slowly in an exact stoichiometry ratio to avoid di-stannylation. Because of the high acid sensitivity, the purification should be restricted to removal of organic by-products by vacuum distillation at 80°C. The results of the NMR and mass analyses are in accordance to the proposed structures **C11** and **C12** and are comparable. Hence, just the analysis of **C12** will be discussed. The FD-MS affords an m/z = 901.7, as expected. In the ^{1}H NMR spectrum, the three aromatic protons are showing a doublet, singlet, and doublet signal at δ = 7.08, 6.98, and 6.93 ppm. The tin-substituted carbon is recorded at δ = 142.6 ppm in the ^{13}C NMR spectrum.

2.2. Model Compounds and Polymers Containing the Indigo Building Block

2.2.1. Synthesis of the CPDT Model Compound

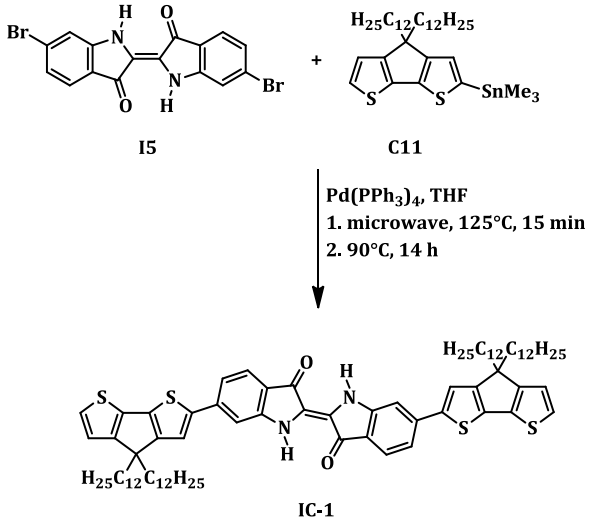

Scheme 28: Synthesis of (*E*)-6,6'-bis(4,4-didodecyl-4*H*-cyclopenta[1,2-*b*:5,4-*b*']dithiophen-2-yl)-[2,2'-biindolinylidene]-3,3'-dione (IC-1)

Scheme 28 shows the Stille cross-coupling of dibromoindigo **I5** and mono-stannylated **C11** with tetrakis(triphenylphosphane)palladium(0) as catalyst. The

microwave assisted cross-coupling reaction, following the literature,[75,76] was performed in tetrahydrofuran at 125°C for 15 minutes, followed by stirring at 90°C for further 14 hours. After an aqueous workup multiple column chromatographies afforded the blue (*E*)-6,6'-bis(4,4-didodecyl-4*H*-cyclopenta[1,2-*b*:5,4-*b*']dithiophen-2-yl)-[2,2'-biindolinylidene]-3,3'-dione (**IC-1**). The model compound **IC-1** was characterised by MALDI-MS, IR, and NMR spectroscopy and was used to investigate the photophysical properties of indigo-CPDT compounds. The m/z = 1288.4 is in accordance to the proposed structure. Figure 16 (top) shows the recorded ^{1}H NMR spectrum of the model compound **IC-1**. The broad singlet signal at δ = 9.07 ppm demonstrates the presence of the amine protons of the indigo unit. Three doublet signals are recorded at δ = 7.60, 7.17, and 6.90 ppm. The expected fourth doublet signal is overlapped by a singlet signal and shows a multiplet signal between δ = 7.12-7.10 ppm, whereas that multiplet contains phenyl protons of the indigo core and protons of the CPDT core. Due to the coupling constants of 4.8 Hz the doublet signals at δ = 7.17 and 6.90 ppm are dedicated to the thiophene rings. Therefore, the doublet signal at δ = 7.60 ppm represents phenyl protons adjacent to further phenyl protons of the indigo core. The singlet signal at δ = 7.28 ppm is dedicated to phenyl protons of the indigo core. A multiplet signal between δ = 1.79-1.77 ppm represents the eight protons of the methylene groups adjacent to the methylene bridge carbons. The methyl groups show a triplet signal at δ = 0.78 ppm. Two multiplet signals between δ = 1.20-1.09 and 0.95-0.93 ppm are dedicated to the remaining methylene protons.

The ^{13}C NMR spectrum of **IC-1** is shown at the bottom of Figure 16. The carbonyl carbons show a signal at δ = 187.1 ppm, comparable to the carbonyl carbons of dibromoindigo **I5** in the solid state NMR (Figure 13). Six tertiary carbons are detected by DEPT spectrum (δ = 126.9, 125.3, 122.2, 120.5, 118.0, and 107.6 ppm). The remaining peaks between δ = 159.6 and 118.5 ppm are quaternary carbons and are in accordance to the proposed structure. Further quaternary carbons are recorded at δ = 54.1 ppm and represent the methylene bridges of the CPDT core. The remaining methylene carbons are recorded between δ = 37.8 and 23.0 ppm. A signal at δ = 14.5 ppm is dedicated to the carbons of the methyl groups.

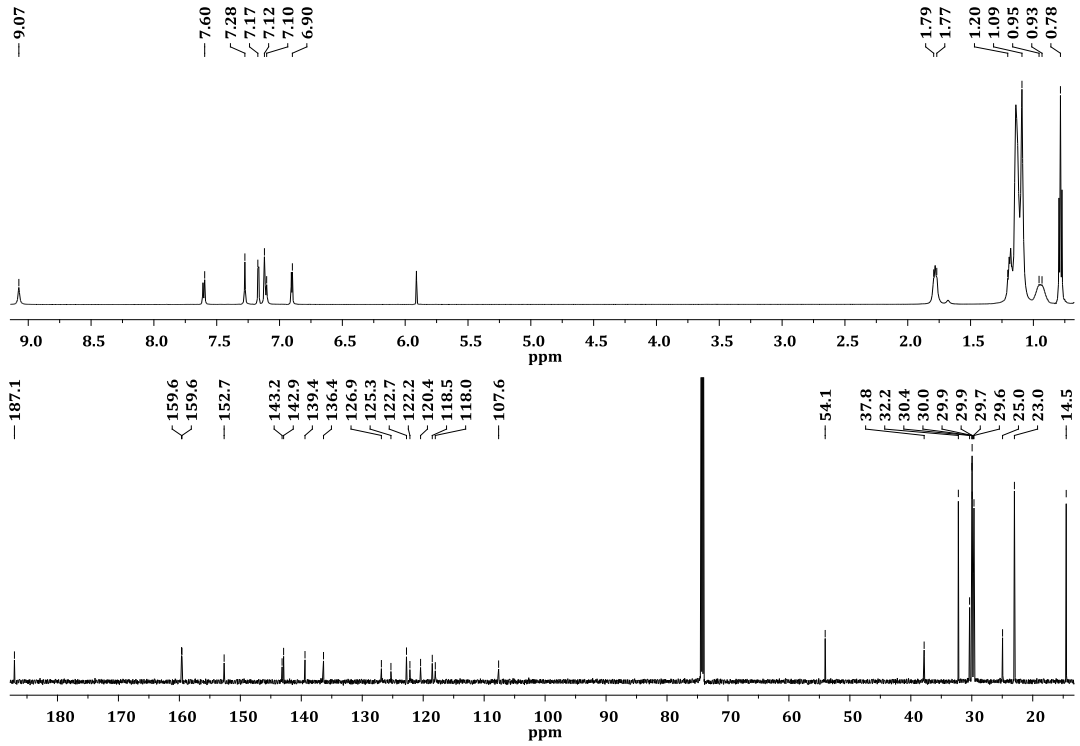

Figure 16 top: ^{1}H NMR spectrum of model compound IC-1; bottom: ^{13}C NMR of model compound IC-1; in $C_2D_2Cl_4$ (5.91 and 74.2 ppm)

In the IR spectrum (Figure 17) the N-H stretching vibrations of the model compound are shifted to 3289 cm^{-1} compared to the N-H stretching vibrations of dibromoindigo **I5** at υ = 3381 cm^{-1} which proofs the conversion into model compound **IC-1**.

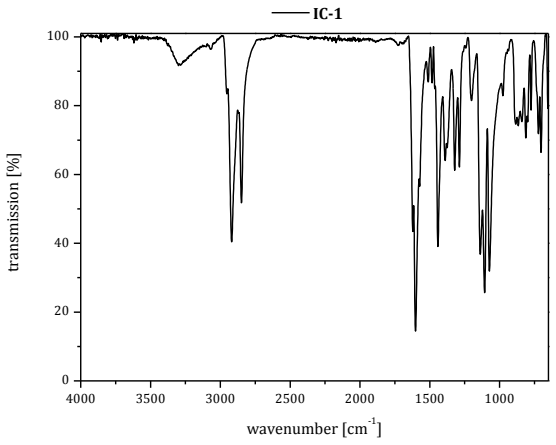

Figure 17: IR spectrum of the CPDT model compound IC-1

2.2.2. Synthesis of the Fluorene Model Compound

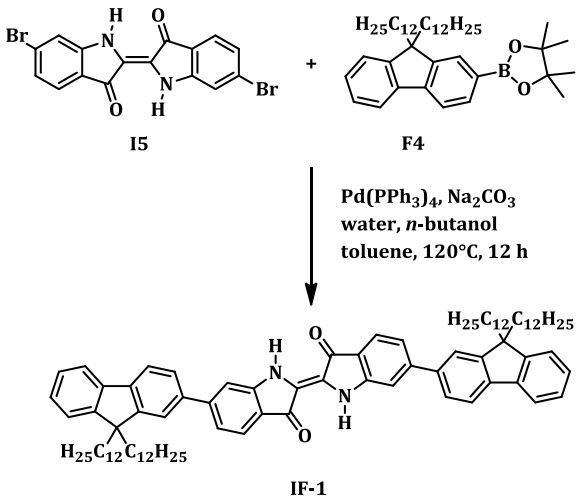

Scheme 29: Synthesis of (*E*)-6,6'-bis(9,9-didodecyl-9*H*-fluoren-2-yl)-[2,2'-biindolinylidene]-3,3'-dione (IF-1)

The Suzuki cross-coupling of dibromoindigo **I5** and the mono-dioxaborolane **F4** was catalysed by tetrakis(triphenylphosphane)palladium(0) in a two phase solvent system and a base, following the literature (Scheme 29).[77] An aqueous workup afforded the crude green (*E*)-6,6'-bis(9,9-didodecyl-9*H*-fluoren-2-yl)-[2,2'-biindolinylidene]-3,3'-dione (**IF-1**), which was purified by multiple silica column chromatographies. The expected m/z = 1262.6 was measured by MALDI-MS. In the ^{1}H NMR spectrum, (Figure 18) the amine protons show a broad singlet signal at δ = 8.97 ppm. The signals of the aromatic protons are recorded as four multiplet signals between δ = 7.76 and 7.25 ppm. The multiplet signal between δ = 1.95-1.92 ppm represents the methylene groups adjacent to the bridging carbon. The remaining 92 protons show multiplet signals according to the proposed structure. In the ^{13}C NMR spectrum, the carbonyl carbons show a signal at δ = 188.0 ppm. The remaining nine quaternary carbons are recorded at δ = 152.5, 151.6, 151.2, 149.9, 142.0, 140.4, 138.8, 132.5, and 118.9 ppm. The signals between δ = 130.9-110.5 ppm represent the aromatic tertiary carbons. A signal at δ = 55.3 ppm is dedicated to the methylene bridged carbons. The methylene carbons of the dodecyl groups show a signal between δ = 40.4-23.0 ppm. The signal at δ = 14.1 ppm represents the methyl groups.

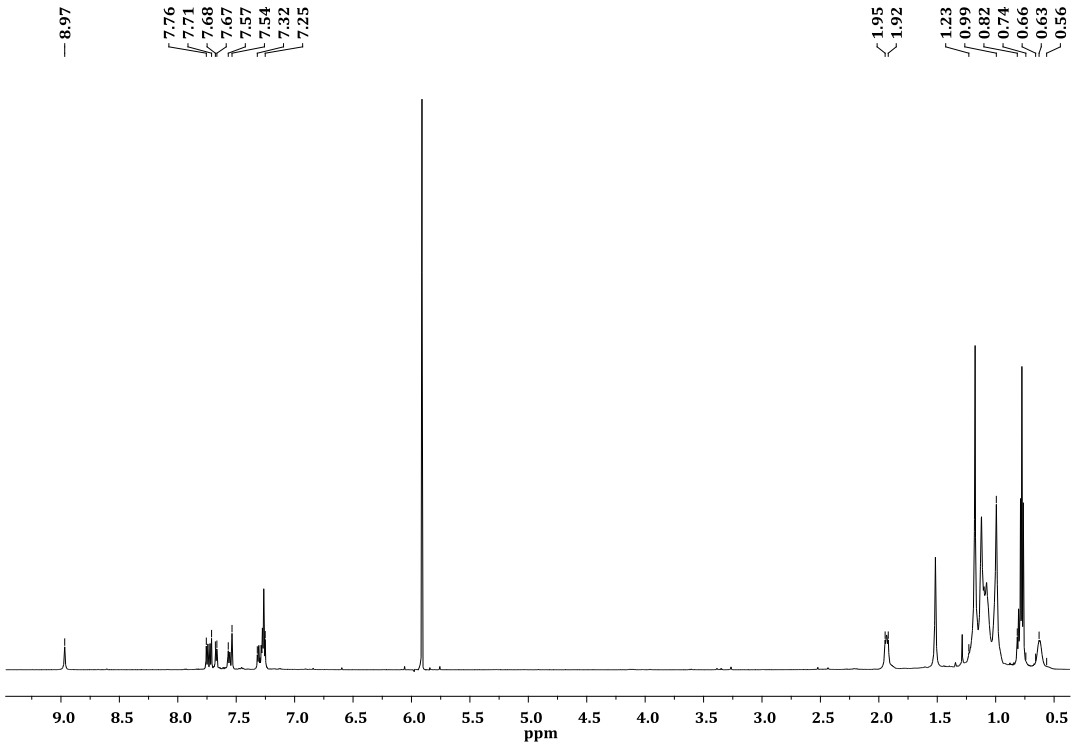

Figure 18: ^{1}H NMR of model compound IF-1; in $C_2D_2Cl_4$ (5.91 ppm)

Figure 19 shows the IR spectrum of **IF-1**. This spectrum is another evidence of the successful reaction. The N-H stretching vibrations are shifted to υ = 3285 cm^{-1} compared to the N-H stretching vibrations of dibromoindigo **I5** (υ = 3381 cm^{-1}). The C-H and CH_3 stretching vibrations are recorded between υ = 2955-2850 cm^{-1}.

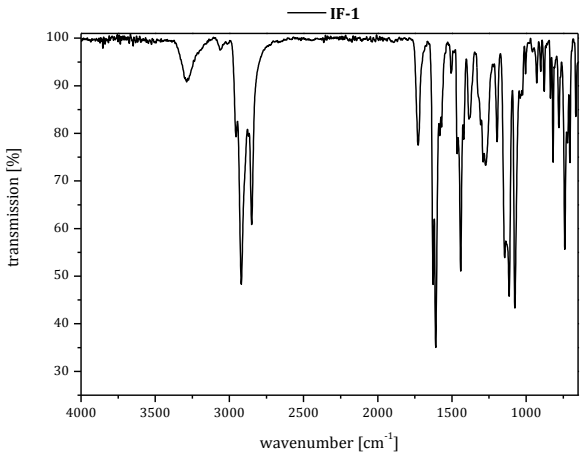

Figure 19: IR spectrum of the fluorene model compound IF-1

2.2.3. Synthesis of Indigo-CPDT and Indigo-Bithiophene Polymers

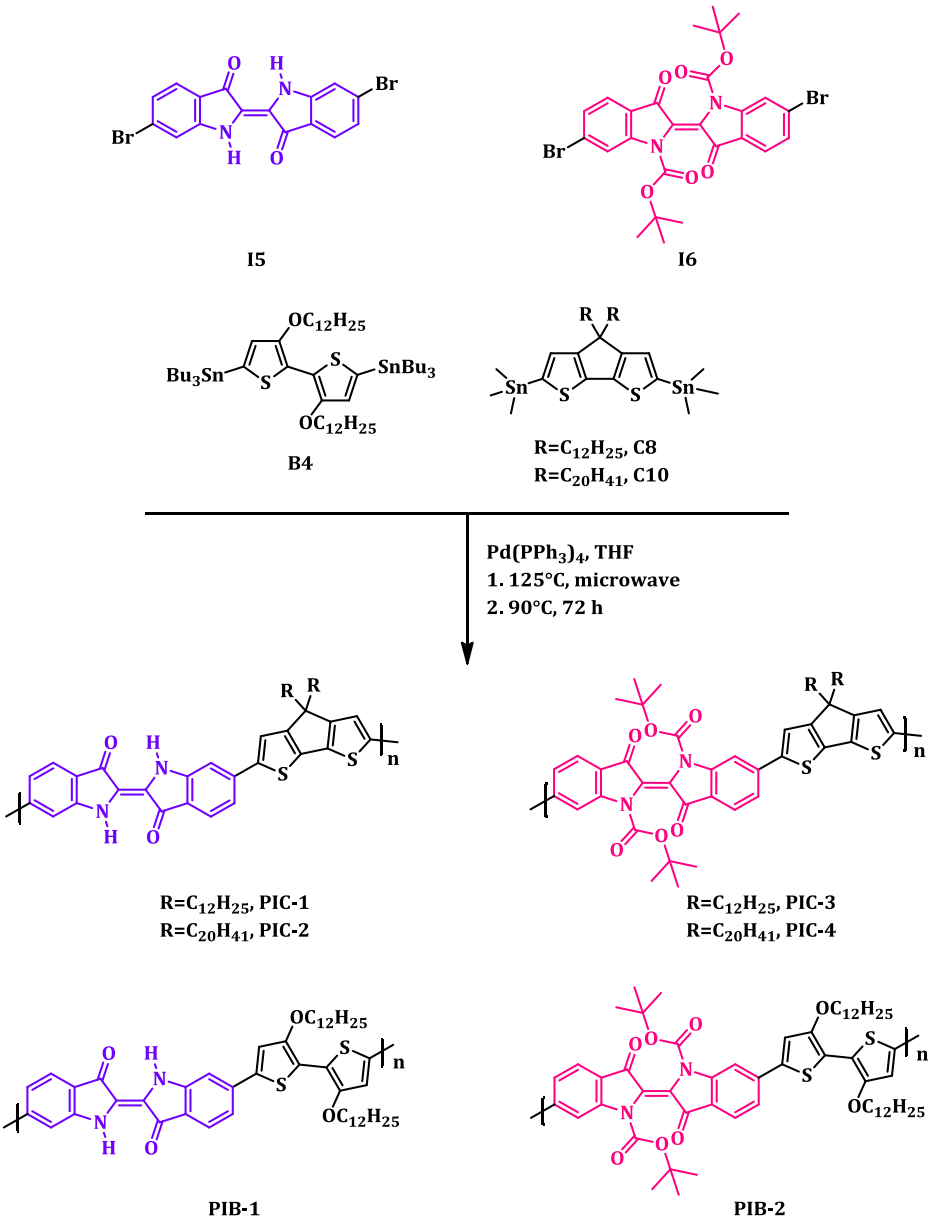

Scheme 30: Overview of the polymers synthesised by Stille cross-coupling

The reaction between stannyl-functionalised bithiophene **B4**, CPDT **C8**, and **C10** was carried out with dibromoindigo **I5** or boc-substituted dibromoindigo **I6** (Scheme 30). Tetrakis(triphenylphosphane)palladium(0) is known to be sensitive against oxygen, therefore the monomers and catalyst were handled under inert conditions.[78] Tetrahydrofuran was added and the reaction was carried out at 125°C in a microwave reactor to initiate the polymer formation. Due to the limited solubility of indigo derivatives, the reaction mixture was stirred for further 72 hours at 90°C. **PIC-1** was

extracted with hydrochloric acid before it was precipitated into cold methanol. The polymers **PIC-2**, **PIC-3**, **PIC-4**, **PIB-1**, and **PIB-2** were directly precipitated into cold methanol.

2.2.4. Synthesis of Indigo-Fluorene Polymers

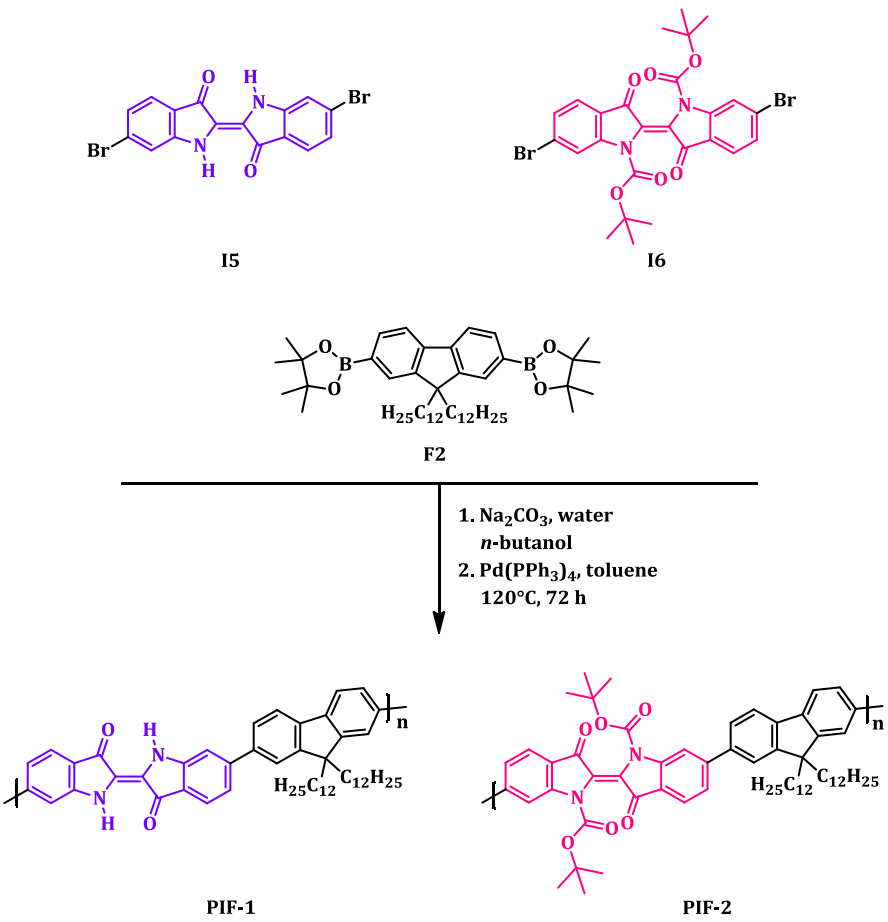

Scheme 31: Overview of the polymers synthesised by Suzuki cross-coupling

The Suzuki cross-coupling reactions of the fluorene-based dioxaboralane **F2** with either dibromoindigo **I5** or boc-substituted dibromoindigo **I6** were catalysed by tetrakis(triphenylphosphane)palladium(0) (Scheme 31). The monomers and base were diluted in water and *n*-butanol. The catalyst was dissolved in toluene and transferred into the monomer solution. The reaction was carried out at 120°C for three days. After an aqueous workup, the polymer solution was treated with sodium diethyldithiocarbamate solution to remove the catalyst. The precipitated polymer was extracted by Soxhlet.

2.2.5. Characterisation of Indigo-CPDT Polymers

Figure 20 shows the NMR spectra of the CPDT-containing polymers in which the signals are broadened as known from polymer NMR spectra.[79,80] The signals at δ = 8.9 ppm are representing the amine protons (green highlighted) of the polymers **PIC-1** and **PIC-2**. The peak shapes and shifts are comparable among the secondary amine polymers (**PIC-1** and **PIC-2**) and among the boc-substituted polymers (**PIC-3** and **PIC-4**). The protons of the methyl groups of the boc-protecting groups (blue highlighted) are recorded at δ = 1.6 ppm.

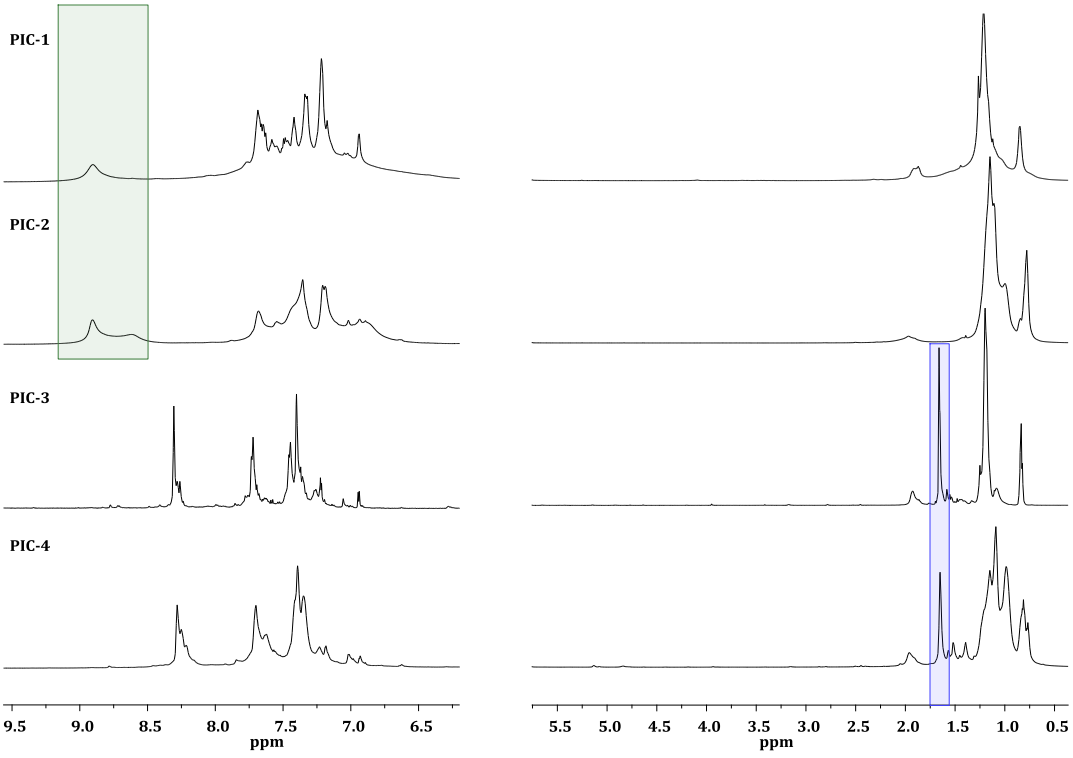

Figure 20: ^{1}H NMR spectra of indigo-CPDT polymers recorded in $C_2D_2Cl_4$ (5.91 ppm); left: Magnified section of the aromatic region, amine protons green highlighted; right: Aliphatic region, methyl groups of the boc-protecting groups blue highlighted

The IR spectra of **PIC-1** and **PIC-2** respectively **PIC-3** and **PIC-4** are comparable. Hence, the IR spectra of **PIC-1** and **PIC-3** will be discussed exemplarily. Figure 21 depicts the overlaid IR spectra. The structural varieties are illustrated in the N-H vibration band of **PIC-1** at υ = 3294 cm^{-1}. Clearly, this vibration band is not observed for **PIC-3**. The characteristic group of **PIC-3** is the boc-protecting group which shows the C=O vibration band of the ester at υ = 1716 cm^{-1}.

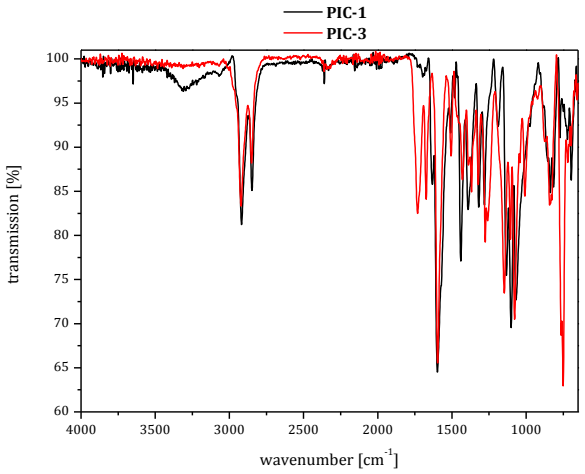

Figure 21: IR spectra of PIC-1 and PIC-3

Table 2 lists the GPC measurements of the indigo-CPDT polymers after Soxhlet extraction. Polymer **PIC-2** seems to undergo decomposition after a short period of time which is observed by the change of colour from blue to red (discussion by absorption spectra in chapter 2.3).

As already described, polymer **PIC-1** is slightly soluble in common organic solvents. This is reflected in the low number-average molecular weight (M_n), which corresponds to only 9-10 repeating units. Hence, the short chains already precipitate and are no longer available for the polymerisation.[81] The high polydispersity (M_w/M_n) could indicate two phenomena, either adsorption during GPC measurement or polymer-polymer interactions due to the hydrogen bonding-capacity of the indigo unit. **PIC-2** contains longer alkyl chains and shows, therefore, a better solubility. The number-average molecular weight for the methylene chloride fraction is 15,100 g/mol and is twice as high as for **PIC-1**. As expected, the chloroform fraction demonstrates higher molecular weights. The more polar boc-substituted polymers **PIC-3** and **PIC-4** tend to have higher polydispersities. The ethyl acetate fraction of **PIC-3** constitutes an exception with the lowest polydispersity of 1.36 for the indigo-CPDT polymers.

Table 2: GPC results measured in tetrahydrofuran; * measured in trichlorobenzene

	fraction	M_n [g/mol]	M_w [g/mol]	M_w/M_n	yield [%]
PIC-1	DCM*	7,400	49,400	6.68	48.1
PIC-2	DCM	15,100	44,800	2.97	41.3
	$CHCl_3$	29,000	120,000	4.13	3.8
PIC-3	EE	10,100	13,800	1.36	26.1
	$CHCl_3$	18,900	167,000	8.85	0.4
PIC-4	EE	10,200	31,500	3.10	61.5

2.2.6. Characterisation of Indigo-Bithiophene Polymers

Figure 22 shows the ^{1}H NMR spectra of the bithiophene unit (**B3**) and the polymer **PIB-2**. The triplet signal of the OCH_2-groups (green highlighted) of the bithiophene unit (**B3**) at $\delta = 4.10$ ppm is a multiplet signal in the polymer spectrum. A singlet signal at $\delta = 1.51$ ppm represents the methyl groups of the boc-protecting groups (blue highlighted) of **PIB-2**.

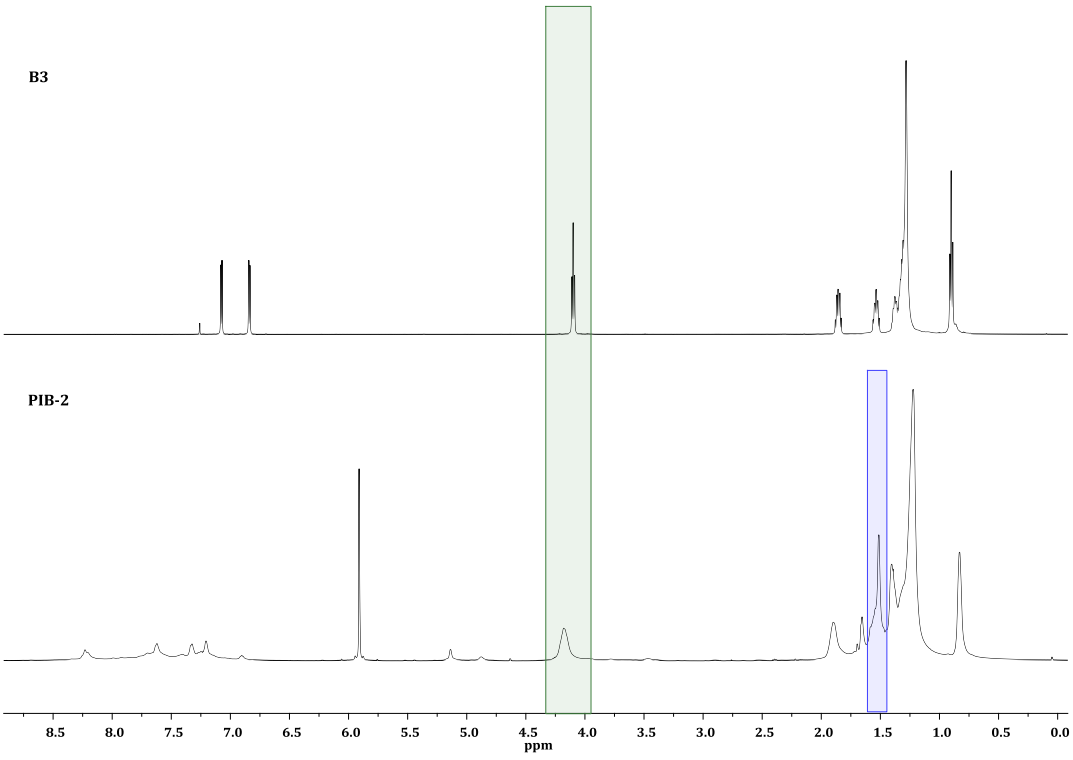

Figure 22: ^{1}H NMR spectra of B3 (top), recorded in $CDCl_3$ (7.26 ppm), and PIB-2 (bottom), recorded in $C_2D_2Cl_4$ (5.91 ppm), ether methylene groups green highlighted, methyl groups of the boc-protecting groups blue highlighted

Figure 23 depicts the overlaid IR spectra of **PIB-1** and **PIB-2**. The aromatic C-H and aliphatic CH_3 stretching vibrations for both polymers are recorded between υ = 2920-2850 cm^{-1}. The N-H stretching vibrations of **PIB-1** show a band at υ = 3280 cm^{-1}. These vibrations are not recorded for the boc-substituted polymer **PIB-2**. The vibration band at υ = 1714 cm^{-1} corresponds to the C=O vibrations of the boc-protecting groups of **PIB-2**.

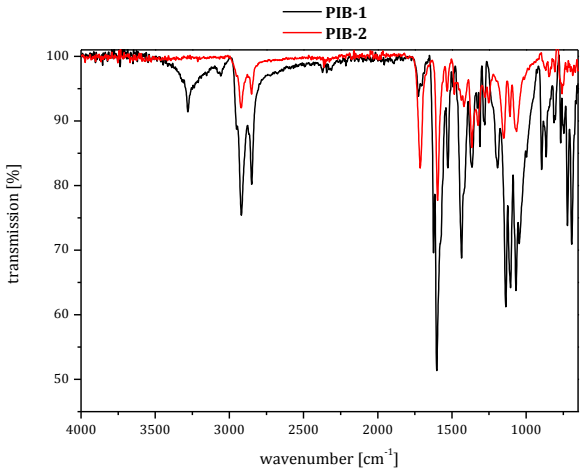

Figure 23: IR spectra of PIB-1 and PIB-2

Table 3 shows the GPC results of the indigo-bithiophene polymers. **PIB-1** is almost insoluble, even in trichlorobenzene at high temperature. The low number-average molecular weight of the trichlorobenzene fraction is 1,800 g/mol. Bao *et al.* described in 1995 a difference between dialkyl and dialkoxy phenylene monomers. They discovered that dialkyl-substituted phenylene monomers when coupled with thiophene or phenylene components result in higher molecular weight polymers, if compared to coupling with corresponding dialkoxy monomers.[82] This could be one reason for the low number-average molecular weight for **PIB-1**. The number-average molecular weight of **PIB-2** has a value of 11,600 g/mol (chloroform fraction). As mentioned before, the boc-substituted polymers showed higher polydispersities. The molecular weights for the chloroform and tetrahydrofuran fractions are comparable.

Table 3: GPC results measured in tetrahydrofuran; * measured in trichlorobenzene

	fraction	M_n [g/mol]	M_w [g/mol]	M_w/M_n	yield [%]
PIB-1	$CHCl_3$	4,300	97,900	22.82	1.7
	TCB*	1,800	3,200	1.78	27.8
PIB-2	$CHCl_3$	11,600	134,000	11.56	9.1
	THF	11,500	169,000	14.74	28.4

2.2.7. Characterisation of Indigo-Fluorene Polymers

Figure 24 depicts the ^{1}H NMR spectra of the two indigo-fluorene polymers. Both spectra show a broad signal at δ = 8.98 ppm (red highlighted), which results from the amine protons. This implies that during the Suzuki cross-coupling 5% of the boc-protecting groups were cleaved. The remaining methyl protons of the boc-protecting groups are recorded between δ = 1.66-1.42 ppm for polymer **PIF-2** (green highlighted).

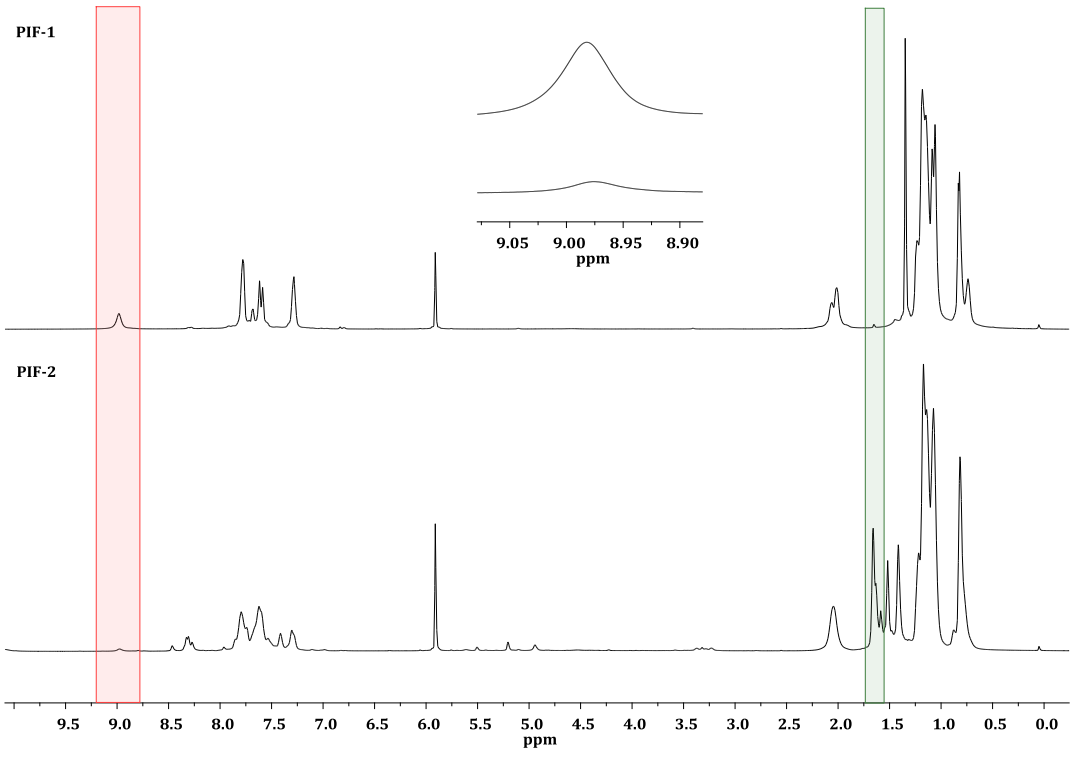

Figure 24: ^{1}H NMR spectra of PIF-1 (top) and PIF-2 (bottom) recorded in $C_2D_2Cl_4$ (5.91 ppm), amine protons red highlighted, methyl groups of the boc-protecting groups green highlighted

The cleavage of the boc-protecting group during the polymerisation can also be seen in the IR spectrum. Figure 25 depicts the overlaid IR spectra of the indigo-fluorene

polymers. The N-H stretching vibration band is detected for both polymers at υ = 3293 cm^{-1}. The stretching vibrations of the C=O of the boc-protecting groups are recorded at υ = 1717 cm^{-1}, which proves that **PIF-2** is a boc-protected polymer.

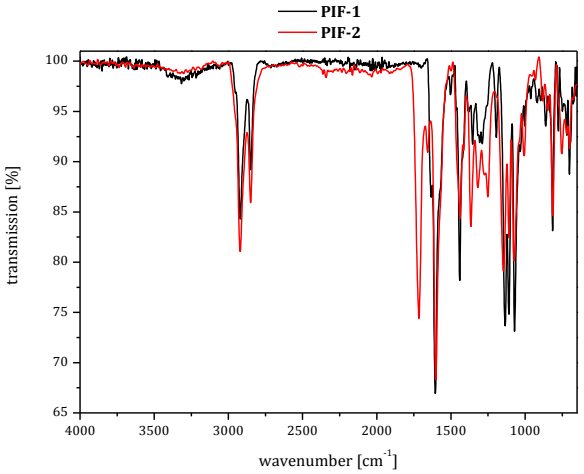

Figure 25: IR spectra of PIF-1 and PIF-2

Table 4 shows the GPC results of the indigo-fluorene polymers **PIF-1** and **PIF-2**. The limited solubility is a reason for the low molecular weights of the **PIF-1** fractions. The better soluble boc-substituted polymer **PIF-2** shows moderate molecular weights. A lower polydispersity for the boc-substituted polymer fractions is observed, if compared to the indigo-CPDT polymers **PIC-3** and **PIC-4**.

Table 4: GPC results measured in tetrahydrofuran

	fraction	M_n [g/mol]	M_w [g/mol]	M_w/M_n	yield [%]
PIF-1	DCM	5,000	6,000	1.21	13.1
	$CHCl_3$	7,200	8,900	1.23	4.0
PIF-2	EE	5,200	11,100	2.12	44.1
	DCM	5,700	23,000	4.06	1.6

2.3. Optical Properties

2.3.1. Absorption Properties

Table 5 summarises the absorption bands of the indigo-CPDT polymers. Figure 26 depicts the absorption spectra. The absorption maxima of **PIC-1** are observed at 658 nm in solution and at 662 nm as thin film in the solid state. A hypsochromic shift for **PIC-2** of

10 nm from solution to thin film is observed and the maximum is recorded at 673 nm in solution. The high energy bands for solution and thin film are located at 389 nm (**PIC-1**) and 404 nm (**PIC-2**). All absorption bands of the boc-substituted polymers (**PIC-3** and **PIC-4**) are distinctly blue-shifted. When comparing the solution and thin film spectra, the high energy band is blue-shifted up to 13 nm (**PIC-3**), the low energy band is shifted up to 9 nm (**PIC-4**). The absorption maxima in solution are observed at 590 nm (**PIC-3**) and 591 nm (**PIC-4**). The thin film absorption maxima are recorded at 585 nm (**PIC-3**) and 582 nm (**PIC-4**). Hence, more energy is needed to excite the boc-substituted polymers.

Table 5: Absorption maxima of PIC-1, PIC-2, PIC-3, and PIC-4 in chloroform and as thin films in the solid state; the underlined values are the most intense absorption maxima

	fraction	λ_{abs} [nm] solution	λ_{abs} [nm] thin film
PIC-1	$CHCl_3$	398, <u>658</u>	389, <u>662</u>
PIC-2	EE	398, <u>673</u>	404, <u>663</u>
PIC-3	$CHCl_3$	456, <u>590</u>	443, <u>585</u>
PIC-4	EE	457, <u>591</u>	454, <u>582</u>

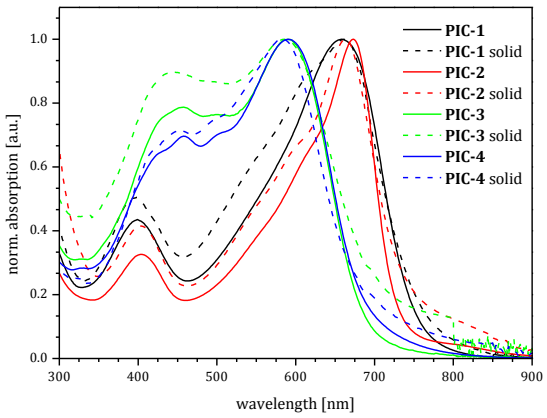

Figure 26: Absorption spectra of the indigo-CPDT polymers measured in chloroform and as thin films

As already mentioned, polymer **PIC-2** changes its absorption spectra, possibly by decomposition, which is not observed for polymer **PIC-1**. Simultaneously, the absorption band of **PIC-1** is broader than for polymer **PIC-2**, possibly related to aggregation processes. **PIC-2** is assumed to be fully soluble (Figure 27).

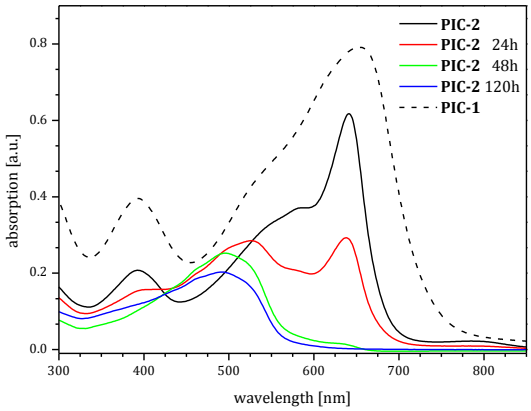

Figure 27: Time-dependent change of the absorption spectrum of PIC-2 in toluene, and of PIC-1 in toluene as reference

Figure 28 shows the absorption spectra of the polymers **PIB-1** and **PIB-2** and Table 6 summarises the absorption maxima measured in tetrahydrofuran and as thin films in the solid state. The solution spectrum of **PIB-1** in tetrahydrofuran shows a broad absorption over a long wavelength range with a maximum at 644 nm. **PIB-2** shows absorption at 482 nm for the chloroform fraction and at 486 nm for the tetrahydrofuran fraction. As thin films, both fractions show absorption maxima at 504 nm.

Table 6: Absorption maxima of the indigo-bithiophene polymers in tetrahydrofuran and as thin films

	fraction	λ_{abs} [nm] solution	λ_{abs} [nm] thin film
PIB-1	$CHCl_3$	644	n/s
PIB-2	$CHCl_3$	482	504
	THF	486	504

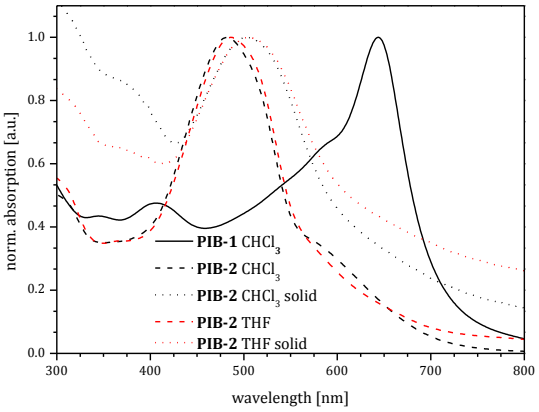

Figure 28: Absorption spectra of indigo-bithiophene polymers measured in tetrahydrofuran and as thin films

Figure 29 shows the absorption spectra of **PIF-1** and **PIF-2** measured in chloroform and as thin films. The results are summarised in Table 7. The absorption maximum of **PIF-1** in solution is at 333 nm and as thin film at 335 nm. A second band is recorded at 444 nm in solution and 447 nm as thin film. This will be discussed later in this chapter. **PIF-2** shows an absorption band at 572 nm in solution and at 569 nm as thin film. Compared with **PIF-1**, the absorption band of **PIF-2** is red-shifted. A shoulder at 434 nm is recorded for **PIF-2** in solution and as thin film.

Table 7: Absorption maxima of PIF-1 and PIF-2 in chloroform and as thin films; the underlined values are the most intense absorption maxima

	fraction	λ_{abs} [nm] solution	λ_{abs} [nm] thin film
PIF-1	DCM	<u>333</u>, 444, 614	<u>335</u>, 447, 632
PIF-2	DCM	<u>362</u>, 434, 572	<u>362</u>, 434, 569

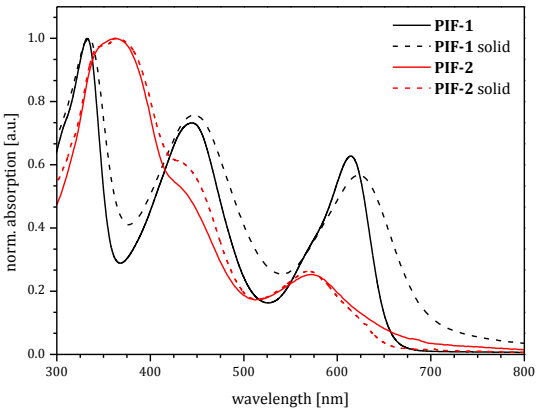

Figure 29: Absorption spectra of PIF-1 and PIF-2 measured in chloroform and as thin films

In summary, the excitation into the first excited state needs less energy for the indigo-CPDT polymers than for the indigo-bithiophene polymers and indigo-fluorene polymers. Moreover, the boc-substituted polymers show higher energy absorption bands, if compared to the unprotected analogues.

2.3.2. Molar Extinction Coefficient

Table 8 presents the molar extinction coefficients of the indigo-containing polymers, except **PIB-1** due to its limited solubility in chloroform. James *et al.* synthesised copolymers composed of dithieno-benzoisoindigo units and thiophene or bithiophene units, respectively. The extinction coefficient of the thiophene copolymer was reported as 49.3 L/g*cm and 37.7 L/g*cm for the dithiophene copolymer.[83] All of our unprotected indigopolymers, excluding **PIC-2**, also show extinction coefficients in this range. The boc-substituted indigopolymers display lower extinction coefficients. This means, that less amount of unprotected indigopolymer (**PIC-1**, **PIC-2**, **PIF-1**) is needed, if compared to the boc-substituted indigopolymers (**PIC-3**, **PIC-4**, **PIF-2**), to observe the same absorption values (colour intensity).

Table 8: Molar extinction coefficients measured in chloroform

	molar extinction coefficient [L/mol*cm]	extinction coefficient [L/g*cm]
PIC-1	35554.9	45.9
PIC-2	63142.3	63.2
PIC-3	42171.2	43.2
PIC-4	34655.2	28.9
PIB-1	n/s	n/s
PIB-2	27431.4	27.6
PIF-1	35604.3	46.7
PIF-2	37980.8	39.4

2.3.3. Photophysical Properties of PIC-1 and PIF-1

The experiments in this chapter were carried out in cooperation with the Universidade de Coimbra, Portugal.[b] To understand the photophysical properties of the polymers **PIF-1** and **PIC-1** so-called model compounds **IF-1** and **IC-1** were included into the investigations. Figures 30 and 31 show the absorption spectra of fluorene- and CPDT-containing compounds and indigo. The results show the low absorption energy band at 617 nm (**PIF-1** and **IF-1**) or 642 nm (**PIC-1**) and at 620 nm (**IC-1**), which are characteristic for the indigo chromophore (H-chromophore). These bands are red-shifted up to 41 nm in comparison to the indigo absorption band at 601 nm. This bathochromic shift is caused by conjugation with the attached aromatic units in the polymers and model compounds, respectively. The higher energy band at 330 nm (**PIF-1** and **IF-1**) or 372 nm (**IC-1**) and 393 nm (**PIC-1**) are dedicated to either the fluorene or CPDT units. Both polymers are showing an "in-between" band/shoulder at 410-431 nm (**IF-1**/**PIF-1**) or 517-550 nm (**IC-1**/**PIC-1**) which are assigned to charge-transfer transition.[84]

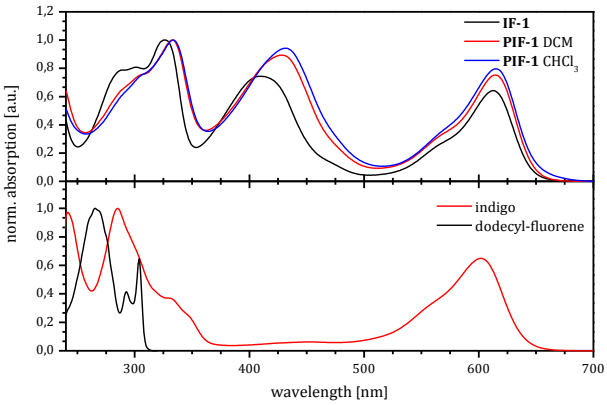

Figure 30: Absorption spectra of PIF-1 (methylene chloride and chloroform fraction), IF-1 (top); indigo and didodecylfluorene (bottom) measured in dioxane

[b] The research leading to the results of **PIF-1** have received funding from Laserlab-Europe and were investigated by myself and PhD João Pina. **PIC-1** was analysed by PhD João Pina, co-worker in the group of Professor J. Sérgio Seixas de Melo.

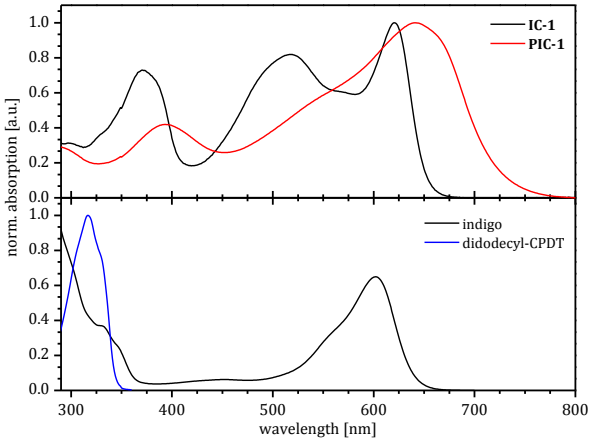

Figure 31: Absorption spectra of PIC-1 (methylene chloride fraction) and IC-1 measured in toluene (top); indigo and didodecyl-CPDT (bottom) measured in dioxane

The fluorescence emission spectra of the fluorene-containing compounds and the CPDT-containing compounds are depicted in Figures 32 and 33. The measurements of **IF-1** and **PIF-1** were carried out in dioxane, those of **IC-1** and **PIC-1** in toluene. The fluorescence emission spectra are pointing out the occurrence of energy transfer across the conjugated indigo-CPDT or indigo-fluorene units. If the model compounds and polymers are excited at the wavelength of the "in-between" band, the fluorescence emissions occur at 645 nm (fluorene compounds) and between 650-656 nm (CPDT compounds), similar to the fluorescence emission of indigo (maximum at 645 nm). The emission at higher energy is caused either by fluorene or by CPDT units.[84]

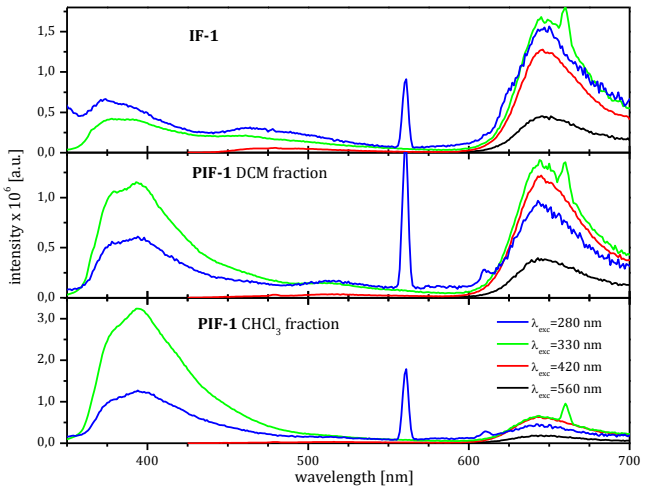

Figure 32: Fluorescence emission spectra of PIF-1 (methylene chloride and chloroform fraction) and IF-1 in dioxane excited at different wavelengths; the sharp peaks at 560 nm (blue line) and 660 nm (green line) result from frequency doubling of the excitation wavelength

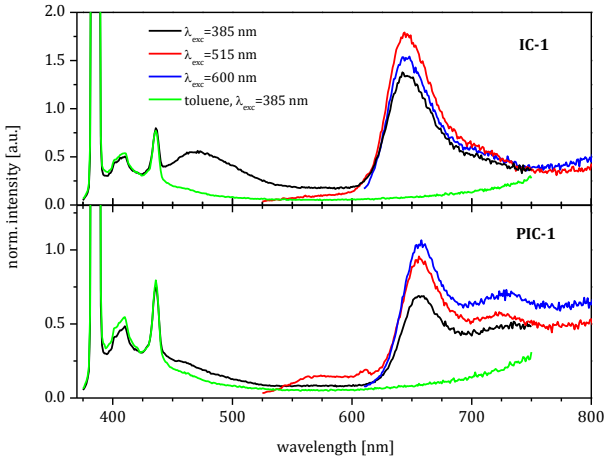

Figure 33: Fluorescence emission spectra of PIC-1 (methylene chloride fraction) and IC-1 in toluene excited at different wavelengths; the spectrum of pure toluene was measured for comparison

Indigo has a fluorescence lifetime of 0.14 ns measured in dimethylformamide.[22] This value is comparable to the fluorescence life time values for the fluorene-containing polymer fractions and the model compound (Table 9). The decay was measured in the emission band of the indigo unit and under excitation into the higher energy band. The results show that the fluorescence decays for the CPDT-containing polymers are faster than for the fluorene-containing polymers. The decays have a value of ca. 0.05 ns for **IC-1** and **PIC-1**.[84]

Table 9: Fluorescence emission decay values (monoexponential decay); fluorene compounds measured in dioxane and CPDT compounds measured in toluene

	fraction	λ_{exc} [nm]	λ_{em} [nm]	τ [ns]
IF-1	--	391	650	0.16
PIF-1	DCM	391	650	0.17
PIF-1	$CHCl_3$	391	650	0.13
IC-1	--	385	620	0.05
PIC-1	$CHCl_3$	385	640	0.07

The phosphorescence emissions of the fluorene-containing compounds were measured in frozen methylcylohexane and are shown in Figure 34. Fluorene-based compounds are known to show phosphorescence emission in contrast to indigo due to efficient deactivation.[22,39,85,86] The phosphorescence emission of **PIF-1** and **IF-1** occurs around 436-493 nm and is related to the fluorene units. Hereby, the spectra of

didodecylfluorene, **IF-1**, as well as the methylene chloride fraction of **PIF-1** are showing vibronic fine-structures. Phosphorescence emission was not recorded for the model compound **IC-1** and the polymer **PIC-1**. However, CPDT and alkylated CPDTs are showing weak phosphorescence emission at ca. 610 nm (Figure 35).[84]

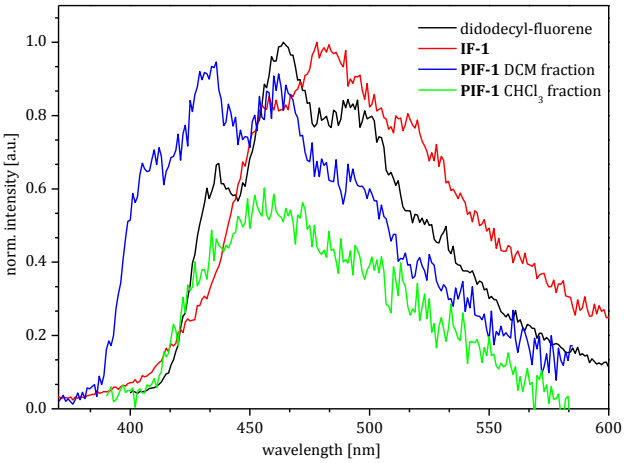

Figure 34: Phosphorescence emission spectra for PIF-1 (methylene chloride and chloroform fraction), didodecylfluorene, and IF-1 in methylcyclohexane at 77K

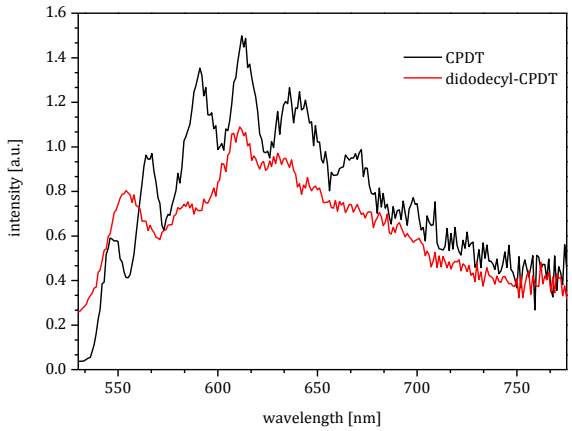

Figure 35: Phosphorescence emission spectra of CPDT and didodecyl-CPDT in methylcyclohexane at 77K

2.3.4. Energy Levels

Figure 36 depicts the thin film in the solid state absorption spectrum of **PIC-1** which was used to calculate the band gap from the offset position of the absorption band.

Therefore, the intersection point of the drawn tangent (red line) and the wavelength axis (dotted red line) was determined.[87]

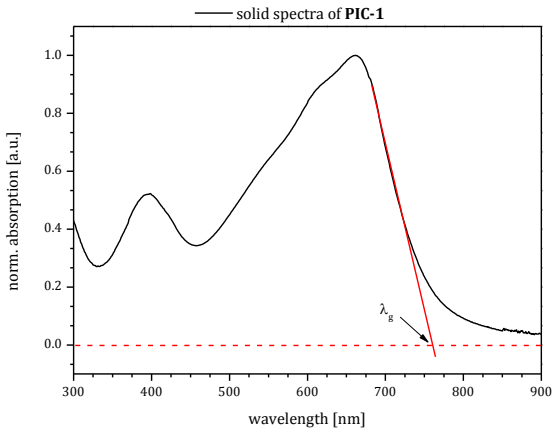

Figure 36: Thin film in the solid state absorption spectrum of PIC-1 and tangent for E_g calculations

The correlation of energy and wavelength was demonstrated by Louis de Broglie whereas the unit is Joule. To convert the unit Joule into Electronvolt the following constants are needed for the equation: h = 6.62606896×10^{-34} Js (Planck constant), c = 299792458 m/s (speed of light), and 1 eV = 1.602176487×10^{-19} J.[87]

$$E\ (J) = \frac{hc}{\lambda}$$

This conversion leads to the first term of the bottom equation, whereas the second term is a correction taking into account of the average exciton binding energy of the organic chromophors.[87]

$$E_g(eV) = \frac{1243.125}{\lambda_g\ (nm)} + 0.3\ eV$$

The optical bad gap is used to conclude about the energy of the lowest unoccupied molecular orbital (LUMO), if the highest occupied molecular orbital (HOMO) energy is recorded by UV photoelectron spectroscopy.

Table 10 shows the measured and calculated energy levels of the indigo-containing polymers. The band gaps of the polymers **PIC-1** and **PIC-2** are 1.94 eV and 1.98 eV, respectively. **PIC-3** has a band gap of 2.05 eV and **PIC-4** of 2.09 eV. The band gaps of the boc-substituted polymers are ca. 6% higher, if compared to those of the unprotected indigopolymers. Different polymer-polymer chain interactions may be one reason, since the boc-protection supresses the formation of intermolecular hydrogen bonds. The band

gap of the boc-substituted indigo-bithiophene polymer **PIB-2** is the lowest band gap for all synthesised indigo-containing polymers with a value of 1.79 eV. A reason for this is the high HOMO-energy level of -5.01 eV. Due to the limited solubility, the polymer **PIB-1** was not analysed in the solid state. With a value of -5.67 eV (**PIF-1**) and -5.80 eV (**PIF-2**) the indigo-fluorene polymers have the lowest HOMO-energy levels. The band gap of **PIF-1** is comparable to the band gap of **PIC-1**. **PIF-2** has a band gap of 2.67 eV and therefore, the highest band gap of the indigo-containing polymers.

Table 10: HOMO- and LUMO-energy levels of the indigo-containing polymers

	fraction	HOMO [eV]	band gap [eV]	LUMO [eV]
PIC-1	$CHCl_3$	-5.52	1.94	-3.58
PIC-2	$CHCl_3$	-5.52	1.98	-3.54
PIC-3	EE	-5.40	2.05	-3.35
PIC-4	EE	-5.30	2.09	-3.21
PIB-2	THF	-5.01	1.79	-3.22
PIF-1	DCM	-5.67	1.95	-3.72
PIF-2	EE	-5.80	2.67	-3.13

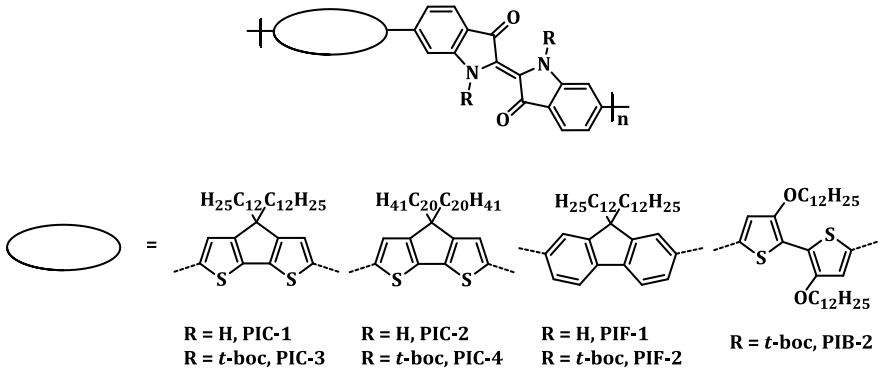

Figure 37: Overview of the chemical structures

2.4. Polymer-Analogous Reactions

2.4.1. Cleaving the Boc–Protecting Group

The next section will demonstrate two different ways to cleave the boc-protecting groups in order to understand which deprotection process is the preferred one. First of

all, the thermal cleavage will be discussed. Secondly, the cleavage under acidic conditions will be presented.

Thermal Cleavage and Thermal Gravimetric Investigations

The protected polymers show an onset of decomposition at the listed temperatures of Table 11, as determined by thermal gravimetric analysis (TGA). **PIC-2** and **PIB-1** show an onset of decomposition at 250°C, whereas the polymer **PIC-1** seems to be slightly more stable. **PIF-1** is more stable than the indigo-CPDT and indigo-bithiophene polymers. Its decomposition starts at 310°C. All boc-substituted polymers show an onset of decomposition at ca. 150°C due to the thermal cleavage of the boc-protecting groups. Differential scanning calorimetry (DSC) curves were also recorded for all eight polymers. The curves neither show endothermic or exothermic (crystallisation or melting) transitions, nor glass transition properties. Therefore, all indigo-containing polymers are expected to be amorphous.

Table 11: TGA results of the indigo-containing polymers

	fraction	on set, 1% [°C]
PIC-1	DCM	270
PIC-2	$CHCl_3$	250
PIC-3	EE	150
PIC-4	EE	150
PIB-1	TCB	250
PIB-2	DCM	150
PIF-1	$CHCl_3$	310
PIF-2	EE	150

The investigations of the thermal cleavage properties of the four boc-substituted indigo-containing polymers were performed with either the solid polymer powders or thin films. TG-analysis already showed that the boc-protected polymers have an onset of decomposing at ca. 150°C, with a peak at ca. 200°C. Hence, the temperature steps were selected at 100, 150, and 200°C, where the IR and UV/Vis spectra monitored after 2 hours (Scheme 32).

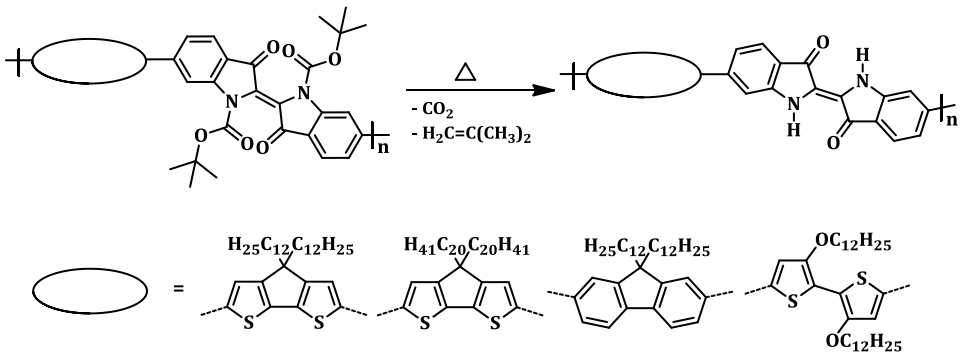

Scheme 32: Cleaving the boc-protecting groups using thermal exposure

All polymers were analysed with the two mentioned spectroscopic methods. Exemplary, **PIC-3** will be discussed concerning IR spectroscopy and **PIF-2** concerning absorption spectroscopy. A similar cleavage is possible for all synthesised polymers. **PIB-2** and **PIC-4** were characterised by these methods as well and show comparable results.

For these measurements, the polymers were heated in a vacuum oven and a small amount was taken out after every heating step to record a solid-state IR spectrum. Figure 38 depicts the overlaid IR spectra. The amine band at $\upsilon = 3300\ cm^{-1}$ increases slightly after every temperature step. This indicates that even below the onset of decomposition at 150°C, parts of the boc-protecting groups are already cleaved. The peak resulting from the C=O vibrations of the boc-protecting groups at $\upsilon = 1730\ cm^{-1}$ slightly disappears during the thermal exposure.

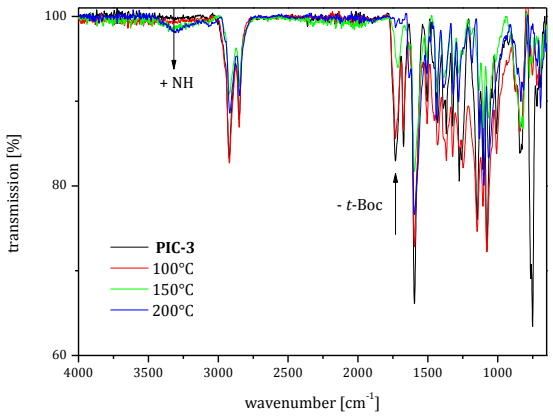

Figure 38: Cleavage of the boc-protecting groups monitored by IR spectroscopy for PIC-3

As already described before, the boc-substituted indigo-fluorene polymer **PIF-2** contains ca. 5% free indigo. This is visible in the absorption spectra in Figure 39.

Nevertheless, a complete cleavage is observed. The lower energy absorption band located at 571 nm for **PIF-2** is bathochromic shifted to 598 nm after heating at 150°C for 2 hours thus indicating the start of the cleavage of the boc-protecting groups. After heating for 2 hours at 200°C, the absorption spectra of **PIF-1** and **PIF-2**, with absorption maxima at 335, 445, and 624 nm are nearly identical thus proving complete cleavage of the boc-protecting groups.

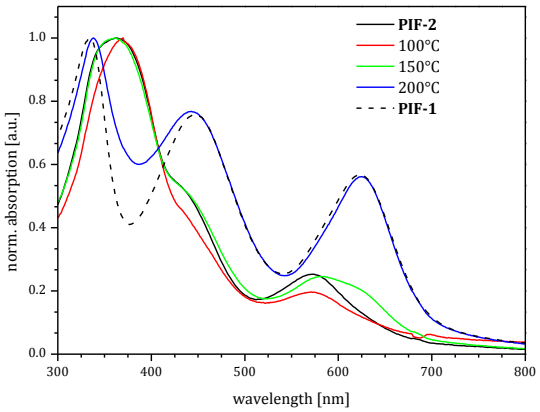

Figure 39: Cleavage of the boc-protecting groups monitored by absorption spectroscopy for PIF-2

Acid Cleavage

To investigate the acid cleavage for **PIC-3** and **PIF-2**, the polymers were dissolved in methylene chloride, treated with trifluoroacetic acid and heated for 30 min (Scheme 33). After an aqueous workup, the polymers were precipitated and Soxhlet extracted. The acid-treated polymers were characterised by GPC, UV/Vis, and IR spectroscopy. A first evidence of the successful reaction is the colour change of the reaction solutions from brown to blue (**PIC-3**) or brown to green (**PIF-2**).

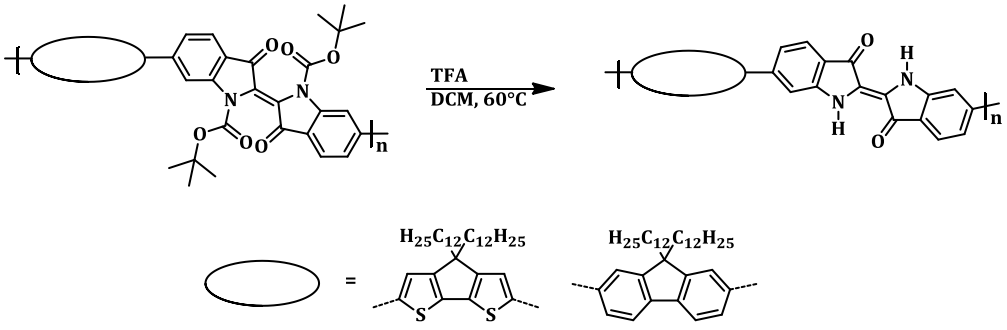

Scheme 33: Cleavage of the boc-protecting groups using TFA

The GPC results of the boc-deprotected polymers are listed in Table 12. Clearly, the GPC results for the methylene chloride fractions are smaller for both polymers due to the weight loss during deprotection. The polymers are getting more and more insoluble, as indicated by the increasing polydispersity caused by polymer-polymer chain interactions.

Table 12: GPC results for the acid treated polymers PIC-3 and PIF-2, measured in tetrahydrofuran; bold values: used fractions of PIC-3 and PIF-2 for cleavage;* measured in trichlorobenzene

	fraction	M_n [g/mol]	M_w [g/mol]	M_w/M_n
PIC-3	**ethyl acetate**	**5,200**	**11,100**	**2.12**
deprotected	DCM	4,400	8,800	2.00
deprotected	$CHCl_3$	14,600	27,800	1.91
deprotected	chlorobenzene*	7,500	18,800	2.50
PIF-2	**ethyl acetate**	**10,100**	**13,800**	**1.36**
deprotected	DCM	6,400	11,800	1.86
deprotected	$CHCl_3$	13,000	29,400	2.26
deprotected	chlorobenzene*	6,200	44,000	7.13
deprotected	dichlorobenzene*	6,000	51,000	8.38

To prove the cleavage of the boc-protecting groups, IR and absorption spectra were recorded. The IR spectra show the now occurring amine band at $\upsilon = 3316\ cm^{-1}$ (**PIF-2**) and $\upsilon = 3326\ cm^{-1}$ (**PIC-3**).

Figures 40 and 41 show the absorption spectra of the chloroform fractions of the acid-treated polymers. The shape of the absorption bands of the indigo-fluorene polymer **PIF-1** could not be restored for the acid-treated polymer **PIF-2**. **PIF-2** with its band at 569 nm shows a red-shift to 615 nm for the acid-treated polymer. The band position is still different, if compared to the unprotected indigo. Therefore, it is assumed that a complete boc-protecting group cleavage is not possible by acid exposure. The initial absorption maximum for the boc-protected polymer **PIC-3** is at 574 nm. After acidic boc-cleaving, the absorption maximum is red-shifted to 647 nm, this value is comparable to that of the polymer **PIC-1**. Therefore, the cleavage seems to work better for the indigo-CPDT polymers.

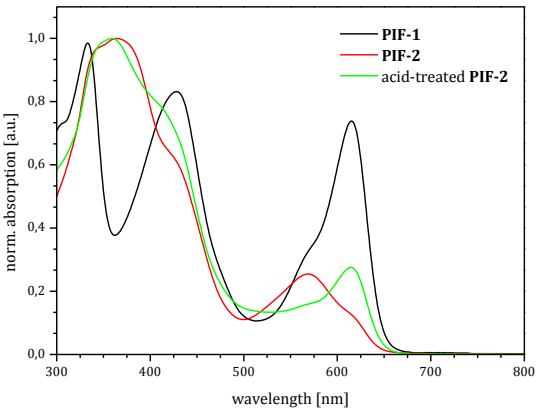

Figure 40: Absorption spectra of unprotected PIF-1, boc-protected PIF-2, and acid-treated PIF-2 in tetrahydrofuran

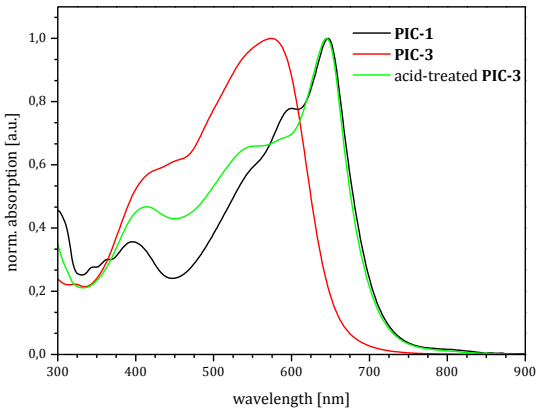

Figure 41: Absorption spectra of unprotected PIC-1, boc-protected PIC-3, and acid-treated PIC-3 in tetrahydrofuran

2.4.2. Oxidation and Reduction Experiments

The redox behaviour of indigo was already discussed in the introduction. These redox properties have been tested for the polymers **PIC-1** and **PIF-1** as well, and will be discussed below (Scheme 34).

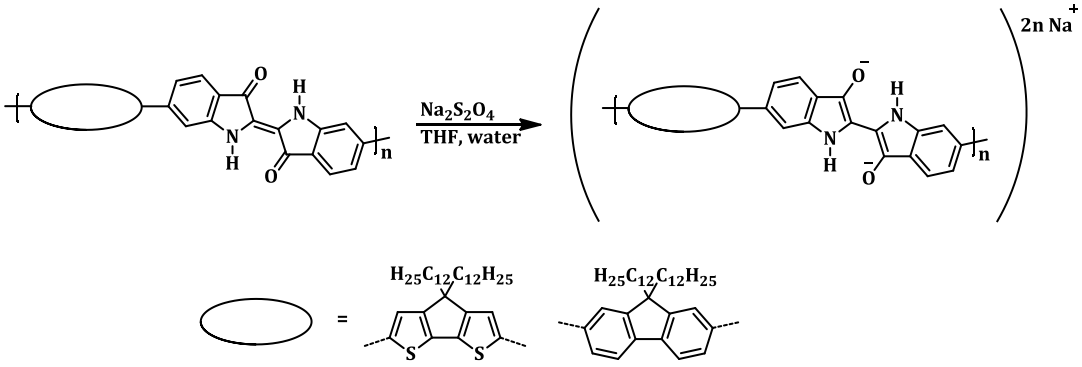

Scheme 34: Reduction of PIC-1 and PIF-1 using sodium dithionite

Stock solutions of the polymers were prepared in tetrahydrofuran and treated with aqueous sodium dithionite solution in a glovebox. The reaction took place in an absorption cuvette under argon atmosphere. The resulting absorption spectra were measured under argon. After the absorption measurements the solutions were treated with oxygen to re-oxidise the polymers. A complete re-oxidation could not be observed by treatment with oxygen. The results are shown in Figures 42 and 43. The absorption

band from the indigo unit disappears by reduction with sodium dithionite and a broad absorption band between 500-300 nm (**PIF-1**) and 550-300 nm (**PIC-1**), respectively, appears. By treating the reduced **PIC-1** solution with oxygen the resulting absorption spectrum shows an increase of the broad band at 455 nm. Nevertheless, **PIC-1** could not be re-oxidised. The indigo-fluorene polymer shows the occurrence of the absorption at 614 nm in accordance with a partial restoration of the indigo unit of **PIF-1**. This means, **PIF-1** can partially undergo a redox cycle ($Na_2S_2O_4$ reduction/ oxygen oxidation).

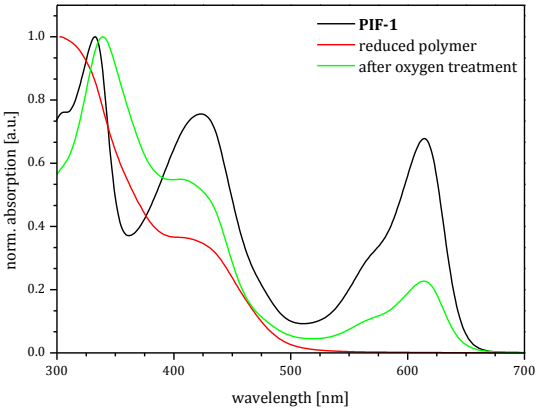

Figure 42: Absorption spectra of PIF-1, after reduction, and after oxygen treatment, all in tetrahydrofuran

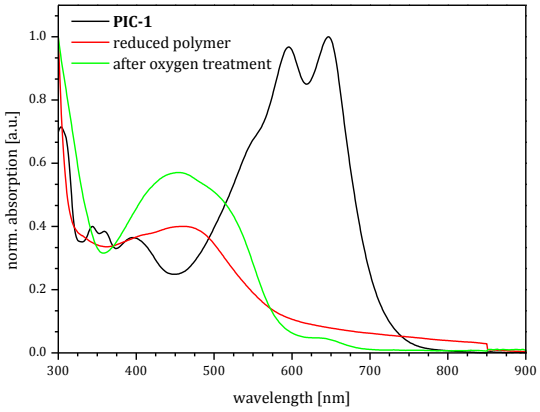

Figure 43: Absorption spectra of PIC-1, after reduction, and after oxygen treatment, all in tetrahydrofuran

2.5. Summary Indigo-Containing Polymers

Figure 44 depicts the eight successfully synthesised and characterised indigo-containing polymers. The group of Li and co-workers,[88] as well as the group of Yamamoto and co-workers[89] synthesised structurally related indigo-containing polymers, also shown in Figure 44.

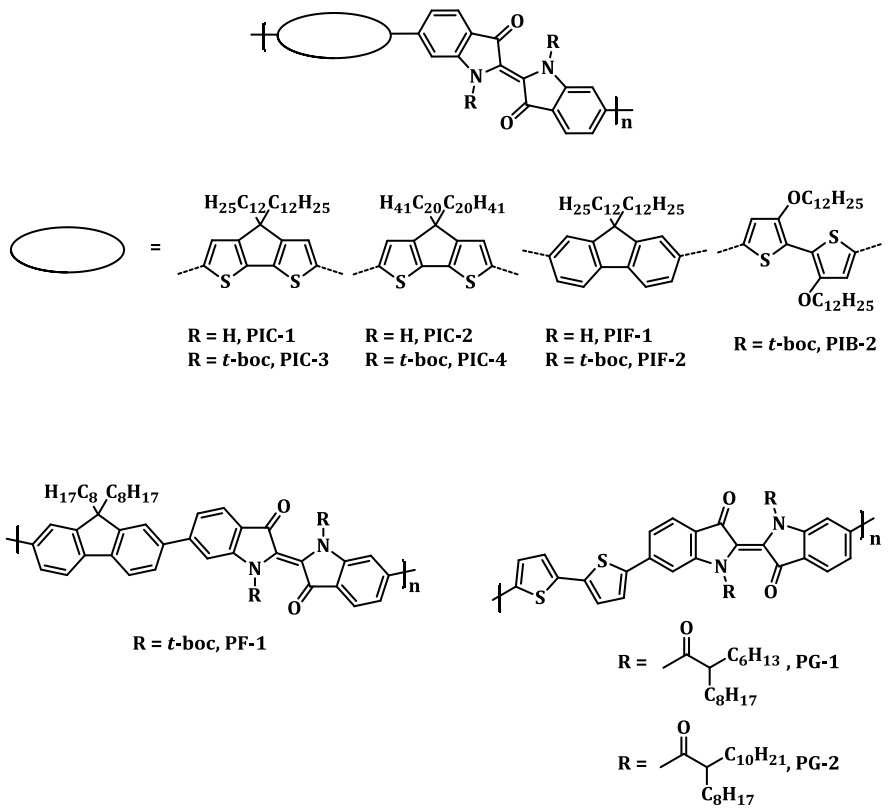

Figure 44 top: Indigo-containing polymers synthesised in this work; bottom left: Indigo-containing polymer of Yamamoto and co-workers[89]; bottom right: Indigo-containing polymers of Li and co-workers[88]

The CPDT-based indigopolymers show molecular weights (M_n) of up to 29,000 g/mol (for the boc-protected **PIC-2**). The boc-protected bithiophene-based indigopolymers show molecular weights (M_n) of up to 11,600 g/mol (**PIB-2**). Most of the CPDT-based and bithiophene-based polymers show broad polydispersity values of up to 14.74 (**PIB-2**). The group of Li and co-workers observed similar polydispersity values of up to 10.6 for their polymers (**PG-1**, **PG-2**).[88] Their molecular weights (M_n) of **PG-1** and **PG-2** are comparable to the molecular weights of our boc-protected bithiophene-based indigopolymers (**PG-1**: M_n = 13,500 g/mol and **PG-2**: M_n = 12,400 g/mol, measured in tetrachloroethane at 130°C).[88] The moderate molecular weights could result from the limited solubility.

The boc-protected indigo-containing polymers need more energy for optical excitation, if compared to the unprotected indigo-containing polymers. For example, the CPDT-based indigopolymer **PIC-1** shows absorption maxima at 658 nm in solution and at 662 nm in thin film. The corresponding boc-protected indigopolymer **PIC-3** shows absorption maxima at 590 nm in solution and at 585 nm as thin film in the solid state. The thiophene-based polymers of Li and co-workers showed absorption maxima in

solution at 527 nm (**PG-1**) or at 572 nm (**PG-2**), and as thin films at 607 nm (**PG-1**) or 620 nm (**PG-2**), respectively.[88] Accordingly, the absorption results of the CPDT-based and bithiophene-based indigopolymers are well matching to the results of Li and co-workers. Nevertheless, the optical band gaps of the CPDT-based (**PIC-4**: 2.09 eV) and bithiophene-based indigopolymers (**PIB-2**: 1.79 eV) are slightly higher, if compared to the thiophene-based indigopolymers by Li and co-workers (**PG-2**: 1.74 eV).[88]

The fluorene-based indigo-containing polymers show moderate molecular weights (M_n) of up to 7,200 g/mol (**PIF-1**) and 5,700 g/mol for the boc-protected polymer (**PIF-2**). The group of Yamamoto and co-workers synthesised a similar boc-protected polymer with shorter alkyl chains. Their polymer **PF-1** showed a low molecular weight (M_n) of ca. 3,000 g/mol caused by the limited solubility.[89]

The absorption maxima at 333, 444, and 614 nm in solution (**PIF-1**) are related either to isolated fluorene units, an intramolecular energy transfer band, or the indigo unit. The absorption maxima for the boc-protected polymer (**PIF-2**) are blue-shifted to 362, 434, and 572 nm, if compared to the deprotected indigo-containing polymer **PIF-1**. The boc-protected, indigo-based polymer **PF-1** of Yamamoto and co-workers showed absorption maxima at 330, 422, and 542 nm.[89] They indicated a band gap energy of 2.0 eV for **PF-1**,[89] whereas the band gap energy for our boc-protected polymer **PIF-2** is 2.67 eV, for the deprotected indigopolymer **PIF-1** 1.95 eV.

Polymer-analogous reactions like reduction and re-oxidation of the indigo unit, as well as the cleavage of the boc-protecting groups were investigated. The reduction of **PIF-1** and **PIC-1** was carried out with sodium dithionite as described for indigoid compounds. Partial re-oxidation is observed for **PIC-1** and only very slightly for **PIF-1**. For cleavage of the boc-protecting groups, thermal and acidic protocols were investigated. Yamamoto and co-workers investigated the acid-induced cleavage of the boc-protecting groups of **PF-1** monitored by IR spectroscopy.[89] Disappearance of the C=O vibration band (approximately at ν = 1717 cm^{-1}) is observed for **PIF-1** and **PF-1**.[89] However, the NH stretching vibrations (ν = 3300 cm^{-1}) of unprotected indigo are already visible for **PF-1** before treating with acid.[89] In our case, this band appears by treatment with acid (**PIF-2**: ν = 3316 cm^{-1}, **PIC-3**: ν = 3326 cm^{-1}). Furthermore it is to mention, that the cleavage of the boc-protecting group is working better by applying heat.

In summary, the series of indigo-containing polymers is a promising class of conjugated main-chain polymers with on-chain dye units that absorb in the Vis region up to 700 nm.

3. BAI-Containing Polymers

3.1. Monomer Synthesis

3.1.1. BAI Synthesis

Diindolonaphthyridine dyes are known since the early 20th century and were used as fabric dyes. He *et al.* reported the possibility to use them as an electron accepting unit in polymeric organic semiconductors.[90] The four step synthesis of 7,14-bis(5'-bromo-3'-dodecyl-[2,2'-bithiophene]-5-yl)diindolo[3,2,1-*de*:3',2',1'-*ij*][1,5]naphthyridine-6,13-dione (**BAI4**) is shown in Scheme 35.[90]

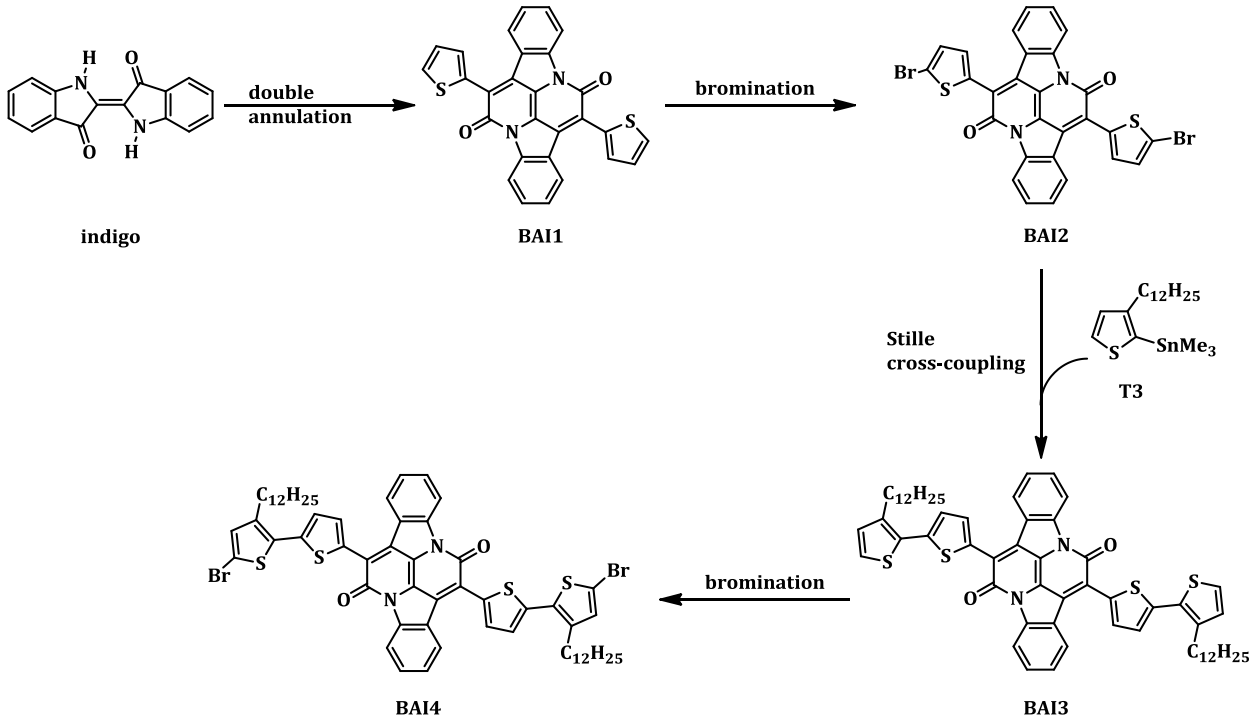

Scheme 35: Synthesis plan of 7,14-bis(5'-bromo-3'-dodecyl-[2,2'-bithiophene]-5-yl)diindolo[3,2,1-*de*:3',2',1'-*ij*][1,5]naphthyridine-6,13-dione (BAI4)[90]

7,14-Di(thiophen-2-yl)diindolo[3,2,1-*de*:3',2',1'-*ij*][1,5]naphthyridine-6,13-dione (**BAI1**) is a thiophene-substituted "bay"-annulated indigo derivate. The 2-positions of the thiophene rings will be substituted by bromide. The following Stille-type coupling reaction of 7,14-bis(5-bromothiophen-2-yl)diindolo[3,2,1-*de*:3',2',1'-*ij*][1,5]naphthyridine-6,13-dione (**BAI2**) and 2-(trimethylstannyl)-3-dodecylthiophene (**T3**) is carried out to introduce an additional solubilising thiophene spacer. 7,14-Bis(3'-

dodecyl-[2,2'-bithiophene]-5-yl)diindolo[3,2,1-*de*:3',2',1'-*ij*][1,5]naphthyridine-6,13-dione (**BAI3**) undergoes a bromination reaction under formation of monomer **BAI4**.

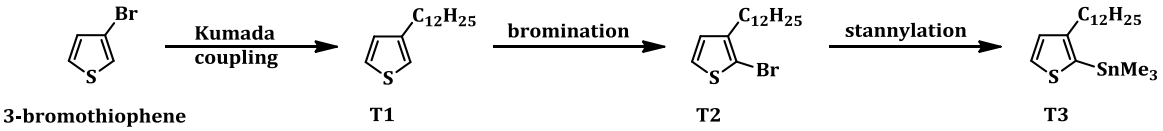

Scheme 36: Synthesis plan of 2-(trimethylstannyl)-3-dodecylthiophene (T3)

For synthesis of monomer **T3**, 3-bromothiophene undergoes a Kumada-coupling to synthesise 3-dodecylthiophene (**T1**). The bromination of **T1** results in 2-bromo-3-dodecylthiophene (**T2**) and is followed by stannylation to afford 2-(trimethylstannyl)-3-dodecylthiophene (**T3**) (Scheme 36).[91]

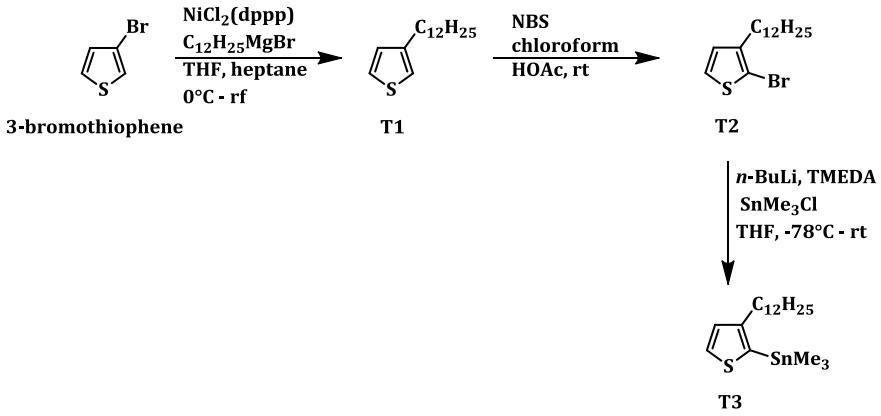

Scheme 37: Synthesis of 2-(trimethylstannyl)-3-dodecylthiophene (T3)

The three step synthesis of the functionalised thiophene monomer **T3** is presented in detail (Scheme 37). First of all, 3-bromothiophene undergoes a Kumada-coupling reaction catalysed by [1,3-bis(diphenylphosphino)propane]dichloronickel(II). Secondly, 3-dodecylthiophene (**T1**) is treated with 1-bromopyrrolidine-2,5-dione to afford 2-bromo-3-dodecylthiophene (**T2**). The bromination step is necessary due to the steric hindrance of the dodecyl group in 3-position, whereas a direct stannylation results in 2-(trimethylstannyl)-4-dodecylthiophene. Finally, lithiation by *n*-butyl lithium and transmetalation with trimethyltin chloride leads to 2-(trimethylstannyl)-3-dodecylthiophene (**T3**). The three products were purified either by distillation or column chromatography. **T1**, **T2**, and **T3** were characterised by NMR spectroscopy and

mass spectrometry. The results of the analyses are in accordance to the proposed structures and are presented in chapter 6.2.

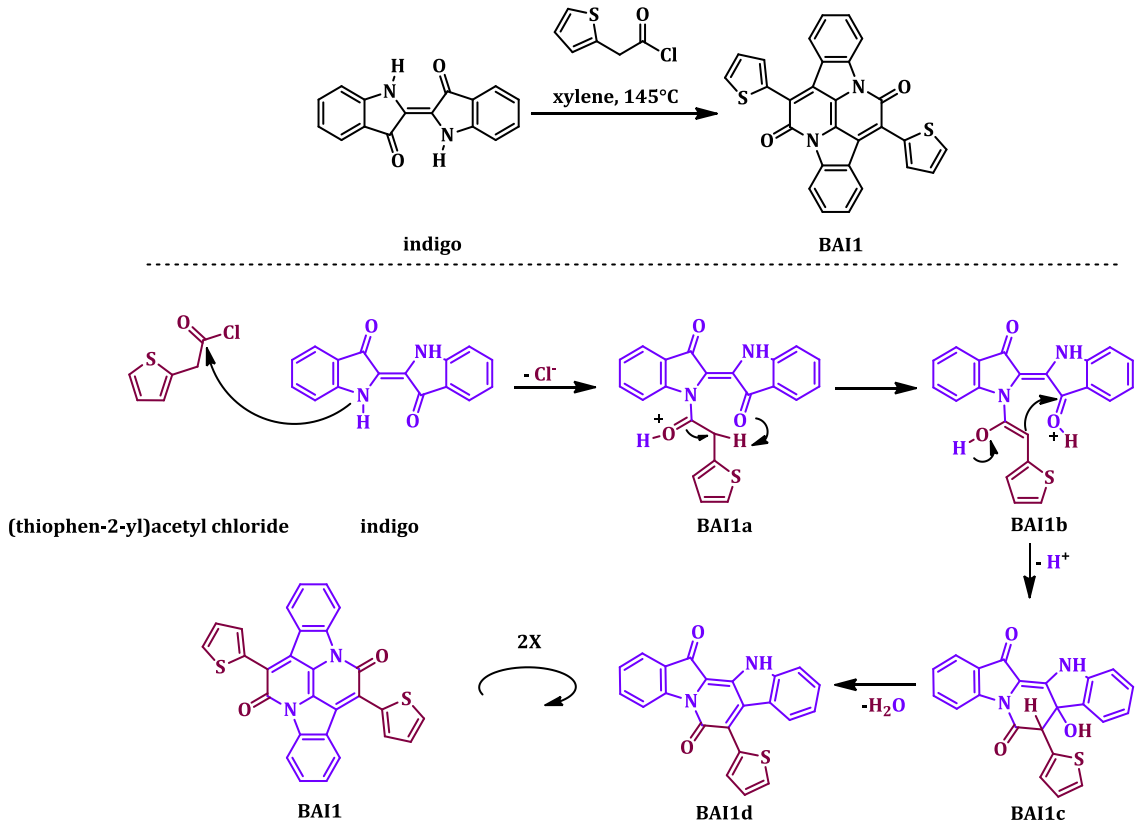

Scheme 38 top: Synthesis of BAI1; bottom: Mechanism of the annulation[47,90,92]

For the synthesis of the BAI monomer, indigo undergoes a double annulation reaction to form the BAI core. It is known, that first an amidation followed by an intramolecular aldol condensation takes place (Scheme 38).[47,90,92] In more detail, 2-(thiophen-2-yl)acetyl chloride and indigo undergo an addition reaction whereas chloride is eliminated. Protonation and rearrangement of the electrons lead to an activation of the carbonyl. The intermediate **BAI1b** undergoes a nucleophilic intramolecular enol addition under formation of the aldol **BAI1c** that dehydrates in the mono-annulated **BAI1d**. To synthesise the double-annulated **BAI1**, a second amidation and aldol condensation at the remaining amine group has to follow. To carry out this reaction sequence, indigo was dissolved in boiling xylene and treated with a solution of 2-(thiophen-2-yl)acetyl chloride in xylene. The mono-annulated indigo **BAI1d** is purple, whereas the double-annulated indigo **BAI1** is red. As soon as the purple colour disappears, the reaction was stopped and the solid product was isolated by filtration. Due to the limited solubility no further purification was applied. The ^{1}H NMR spectrum

shows two doublet signals at δ = 8.51 and 8.05 ppm. These signals belong to the phenyl groups. The remaining protons of the phenyl ring show multiplet signals at δ = 7.55-7.52 and 7.27-7.21 ppm, whereas the last multiplet signal also involves two protons of the thiophene rings. The signals between δ = 7.71-7.63 ppm represent the remaining thiophene protons. In the ^{13}C NMR spectrum, the carbonyl carbons show a signal at δ = 158.9 ppm. The signal at δ = 126.4 ppm is dedicated to the tertiary carbons adjacent to sulphur. A MALDI-MS measurement shows the expected peak at m/z = 475.1. In order to prove the complete annulation, an IR spectrum was recorded (Figure 45). The blue line shows the indigo spectrum and the red spectrum **BAI1**. Typically, the N-H stretching vibrations of indigo show a band at υ = 3258 cm^{-1}. Clearly, this band could not be detected for the annulated indigo compound **BAI1**. The vibration band at υ = 3068 cm^{-1} is dedicated to aromatic C-H stretching vibrations. The C=O stretching vibration band is recorded for both compounds at υ = 1625 cm^{-1}.

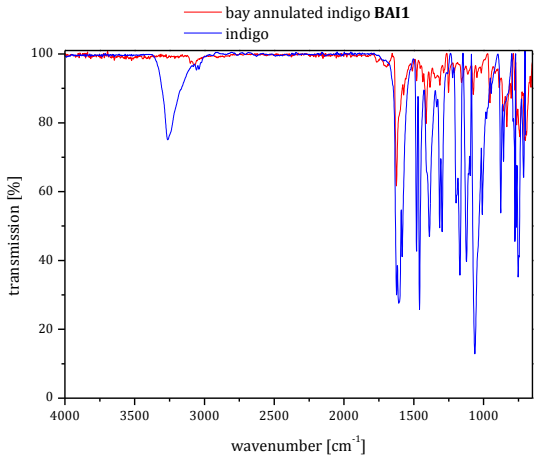

Figure 45: IR spectra of indigo (blue line) and BAI1 (red line)

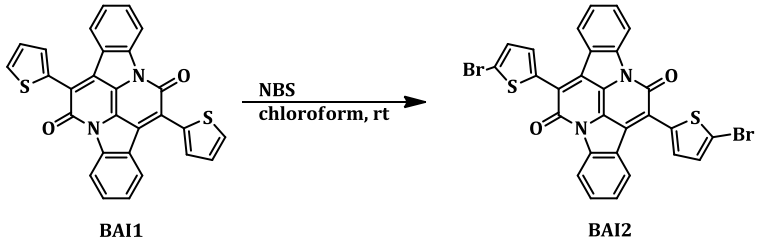

Scheme 39: Bromination of BAI1 to 7,14-bis(5-bromothiophen-2-yl)diindolo[3,2,1-*de*:3',2',1'-*ij*][1,5]naphthyridine-6,13-dione (BAI2)

To accomplish a dibromination of **BAI1**, it was suspended in chloroform and treated with 1-bromopyrrolidine-2,5-dione under exclusion of light (Scheme 39). MALDI-MS and NMR spectra were measured. The m/z = 631.8 is in accordance to the proposed structure. Due to the electron withdrawing inductive effect of the bromo-substituent, the signals of the aromatic protons are shifted downfield in the ^{1}H NMR spectrum. Therefore, two doublet signals of the thiophene rings are recorded at δ = 7.50 and 7.21 ppm. In the ^{13}C NMR spectrum, the peak at δ = 118.4 ppm represents the bromo-substituted carbons.

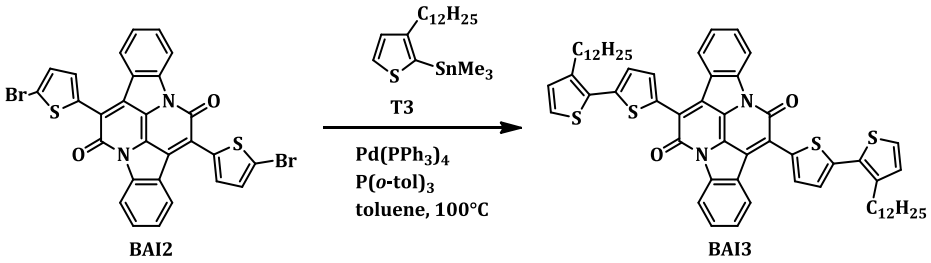

Scheme 40: Stille-type coupling to 7,14-bis(3'-dodecyl-[2,2'-bithiophene]-5-yl)diindolo[3,2,1-*de*:3',2',1'-*ij*][1,5]naphthyridine-6,13-dione (BAI3)

According to a literature procedure,[90] the Stille cross-coupling of **BAI2** and **T3** is catalysed by tetrakis(triphenylphosphane)palladium(0) and tri-*o*-tolylphosphine as ligand (Scheme 40). After purification, the product **BAI3** was isolated and shows an m/z = 973.3, measured by MALDI-MS, as expected. In the ^{1}H NMR spectrum, the doublet signals of the four phenylic protons are slightly shifted, compared to the precursor **BAI2**. Two additional doublet signals of the dodecylthiophene groups are detected at δ = 7.22 and 6.97 ppm. The three multiplet signals between δ = 7.76 and 7.26 ppm represent the remaining protons. In the ^{13}C NMR spectrum, a signal at δ = 158.7 ppm is dedicated to the carbonyl carbons. Two signals at δ = 120.4 and 126.3 ppm represent the tertiary carbons of the dodecylthiophene groups. The proton and carbon signals of the dodecyl chain, as well as the remaining carbon signals are in accordance to the proposed structure.

Figure 46 shows the IR spectrum of the dodecylthiophene-substituted **BAI3**. The aromatic C-H stretching vibrations are shown as a broad band at υ = 2952-2915 cm^{-1} resulting from the BAI core. The weak band at υ = 3073 cm^{-1} represents the aromatic C-H vibrations and a band at υ = 2848 cm^{-1} the CH_3 stretching vibrations of the

dodecylthiophene groups. A signal at $\upsilon = 1624\ cm^{-1}$ is dedicated to the stretching vibrations of the C=O group.

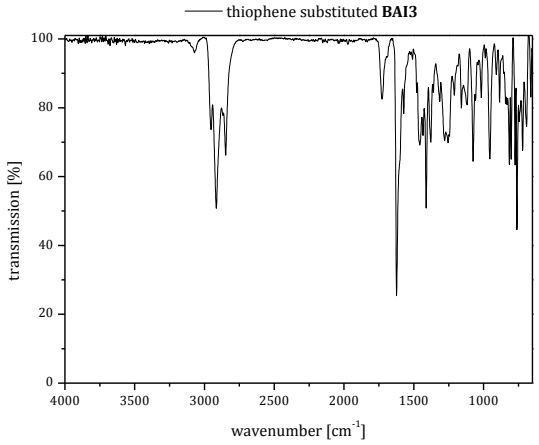

Figure 46: IR spectrum of BAI3

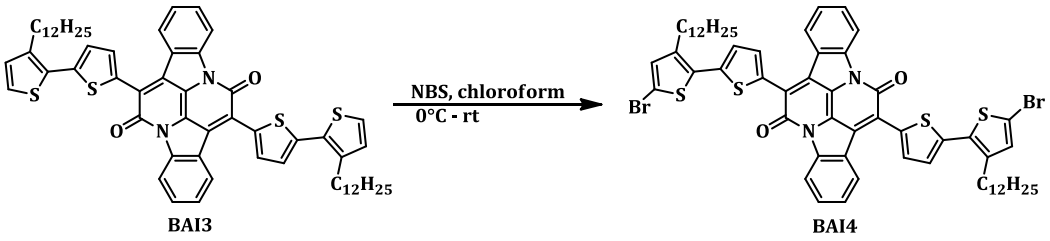

Scheme 41: Synthesis of the monomer 7,14-bis(5'-bromo-3'-dodecyl-[2,2'-bithiophene]-5-yl)diindolo[3,2,1-*de*:3',2',1'-*ij*][1,5]naphthyridine-6,13-dione (BAI4)

The final bromination reaction of **BAI3** was performed in the absence of light (Scheme 41) and yielded **BAI4**, with an m/z = 1133.2 (MALDI-MS), as expected. In the ^{1}H NMR spectrum, the proton signals at position five of the two dodecylthiophene groups are no longer recorded. A singlet signal at $\delta = 6.92$ ppm is recorded for the protons in position four. In the ^{13}C NMR spectrum, a signal at $\delta = 111.7$ ppm represents the bromo-substituted carbons. All remaining proton and carbon signals are in accordance to the proposed structure.

3.1.2. Benzodithiophene Synthesis

The π-π stacking of benzodithiophene (**BDT**) units in the solid state is known to afford oligomers and polymers with high hole mobilities of up to $0.25\ cm^2/Vs$.[93]

Another interesting aspect is the low amount of steric hindrance caused by branched alkyl chains in **BDT** derivatives. The low steric hindrance and the good solubility also support the formation of high molecular weight polymers.[94]

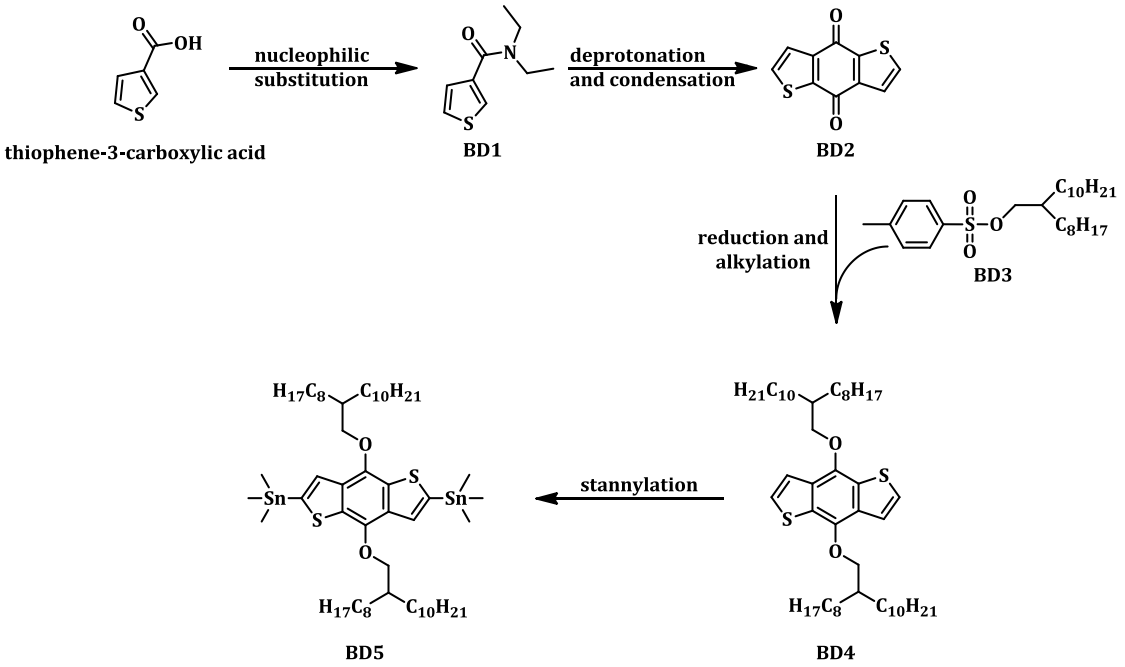

Scheme 42: Synthesis plan of 4,8-bis((2-octyldodecyl)oxy)-2,6-bis(trimethylstannyl)-benzo[1,2-*b*:4,5-*b*']dithiophene (BD5)[95]

Five steps are necessary to synthesise the stannylated **BDT** monomer 4,8-bis((2-octyldodecyl)oxy)-2,6-bis(trimethylstannyl)benzo[1,2-*b*:4,5-*b*']dithiophene (**BD5**) (Scheme 42). The synthesis of *N,N*-diethylthiophene-3-carboxamide (**BD1**) is followed by deprotonation and condensation into benzo[1,2-*b*:4,5-*b*']dithiophene-4,8-dione (**BD2**). Reduction and alkylation of **BD2** with 2-octyldodecyl-4-methylbenzenesulfonate (**BD3**) results in the formation of 4,8-bis((2-octyldodecyl)oxy)benzo[1,2-*b*:4,5-*b*']dithiophene (**BD4**). The planned Stille-type coupling with **BAI4** requires the presence of stannyl groups, which are introduced by treatment with trimethyltin chloride.

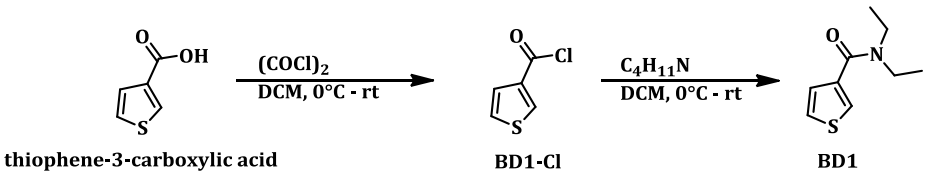

Scheme 43: Synthesis of *N,N*-diethylthiophene-3-carboxamide BD1

For the synthesis of **BD1**, the reaction of thiophene-3-carboxylic acid with oxalyl dichloride under dimethylformamide catalysis affords thiophene-3-carbonyl chloride (**BD1-Cl**). Thiophene-3-carboxylic acid was dissolved in methylene chloride and treated with oxalyl chloride and dimethylformamide. For the following nucleophilic substitution, **BD1-Cl** was dissolved in methylene chloride and added to a solution of diethylamine in methylene chloride (Scheme 43). After an aqueous workup, the pure product was isolated. **BD1** was analysed by GC-MS resulting in an m/z = 183.1 and NMR spectroscopy. In the ^{1}H NMR spectrum, the three aromatic protons are shown as multiplet, doublet of doublets, and doublet signals at δ = 7.41-7.36, 7.25, and 7.11 ppm. The methylene group is recorded as a quartet signal at δ = 3.37 ppm. A triplet signal at δ = 1.12 ppm is dedicated to the methyl group. In the ^{13}C NMR spectrum, the carbonyl carbon shows a signal at δ = 166.4 ppm. The signal at δ = 138.2 ppm represents the quaternary carbon of the thiophene. The signals at δ = 127.2, 125.7, and 125.2 ppm demonstrate the tertiary carbons of thiophene. A signal at δ = 41.7 ppm is dedicated to the methylene carbon and the methyl carbon is recorded at δ = 13.8 ppm.

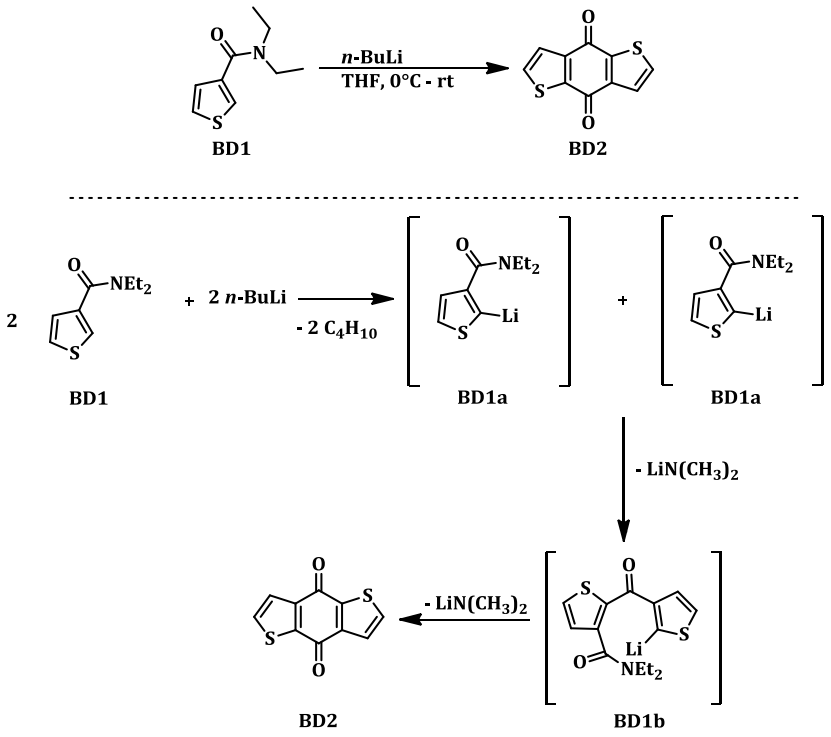

Scheme 44 top: Synthesis of benzo[1,2-*b*:4,5-*b*']dithiophene-4,8-dione (BD2); bottom: Formation of benzodithiophene BD2[96]

Benzodithiophene derivatives can be synthesised either by starting from the central benzene core and annulation of the thiophene rings or by starting from the thiophene rings under formation of the central benzene core which requires less synthesis steps. The latter method was used in this work. The mechanism of the reaction of *N,N*-diethylthiophene-3-carboxamide with *n*-butyl lithium was examined by Slocum and Gierer in 1974 (Scheme 44).[96] The lithiated intermediate condenses *via* dimerisation by formal cleavage of $LiNEt_2$. The intermediate **BD1b** is highly reactive and condenses intramolecularly to benzodithiophene (**BD2**). After an aqueous workup, the crude **BD2** was recrystallised from glacial acetic acid. The expected m/z = 219.9 was measured by GC-MS. In the ^{1}H NMR spectrum, two doublet signals at δ = 7.71 and 7.67 ppm are recorded. The carbonyl carbons are shifted downfield to δ = 174.7 ppm compared to amid **BD1**. Two quaternary carbon signals of the phenyl ring are recorded at δ = 145.1 and 143.0 ppm. The signals at δ = 133.7 and 126.8 ppm are dedicated to the tertiary carbons of the thiophene rings.

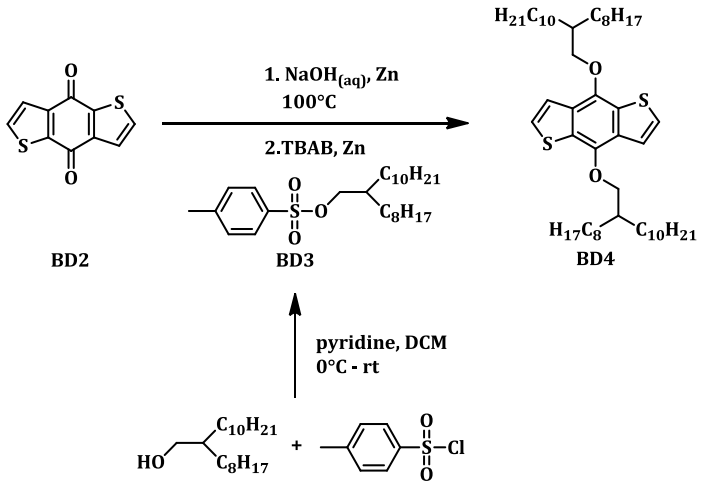

Scheme 45: Synthesis of 4,8-bis((2-octyldodecyl)oxy)benzo[1,2-*b*:4,5-*b*']dithiophene (BD4)

The reduction reaction is followed by an alkylation with activated octyldodecyl tosylate (2-octyldodecyl-4-methylbenzenesulfonate, **BD3**) (Scheme 45). Thereby, 2-octyldodecan-1-ol, pyridine, and 4-methylbenzene-1-sulfonyl chloride were reacted following a procedure of Gege *et al.*.[97] An aqueous workup and column chromatography afforded the pure tosylate **BD3**. ^{1}H NMR and ^{13}C NMR spectroscopy, as well as the LC-MS are in accordance to the proposed structure (chapter 6.2). Benzo[1,2-*b*:4,5-*b*']dithiophene-4,8-diol as the product of the reduction with zinc is not stable against oxygen and would oxides back to benzo[1,2-*b*:4,5-*b*']dithiophene-4,8-dione (**BD2**)

immediately.[98] This is the reason for the one-pot reduction and alkylation. An aqueous workup was followed by column chromatography. The APCI-MS spectrum shows an m/z = 783.6, as expected. In the ^{1}H-NMR spectrum, two doublet signals at δ = 7.47 and 7.36 ppm represent the two aromatic protons of the thiophene rings. The methylene groups adjacent to oxygen are shifted downfield and show a doublet at δ = 4.17 ppm. The signals between δ = 1.91-0.89 ppm represent the remaining alkyl proton signals. The reduction of the carbonyl groups to an ether functionality shifts the corresponding carbon signal to δ = 144.9 ppm. Two quaternary carbon signals of the phenyl ring are recorded at δ = 131.6 and 130.1 ppm. The tertiary carbons are highfield-shifted to δ = 126.0 and 120.4 ppm. Due to the positive inductive effect of ester functions, the carbons of the methylene groups are shifted to δ = 76.6 ppm.

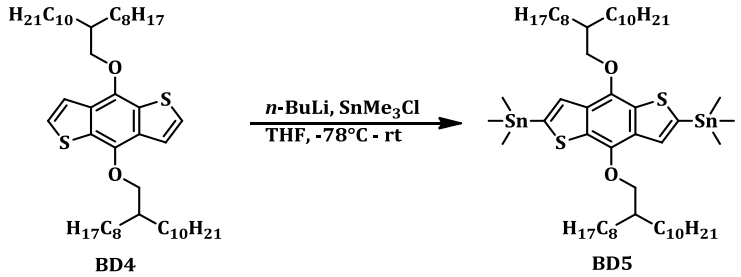

Scheme 46: Synthesis of 4,8-bis((2-octyldodecyl)oxy)-2,6-bis(trimethylstannyl)benzo[1,2-*b*:4,5-*b*']-dithiophene (BD5)

To synthesise the di-stannylated **BD5**, **BD4** was treated with *n*-butyl lithium followed by treating with trimethyltin chloride (Scheme 46). The product was afforded as slowly solidifying oil. In the ^{1}H NMR spectrum, the singlet signal at δ = 7.25 ppm shows satellites resulting from the coupling with tin (Figure 47). Compared to **BD4**, the signals for the alkyl chains are negligible shifted. The protons of the methyl groups adjacent to the tin are detected at δ = 0.45 ppm, and showing satellites as well. In the ^{13}C NMR spectrum, the tin substituted carbons are shifted to δ = 133.1 ppm. Due to adjacent tin, the methyl groups signals are detected at δ = -8.2 ppm. The peak at δ = -24.6 ppm in the ^{119}Sn NMR spectrum, as well as the FD-MS of m/z = 1108.3 support the successful di-stannylation.

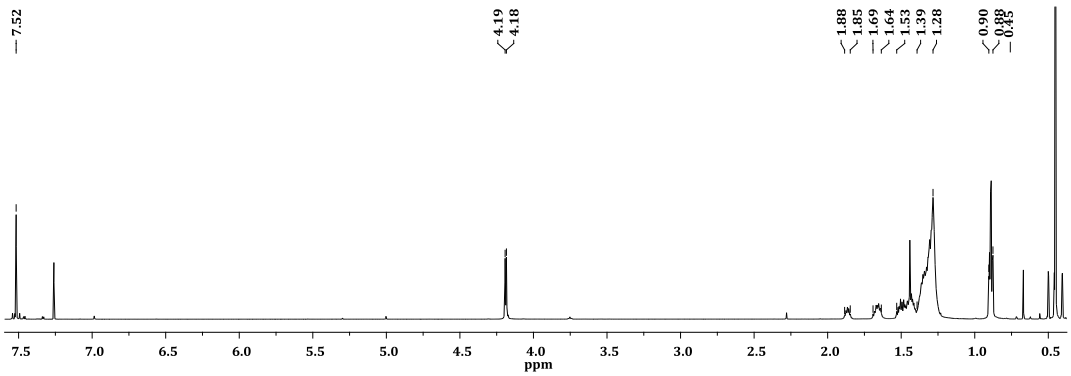

Figure 47: ^{1}H NMR of 4,8-bis((2octyldodecyl)oxy)-2,6-bis(trimethylstannyl)benzo[1,2-*b*:4,5-*b*']dithiophene (BD5); $CDCl_3$ (7.26 ppm)

3.2. Polymers Containing the BAI Building Block

3.2.1. Synthesis

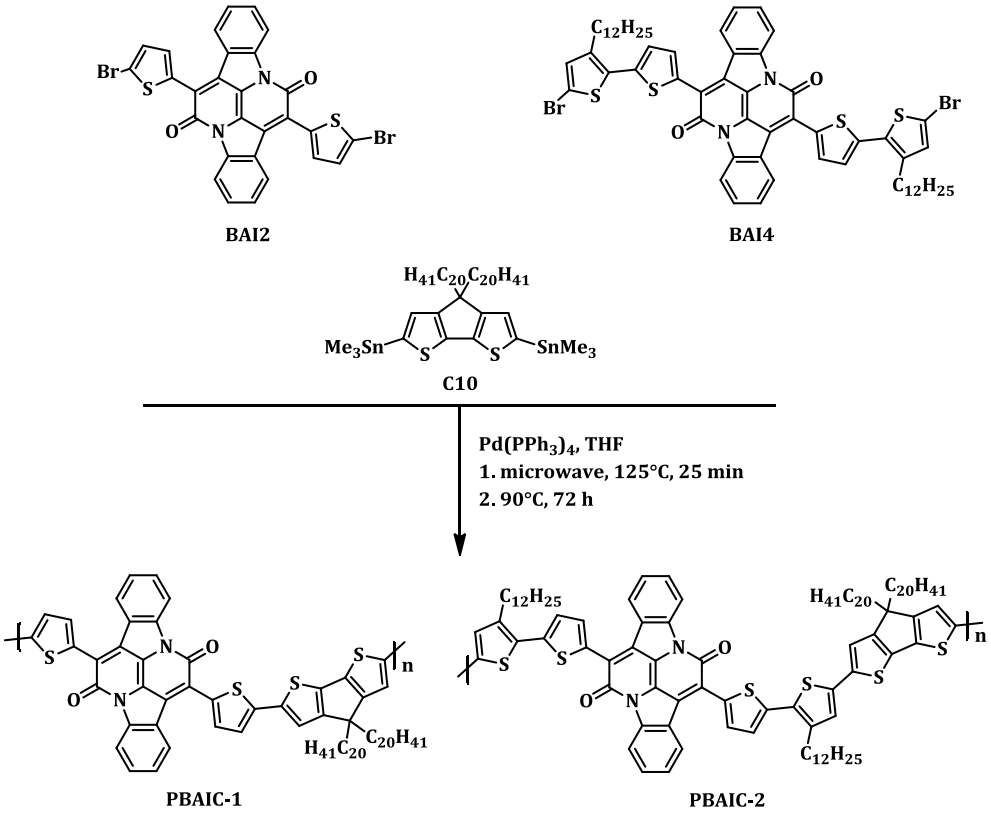

Scheme 47: Synthesis of the polymers PBAIC-1 and PBAIC-2

The Stille-type cross-coupling of the two different BAI derivatives (**BAI2** and **BAI4**) with di-stannylated CPDT **C10** was carried out in analogy to the synthesis of the indigo-

containing polymers (chapter 2.2). Tetrakis(triphenylphosphane)palladium(0) was used as catalyst for the microwave assisted coupling reaction. After irradiation at 125°C for 25 minutes, the reaction mixture was stirred at 90°C for further 72 hours (Scheme 47). The polymers **PBAIC-1** and **PBAIC-2** were precipitated into cold methanol and Soxhlet extracted.

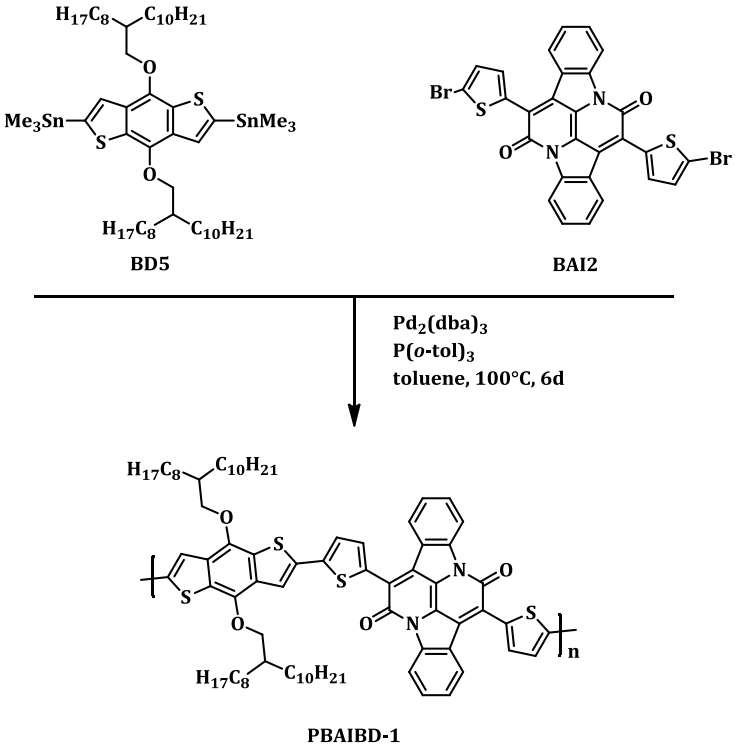

Scheme 48: Synthesis of PBAIBD-1

For the synthesis of the BAI-benzodithiophene polymer **PBAIBD-1**, the reaction conditions were modified according to the report by He *et al.*.[90] Under inert conditions, tris(dibenzylideneacetone)dipalladium(0) as catalyst and tri-*o*-tolylphosphine as ligand, as well as the monomers **BD5** and **BAI2** were dissolved in toluene and heated to 100°C. After six days, the polymer was precipitated and Soxhlet extracted (Scheme 48).

3.2.2. Characterisation

Figure 48 shows the three stacked ^{1}H NMR spectra of the BAI-containing polymers. The signals at δ = 8.7-8.6 and 8.4-8.2 ppm are recorded for four of the phenyl protons of the BAI unit (green highlighted) for all three polymers. **PBAIC-2** is the polymer with the dodecylthiophene spacer, for whom signals between δ = 7.1-6.9 ppm for the tertiary

protons and the methylene groups adjacent to the thiophene rings at δ = 2.8 ppm (blue highlighted) are detected. The broad signal at δ = 4.12 ppm results from the ether methylene groups (red highlighted) of the **PBAIBD-1** polymer.

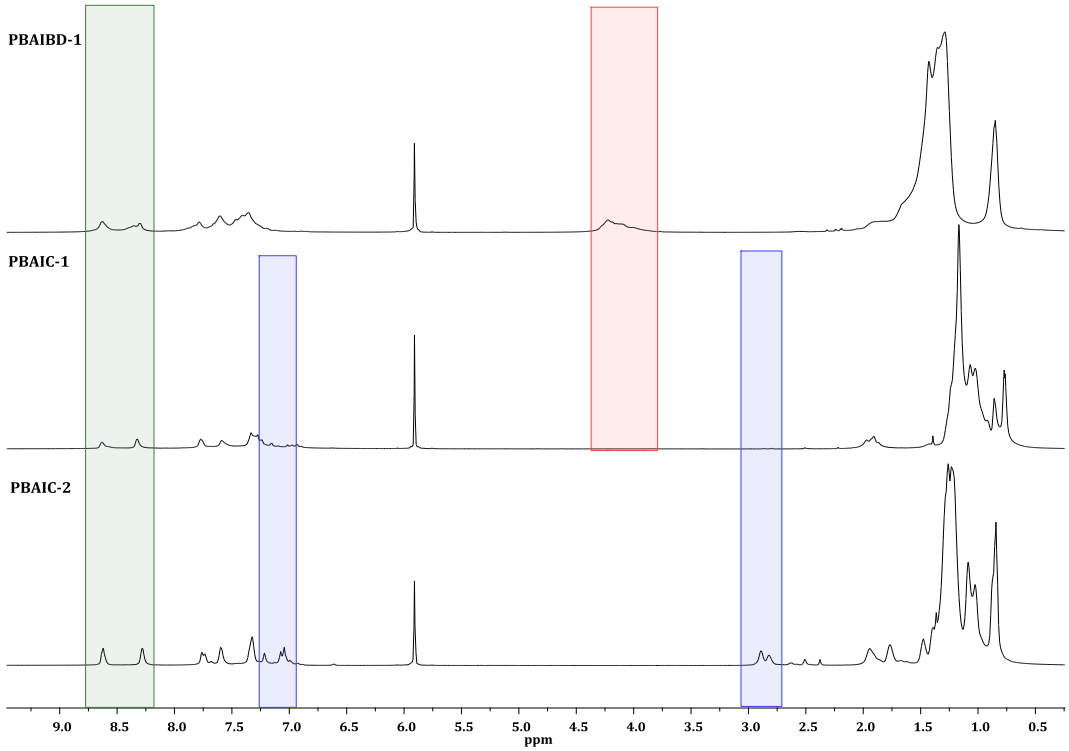

Figure 48: ^{1}H NMR spectra of PBAIBD-1 (top), PBAIC-1 (middle), and PBAIC-2 (bottom) recorded in $C_2D_2Cl_4$ (5.91 ppm); phenyl protons of the BAI unit green highlighted, protons of the thiophene spacer blue highlighted, and ether methylene protons red highlighted

Figure 49 shows the IR spectra of the BAI-containing polymers. The bands at υ = 3066 and 2920 cm^{-1} are resulting from the aromatic C-H stretching vibrations for all three polymers. A band at υ = 2850 cm^{-1} is dedicated to CH_3 stretching vibrations. The C=O stretching vibrations of the polymers are recorded at υ = 1630 cm^{-1}. **PBAIBD-1** shows an additional band at υ = 1240 cm^{-1}, which results from the C-O stretching vibrations of the alkoxy groups.

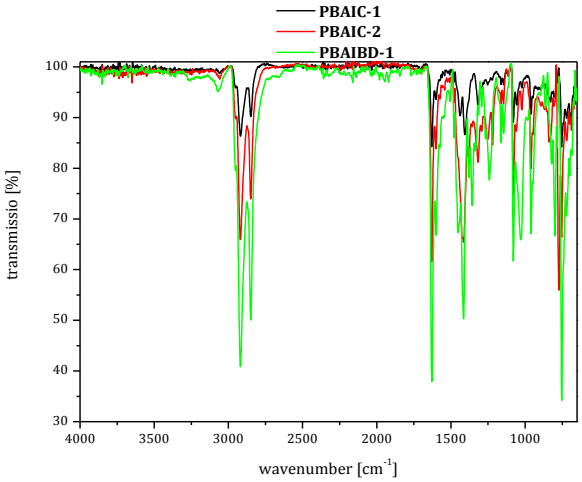

Figure 49: IR spectra of the BAI-containing polymers; PBAIC-1 (black), PBAIC-2 (red), and PBAIBD-1 (green)

PBAIC-1 and **PBAIBD-1** show low molecular weights, resulting either from precipitation due to limited solubility or caused by the specific ligand-catalyst system used for **PBAIBD-1** (Table 13). Bao *et al.* described the decomposition of the ligand before high molecular weight polymers are formed.[82] The aggregation and, therefore, the low solubility of polymer **PBAIC-1** is illustrated by the difference of the GPC data in tetrahydrofuran and trichlorobenzene at high temperature. An interaction of the polymer chains can occur during the GPC measurements. To prevent aggregation of **PBAIC-1** (chloroform fraction), high temperature GPC measurements in trichlorobenzene at 160°C were carried out and showed a narrowed polydispersity. The two dodecylthiophene spacers of polymer **PBAIC-2** increase the solubility of monomer and polymer. Hence, polymers with average degree of polymerisation of 10 (methylene chloride fraction) and 28 (chloroform fraction) were isolated after Soxhlet extraction. The polydispersity values for these investigated polymer fractions are 1.36 (methylene chloride fraction) and 1.29 (chloroform fraction).

Table 13: GPC measurements recorded in tetrahydrofuran; * measured in trichlorobenzene at 160°C

	fraction	M_n [g/mol]	M_w [g/mol]	M_w/M_n	Yield [%]	on set, 1% [°C]
PBAIC-1	DCM	10,900	22,100	2.04	28.3	n/s
	$CHCl_3$	16,600	203,000	12.24	2.7	350
	$CHCl_3^*$	8,300	11,500	1.39	--	--
PBAIC-2	DCM	17,900	24,200	1.36	56.2	360
	$CHCl_3$	47,400	61,300	1.29	25.6	n/s
PBAIBD-1	hexane	8,400	11,200	1.33	28.1	n/s
	$CHCl_3$	3,900	9,000	2.31	42.6	280

All BAI-containing polymers show an amorphous behaviour, as the indigo-containing polymers. Due to a higher decomposition temperature, the polymers **PBAIC-1** and **PBAIC-2** are more stable against thermal exposure.

3.3. Optical properties

3.3.1. Absorption Properties

Figures 50 and 51 depict the absorption spectra of the three BAI-containing polymers measured in chloroform and as thin films in the solid state. Table 14 summarises the absorption maxima. The shapes of the absorption bands are similar for the three polymers. All absorption spectra show a band at high energy in the range of 389-456 nm, the solid state absorption bands are red-shifted compared to the spectra measured in solution, except **PBAIC-2** showing a hypsochromic shift. This phenomenon is not recorded for the lower energy absorption band. The lowest energy absorption maximum in solution is recorded for **PBAIC-1** at 819 nm, whereas the lowest energy absorption maximum in the solid state is recorded for **PBAIC-2** at 928 nm. The absorption maximum of **PBAIBD-1** is recorded at 649 nm in solution and at 748 nm as thin film (methylene chloride fraction).

Table 14: Absorption maxima of the three BAI-containing polymers, measured in chloroform and as thin films in the solid state, the underlined values are the most intense absorption maxima

	fraction	λ_{abs} [nm] solution	λ_{abs} [nm] thin film
PBAIC-1	DCM	413, <u>819</u>	420, <u>835</u>
	$CHCl_3$	411, <u>794</u>	407, <u>803</u>
PBAIC-2	DCM	450, <u>720</u>	381/513, <u>928</u>
	$CHCl_3$	456, <u>742</u>	483, <u>875</u>
PBAIBD-1	hexane	389, <u>649</u>	421, <u>748</u>
	$CHCl_3$	418, <u>766</u>	431, <u>799</u>

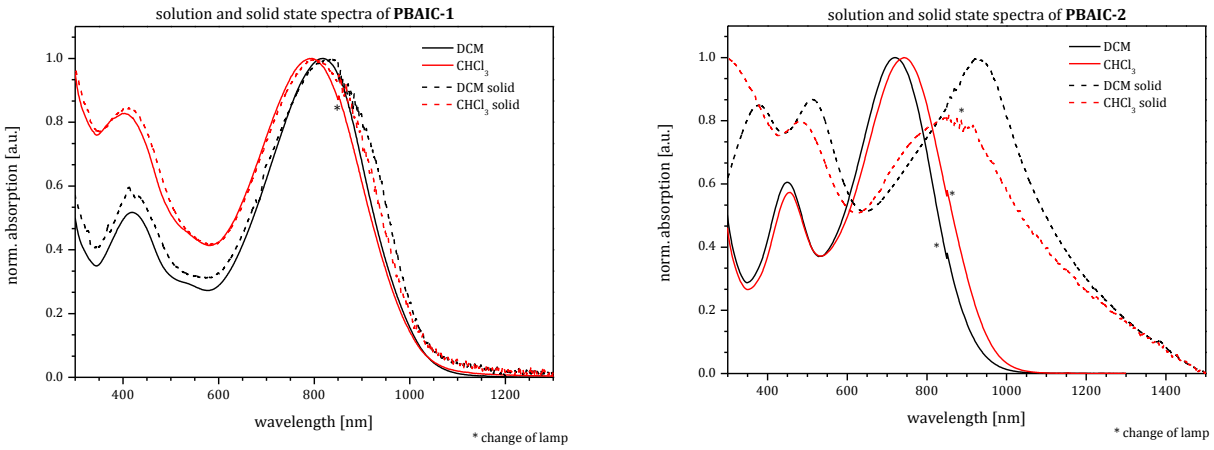

Figure 50: Absorption spectra of PBAIC-1 and PBAIC-2 in chloroform and as thin films

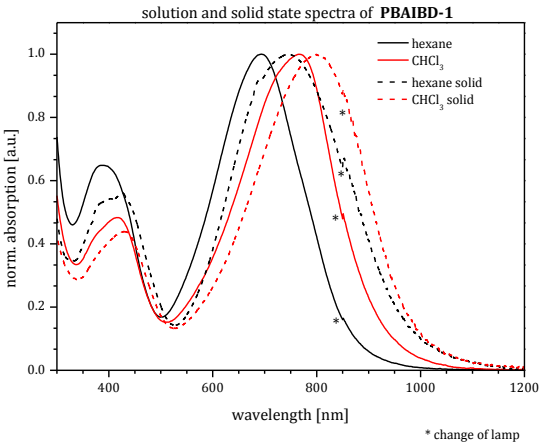

Figure 51: Absorption spectra of PBAIBD-1 in chloroform and as thin films

3.3.2. Molar Extinction Coefficient

Table 15 lists the extinction coefficients of the BAI-containing polymers. The values of the extinction coefficients are lower, if compared to the indigo-containing polymers (Table 8, chapter 2.3). They are in the same range as the boc-protected indigopolymers, possibly due to the missing secondary amine function. The introduction of the dodecylthiophene spacer does not influence the extinction coefficients (29.8 L/g*cm (**PBAIC-1**) vs. 30.2 L/g*cm (**PBAIC-2**)).

Table 15: Molar extinction coefficients measured in chloroform

	molar extinction coefficient [L/mol*cm]	extinction coefficient [L/g*cm]
PBAIC-1	36138.4	29.8
PBAIC-2	51744.8	30.2
PBAIBD-1	49836.7	39.7

3.3.3. Energy Levels

The method of calculation is already mentioned in chapter 2.3. Table 16 shows the recorded and calculated energy levels for the BAI-containing polymers. The two polymers without dodecylthiophene spacer (**PBAIC-1** and **PBAIBD-1**) show higher band gap energies than the polymer with dodecylthiophene spacers (**PBAIC-2**). The HOMO-levels of the CPDT-based polymers are comparable with values of -5.03 eV (**PBAIC-1**) and -5.07 eV (**PBAIC-2**), respectively. The band gap energy of **PBAIC-2** is 1.29 eV, the lowest energy determined in the series of all synthesised polymers within this thesis.

Table 16: Energy levels of the BAI-containing polymers

	fraction	HOMO [eV]	Band gap [eV]	LUMO [eV]
PBAIC-1	DCM	-5.03	1.48	-3.55
PBAIC-2	$CHCl_3$	-5.07	1.29	-3.78
PBAIBD-1	$CHCl_3$	-5.52	1.54	-3.98

3.4. Summary BAI-Containing Polymers

In Figure 52, the three successfully synthesised BAI-containing polymers are depicted. **PH-1** is one structural related polymer synthesised by He *et al.*.[90] The reasonable yields of up to 82% for **PBAIC-2** (methylene chloride and chloroform fractions) are comparable with the yields of the polymer **PH-1** by He *et al*. (86%).[90]

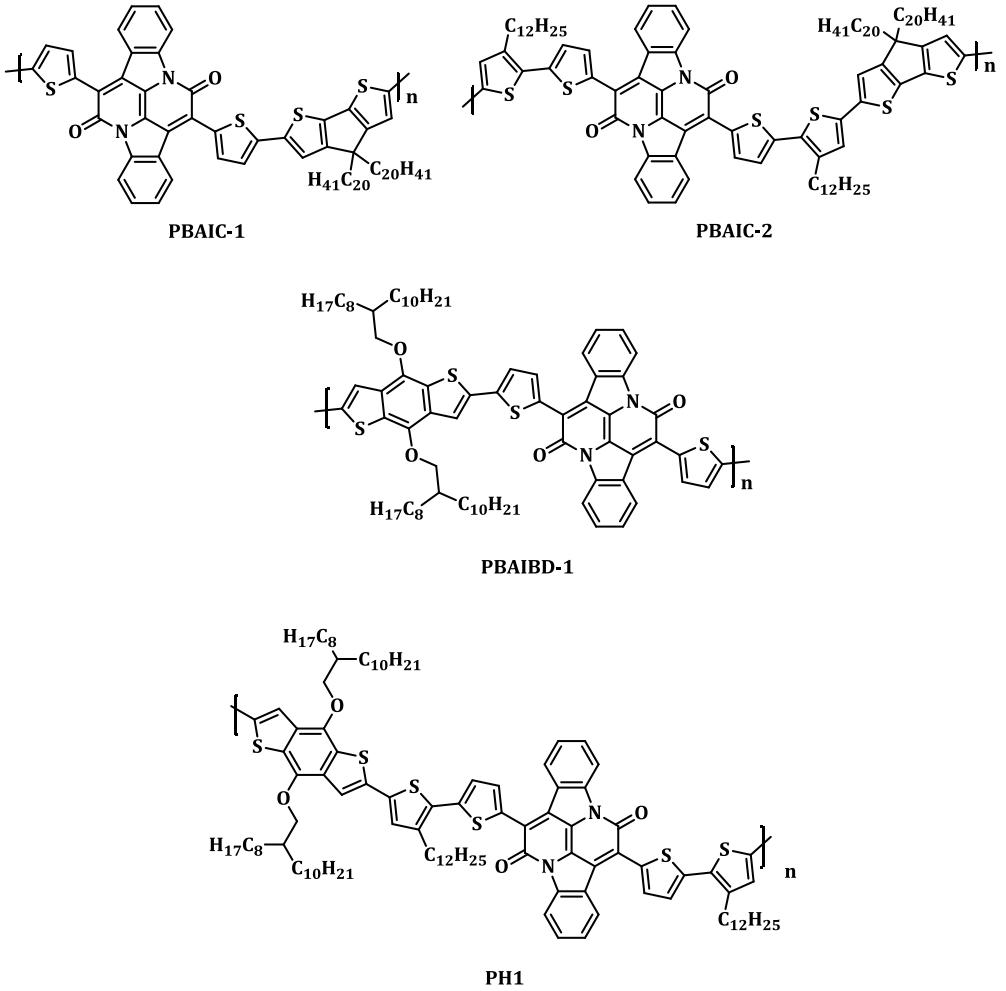

Figure 52 top: Chemical structure of the three BAI-containing polymers; bottom: Chemical structure of PH-1 by He *et al.*[90]

PBAIC-1 and **PBAIBD-1** show moderate molecular weights (M_n) of approximately 8,300 g/mol. The additional two dodecylthiophene groups of **PBAIC-2** lead to an improvement of solubility. This causing the higher molecular weight (M_n) of up to 47,400 g/mol with a narrower polydispersity of 1.29. Polymer **PH-1** by He *et al.* showed a molecular weight (M_n) of up to 41,200 g/mol with a polydispersity of 2.47.[90] In comparison, the molecular weight of **PBAIC-2** is slightly higher at a narrower

polydispersity in relation to **PH-1**. In accordance with our results, it is obvious that additional solubilising groups, as dodecylthiophene are crucial for BDT- and CPDT-based indigopolymers to gain high molecular weight polymers.

The optical properties of the BAI-containing polymers were investigated in solution and as thin films in the solid state. The absorption maxima at 794 nm for **PBAIC-1** in solution and at 928 nm for **PBAIC-2** in the solid state are shifted to lower absorption energies, if compared to polymer **PH-1** (solution: 729 nm, solid: 783 nm).[90] Nevertheless, the optical HOMO-LUMO gap values of 1.29 eV (**PBAIC-2**) and 1.24 eV (**PH-1**) are comparable.[90]

In summary, BAI-containing polymers are a promising class of low band gap polymers with optical absorptions widely shifted into the NIR region.

4. Applications

4.1. Solar Cell Investigations

Scheme 49 shows the structures of the three polymers **PIB-2**, **PIC-1**, and **PBAIC-1** which were tested in bulk-heterojunction-type (BHJ) photovoltaic cells. The performances of **PIB-2** and **PBAIC-1** were determined in cooperation with the group of Professor Thomas Riedl from Bergische Universität Wuppertal. **PIC-1** was investigated in cooperation with the group of Professor Ergang Wang from Chalmers University of Technology.

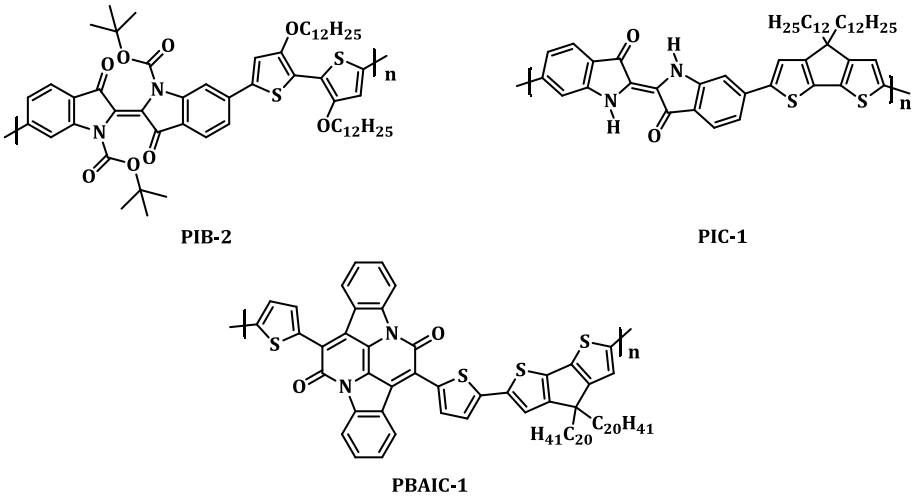

Scheme 49: PIB-2, PIC-1, and PBAIC-1 used for solar cell investigations

Figure 53 shows the three device structures of the fabricated BHJ solar cells. Cell type 1 is a so-called inverted solar cell.[99–101] Indium-tin-oxide (ITO) is the bottom electrode and is placed on a glass substrate. On top of the ITO layer, zinc oxide is used as the electron transport layer. The BHJ is a mixture of $PC_{71}BM$ (acceptor) and one of the three polymers (donor). To increase the performance of solar cells, an additive like diiodooctane (DIO) can be added to the BHJ mixture. BHJ layers are used to increase the interfacial area between donor and acceptor. The counter electrode for cell type 1 is molybdenum trioxide/silver.[99–101] Cell types 2 and 3 are conventional device structures with cathodes either composed of calcium/silver[102] or lithium fluoride/aluminium.[103] PEDOT:PSS (poly(3,4-ethylenedioxythiophene): poly(styrenesulfonate)) is used to increase the charge carrier extraction into the ITO electrode.[104–106]

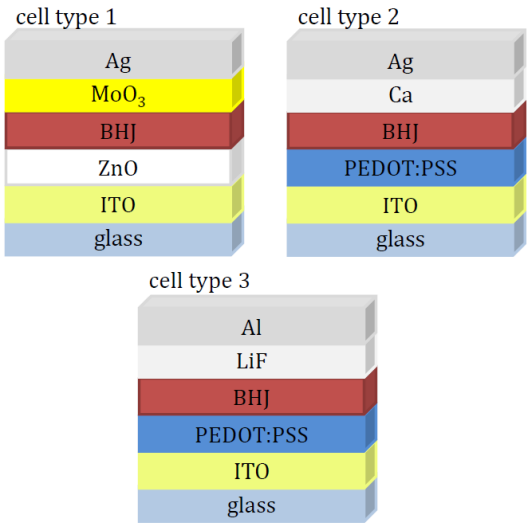

Figure 53: Device structure of the three used solar cell architectures

Table 17 reports the photovoltaic properties. The best results were obtained for **PIB-2** (tetrahydrofuran fraction) with 2.9% DIO as additive and cell type 1 (inverted structure). A power conversion efficiency (PCE) of 0.49% was measured with a fill factor (FF) of 47% for **PIB-2** as donor and $PC_{71}BM$ as acceptor. The results for the methylene chloride fraction of **PIB-2** are comparable. **PIB-2** was also annealed for 30 minutes at 200°C to cleave the boc-group which leads to PCEs of less than 0.1%. A PCE of 0.47% was measured for **PBAIC-1** with a FF of 39% by using the "conventional"-solar cell type 2. **PIC-1** achieved a PCE of 0.19% and a FF of 26% by using solar cell type 3 and 2.5% DIO as additive.

Table 17: Solar cell results; DIO: diiodooctane

	fraction	cell type	DIO [%]	PCE [%]	V_{OC} [V]	J_{SC} [mA/cm²]	FF [%]
PIB-2	DCM	1	0	0.10	0.22	1.2	36
	DCM	1	2.9	0.46	0.59	1.7	46
	THF	1	0	0.28	0.44	1.6	39
	THF	**1**	**2.9**	**0.49**	**0.59**	**1.8**	**47**
PBAIC-1	DCM	1	0	0.37	0.54	2.3	31
	DCM	**2**	**0**	**0.47**	**0.49**	**2.5**	**39**
PIC-1	DCM	3	2.5	0.19	0.33	1.2	26

Liu *et al.* reported a boc-protected indigo-containing polymer (**PLi-1**), which is shown in Figure 54.[101] Polymer **PLi-2** results from thermal cleavage at 200°C for 10 minutes. The photovoltaic performances were investigated by Liu *et al.* using an inverted device structure: ITO/PFN-OX/copolymer:$PC_{71}BM$/MoO_3/Al.[101] The boc-protected **PLi-1** leads to PCEs up to 0.75% (FF: 34.5%) and the annealed polymer **PLi-2** shows PCEs up to 0.55% (FF: 37.6%).[101]

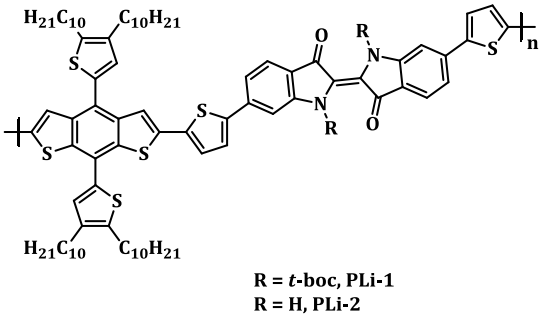

Figure 54: Chemical structure of the indigo-containing polymers by Liu *et al.*[101]

The annealing process seems to be counterproductive to obtain valuable PCEs as observed for **PIB-2** and **PLi-2** by Liu *et al.*.[101] One reason for the decreased PCEs by annealing can be the roughening of the film surface, which impedes the charge carrier collection, as described by Liu *et al.*.[101]

In summary, it could be stated that the indigo-containing polymer solar cells show similar PCEs, if compared to the solar cells by Liu *et al.*.[101] Nevertheless, the solar cell performances are in need of further improvement.

4.2. Organic Field Effect Transitor Investigations

In coopertation with the group of Professor Franco Cacialli from the London Centre for Nanotechnology (LCN), UCL, the charge carrier mobility of polymer **PBAIC-2** in p-doped organic field effect transistors (OFET) was investigated. Figure 55 shows the different OFET device structures[107] and the chemical structure of polymer **PBAIC-2**.

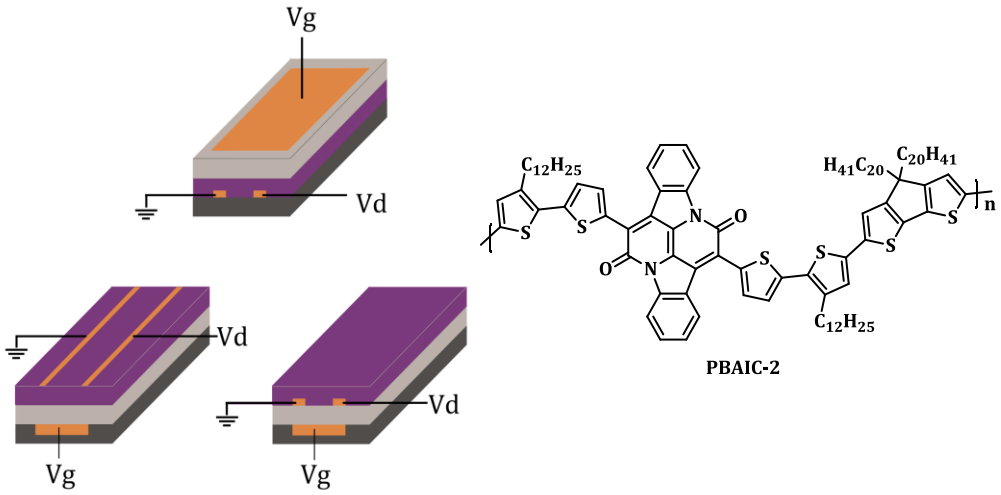

Figure 55 left: OFET structures; top: top-gate/bottom-contact (TGBC); down left: bottom-gate/top-contact (BGTC); bottom right: bottom-gate/bottom-contact (BGBC);[107] right: Chemical structure of PBAIC-2

Transistors consist of a substrate layer (dark grey), a source/drain and a gate electrode layer (orange), the semiconductor layer (violet), and a dielectric layer (bright grey). Two different architectures for transistors are known, the top-gate and bottom-gate construction.[108] In the top-gate/bottom-contact (TGBC) configuration, the gate electrode is placed on top and source/drain electrodes are placed directly on the substrate. The semiconductor layer is beyond the dielectric layer. Silicon dioxide is an example for the insulating material of the dielectric layer. TGBC structures are suitable for printing techniques in which every layer is printed one after the other.[107] In the bottom-gate/bottom-contact (BGBC) structure, the gate electrode is on top of the substrate layer, followed by the dielectric and the source/drain layer. On top of this device structure the semiconductor is located. The advantage of the BGBC structure is the possibility to manufacture small devices.[107] To investigate the OFET properties of **PBAIC-2**, the bottom-gate/top-contact (BGTC) device structure was used, in which the gate electrode is placed on the substrate layer, followed by the dielectric layer and the semiconductor layer. As already assumed by the name (top-contact), source/drain are

on top of this device. Charge carrier mobility tends to be higher for this device structure compared to the BGTC structure.[109] The n-doped silicon substrate was passivated with hexamethyldisilazane to obtain a p-doped silicon structure. Hence, the semiconductor **PBAIC-2** represents the n-type part of the OFET. The mobility (μ) is defined as the speed of charge carrier drifting into the active layer per unit electric field.[110] The here prepared OFET shows an extrapolated hole mobility of $\mu = 0.77 \pm 0.08 \times 10^{-4}$ cm²/Vs. Another performance parameter is the threshold voltage (V_t).[110] This parameter demonstrates the voltage at which the field effect is functioning. It describes the number of charge carrier traps between the semiconductor and dielectric interface. Before charge carriers flow between the source/drain, these traps have to be filled.[111] The threshold voltage of the OFET has a value of around $V_t = -7$ V. The output characteristics and the transfer characteristics are shown in Figure 56.

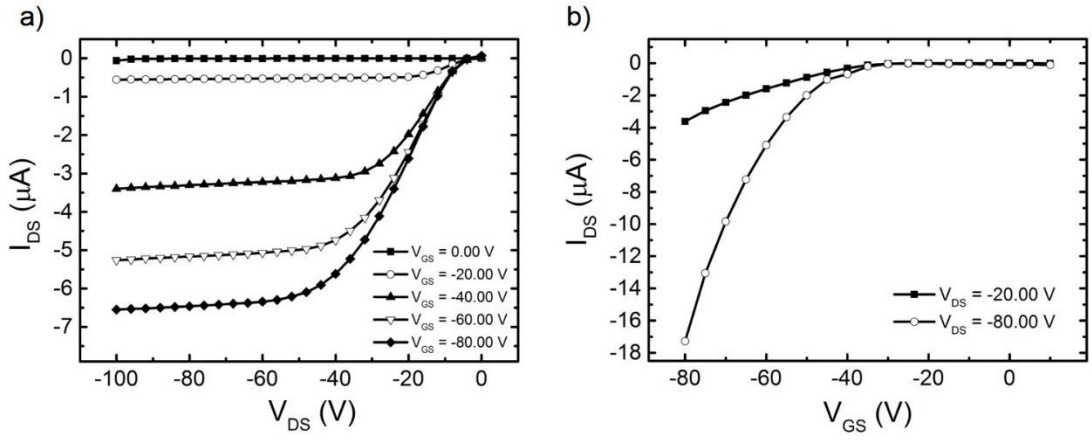

Figure 56 a: Output (I_{DS}-V_{DS}); b: Transfer (I_{DS}-V_{GS}) characteristics of an OFET based on polymer PBAIC-2

The group of Hugo Bronstein and co-workers synthesised a BAI-thiophene polymer (**PBT-1**) which is shown in Figure 57. They extrapolated a hole mobility of up to $\mu = 0.23 \pm 0.01$ cm²/Vs with a threshold voltage of up to $V_t = -131$ V.[48] The TGBC devices were annealed at 200°C. To design high performance OFETs, the planarity of the organic semiconducting polymer is important, since a planarised polymer structure supports the stacking of the polymer chains.

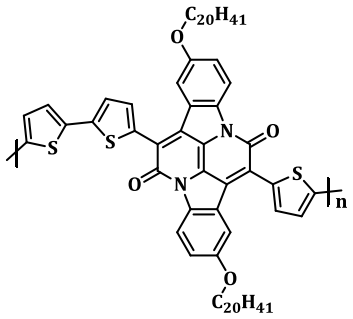

PBT-1

Figure 57: Structure of PBT-1 synthesised by Bronstein and co-workers [48]

5. Summary and Outlook

5.1. Summary

This thesis reports the synthesis and characterisation of eleven conjugated polymers containing either indigo or BAI units. The polymers are showing moderate to high molecular weights, which depends on the obtained solubility. The highest number-average molecular weight of 47,400 g/mol and the highest weight-average molecular weight of 61,300 g/mol, (resulting in an M_w/M_n of 1.29) are obtained for **PBAIC-2**. Absorption properties of the polymers are remarkable. Table 18 demonstrates the possibility to introduce the unique indigo properties into soluble indigo-containing polymers which results in absorption maxima of up to 794 nm (**PBAIC-1**). All boc-protected polymers need more energy to be excited resulting in a hypsochromic shift of the long wavelength absorption band, if compared to the indigo-containing polymers. The long wavelength absorption bands of the BAI-containing polymers are shifted bathochromically in comparison to the indigo-containing polymers, also leading to lower band gap energies with the lowest one of 1.29 eV for **PBAIC-2**.

Table 18: Overview of the absorption bands of the synthesised polymers; the underlined values are the most intense absorption maxima

	λ_{abs} [nm] solution
PIC-1	398, <u>658</u>
PIC-2	398, <u>673</u>
PIC-3	456, <u>590</u>
PIC-4	457, <u>591</u>
PIB-1	<u>644</u>
PIB-2	<u>482</u>
PIF-1	<u>333</u>, 444, 614
PIF-2	<u>362</u>, 434, 572
PBAIC-1	411, <u>794</u>
PBAIC-2	456, <u>742</u>
PBAIBD-1	418, <u>766</u>

In cooperation with the group of Prof. J. S. Seixas de Melo from the Universidade de Coimbra, Portugal, the photophysical properties of **PIF-1** and **IF-1**, as well as **PIC-1** and **IC-1** were investigated showing an intrachain energy transfer that results in an 'in-between' absorption band.

Polymer-analogous cleavage of the boc-protecting groups results in deprotected indigo-containing polymers. The degree of cleavage by acid is not complete. Hence, the deprotection of the boc-protected indigo-containing polymers is working better under thermal conditions.

Reduction of **PIC-1** and **PIF-1** is possible as described for reduction of indigoid compounds with sodium dithionite. A re-oxidation was not observed for **PIC-1** and only partially obtained for **PIF-1**.

These investigations show that the properties of monomeric indigo can be transferred to indigo-containing polymers as demonstrated for the optical properties.

PIC-1, **PIB-2**, and **PBAIB-2** were used for the fabrication of solar cells. They were investigated either with or without DIO as processing additive. These measurements were realised in cooperation with the group of Prof. Riedl (Wuppertal) and the group of Prof. Wang (Gothenburg), respectively. The best results were obtained for polymer **PIB-2** with DIO as additive. A PCE value of 0.49% and a FF of 47% are measured for a solar cell in inverted architecture.

In cooperation with the group of Prof. Franco Cacialli from the London Centre for Nanotechnology (LCN), UCL, the charge carrier mobility was investigated. Therefore, a bottom-gate/top-contact transistor was produced with **PBAIC-2** as semiconductor layer. The extrapolated hole mobility was $\mu = 0.77 \pm 0.08 \times 10^{-4}$ cm^2/Vs with a threshold voltage of $V_t = -7$ V.

5.2. Outlook

The solubility of the BAI-containing polymers needs to be improved. Several possible approaches can lead to better soluble BAI-containing polymers. One alternative could be to introduce branched alkyl chains to the thiophene spacer. Another alternative could be the substitution by solubilising groups at the benzene rings. It could be possible to introduce up to four alkyl or alkoxy groups, as shown in Figure 58.

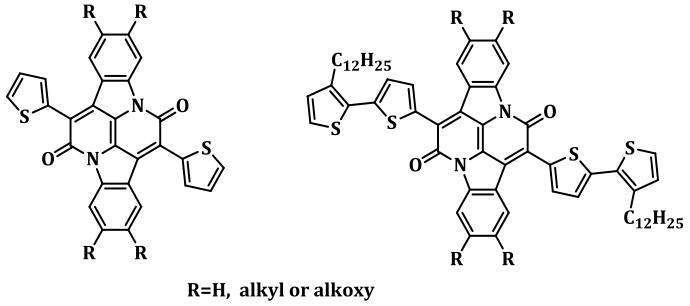

Figure 58: Alkylated BAI derivatives

The photophysical properties of the indigo-bithiophene polymers (**PIB-1** and **PIB-2**) and all here synthesised BAI-containing polymers are highly interesting to be investigated. To understand the photophysical properties, it is necessary to synthesise model compounds.

The design of indigo-containing polymers by using indigo derivatives like selenoindigo, oxindigo, and thioindigo as described in the introduction is another interesting topic. The synthesis of thioindigo was published by Fierz-David and Blangey, and is shown in Scheme 50.[112] Lüthy modified this route to synthesise the functionalised 6,6'-dibromothioindigo and started from 2-amino-4-bromobenzoic acid.[113] The next step would be the synthesis of thioindigo-containing polymers.

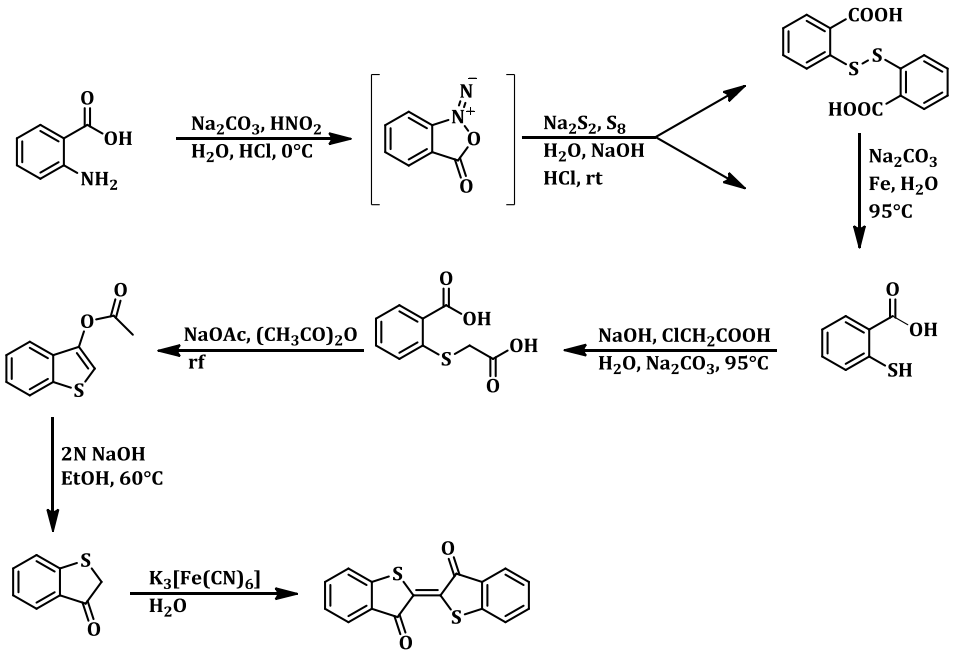

Scheme 50: Synthesis route for thioindigo[112]

6. Experimental Part

6.1. General Information

6.1.1. Materials

All commercially available chemicals and solvents were used without further purification. Dry solvents were bought from Acros and stored over molecular sieve. All reactions were performed under argon atmosphere, if not specified otherwise. Degassing the solvents was performed using argon (12 hours) *via* Schlenk-technique.
9,9-Didodecyl-9*H*-fluorene and 2-(9,9-didodecyl-9*H*-fluorene-2,7-diyl)bis(4,4,5,5-tetramethyl-1,3,2-dioxaborolane) were synthesised by Dr. Nils Fröhlich.

6.1.2. Instrumentation

Flash chromatography systems and columns

For the flash column chromatography either a Reveleris X2 flash by Grace system or an Isolera One system by Biotage chromatography were used. For both systems columns with a pore size of 40 µm by Grace were used.

Silica gel

For the column chromatography two different silica gels were used, either with pore size of 0.035-0.070 mm by Acros or with pore size of 0.063-0.200 mm by Merck.

NMR spectroscopy

The Nuclear Magnetic Resonance (NMR) spectra were recorded on a Bruker Avance 400 or Avance III 600 spectrometer. Deuterated solvents were used as references. For the solid state $^{13}C\{^{1}H\}$ CPMAS NMR spectra a Bruker Avance III 300 was used at the Westfälische Wilhelms-Universität Münster. The following abbreviations were used: Ar-H: aromatic tertiary carbon, Ar-R: aromatic quaternary carbon, s: singlet signal, bs: broad singlet signal, d: doublet signal, dd: doublet of doublets signal, t: triplet signal, q: quartet signal, m: multiplet signal.

GC-MS

Gas Chromatography (GC) Mass Spectrometry measurements were recorded on either a GC17AQP5050 or a 7890GC gas chromatograph by Shimadzu with 5975C MS detector by Agilent Technologies.

LC-MS

Liquid Chromatography (LC) Mass Spectrometry was performed on a Bruker Daltonics microTOF with an Agilent 1100 series HPLC unit.

APCI-MS

Atmospheric Pressure Laser Ionisation (APCI) measurements were carried out using a microTOF by Bruker Daltronik Bremen. The APCI-source was built by the University of Wuppertal using a Corona discharge needle.

FD-MS

Field Desorption (FD) mass measurements were recorded with Sektor Feld MS, ZAB2-SE-FPD, VG Instruments at the Max Plank Institute for Polymer Research in Mainz.

MALDI

Matrix Assisted Laser Desorption Ionisation (MALDI) measurements were carried out using a Bruker Reflex TOF at the Max Plank Institute for Polymer Research in Mainz.

GPC

Gel Permeation Chromatography (GPC) measurements were recorded with a PSS/ Agilent SECurity GPC System using a pre-column (8x50 mm, particle size 5 µm) and two PSS SDV analytical linear M columns (8x300 nm, particle size 5 µm). For the measurements with tetrahydrofuran ALS G1328A (DAD) and RID G1362A were used as detectors. A VWD G1329A ALS (UV) and RID C1362A (RI) were used for the measurements in toluene and chloroform. The high temperature measurements were recorded in trichlorobenzene. Either a Waters Alliance 200 with a RID detector, one pre-column (PLgel Guard) and one column (PLgel MIXED-B) were used at 135°C for separation or a PG 14, Agilent PL-210-HT four columns (PSS SDV 5 µm, guard, ID

8x50 mm, PSS SDV 5 µm, 10e5 A, ID 8x300 mm, PSS SDV 5 µm, 10e3 A, ID 8x300 mm and PSS SDV 5 µm, lin s, ID 8x300 mm) with an Agilent PL220 RI detector were used at 160°C.

TGA/DSC

Thermogravimetric Analysis (TGA) and Differential Scanning Calorimetry (DSC) measurements were recorded with a TGA/DSC1 STAR System by Mettler Toledo. The heating rate was 10K/min and Argon was used as carrier gas.

UV/Vis spectroscopy

Ultraviolet-visible (UV/Vis) spectroscopy measurements were carried out using a Jasco V-670 UV/Vis spectrometer.

PL spectroscopy

Photoluminescence (PL) spectra were recorded on a Horiba FluoroMax4.

IR spectroscopy

Infrared (IR) spectroscopy was carried out using a Jasco FT/IR-4200 spectrometer with an ATR unit by Specane.

Photoelectron spectroscopy

The HOMO-levels of the polymers were recorded with a Photoelectron-Spectrometer by Riken Keiki, model AC-2, with energy seek area of 3.4-6.2 eV, in spin-cast films on ITO surface at ambient conditions.

6.2. Monomer Synthesis

2-Hydroxy-1,2-di(thiophen-3-yl)ethanone (C1)

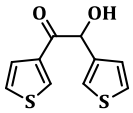

Thiophene-3-carbaldehyde (80.71 g, 719.01 mmol), 3-benzyl-5-(2-hydroxyethyl)-4-methyl-3-thiazoliumchloride (4.81 g, 17.81 mmol) and trimethylamine (24.01 g, 237.01 mmol) were dissolved in ethanol (202 mL). The reaction mixture was heated to 80°C and stirred for 3 hours. After cooling to room temperature, the solution was poured into iced water. The yellowish crude product was filtered off, washed with water, and recrystallised from ethanol to yield the desired white product (56.87 g, 70.1%).

^{1}H NMR (600 MHz, $CDCl_3$) δ [ppm] = 8.05 (dd, J = 2.9, 1.2 Hz, 1H, Ar-H), 7.51 (dd, J = 5.1, 1.3 Hz, 1H, Ar-H), 7.33 (dd, J = 2.8, 1.1 Hz, 1H, Ar-H), 7.30-7.27 (m, 2H, Ar-H), 7.00 (dd, J = 5.0, 1.3 Hz, 1H, Ar-H), 5.84 (d, J = 5.9 Hz, 1H, CH-OH), 4.33 (d, J = 6.0 Hz, 1H, OH). **^{13}C NMR** (151 MHz, $CDCl_3$) δ [ppm] = 192.6 (C=O), 140.1 (Ar-R), 138.1 (Ar-R), 134.3 (Ar-H), 127.4 (Ar-H), 127.2 (Ar-H), 126.7 (Ar-H), 126.4 (Ar-H), 124.3 (Ar-H), 72.6 (CH-OH). **GC-MS**: m/z [M^+] = 224.0.

1,2-Di(thiophen-3-yl)ethane-1,2-dion (C2)

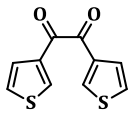

Copper(II)sulphate*5H_2O (45.81 g, 182.99 mmol) was dissolved in a mixture of pyridine (75 mL) and water (40 mL) and heated to 60°C. 2-Hydroxy-1,2-di(thiophen-3-yl)ethanone (18.69 g, 83.01 mmol) was added in one portion. The solution was heated to 80°C for 1 hour. At room temperature, 10% hydrochloric acid was added. After extraction with diethyl ether, the organic phase was dried over magnesium sulphate and the solvent was removed under reduced pressure. 1,2-Di(thiophen-3-yl)ethane-1,2-dione was recrystallised from isopropanol to afford yellow crystals (15.95 g, 86.1%).

^{1}H NMR (600 MHz, $C_2D_2Cl_4$) δ [ppm] = 8.30 (s, 2H, Ar-H), 7.63 (d, J = 4.7 Hz, 2H, Ar-H), 7.36 (dd, J = 4.9, 2.8 Hz, 2H, Ar-H). **^{13}C NMR** (151 MHz, $C_2D_2Cl_4$) δ [ppm] = 186.2 (C=O), 137.9 (Ar-H), 137.8 (Ar-R), 127.8 (Ar-H), 127.5 (Ar-H). **GC-MS**: m/z [M^+] = 221.9.

2-Hydroxy-2,2-di(thiophen-3-yl)acetic acid (C3)

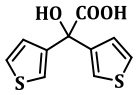

Potassium hydroxide (44.41 g, 790.98 mmol) was dissolved in a mixture of water (100 mL) and ethanol (100 mL). 1,2-Di(thiophen-3-yl)ethane-1,2-dione (51.71 g, 233.01 mmol) was added and the reaction mixture was dived into a 90°C hot oil bath. After 15 minutes the reaction mixture was cooled to 0°C. The pH was adjusted to 1 by adding concentrated hydrochloric acid. Ethanol was removed under reduced pressure. The remaining aqueous phase was extracted with diethyl ether and the combined organic phase was extracted with saturated sodium carbonate solution. The aqueous solution mixture was acidified with 10% hydrochloric acid which leads to a precipitate. The precipitate was filtered off and dissolved in diethyl ether, washed with water and dried over magnesium sulphate. The solvent was removed under reduced pressure. Crude, beige 2-hydroxy-2,2-di(thiophen-3-yl)acetic acid (45.15 g, 81.1%) was used in the next step without further purification.

^{1}H NMR (400 MHz, MeOD) δ [ppm] = 7.36-7.32 (m, 4H, Ar-H), 7.17-7.13 (m, 2H, Ar-H), 4.89 (s, 2H, OH). **^{13}C NMR** (101 MHz, MeOD) δ [ppm] = 175.9 (C=O), 145.4 (Ar-R), 128.3 (Ar-H), 126.3 (Ar-H), 123.6 (Ar-H), 77.9 (HO-C-COOH). **GC-MS**: m/z [M-OH] = 224.0.

4H-Cyclopenta[1,2-b:5,4-b´]dithiophene-4-carboxylic acid (C4)

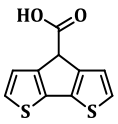

2-Hydroxy-2,2-di(thiophen-3-yl)acetic acid (16.14 g, 67.21 mmol) was dissolved in benzene (175 mL) and cooled to 5°C. Aluminium trichloride (29.93 g, 223.99 mmol) was added to the reaction. The reaction solution was heated to 100°C and stirred for

30 minutes. After cooling the reaction mixture to room temperature, water and 4N hydrochloric acid were added and the mixture was extracted with diethyl ether. The organic phase was dried over magnesium sulphate and the solvent was removed under reduced pressure. 4*H*-Cyclopenta[1,2-*b*:5,4-*b*']dithiophene-4-carboxylic acid was purified by recrystallization from diisopropyl ether to afford a slightly violet product (15.33 g, 95.1%).

^{1}H NMR (600 MHz, $(CD_3)_2CO$) δ [ppm] = 11.18 (s, 1H, COOH), 7.38 (d, J = 4.9 Hz, 2H, Ar-H), 7.26-7.25 (m, 2H, Ar-H), 4.76 (s, 2H, CH-COOH). **^{13}C NMR** (151 MHz, $(CD_3)_2CO$) δ [ppm] = 170.0 (C=O), 149.1 (Ar-R), 139.0 (Ar-R), 126.2 (Ar-H), 124.6 (Ar-H), 49.9 (CH-COOH). **GC-MS**: m/z [M-COOH] = 178.0.

4H-Cyclopenta[1,2-b:5,4-b´]dithiophene (C5)

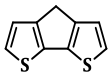

4*H*-Cyclopenta[1,2-*b*:5,4-*b*']dithiophene-4-carboxylic acid (7.68 g, 34.61 mmol) and copper (1.65 g, 25.89 mmol) were dissolved in freshly distilled quinoline (50 mL). The reaction mixture was heated to 245°C for 45 minutes. At room temperature, the suspension was poured into a mixture of ice and hydrochloric acid. After adding diethyl ether, the mixture was filtered off and the filtrate washed with 10% hydrochloric acid, water, and sodium carbonate solution. The organic phase was dried over magnesium sulphate and the solvent was removed under reduced pressure. 4*H*-Cyclopenta[1,2-*b*:5,4-*b*']dithiophene was purified by silica gel column chromatography (eluent: hexane) to afford the greyish product (4.29 g, 69.6%).

^{1}H NMR (400 MHz, $C_2D_2Cl_4$) δ [ppm] = 7.14 (d, J = 4.9 Hz, 2H, Ar-H), 7.05 (d, J = 4.9 Hz, 2H, Ar-H), 3.48 (s, 2H, Ar_2-CH_2). **^{13}C NMR** (101 MHz, $C_2D_2Cl_4$) δ [ppm] = 150.1 (Ar-R), 138.8 (Ar-R), 125.0 (Ar-H), 123.4 (Ar-H), 32.2 (Ar_2-CH_2). **GC-MS**: m/z [M^+] = 178.0.

4,4-Didodecyl-4H-cyclopenta[1,2-b:5,4-b']dithiophene (C6)

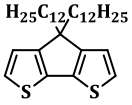

4*H*-Cyclopenta[1,2-*b*:5,4-*b*']dithiophene (0.85 g, 4.75 mmol), potassium hydroxide (1.07 g, 18.99 mmol), and potassium iodide (0.03 g, 0.19 mmol) were suspended in dimethyl sulfoxide (30 mL). 1-Bromododecane (2.37 g, 9.53 mmol) was added and the reaction was stirred at room temperature for 14 hours. After adding water, the reaction mixture was poured into brine. The mixture was extracted with diisopropyl ether and the combined organic phase was dried over magnesium sulphate and the solvent was removed under reduced pressure. The desired product was obtained as yellowish oil (1.21 g, 49.1%) after a silica gel column chromatography (eluent: hexane).

^{1}H NMR (600 MHz, $CDCl_3$) δ [ppm] = 7.14 (d, J = 4.9 Hz, 2H, Ar-H), 6.93 (d, J = 4.9 Hz, 2H, Ar-H), 1.95-1.74 (m, 4H, C-$(CH_2)_2$), 1.43 (dt, J = 14.7, 7.2 Hz, 4H, C-$(CH_2$-$CH_2)_2$), 1.38-1.02 (m, 32H, CH_2), 0.98-0.92 (m, 4H, CH_2-CH_3), 0.90-0.87 (m, 6H, CH_3). **^{13}C NMR** (151 MHz, $CDCl_3$) δ [ppm] = 158.8 (Ar-R), 137.0 (Ar-R), 124.8 (Ar-H), 122.0 (Ar-H), 53.3 (C-$(CH_2)_2$), 37.7 (CH_2), 32.8 (CH_2), 31.8 (CH_2), 29.5 (CH_2), 29.4 (CH_2), 29.3 (CH_2), 29.2 (CH_2), 28.7 (CH_2), 28.01 (CH_2), 24.4 (CH_2), 22.5 (CH_2), 13.9 (CH_3). **GC-MS**: m/z [M^+] = 515.4.

4,4-Didodecyl-2,6-bis(trimethylstannyl)-4H-cyclopenta[1,2-b:5,4-b']dithiophene (C8)

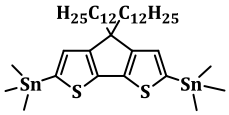

4,4-Didodecyl-4*H*-cyclopenta[1,2-*b*:5,4-*b*']dithiophene (2.91 g, 5.41 mmol) was dissolved in dry tetrahydrofuran (25 mL) and cooled to -78°C. During 20 minutes, *n*-butyl lithium (7.7 mL, 21.65 mmol, 2.8 M) was added and the solution was stirred for 60 minutes at -78°C, followed by heating to 75°C for 45 minutes. Trimethyltin chloride (21.7 mL, 21.65 mmol, 1 M) was added dropwise to the cold solution. The reaction mixture was heated to reflux for 45 minutes. After stirring at 20°C for additional 12 hours, the reaction mixture was poured into diluted ammonium chloride solution, extracted with diethyl ether and dried over magnesium sulphate. Evaporation of the solvent is followed by heating to 80°C at a vacuum of $1x10^{-3}$ mbar for 12 hours. A column chromatography using alumina oxide with 10% water as stationary phase (eluent: hexane with 3% trimethylamine) afforded a mixture of 80.5% 4,4-didodecyl-

2,6-bis(trimethylstannyl)-4*H*-cyclopenta[1,2-*b*:5,4-*b*']dithiophene, 18% 4,4-didodecyl-2-(trimethylstannyl)-4*H*-cyclopenta[1,2-*b*:5,4-*b*']dithiophene, and 1.5% 4,4-didodecyl-4*H*-cyclopenta[1,2-*b*:5,4-*b*']dithiophene. The product mixture (3.56 g, 78.1%) was used without further purification.

^{1}H NMR (600 MHz, $C_2D_2Cl_4$) δ [ppm] = 6.93-6.84 (m, 2H, Ar-H), 1.95-1.74 (m, 4H, C-$(CH_2)_2$), 1.75-1.67 (m, 4H, C-$(CH_2$-$CH_2)_2$), 1.27-1.09 (m, 32H, CH_2), 1.00-0.97 (m, 4H, CH_2-CH_3), 0.81 (t, J = 7.1 Hz, 6H, CH_3) 0.31 (s, 18H, Sn-CH_3). **^{13}C NMR** (151 MHz, $C_2D_2Cl_4$) δ [ppm] = 160.9 (Ar-R), 142.2 (Ar-Sn), 137.2 (Ar-R), 129.9 (Ar-H), 52.4 (C-$(CH_2)_2$), 37.6 (CH_2), 32.2 (CH_2), 30.3 (CH_2), 30.0 (CH_2), 30.0 (CH_2), 29.9 (CH_2), 29.7 (CH_2), 24.9 (CH_2), 23.0 (CH_2), 14.5 (CH_3), -7.6 (Sn-CH_3).

Calculation of the ratio:

The ^{1}H NMR spectra of the mixture was compared with the spectra of **C6** and **C11** to identify the peaks. Three peaks are depicted in the spectra, whereas the signal between δ = 7.08-7.07 ppm results from the non-stannylated CPDT. The signal between δ = 7.04-7.03 ppm is dedicated to the mono-stannylated CPDT and the signal between δ = 6.93-6.84 ppm contains proton signals of all three compounds. The integration is set to the non-stannylated compound, this integral (I_{non}) contains two protons. The adjacent peak assigned to one of the three proton signals of the mono-stannylated CPDT and has an integral (I_{mono}) of fourteen. The integral (I_{mix}) contains protons of the non-stannylated, mono-stannylated, and di-stannylated compounds and has a value of 155. The following equation shows the relation between these integrals:

$$I_{di} = I_{mix} - I_{non} - 2 * I_{mono}$$

$$I_{di} = 155 - 2 - 2 * 14$$

$$I_{di} = 125$$

Therefore, 125 protons are dedicated to the di-stannylated compound. By converting the proton ratio into the molar ratio a relation of 1:14:62 (non-stannylated: mono-stannylated: di-stannylated compound) is calculated by the following equation:

$$ratio = \frac{I_{non}}{2} : I_{mono} : \frac{I_{di}}{2}$$

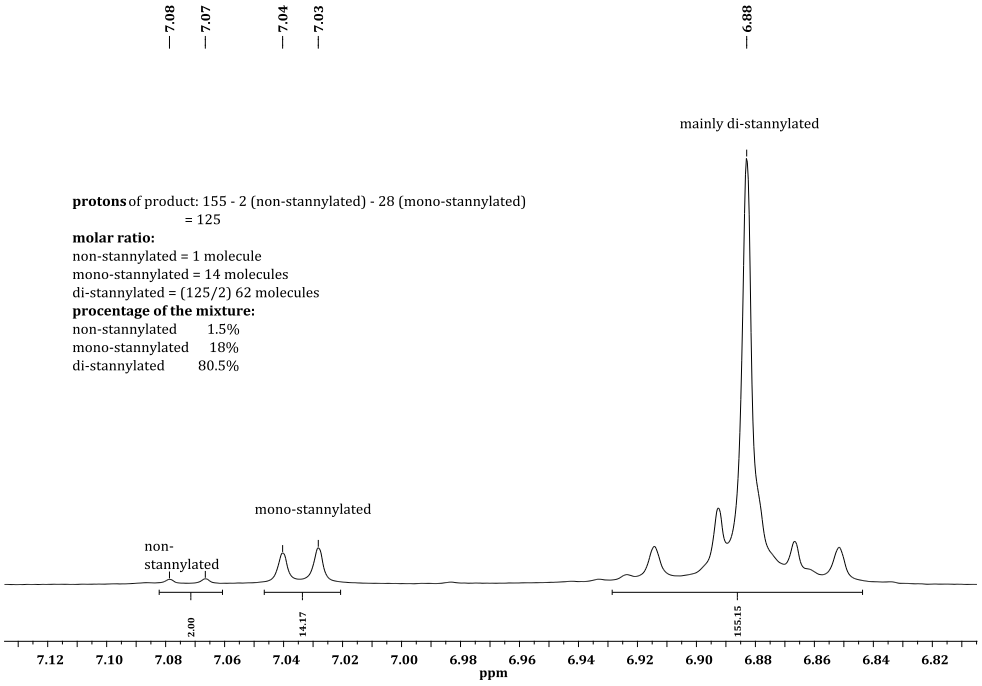

Figure 59: Section of ^{1}H NMR spectrum recorded in $C_2D_2Cl_4$ (5.91 ppm) of the mixture including calculation of the ratio of di-stannylated C8, mono-stannylated, and non-stannylated C6

4,4-didodecyl-2-(trimethylstannyl)-4H-cyclopenta[1,2-b:5,4-b']dithiophene (C11)

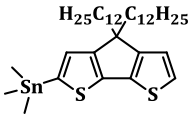

In a dry flask, 4,4-didodecyl-4*H*-cyclopenta[1,2-*b*:5,4-*b*']dithiophene (0.94 g, 1.82 mmol) was dissolved in dry tetrahydrofuran (10 mL). The solution was cooled to -78°C and *n*-butyl lithium (0.7 mL, 1.82 mmol, 2.8 M) was added and the solution was stirred for 1 hour at this temperature. Stirring an additional hour at 20°C is followed by cooling to -78°C. Trimethyltin chloride (1.8 mL, 1.82 mmol, 1 M) was added and the solution was allowed to warm up to room temperature overnight. The reaction mixture was poured into diluted ammonium chloride solution and extracted with diethyl ether. Drying over magnesium sulphate is followed by removal of the solvent under reduced pressure. The crude product was dried at 80°C at a vacuum of $1x10^{-3}$ mbar for 12 hours. Aluminium oxide with 10% water as stationary phase (eluent: hexane with 3% trimethylamine) was used for column chromatography to obtain the desired product

(1.04 g, 84.1%) in a mixture with the starting material. The 6/4 mixture was used without further purification.

^{1}H NMR (600 MHz, $CDCl_3$) δ [ppm] = 7.11 (d, J = 4.8 Hz, 1H, Ar-H), 6.95 (s, 1H, Ar-H), 6.93 (d, J = 4.8 Hz, 1H, Ar-H) 1.84-1.80 (m, 4H, C-$(CH_2)_2$), 1.27-1.09 (m, 36H, CH_2), 1.02-0.89 (m, 4H, CH_2-CH_3), 0.89 (t, J = 7.1 Hz, 6H, CH_3), 0.39 (s, 9H, Sn-CH_3). **^{13}C NMR** (151 MHz, $CDCl_3$) δ [ppm] = 158.3 (Ar-R), 142.3 (Ar-Sn), 137.5 (Ar-R), 136.8 (Ar-R), 136.6 (Ar-R), 129.4 (Ar-H), 124.2 (Ar-H), 121.8 (Ar-H), 52.9 (C-$(CH_2)_2$), 37.8 (CH_2), 32.1 (CH_2), 30.2 (CH_2), 30.2 (CH_2), 29.8 (CH_2), 29.8 (CH_2), 29.7 (CH_2), 24.7 (CH_2), 22.8 (CH_2), 14.3 (CH_3), -7.9 (Sn-CH_3).

9-(Iodomethyl)nonadecane (C7a)

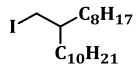

2-Octyldodecan-1-ol (36.41 mL, 102.01 mmol), 1*H*-imidazole (8.35 g, 123.01 mmol), and triphenylphosphine (32.21 g, 123.01 mmol) were dissolved in methylene chloride (145 mL) and treated with iodine (31.09 g, 123.01 mmol) at 0°C. The reaction was stirred for 3 days at room temperature. Sodium sulphite solution was added and the organic phase was washed with water and brine. The organic phase was dried over magnesium sulphate and the solvent was removed under reduced pressure. The crude product was filtered over silica gel to afford the desired product (40.01 g, 95.9%) as colourless oil.

^{1}H NMR (400 MHz, $CDCl_3$) δ [ppm] = 3.27 (d, J = 4.6 Hz, 2H, I-CH_2), 1.39-1.17 (m, 32H, CH_2), 1.13-1.12 (m, 1H, CH), 0.89 (t, J = 6.8 Hz, 6H, CH_3). **^{13}C NMR** (101 MHz, $CDCl_3$) δ [ppm] = 38.9 (CH), 34.6 (CH_2), 32.1 (CH_2), 32.1 (CH_2), 29.9 (CH_2), 29.8 (CH_2), 29.8 (CH_2), 29.7 (CH_2), 29.5 (CH_2), 29.5 (CH_2), 26.7 (CH_2), 22.8 (CH_2), 16.8 (CH_2), 14.6 (CH_3). **GC-MS**: m/z [M-IH] = 281.4.

4,4-Bis(2-octyldodecyl)-4H-cyclopenta[1,2-b:5,4-b']dithiophene (C7)

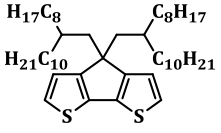

4*H*-Cyclopenta[1,2-*b*:5,4-*b*']dithiophene (3.73 g, 20.91 mmol), potassium iodide (0.16 g, 0.94 mmol), and potassium hydroxide (4.72 g, 84.01 mmol) were dissolved in dimethyl sulfoxide (60 mL). The reaction solution was heated to 60°C. 9-(Iodomethyl)nonadecane (18.33 g, 44.89 mmol) was added to the reaction. The reaction was stirred at 60°C for 3 days. Water and brine were added and the mixture was extracted with diethyl ether. The organic phase was dried over magnesium sulphate and the solvent was removed under reduced pressure. After a silica gel column chromatography (eluent: hexane), several RP18-silica gel column chromatographies (eluent: tetrahydrofuran/ water 8/2) lead to the product as brownish oil (12.19 g, 79.1%).

^{1}H NMR (400 MHz, $C_2D_2Cl_4$) δ [ppm] = 7.03 (d, J = 4.9 Hz, 2H, Ar-H), 6.85 (d, J = 4.9 Hz, 2H, Ar-H), 1.78 (d, J = 5.0 Hz, 4H, C-$(CH_2)_2$), 1.28-0.98 (m, 44H, CH_2), 0.89 (m, 14H, CH_2), 0.84-0.74 (m, 22H, CH_3, CH_2), 0.62-0.49 (m, 2H, CH). **^{13}C NMR** (101 MHz, $C_2D_2Cl_4$) δ [ppm] = 157.9 (Ar-R), 136.9 (Ar-R), 124.3 (Ar-H), 122.7 (Ar-H), 53.5 (C-$(CH_2)_2$), 44.0 (CH_2), 35.3 (CH_2), 33.8 (CH), 32.5 (CH_2), 32.2 (CH_2), 30.0 (CH_2), 30.0 (CH_2), 30.0 (CH_2), 29.9 (CH_2), 29.9 (CH_2), 29.7 (CH_2), 29.6 (CH_2), 26.6 (CH_2), 23.1 (CH_2), 23.0 (CH_2), 14.6 (CH_3). **FD-MS**: m/z [M^+] = 739.3.

2,6-Dibromo-4,4-bis(2-octyldodecyl)-4H-cyclopenta[1,2-b:5,4-b']dithiophene (C9)

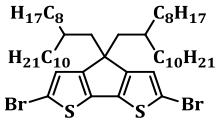

Benzyltrimethylammonium tribromide (4.11 g, 10.55 mmol) and zinc chloride (1.58 g, 11.60 mmol) were treated with 4,4-bis(2-octyldodecyl)-4*H*-cyclopenta[1,2-*b*:5,4-*b*']dithiophene (3.71 g, 5.02 mmol) in dimethylformamide (80 mL). The reaction was stirred at 20°C for 2.5 hours. Water and a solution of 5% sodium bisulphate were added and the mixture was extracted with hexane. To obtain the desired brownish product, (3.91 g, 87.1%) several columns on a flash chromatography system (eluent: hexane) were necessary.

^{1}H NMR (600 MHz, $C_2D_2Cl_4$) δ [ppm] = 6.88 (s, 2H, Ar-H), 1.73 (d, J = 5.1 Hz, 4H, C-$(CH_2)_2$), 1.32-1.02 (m, 44H, CH_2), 0.97-0.85 (m, 14H, CH_2), 0.82 (t, J = 7.2 Hz, 18H, CH_3), 0.53 (dt, J = 10.9, 5.4 Hz, 2H, CH). **^{13}C NMR** (151 MHz, $C_2D_2Cl_4$) δ [ppm] = 155.8 (Ar-R),

136.8 (Ar-R), 125.7 (Ar-H), 110.9 (Ar-Br), 55.3 (C-$(CH_2)_2$), 43.7 (CH_2), 35.4 (CH_2), 33.9 (CH), 32.3 (CH_2), 32.2 (CH_2), 30.1 (CH_2), 30.1 (CH_2), 30.0 (CH_2), 30.0 (CH_2), 29.9 (CH_2), 29.7 (CH_2), 29.7 (CH_2), 23.1 (CH_2), 14.6 (CH_3). **APCI-MS**: m/z [M^+] = 896.5.

4,4-Bis(2-octyldodecyl)-2,6-bis(trimethylstannyl)-4H-cyclopenta[1,2-b:5,4-b']dithiophene (C10)

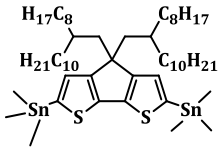

2,6-Dibromo-4,4-bis(2-octyldodecyl)-4*H*-cyclopenta[1,2-*b*:5,4-*b*']dithiophene (2.33 g, 2.59 mmol) was dissolved in dry tetrahydrofuran (44 mL) and *N,N,N',N'*-tetramethylmethanediamine (1.4 mL, 10.37 mmol) was added. The solution was cooled to -78°C. *n*-Butyl lithium (4.3 mL, 10.37 mmol, 2.4 M) was added and the mixture was stirred for 60 minutes at -78°C. After reacting at 20°C for 60 minutes, the mixture was cooled to -78°C again. Trimethyltin chloride (10.4 mL, 10.37 mmol, 1 M) was added in one shot. The reaction was allowed to warm to room temperature overnight and poured into ammonia chloride solution and extracted with diethyl ether. After the solvent was dried over magnesium sulphate, it was removed under reduced pressure. The red-brownish oil (2.27 g, 82.1%) was used without further purification.

^{1}H NMR (400 MHz, $C_2D_2Cl_4$) δ [ppm] = 6.94 (s, 2H, Ar-H), 1.85 (d, J = 4.7 Hz, 4H, C-$(CH_2)_2$), 1.38-1.07 (m, 50H, CH_2), 0.96-0.86 (m, 26H, CH_2, CH_3), 0.65-0.56 (m, 2H, CH), 0.37 (s, 18H, CH_3). **^{13}C NMR** (101 MHz, $C_2D_2Cl_4$) δ [ppm] = 160.0 (Ar-R), 142.8 (Ar-Sn), 136.3 (Ar-R), 130.6 (Ar-H), 52.5 (C-$(CH_2)_2$), 43.9 (CH_2), 35.8 (CH_2), 34.0 (CH), 32.2 (CH_2), 32.2 (CH_2), 30.2 (CH_2), 30.0 (CH_2), 30.0 (CH_2), 30.0 (CH_2), 29.7 (CH_2), 26.9 (CH_2), 23.0 (CH_2), 14.6 (CH_3), -7.8 (CH_3). **^{119}Sn NMR** (149 MHz, $C_2D_2Cl_4$) δ [ppm] = -28.5. **FD-MS**: m/z [M^+] = 1064.8.

4,4-Bis(2-octyldodecyl)-2-(trimethylstannyl)-4H-cyclopenta[1,2-b:5,4-b']dithiophene (C12)

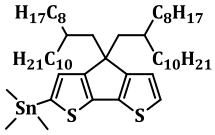

4,4-Bis(2-octyldodecyl)-4*H*-cyclopenta[1,2-*b*:5,4-*b*']dithiophene (1.44 g, 1.95 mmol) was dissolved in tetrahydrofuran (25 mL). At -78°C, the solution was treated with *n*-butyl lithium (0.9 mL, 1.95 mmol, 2.2 M). After the reaction was stirred for 1 hour at -78°C, it was heated to 20°C for an additional hour, followed by cooling to -78°C and treating with trimethyltin chloride (2.0 mL, 1.95 mmol, 1 M). The reaction mixture was allowed to warm up to room temperature overnight and was poured into ammonium chloride solution. After the mixture was extracted with diethyl ether, the combined organic phase was dried over magnesium sulphate and the solvent was removed under reduced pressure. The product was dried at 80°C and a vacuum of $1x10^{-3}$ mbar for 12 hours. The brown oil (1.51 g, 85.1%) was used for the next reaction without further purification.

^{1}H NMR (400 MHz, $C_2D_2Cl_4$) δ [ppm] = 7.08 (d, J = 4.9 Hz, 1H, Ar-H), 6.98 (s, 1H, Ar-H), 6.93 (d, J = 4.9 Hz, 1H, Ar-H), 1.89-1.87 (m, 4H, C-$(CH_2)_2$), 1.37-1.08 (m, 50H, CH_2), 0.92-0.88 (m, 26H, CH_2, CH_3), 0.66-0.63 (m, 2H, CH), 0.39 (s, 9H, CH_3). **^{13}C NMR** (101 MHz, $C_2D_2Cl_4$) δ [ppm] = 160.0 (Ar-R), 157.8 (Ar-R), 142.6 (Ar-Sn), 137.2 (Ar-R), 136.7 (Ar-R), 130.5 (Ar-H), 123.9 (Ar-H), 122.8 (Ar-H), 53.1 (C-$(CH_2)_2$), 44.0 (CH_2), 32.3 (CH_2), 32.3 (CH), 32.2 (CH_2), 32.2 (CH_2), 30.2 (CH_2), 30.1 (CH_2), 30.0 (CH_2), 29.9 (CH_2), 29.7 (CH_2), 29.7 (CH_2), 26.8 (CH_2), 23.1 (CH_2), 14.5 (CH_3), -7.9 (CH_3). **^{119}Sn NMR** (149 MHz, $C_2D_2Cl_4$) δ [ppm] = -28.5. **FD-MS**: m/z [M^+] = 901.7.

2-Bromo-9,9-didodecyl-9H-fluorene (F3)

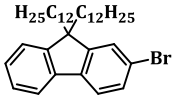

2-Bromo-9*H*-fluorene (10.10 g, 41.71 mmol), tetra-*n*-butylammonium bromide (4.17 g, 12.94 mmol), sodium hydroxide (27.37 g, 342.01 mmol), and 1-bromododecane (22.01 mL, 90.99 mmol) were dissolved in dimethyl sulfoxide (100 mL) and water

(20 mL). The reaction mixture was heated to 80°C for 3 hours. The mixture was poured on water, extracted with diethyl ether and washed with brine. The solvent was dried over magnesium sulphate und removed under reduced pressure. To obtain the desired brownish oil (20.88 g, 87.1%), a silica gel column chromatography (eluent: hexane) was done.

^{1}H NMR (600 MHz, $C_2D_2Cl_4$) δ [ppm] = 7.61-7.57 (m, 1H, Ar-H), 7.48 (d, J = 8.0 Hz, 1H, Ar-H), 7.42-7.36 (m, 2H, Ar-H), 7.28-7.22 (m, 3H, Ar-H), 1.95-1.73 (m, 4H, CH_2), 1.25-0.92 (m, 36H, CH_2), 0.80 (t, J = 7.1 Hz, 6H, CH_3), 0.61-0.49 (m, 4H, CH_2). **^{13}C NMR** (151 MHz, $C_2D_2Cl_4$) δ [ppm] = 153.4 (Ar-R), 150.6 (Ar-R), 140.4 (Ar-R), 140.1 (Ar-R), 130.1 (Ar-H), 127.8 (Ar-H), 127.1 (Ar-H), 126.4 (Ar-H), 123.3 (Ar-H), 121.3 (Ar-H), 121.1 (Ar-Br), 120.1 (Ar-H), 55.6 (C-(CH_2)$_2$), 40.3 (CH_2), 32.2 (CH_2), 30.3 (CH_2), 29.9 (CH_2), 29.8 (CH_2), 29.6 (CH_2), 29.5 (CH_2), 23.0 (CH_2), 14.5 (CH_3). **APCI-MS**: m/z [M^+] = 582.4.

2-(9,9-Didodecyl-9H-fluoren-2-yl)-4,4,5,5-tetramethyl-1,3,2-dioxaborolane (F4)

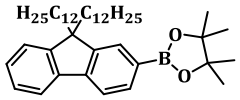

2-Bromo-9,9-didodecyl-9*H*-fluorene (7.01 g, 12.03 mmol), 4,4,4‘,4‘,5,5,5‘,5‘-octamethyl-2,2‘-bi(1,3,2-dioxaborolane) (4.02 g, 15.75 mmol), potassium acetate (5.67 g, 57.81 mmol), and [1,1’-bis(diphenylphosphino)ferrocene]dichloropalladium(II) (0.44 g, 0.59 mmol) were dissolved in dry dioxane (250 mL) and stirred for 16 hours at 90°C. The reaction mixture was diluted with chloroform and water was added. After extraction with chloroform and drying over magnesium sulphate the solvent was removed under reduced pressure. A purification by silica gel and zeolite flash column chromatography (eluent: hexane/DCM 4/1) was done. The yellowish product (4.96 g, 65.6%) was purified by recrystallization from hot hexane.

^{1}H NMR (600 MHz, $C_2D_2Cl_4$) δ [ppm] = 7.71 (d, J = 7.6 Hz, 1H, Ar-H), 7.69 (s, 1H, Ar-H), 7.67-7.64 (m, 1H, Ar-H), 7.61 (d, J = 7.5 Hz, 1H, Ar-H), 7.31-7.23 (m, 3H, Ar-H), 1.91-1.88 (m, 4H, CH_2), 1.38-1.34 (m, 4H, CH_2), 1.29 (s, 12H, CH_3), 1.23-1.03 (m, 32H, CH_2) 0.80 (t, J = 7.1 Hz, 6H, CH_3), 0.56-0.55 (m, 4H, CH_2). **^{13}C NMR** (151 MHz, $C_2D_2Cl_4$) δ [ppm] = 151.6 (Ar-R), 150.3 (Ar-R), 144.2 (Ar-R), 141.0 (Ar-R), 133.8 (Ar-H), 129.3 (Ar-H), 128.0 (Ar-B), 127.9 (Ar-H), 126.9 (Ar-H), 123.4 (Ar-H), 120.4 (Ar-H), 119.2

(Ar-H), 83.9 (C-(CH_3)$_2$), 55.2 (C-(CH_2)$_2$), 40.3 (CH_2), 32.2 (CH_2), 30.3 (CH), 29.9 (CH_2), 29.9 (CH_2), 29.6 (CH_2), 29.5 (CH_2), 25.3 (CH_3), 24.1 (CH_2), 23.0 (CH_2), 14.5 (CH_3). **APCI-MS**: m/z [M^+] = 628.5.

4-Methyl-3-nitroaniline (I1)

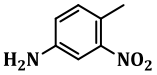

p-Toluidine (25.50 g, 238.01 mmol) was suspended in (70.0 mL, 1312.99 mmol) concentrated sulfuric acid under cooling. Sulfuric acid (45.0 mL, 844.01 mmol) was added dropwise to a solution of 13.0 mL (312.01 mmol) cold nitric acid. The obtained nitration acid was added to the *p*-toluidine suspension at -5°C. The suspension was stirred in the cold and poured into ice after 14 hours. The dark yellow solid was filtered off and washed with water.

The intermediate salt was treated with 2N sodium hydroxide solution and washed excessively with water. The solid was dissolved in chloroform, dried over magnesium sulphate and the solvent was removed under reduced pressure. The resulting product was purified by sublimation to afford the orange target compound (18.39 g, 50.8%).

^{1}H NMR (600 MHz, $C_2D_2Cl_4$) δ [ppm] = 7.17 (d, J = 2.5 Hz, 1H, Ar-H), 7.02 (d, J = 8.2 Hz, 1H, Ar-H), 6.74 (dd, J = 8.2, 2.5 Hz, 1H, Ar-H), 3.79 (s, 2H, NH_2), 2.36 (s, 3H, Ar-CH_3). **^{13}C NMR** (151 MHz, $C_2D_2Cl_4$) δ [ppm] = 149.7 (Ar-NO_2), 145.6 (NH_2), 133.8 (Ar-H), 123.0 (Ar-CH_3), 120.3 (Ar-H), 110.4 (Ar-H), 19.8 (CH_3). **GC-MS**: m/z [M^+] = 152.0. **FT-IR** (ATR): υ [cm^{-1}] = 3477, 3449, 3380, 3353, 3215, 3077, 2964, 2932, 1624, 1610, 1516, 1495, 1456, 1421, 1345, 1307, 1258, 863, 821.

4-Bromo-1-methyl-2-nitrobenzene (I2)

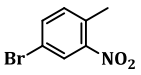

4-Methyl-3-nitroaniline (20.01 g, 131.01 mmol) was dissolved in water (75 mL) and hydrobromic acid (45.1 mL, 398.01 mmol) and cooled to 0°C. Sodium nitrite (16.41 g, 238.01 mmol) was dissolved in water and cooled to 0°C. The sodium nitrite solution was added to the aniline solution, holding the temperature at 0°C. Copper(I) bromide

(18.97 g, 132.01 mmol) was dissolved in hydrobromic acid (17.5 mL, 154 mmol) and heated to reflux. The diazonium salt solution was added to the refluxing solution of copper(I) bromide. After stirring overnight, the suspension was cooled to room temperature and extracted with diethyl ether. The combined organic phase was washed with ammonium chloride solution and water followed by drying over magnesium sulphate. Diethyl ether was removed under reduced pressure and the resulting dark yellow solid was purified by silica gel column chromatography (eluent: hexane/methylene chloride 6/4) affording the bright yellow product (14.38 g, 50.6%).

^{1}H NMR (600 MHz, $CDCl_3$) δ [ppm] = 8.10 (d, J = 2.1 Hz, 1H, Ar-H), 7.61 (dd, J = 2.1 Hz, 1H, Ar-H), 7.25 – 7.20 (m, 1H, Ar-H), 2.54 (s, 3H, Ar-CH_3). **^{13}C NMR** (151 MHz, $CDCl_3$) δ [ppm] = 149.8 (Ar-NO_2), 136.1 (Ar-H), 134.2 (Ar-H), 132.6 (Ar-CH_3), 127.7 (Ar-H), 119.8 (Ar-Br), 20.1 (CH_3). **GC-MS**: m/z [M^+] = 217.0. **FT-IR** (ATR): υ [cm^{-1}] = 3109, 3081, 3066, 2995, 2978, 2931, 2850, 1941, 1521, 1443, 1377, 1333, 1281, 1264, 1159, 1099, 1033, 875, 828, 752.

4-Bromo-2-nitrobenzylidene diacetate (I3)

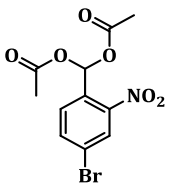

4-Bromo-1-methyl-2-nitrobenzene (37.07 g, 172.01 mmol) was dissolved in a mixture of acetic acid (65.0 mL) and acetic anhydride (14.5 mL) and treated with concentrated sulphuric acid (35.0 mL). The solution was cooled to 5–10°C. Chromium trioxide (47.01 g, 470.01 mmol) was suspended in a mixture of water (25.0 mL) and acetic acid (166.0 mL) and added to the cooled nitrobenzene solution; the temperature was hold between 5–10°C. After stirring for an additional hour, the suspension was poured into ice, and the white precipitate was isolated by filtration. The colourless solid was purified by silica gel column filtration (eluent: methylene chloride/hexane 4/6 to 100% methylene chloride) to yield 20.01 g (35.1%).

^{1}H NMR (400 MHz, $C_2D_2Cl_4$) δ [ppm] = 8.09 (d, J = 1.9 Hz, 1H, Ar-H), 8.01 (s, 1H, Ar-CH), 7.77 (dd, J = 8.4, 1.4 Hz, 1H, Ar-H), 7.54 (d, J = 8.4 Hz, 1H, Ar-H), 2.06 (s, 6H, CO-CH_3). **^{13}C NMR** (101 MHz, $C_2D_2Cl_4$) δ [ppm] = 168.8 (C=O), 148.2 (Ar-NO_2), 137.1

(Ar-H), 129.9 (Ar-H), 129.8 (Ar-CH), 128.3 (Ar-H), 124.4 (Ar-Br), 85.6 (CH), 20.9 (CH_3). **LC-MS**: m/z [M – H,+Na^+] = 354.0. **FT-IR** (ATR): υ [cm^{-1}] = 3109, 3003, 1757, 1530, 1346, 1229, 1196, 1060, 1048, 1010, 998, 974, 953, 909, 896, 938, 825, 759, 727.

4-Bromo-2-nitrobenzaldehyde (I4)

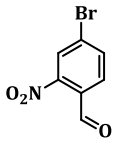

4-Bromo-2-nitrobenzylidene diacetate (19.14 g, 57.01 mmol) was dissolved in ethanol (220.1 mL) and treated with an aqueous potassium hydroxide solution (4.88 g in 100 mL water) at 8°C. After 1 hour of stirring the precipitate was filtered off and washed with water. The crude yellowish compound was purified by silica gel column chromatography (eluent: hexane/methylene chloride 1/1) to yield 11.67 g (88.0%).

^{1}H NMR (400 MHz, $C_2D_2Cl_4$) δ [ppm] = 10.25 (s, 1H, CO-H), 8.16 (d, J = 1.8 Hz, 1H, Ar-H), 7.87 (dd, J = 7.8, 1.8 Hz, 1H, Ar-H), 7.73 (d, J = 8.2 Hz, 1H, Ar-H). **^{13}C NMR** (101 MHz, $C_2D_2Cl_4$) δ [ppm] = 187.6 (CHO), 149.9 (Ar-NO_2), 137.6 (Ar-H), 131.3 (Ar-H), 129.9 (Ar-Br), 128.6 (Ar-CHO), 127.9 (Ar-H). **LC-MS**: m/z [M–H^+] = 227.2. **FT-IR** (ATR): υ [cm^{-1}] = 3091, 3080, 2961, 2923, 2855, 1685, 1588, 1522, 1341, 1258, 1186, 1148, 906, 875, 837, 816, 754, 720.

(E)-6,6'-Dibromo-[2,2'-biindolinylidene]-3,3'-dione (I5)

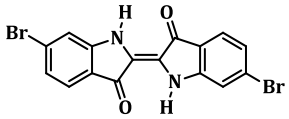

4-Bromo-2-nitrobenzaldehyde (5.28 g, 23.01 mmol) was dissolved in acetone (230 mL) and treated step by step with water (250 mL). The pH of the solution was set to 10 by adding 2N sodium hydroxide solution slowly. Additional to a change of colour from yellow over orange to red brown, gas evolved. After stirring for 4 days, the obtained precipitate was isolated by filtration and washed with water and acetone. 2.66 g (55.2%) of the purple dibromoindigo were obtained.

^{13}C NMR (75 MHz, solid) δ [ppm] = 187.1, 151.4, 121.2, 116.5. **MALDI-TOF**: m/z [M^+] = 419.0. **FT-IR** (ATR): υ [cm^{-1}] = 3381, 3347, 3080, 1885, 1704, 1665, 1631, 1607, 1575, 1473, 1436, 1386, 1311, 1279, 1246, 1203, 1154, 1105, 1080, 1046, 896, 848, 812, 763, 726, 692.

(E)-Di-tert-butyl-6,6'-dibromo-3,3'-dioxo-[2,2'-biindolinylidene]-1,1'-dicarboxylate (I6)

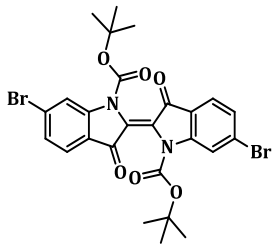

4-Dimethylaminopyridine (0.63 g, 5.01 mmol), di-*tert*-butyl dicarbonate (2.82 g, 13.01 mmol), and (*E*)-6,6'-dibromo-[2,2'-biindolinylidene]-3,3'-dione (2.17 g, 5.01 mmol) were suspended in methylene chloride (110 mL) and stirred for 4 days. This solution was filtered over silica gel with a solvent mixture of hexane/ethyl acetate 9/1. To afford the desired product, several recrystallizations from ethyl acetate were necessary. 1.17 g (36.5%) of the pink product were obtained.

^{1}H NMR (600 MHz, $C_2D_2Cl_4$) δ [ppm] = 8.26 (s, 2H, Ar-H), 7.61 (d, J = 8.1 Hz, 2H, Ar-H), 7.36 (dd, J = 8.2, 1.6 Hz, 2H, Ar-H), 1.61 (s, 18H, CH_3). **^{13}C NMR** (151 MHz, $C_2D_2Cl_4$) δ [ppm] = 182.5 (C=O), 149.7 (Ar-R), 149.6 (Ar-R), 131.2 (NC=CN), 127.9 (Ar-H), 125.1 (Ar-H), 121.8 (Ar-Br), 120.4 (Ar-H), 85.4 (C-$(CH_3)_3$), 28.2 (CH_3). **APCI-MS**: m/z [M^+] = 621.0. **FT-IR** (ATR): υ [cm^{-1}] = 3119, 2999, 2964, 1739, 1674, 1595, 1581, 1420, 1367, 1313, 1267, 1254, 1240, 1184, 1137, 1083, 1052, 1003, 872, 840, 828, 773, 704.

3-Dodecylthiophene (T1)

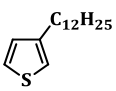

3-Bromothiophene (10.98 g, 67.30 mmol) and [1,3-bis(diphenylphosphino)-propane]dichloronickel(II) (0.37 g, 0.67 mmol) were dissolved in heptane (100 mL) and

tetrahydrofuran (60 mL) and cooled to 0°C. Dodecylmagnesium bromide (94.0 ml, 94.01 mmol, 1 M) was added dropwise to the cold solution. The reaction mixture was heated for 12 hours at 85°C. After the reaction mixture was cooled to 20°C, 1N hydrochloric acid was added and the mixture was washed with water. The solvent was removed under reduced pressure after it was dried over magnesium sulphate. The brown oil was precleaned by silica gel filtration column (eluent: hexane). The following distillation afforded a yellowish oil (13.52 g, 80.1%).

^{1}H NMR (400 MHz, $C_2D_2Cl_4$) δ [ppm] = 7.21 (dd, J = 4.9, 2.9 Hz, 1H, Ar-H), 6.92 (m, 2H, Ar-H), 2.61 (t, J = 7.5 Hz, 2H, Ar-CH_2), 1.68-1.53 (m, 2H, ArCH_2-CH_2), 1.31-1.27 (m, 18H, CH_2), 0.90 (t, J = 6.7 Hz, 3H, CH_3). **^{13}C NMR** (101 MHz, $C_2D_2Cl_4$) δ [ppm] = 143.6 (Ar-alkyl), 128.7 (Ar-H), 125.4 (Ar-H), 120.1 (Ar-H), 32.8 (Ar-CH_2), 30.9 (ArCH_2-CH_2), 30.6 (CH_2), 30.1 (CH_2), 30.1 (CH_2), 30.0 (CH_2), 29.9 (CH_2), 29.8 (CH_2), 29.7 (CH_2), 23.1 (CH_2), 14.5 (CH_3). **GC-MS**: m/z [M^+] = 252.2.

2-Bromo-3-dodecylthiophene (T2)

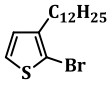

3-Dodecylthiophene (5.01 g, 19.81 mmol) was dissolved in chloroform (30 mL) and acetic acid (30 mL). In portions, 1-bromopyrrolidine-2,5-dione (3.53 g, 19.81 mmol) was added. In the absence of light the reaction mixture was stirred for 2 hours. The solution was treated with water, extracted with chloroform and washed with 2N sodium hydroxide solution. The organic phase was dried over magnesium sulphate and concentrated under reduced pressure. The crude orange oil was purified by silica gel flash chromatography (eluent: hexane). 2-Bromo-3-dodecylthiophene was obtained as yellowish oil (5.59 g, 85.1%).

^{1}H NMR (400 MHz, $C_2D_2Cl_4$) δ [ppm] = 7.13 (d, J = 5.6 Hz, 1H, Ar-H), 6.74 (d, J = 5.6 Hz, 1H, Ar-H), 2.49 (t, J = 7.4 Hz, 2H, Ar-CH_2), 1.15 (m, 2H, ArCH_2-CH_2), 1.25-1.20 (m, 18H, CH_2), 0.82 (t, J = 6.8 Hz, 3H, CH_3). **^{13}C NMR** (101 MHz, $C_2D_2Cl_4$) δ [ppm] = 142.4 (Ar-alkyl), 128.7 (Ar-H), 125.6 (Ar-H), 109.0 (Ar-Br), 32.2 (Ar-CH_2), 30.0 (ArCH_2-CH_2), 30.0 (CH_2), 29.9 (CH_2), 29.7 (CH_2), 29.7 (CH_2), 29.7 (CH_2), 29.6 (CH_2), 23.1 (CH_2), 14.6 (CH_3). **GC-MS**: m/z [M^+] = 332.1.

2-(Trimethylstannyl)-3-dodecylthiophene (T3)

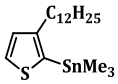

2-Bromo-3-dodecylthiophene (7.04 g, 21.25 mmol) and tetramethylethylendiamine (3.3 mL, 21.87 mmol) were dissolved in tetrahydrofuran (700 mL). The solution was cooled to -78°C and *n*-butyl lithium (8.9 ml, 21.25 mmol, 2.8 M) was added dropwise. The solution was stirred for another hour at -78°C, followed by adding trimethyltin chloride (27.6 ml, 27.60 mmol, 1 M) in one shot. The reaction was allowed to warm up to room temperature overnight. Saturated ammonium chloride solution was added and the solution was extracted three times with diethyl ether. The combined organic phase was dried over magnesium sulphate. 2-(Trimethylstannyl)-3-dodecylthiophene was obtained after removing the solvent under reduced pressure and heating at 50°C under high vacuum as a yellowish oil (8.69 g, 99.0%).

^{1}H NMR (600 MHz, $C_2D_2Cl_4$) δ [ppm] = 7.55-7.52 (m, 1H, Ar-H), 7.14-7.10 (m, 1H, Ar-H), 2.68-2.61 (m, 2H, Ar-CH_2), 1.70-1.56 (m, 2H, ArCH_2-CH_2), 1.43-1.22 (m, 18H, CH_2), 0.92 (m, 3H, CH_3), 0.41 (s, 9H, CH_3). **^{13}C NMR** (151 MHz, $C_2D_2Cl_4$) δ [ppm] = 151.2 (Ar-alkyl), 131.6 (Ar-Sn), 130.8 (Ar-H), 129.8 (Ar-H), 32.9 (Ar-CH_2), 32.5 (Ar-CH_2CH_2), 32.3 (CH_2), 30.0 (CH_2), 30.0 (CH_2), 30.0 (CH_2), 29.9 (CH_2), 29.9 (CH_2), 29.7 (CH_2), 23.1 (CH_2), 14.5 (CH_3), -7.5 (Sn-CH_3). **^{119}Sn NMR** (149 MHz, $C_2D_2Cl_4$) δ [ppm] = -36.6. **FD-MS**: m/z [M^+] = 416.9.

7,14-Di(thiophen-2-yl)diindolo[3,2,1-de:3',2',1'-ij][1,5]naphthyridine-6,13-dione (BAI1)

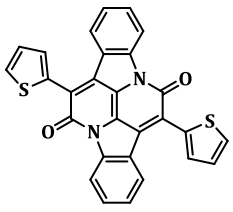

(*E*)-[2,2'-Biindolinylidene]-3,3'-dione (12.23 g, 46.60 mmol) was dissolved in xylene (606 ml) and heated to 145°C. 2-(Thiophen-2-yl)acetyl chloride (23.0 ml, 187.01 mmol) was dissolved in xylene (60 ml) and added during 30 minutes to the indigo solution. The reaction was monitored by TLC and was allowed to stir for 48 hours. The dark red solid

was filtered off and rinsed with tetrahydrofuran. The product (8.53 g, 38.5%) was used for the next step without further purification.

^{1}H NMR (600 MHz, $C_2D_2Cl_4$) δ [ppm] = 8.51 (d, J = 7.8 Hz, Ar-H), 8.05 (d, J = 7.7 Hz, Ar-H), 7.71-7.66 (m, Ar-H), 7.64-7.64 (m, Ar-H), 7.55-7.52 (m, Ar-H), 7.27-7.21 (m, Ar-H). **^{13}C NMR** (151 MHz, $C_2D_2Cl_4$) δ [ppm] = 158.9 (C=O), 144.5 (Ar-R), 134.9 (Ar-R), 132.4 (Ar-H), 130.4 (Ar-H), 130.1 (Ar-R), 130.1 (Ar-H), 126.8 (Ar-H), 126.4 (Ar-H), 125.8 (Ar-R), 125.4 (Ar-H), 125.0 (Ar-R), 122.3 (Ar-R), 118.0 (Ar-H). **MALDI-MS**: m/z [M^+] = 475.1. **FT-IR** (ATR): υ [cm^{-1}] = 3102, 3073, 1625, 1413, 955, 859, 834, 763, 740, 708, 701, 692.

7,14-Bis(5-bromothiophen-2-yl)diindolo[3,2,1-de:3',2',1'-ij][1,5]naphthyridine-6,13-dione (BAI2)

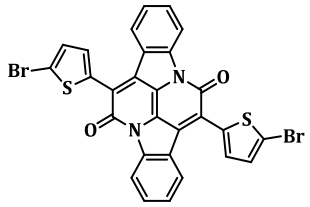

7,14-Di(thiophen-2-yl)diindolo[3,2,1-*de*:3',2',1'-*ij*][1,5]naphthyridine-6,13-dione (9.20 g, 19.41 mmol) was suspended in chloroform (700 ml). 1-Bromopyrrolidine-2,5-dione (3.45 g, 19.41 mmol) was added in portions. After 15 hours, the reaction solution was filtered off and washed with water, acetone, and chloroform. The obtained reddish black product (8.54 g, 69.7%) was used without further purification.

^{1}H NMR (600 MHz, $C_2D_2Cl_4$) δ [ppm] = 8.53 (d, J = 7.8 Hz, Ar-H), 8.14 (d, J = 7.7 Hz, Ar-H), 7.59-7.56 (m, Ar-H), 7.50 (d, J = 3.72 Hz, Ar-H), 7.32-7.29 (m, Ar-H), 7.21 (d, J = 3.8 Hz, Ar-H). **^{13}C NMR** (151 MHz, $C_2D_2Cl_4$) δ [ppm] = 158.2 (C=O), 144.3 (Ar-R), 136.8 (Ar-R), 132.7 (Ar-H), 130.3 (Ar-H), 130.0 (Ar-R), 129.6 (Ar-H), 126.7 (Ar-H), 125.7 (Ar-R), 125.3 (Ar-H), 124.3 (Ar-R), 122.4 (Ar-R), 118.4 (Ar-Br), 118.2 (Ar-H). **MALDI-MS**: m/z [M^+] = 631.8. **FT-IR** (ATR): υ [cm^{-1}] = 3102, 3073, 1765, 1704, 1624, 1413, 1252, 1074, 955, 859, 834, 802, 775, 763, 742, 701, 690.

7,14-Bis(3'-dodecyl-[2,2'-bithiophene]-5-yl)diindolo[3,2,1-de:3',2',1'-ij][1,5]naphthyridine-6,13-dione (BAI3)

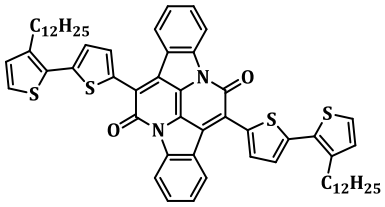

Tri-*o*-tolylphosphine (0.66 g, 2.17 mmol), tetrakis(triphenylphosphane)palladium(0) (0.63 g, 0.54 mmol), 7,14-bis(5-bromothiophen-2-yl)diindolo[3,2,1-*de*:3',2',1'-*ij*][1,5]naphthyridine-6,13-dione (11.41 g, 18.04 mmol), and 2-(trimethylstannyl)-3-dodecylthiophene (17.98 g, 43.31 mmol) were dissolved in toluene (225 mL) and heated to 100°C for 4 days. After concentration of the solution, several silica gel column chromatographies (eluent: hexane/chloroform 1/1 and 5.5/4.5) were needed to purify the purple product (0.27 g, 1.5% yield).

^{1}H NMR (600 MHz, $C_2D_2Cl_4$) δ [ppm] = 8.57 (d, J = 7.7 Hz, 2H, Ar-H), 8.24 (d, J = 7.3 Hz, 2H, Ar-H), 7.76-7.63 (m, 4H, Ar-H), 7.61-7.51 (m, 2H, Ar-H), 7.35-7.26 (m, 2H, Ar-H), 7.22 (d, J = 5.1 Hz, 2H, Ar-H), 6.97 (d, J = 5.1 Hz, 2H, Ar-H), 2.88-2.86 (m, 2H, Ar-CH_2), 2.62-2.60 (m, 2H, CH_2), 1.98-0.86 (m, 40H, CH_2), 0.95-0.78 (m, 6H, CH_3). **^{13}C NMR** (151 MHz, $C_2D_2Cl_4$) δ [ppm] = 158.7 (C=O), 132.7 (Ar-H), 132.6 (Ar-R), 132.5 (Ar-R), 131.3 (Ar-R), 130.5 (Ar-H), 129.0 (Ar-H), 126.3 (Ar-H), 125.3 (Ar-H), 124.7 (Ar-H), 120.4 (Ar-H), 118.0 (Ar-H), 32.1 (CH_2), 30.7 (CH_2), 30.7 (CH_2), 30.5 (CH_2), 29.9 (CH_2), 29.8 (CH_2), 29.8 (CH_2), 29.7 (CH_2), 29.6 (CH_2), 29.4 (CH_2), 22.8 (CH_2), 14.1 (CH_3). **MALDI-MS**: m/z [M^+] = 973.3. **FT-IR** (ATR): υ [cm^{-1}] = 3073, 2952, 2915, 2848, 1727, 1624, 1573, 1457, 1435, 1412, 1379, 1279, 1254, 1159, 1119, 1075, 956, 816, 802, 774, 761, 720, 692.

7,14-Bis(5'-bromo-3'-dodecyl-[2,2'-bithiophene]-5-yl)diindolo[3,2,1-de:3',2',1'-ij][1,5]naphthyridine-6,13-dione (BAI4)

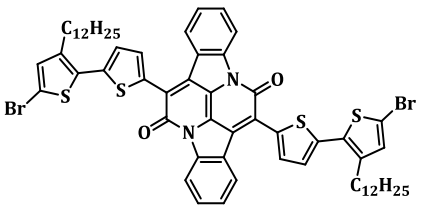

7,14-Bis(3'-dodecyl-[2,2'-bithiophene]-5-yl)diindolo[3,2,1-*de*:3',2',1'-*ij*][1,5]naphthyridine-6,13-dione (0.27 g, 0.28 mmol) was dissolved in chloroform (28 mL) and cooled to 0°C. 1-Bromopyrrolidine-2,5-dione (0.10 g, 0.57 mmol) was added in portions. The reaction was stirred 12 hours at 20°C, followed by washing with water and brine. After the solvent was removed under reduced pressure, 7,14-bis(5'-bromo-3'-dodecyl-[2,2'-bithiophene]-5-yl)diindolo[3,2,1-*de*:3',2',1'-*ij*][1,5]naphthyridine-6,13-dione (0.27 g, 87.1%) was obtained as a purple solid.

^{1}H NMR (600 MHz, $C_2D_2Cl_4$) δ [ppm] = 8.46-8.42 (m, 2H, Ar-H), 8.18-8.17 (m, 2H, Ar-H), 7.66-7.63 (m, 2H, Ar-H), 7.53-7.46 (m, 2H, Ar-H), 7.30-7.25 (m, 2H, Ar-H), 7.19-7.17 (m, 2H, Ar-H), 6.92 (s, 2H, Ar-H), 2.78-2.76 (m, 2H, Ar-CH_2), 2.51-2.49 (m, 2H, CH_2), 1.64-1.55 (m, 4H, CH_2), 1.36-1.09 (m, 36H, CH_2), 0.82-0.77 (m, 6H, CH_3). **^{13}C NMR** (151 MHz, $C_2D_2Cl_4$) δ [ppm] = 158.7 (Ar-R), 144.8 (Ar-R), 144.2 (Ar-R), 140.8 (Ar-R), 134.8 (Ar-R), 132.2 (Ar-H), 131.3 (Ar-R), 131.0 (Ar-R), 130.5 (Ar-H), 129.7 (Ar-R), 126.5 (Ar-H), 126.1 (Ar-H), 125.5 (Ar-H), 124.7 (Ar-R), 123.1 (Ar-H), 120.5 (Ar-R), 118.1 (Ar-H), 111.7 (Ar-Br), 32.1 (Ar-CH_2), 30.7 (ArCH_2-CH_2), 29.8 (CH_2), 29.8 (CH_2), 29.7 (CH_2), 29.7 (CH_2), 29.6 (CH_2), 29.6 (CH_2), 29.5 (CH_2), 29.4 (CH_2), 22.8 (CH_2), 14.2 (CH_3). **MALDI-MS**: m/z [M^+] = 1133.2. **FT-IR** (ATR): υ [cm^{-1}] = 3061, 2952, 2919, 2849, 1721, 1624, 1602, 1432, 1414, 1382, 1291, 1249, 1079, 1061, 962, 839, 792, 751, 720.

N,N-Diethylthiophene-3-carboxamide (BD1)

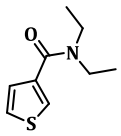

Thiophene-3-carboxylic acid (12.99 g, 101.01 mmol) was dissolved in methylene chloride (60 mL) and cooled to 0°C. Oxalyl dichloride (17.4 mL, 203.02 mmol) was added dropwise followed by one drop of dimethylformamide and the solution was stirred for 12 hours at 20°C. Excessive oxalyl dichloride was removed under reduced pressure. The yellowish solid was dissolved in methylene chloride and added dropwise to a cold solution of diethylamine (21.2 mL, 203.01 mmol) in methylene chloride (60 mL). The solution was stirred for 30 minutes at room temperature. Water was added and the aqueous solution was extracted with chloroform. The combined organic phase was washed with water, dried over magnesium sulphate and the solvent was

removed under reduced pressure. No further purification was necessary to obtain the product as yellow oil (18.43 g, 99.1%)

^{1}H NMR (600 MHz, $C_2D_2Cl_4$) δ [ppm] = 7.41-7.36 (m, 1H, Ar-H), 7.25 (dd, J = 4.8, 3.2 Hz, 1H, Ar-H), 7.11 (d, J = 5.0 Hz, 1H, Ar-H), 3.37 (q, J = 14.2, 7.0 Hz, 4H, CH_2), 1.12 (t, J = 7.2 Hz, 6H, CH_3). **^{13}C NMR** (151 MHz, $C_2D_2Cl_4$) δ [ppm] = 166.4 (C=O), 138.2 (Ar-R), 127.2 (Ar-H), 125.7 (Ar-H), 125.2 (Ar-H), 41.7 (N-CH_2), 13.8 (CH_2-CH_3). **GC-MS**: m/z [M^+] = 183.1.

Benzo[1,2-b:4,5-b']dithiophene-4,8-dione (BD2)

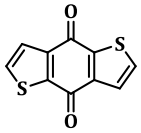

N,N-Diethylthiophene-3-carboxamide (8.01 g, 43.71 mmol) was dissolved in tetrahydrofuran (160 mL) and cooled to 0°C. Under cooling, *n*-butyl lithium (17.2 mL, 48.1 mmol) was added dropwise. After 12 hours of stirring at room temperature, water was added and the dark yellow solid was filtered off. The solid was washed excessively with water, methanol, and hexane followed by recrystallization from glacial acetic acid to afford the yellow product (2.81 g, 58.3%).

^{1}H NMR (600 MHz, $CDCl_3$) δ [ppm] = 7.71 (d, J = 5.0 Hz, 1H, Ar-H), 7.67 (d, J = 5.0 Hz, 1H, Ar-H). **^{13}C NMR** (151 MHz, $CDCl_3$) δ [ppm] = 174.7 (C=O), 145.1 (Ar-R), 143.0 (Ar-R), 133.7 (Ar-H), 126.8 (Ar-H). **GC-MS**: m/z [M^+] = 219.9. **FT-IR** (ATR): υ [cm^{-1}] = 3272, 3094, 3077, 1643, 1621, 1492, 1382, 1281, 1199, 1095, 1007, 919, 547, 831, 764, 754, 724, 694.

2-Octyldodecyl-4-methylbenzenesulfonate (BD3)

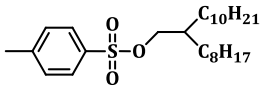

2-Octyldodecan-1-ol (10.15 g, 34.01 mmol) was dissolved in pyridine (27.1 mL, 334.01 mmol) and dry methylene chloride (100 mL) and cooled to 0°C. 4-Methylbenzene-1-sulfonyl chloride (6.41 g, 33.61 mmol) was dissolved in dry methylene chloride (70 mL) and added dropwise to the cold solution. The reaction mixture was

stirred for 24 hours at 20°C and poured into chloroform. The organic phase was washed with 2N hydrochloric acid and brine, dried over magnesium sulphate and the solvent was removed under reduced pressure. To afford the product as colourless oil (11.86 g, 77.1%) a silica gel column chromatography was performed (eluent: hexane/ethyl acetate 9.75/0.25).

^{1}H NMR (400 MHz, $CDCl_3$) δ [ppm] = 7.78 (d, J = 8.3 Hz, 2H, Ar-H), 7.33 (d, J = 8.0 Hz, 2H, Ar-H), 3.91 (d, J = 5.4 Hz, 2H, O-CH_2), 2.44 (s, 3H, Ar-CH_3), 1.63-1.52 (m, 1H, CH), 1.36-1.03 (m, 32H, CH_2), 0.88 (t, J = 6.9 Hz, 6H, CH_3). **^{13}C NMR** (101 MHz, $CDCl_3$) δ [ppm] = 144.7 (Ar-S), 133.4 (Ar-R), 129.8 (Ar-H), 128.1 (Ar-H), 73.0 (O-CH_2), 37.7 (CH-$(CH_2)_2$), 32.0 (CH_2), 32.0 (CH_2), 30.1 (CH_2), 30.0 (CH_2), 29.8 (CH_2), 29.7 (CH_2), 29.6 (CH_2), 26.5 (CH_2), 29.4 (CH_2), 26.6 (CH_2), 22.8 (CH_2), 22.8 (CH_2), 21.7 (CH_3), 14.2 (CH_3). **LC-MS**: m/z [M-IH] = 280.3.

4,8-Bis((2-octyldodecyl)oxy)benzo[1,2-b:4,5-b']dithiophene (BD4)

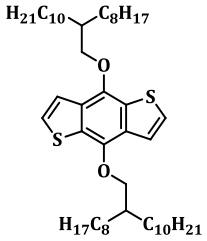

Benzo[1,2-*b*:4,5-*b*']dithiophene-4,8-dione (0.51 g, 2.31 mmol) and zinc (0.33 g, 5.01 mmol) were dissolved in a solution of sodium hydroxide (3.85 g, 96.01 mmol) in water (23 mL). The dark red solution was heated to 100°C for 1 hour. 2-Octyldodecyl-4-methylbenzenesulfonate (3.26 g, 7.21 mmol) and tetrabutylammonium bromide (0.25 g, 0.77 mmol) were added. To keep the reaction solution yellowish, another portion of zinc (0.81 g, 12.38 mmol) was added. The reaction solution was poured into water, extracted several times with diethyl ether and dried over magnesium sulphate. The organic solvent was removed under reduced pressure. The brown oil was purified by silica gel column and several flash column chromatographies (eluent for both: chloroform/hexane 9/1) to afford the purified product (1.07 g, 59.5%).

^{1}H NMR (400 MHz, $CDCl_3$) δ [ppm] = 7.47 (d, J = 5.5 Hz, 2H, Ar-H), 7.36 (d, J = 5.5 Hz, 2H, Ar-H), 4.17 (d, J = 5.1 Hz, 4H, O-CH_2), 1.91-1.86 (m, 2H, CH), 1.71-1.58 (m, 4H, CH_2), 1.57-1.19 (m, 56H, CH_2), 0.93-0.89 (m, 16H, CH_2, CH_3). **^{13}C NMR** (101 MHz, $CDCl_3$)

δ [ppm] = 144.9 (Ar-R), 131.6 (Ar-R), 130.1 (Ar-R), 126.0 (Ar-H), 120.4 (Ar-H), 76.6 (CH_2), 39.4 (CH), 32.1 (CH_2), 32.1 (CH_2), 31.5 (CH_2), 30.2 (CH_2), 29.9 (CH_2), 29.8 (CH_2), 29.8 (CH_2), 29.8 (CH_2), 29.5 (CH_2), 27.2 (CH_2), 22.9 (CH_2), 14.3 (CH_3). **APCI-MS**: m/z [M^+] = 783.6.

4,8-Bis((2-octyldodecyl)oxy)-2,6-bis(trimethylstannyl)benzo[1,2-b:4,5-b']-dithiophene (BD5)

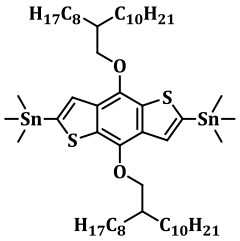

4,8-Bis((2-octyldodecyl)oxy)benzo[1,2-*b*:4,5-*b*']dithiophene (0.45 g, 0.58 mmol) was dissolved in dry tetrahydrofuran (6.2 mL) and cooled to -78°C. *n*-Butyl lithium (0.5 mL, 1.46 mmol, 2.8 M) was added dropwise and the solution was stirred at -78°C for 30 minutes, followed by stirring for 2 hours at 20°C. After the solution was cooled to -78°C trimethyltin chloride (1.8 mL, 1.8 mmol, 1 M) was added and the reaction mixture was allowed to warm up to room temperature overnight. The reaction solution was poured into ammonium chloride solution and extracted with diethyl ether, dried over magnesium sulphate and the solvent was removed under reduced pressure. The colourless solid (0.63 g, 98.1%) was used for the next step without further purification.

^{1}H NMR (600 MHz, $CDCl_3$) δ [ppm] = 7.52 (s, 2H, Ar-H), 4.19 (d, J = 5.3 Hz, 4H, O-CH_2), 1.88-1.85 (m, 2H, CH), 1.69-1.64 (m, 4H, CH_2), 1.53-1.40 (m, 16H, CH_2), 1.39-1.28 (m, 44H, CH_2), 0.90-0.88 (m, 12H, CH_3), 0.45 (s, 18H, CH_2). **^{13}C NMR** (151 MHz, $CDCl_3$) δ [ppm] = 143.4 (Ar-R), 140.5 (Ar-R), 134.0 (Ar-R), 133.1 (Ar-Sn), 128.2 (Ar-H), 76.1 (O-CH_2), 39.4 (CH-$(CH_2)_2$), 32.1 (CH_2), 32.1 (CH_2), 31.6 (CH_2), 30.5 (CH_2), 30.4 (CH_2), 29.9 (CH_2), 29.9 (CH_2), 29.9 (CH_2), 29.9 (CH_2), 29.6 (CH_2), 29.5 (CH_2), 22.9 (CH_2), 14.3 (CH_3), -8.2 (Sn-CH_3). **^{119}Sn NMR** (224 MHz, $C_2D_2Cl_4$) δ [ppm] = -24.6. **FD-MS**: m/z [M^+] = 1108.3.

3-(Dodecyloxy)thiophene (B1)

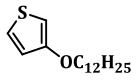

3-Methoxythiophene (4.4 mL, 43.01 mmol), *p*-toluenesulfonic acid monohydrate (0.83 g, 4.38 mmol), and dodecan-1-ol (19.7 mL, 88.01 mmol) were dissolved in toluene (40 mL) and stirred for 15 hours at 130°C. The solution was diluted with methylene chloride, washed with water and dried over magnesium sulphate. The solvent was removed under reduced pressure and the yellowish product was purified by silica gel chromatography (eluent: hexane/methylene chloride 3/1) to afford a colourless solid (7.54 g, 64.1%).

^{1}H NMR (400 MHz, $CDCl_3$) δ [ppm] = 7.17 (dd, J = 5.2, 3.1 Hz, 1H, Ar-H), 6.76 (dd, J = 5.2, 3.1 Hz, 1H, Ar-H), 6.23 (dd, J = 3.5, 1.5 Hz, 1H, Ar-H), 3.94 (t, J = 6.6 Hz, 2H, O-CH_2), 1.84-1.72 (m, 2H, OCH_2-CH_2), 1.48-1.41 (m, 2H, $O(CH_2)_2$-CH_2), 1.36-1.28 (m, 18H, CH_2), 0.89 (t, J = 6.9 Hz, 3H, CH_3). **^{13}C NMR** (101 MHz, $CDCl_3$) δ [ppm] = 158.2 (Ar-O), 124.6 (Ar-H), 119.7 (Ar-H), 97.1 (Ar-H), 70.4 (O-CH_2), 32.1 (OCH_2-CH_2), 29.8 (CH_2), 29.8 (CH_2), 29.7 (CH_2), 29.7 (CH_2), 29.6 (CH_2), 29.5 (CH_2), 29.4 (CH_2), 26.2 (CH_2), 22.8 (CH_2), 14.3 (CH_3). **APCI-MS**: m/z [M^+] = 269.2. **FT-IR** (ATR): υ [cm^{-1}] = 3110, 2954, 2916, 2871, 2848, 1547, 1472, 1462, 1423, 1379, 1361, 1234, 1182, 1161, 1068, 1045, 1027, 1007, 944, 872, 824, 851, 829, 719, 685.

2-Bromo-3-(dodecyloxy)thiophene (B2)

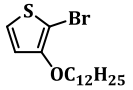

3-(Dodecyloxy)thiophene (4.01 g, 14.90 mmol) was dissolved in dimethylformamide (30 mL) and cooled to 0°C. 1-Bromopyrrolidene-2,5-dione (2.50 g, 14.05 mmol) was added in portions to the orange solution. After 4 hours of stirring at 0°C, the solution was diluted with diethyl ether and washed with water. The organic phase was dried over magnesium sulphate and the solvent was removed under reduced pressure. The crude product was dissolved in hexane and filtered over silica gel to afford a grey solid (3.12 g, 60.2%).

^{1}H NMR (400 MHz, $CDCl_3$) δ [ppm] = 7.18 (dd, J = 5.9 Hz, 1H, Ar-H), 6.74 (dd, J = 5.9 Hz, 1H, Ar-H), 4.03 (t, J = 6.6 Hz, 2H, O-CH_2), 1.80-1.73 (m, 2H, OCH_2-CH_2), 1.51-1.41 (m, 2H, CH_2), 1.40-1.19 (m, 18H, CH_2), 0.90 (t, J = 6.9 Hz, 3H, CH_3). **^{13}C NMR** (101 MHz, $CDCl_3$) δ [ppm] = 154.7 (Ar-O), 124.2 (Ar-H), 117.7 (Ar-H), 97.8 (Ar-Br), 72.4 (O-CH_2), 32.7 (OCH_2-CH_2), 29.8 (CH_2), 29.8 (CH_2), 29.7 (CH_2), 29.7 (CH_2), 29.6 (CH_2), 29.5 (CH_2), 29.4 (CH_2), 26.0 (CH_2), 22.8 (CH_2), 14.3 (CH_3). **APCI-MS**: m/z [M^+] = 348.1.

3,3'-Bis(dodecyloxy)-2,2'-bithiophene (B3)

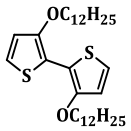

2,2'-Bipyridine (1.00 g, 6.42 mmol), bis(1,5-cyclooctadiene)nickel(0) (1.72 g, 6.26 mmol) and cyclooctadiene (0.5 ml, 4.15 mmol) were dissolved in dimethylformamide (20 mL), and heated to 80°C for 1 hour. 2-Bromo-3-(dodecyloxy)thiophene (1.44 g, 4.15 mmol) was dissolved in toluene (25 mL) and transferred into the catalyst solution at room temperature. After stirring the reaction mixture at 80°C for 48 hours, methylene chloride was added and the mixture washed with water, 2N hydrochloric acid, and 2N sodium hydroxide solution. The organic phase was dried over magnesium sulphate and the solvent was removed under reduced pressure. The crude product was purified by silica gel chromatography (eluent: hexane/methylene chloride 8/2) to afford a pale yellow product (0.86 g, 39.1%).

^{1}H NMR (600 MHz, $CDCl_3$) δ [ppm] = 7.08 (dd, J = 5.6 Hz, 2H, Ar-H), 6.84 (dd, J = 5.6 Hz 2H, Ar-H), 4.10 (t, J = 6.5 Hz, 4H, O-CH_2), 1.87-1.83 (m, 4H, OCH_2-CH_2), 1.60-1.48 (m, 4H, CH_2), 1.45-1.04 (m, 32H, CH_2), 0.88 (t, J = 6.3 Hz, 6H, CH_3). **^{13}C NMR** (151 MHz, $CDCl_3$) δ [ppm] = 152.1 (Ar-O), 121.7 (Ar-H), 116.2 (Ar-H), 114.3 (Ar-Ar), 72.1 (O-CH_2), 32.1 (OCH_2-CH_2), 29.9 (CH_2), 29.8 (CH_2), 29.8 (CH_2), 29.7 (CH_2), 29.7 (CH_2), 29.5 (CH_2), 29.5 (CH_2), 26.1 (CH_2), 22.8 (CH_2), 14.3 (CH_3). **APCI-MS**: m/z [M^+] = 535.4. **FT-IR** (ATR): υ [cm^{-1}] = 2937, 2919, 2848, 1521, 1470, 1484, 1415, 1398, 1363, 1355, 1249, 1048, 932, 822, 723, 684.

3,3'-Bis(dodecyloxy)-5,5'-bis(tributylstannyl)-2,2'-bithiophene (B4)

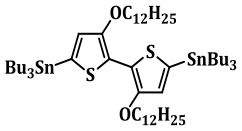

3,3'-Bis(dodecyloxy)-2,2'-bithiophene (0.67 g, 1.25 mmol) was dissolved in tetrahydrofuran (20 mL), cooled to -78°C and *n*-butyl lithium (1.0 mL, 2.80 mmol) was added dropwise. The solution was stirred for 1 hour at -78°C and an additional hour at 20°C. After the solution was cooled to -78°C, tributyltin chloride (0.75 mL, 2.76 mmol) was added in one portion. The mixture was allowed to warm up to room temperature and stirred for 1 hour at 20°C, followed by dilution with ethyl acetate and washing with water and 2N sodium hydroxide solution. The solvent was removed under reduced pressure and the resulting yellowish oil was purified by column chromatography using aluminium oxide, with 10% water (eluent: hexane/trimethylamine 97/3) to afford the yellowish oil (1.12 g, 80.1%).

^{1}H NMR (600 MHz, $CDCl_3$) δ [ppm] = 6.85 (s, 2H, Ar-H), 4.12 (t, J = 6.5 Hz, 4H, O-CH_2), 1.94-1.81 (m, 4H, OCH_2-CH_2), 1.66-1.52 (m, 16H, CH_2), 1.42-1.23 (m, 40H, CH_2), 1.13-1.09 (m, 10H, CH_2), 0.98-0.83 (m, 30H, CH_2, CH_3). **^{13}C NMR** (151 MHz, $CDCl_3$) δ [ppm] = 153.9 (Ar-O), 132.7 (Ar-Sn), 124.0 (Ar-H), 120.5 (Ar-Ar), 72.1 (O-CH_2), 32.1 (OCH_2-CH_2), 30.1 (CH_2), 30.0 (CH_2), 29.9 (CH_2), 29.8 (CH_2), 29.7 (CH_2), 29.5 (CH_2), 29.1 (CH_2), 27.4 (CH_2), 26.4 (CH_2), 22.9 (CH_2), 14.3 (CH_3), 13.8 (CH_3), 10.9 (CH_2). **^{119}Sn NMR** (149 MHz, $CDCl_3$) δ [ppm] = -38.5. **FD-MS**: m/z [M^+] = 1111.9.

6.3. Model Compounds and Polymer Synthesis

(E)-6,6'-Bis(4,4-didodecyl-4H-cyclopenta[1,2-b:5,4-b']dithiophen-2-yl)-[2,2'-biindolinylidene]-3,3'-dione (IC-1)

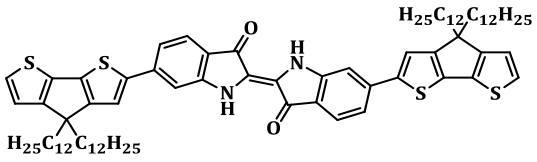

Under inert conditions, tetrakis(triphenylphosphane)palladium(0) (42 mg, 0.04 mmol), (*E*)-6,6'-dibromo-[2,2'-biindolinylidene]-3,3'-dione (155 mg, 0.37 mmol),

and a 60:40 mixture of mono-stannylated 4,4-didodecyl-2,6-bis(trimethylstannyl)-4*H*-cyclopenta[1,2-*b*:5,4-*b*']dithiophene and non-substituted 4,4-didodecyl-4*H*-cyclopenta[1,2-*b*:5,4-*b*']dithiophene (containing 0.89 mmol stannyl equivalents) were dissolved in 15 mL of tetrahydrofuran. Microwave-assistant heating was carried out at 125°C for 15 minutes, followed by stirring for 14 h at 90°C. The blue solution was diluted with chloroform and washed with 2M hydrochloric acid solution. After multiple silica column chromatographies (eluent: hexane/methylene chloride 5/5) the blue model compound was obtained (yield: 187 mg, 39.1%).

^{1}H NMR (600 MHz, $C_2D_2Cl_4$) δ [ppm] = 9.07 (bs, 2H, NH_2), 7.60 (d, J = 8.0 Hz, 2H, Ar-H), 7.28 (s, 2H, Ar-H), 7.17 (d, J = 4.8 Hz, 2H, Ar-H), 7.12-7.10 (m, 4H, Ar-H), 6.90 (d, J = 4.8 Hz, 2H, Ar-H), 1.79–1.77 (m, 8H, C-$(CH_2)_2$), 1.20–1.09 (m, 72H, CH_2), 0.95–0.93 (m, 8H, CH_2-CH_3), 0.78 (t, J = 7.1 Hz, 12H, CH_3). **^{13}C NMR** (151 MHz, $C_2D_2Cl_4$) δ [ppm] = 187.1 (C=O), 159.6 (Ar-R), 159.6 (Ar-R), 152.7 (Ar-R), 143.2 (Ar-R), 142.9 (Ar-R), 139.4 (Ar-R), 136.4 (Ar-R), 126.9 (Ar-H), 125.3 (Ar-H), 122.7 (Ar-R), 122.2 (Ar-H), 120.4 (Ar-H), 118.5 (Ar-R), 118.0 (Ar-H), 107.6 (Ar-H), 54.1 (C-$(CH_2)_2$), 37.8 (CH_2), 32.2 (CH_2), 30.4 (CH_2), 30.0 (CH_2), 29.9 (CH_2), 29.9 (CH_2), 29.7 (CH_2), 29.6 (CH_2), 25.0 (CH_2), 23.0 (CH_2), 14.5 (CH_3). **MALDI-TOF**: m/z [M^+] = 1288.4. **UV-Vis** (in toluene): $\lambda_{max,abs}$ = 620 nm. **PL** (in toluene, 600 nm): $\lambda_{max,em}$ = 650 nm. **FT-IR** (ATR): υ [cm^{-1}] = 3289, 2919, 2870, 2849, 1622, 1573, 1464, 1442, 1389, 1376, 1322, 1288, 1139, 1073, 976, 884, 866, 841, 812, 798, 774, 722, 703.

(E)-6,6'-Bis(9,9-didodecyl-9H-fluoren-2-yl)-[2,2'-biindolinylidene]-3,3'-dione (IF-1)

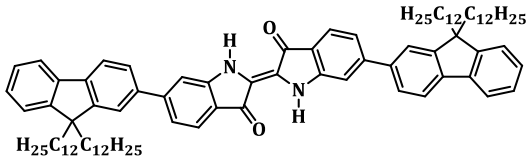

(*E*)-6,6'-Dibromo-[2,2'-biindolinylidene]-3,3'-dione (1.01 g, 2.38 mmol), 2-(9,9-didodecyl-9*H*-fluoren-2-yl)-4,4,5,5-tetramethyl-1,3,2-dioxaborolane (3.14 g, 5.01 mmol), and sodium carbonate (0.33 g, 3.09 mmol) were suspended in a mixture of water and *n*-butanol (10 mL/50 mL) under inert conditions. Tetrakis(triphenylphosphane)-palladium(0) (0.14 g, 0.12 mmol) was dissolved in toluene (50 mL) and added to the

solution. After 12 hours of stirring at 120°C, the dark green solution was diluted with chloroform. The organic layer was washed with 2N hydrochloric acid, sodium carbonate solution, aqueous ethylenediaminetetraacetic acid solution, and brine. The solvent was removed under reduced pressure. Purification by multiple silica column chromatographies (eluent: hexane/methylene chloride 1/4) gave the model compound as a dark green solid (yield: 451 mg, 15.1%).

^{1}H NMR (600 MHz, $C_2D_2Cl_4$) δ [ppm] = 8.97 (bs, 2H, NH), 7.76-7.71 (m, 4H, Ar-H), 7.68-7.67 (m, 2H, Ar-H), 7.57-7.54 (m, 4H, Ar-H), 7.32-7.25 (m, 10H, Ar-H), 1.95-1.92 (m, 8H, CH_2), 1.23-0.99 (m, 72H, CH_2), 0.82-0.74 (m, 12H, CH_3), 0.66-0.56 (m, 8H, CH_2). **^{13}C NMR** (101 MHz, $CDCl_3$) δ [ppm] = 188.0 (C=O), 152.5 (Ar-R), 151.6 (Ar-R), 151.2 (Ar-R), 149.9 (Ar-R), 142.0 (Ar-R), 140.4 (Ar-R), 138.8 (Ar-R), 132.5 (Ar-R), 130.9 (Ar-H), 128.8 (Ar-H), 127.5 (Ar-H), 126.3 (Ar-H), 124.8 (Ar-H), 123.0 (Ar-H), 122.2 (Ar-H), 121.6 (Ar-H), 120.1 (Ar-H), 118.9 (Ar-R), 110.5 (Ar-H), 55.3 (C-(CH_2)$_2$), 40.4 (CH_2), 38.8 (CH_2), 32.9 (CH_2), 30.4 (CH_2), 30.0 (CH_2), 29.7 (CH_2), 29.6 (CH_2), 29.5 (CH_2), 29.3 (CH_2), 29.3 (CH_2), 28.9 (CH_2), 23.8 (CH_2), 23.8 (CH_2), 23.0 (CH_2), 14.1 (CH_3). **MALDI-MS**: m/z [M^+] = 1262.6. **UV-Vis** (in dioxane): $\lambda_{max,abs}$ = 617 nm. **PL** (in dioxane, 560 nm): $\lambda_{max,em}$ = 645 nm. **FT-IR** (ATR): υ [cm^{-1}] = 3285, 2955, 2920, 2871, 2850, 1728, 1628, 1609, 1582, 1465, 1442, 1420, 1290, 1274, 1145, 1115, 1076, 819, 740, 721, 705.

PBAIBD-1

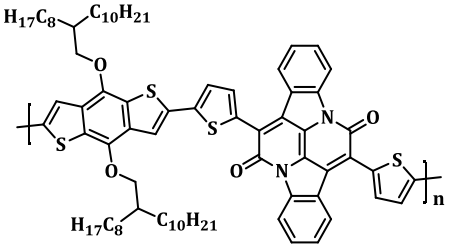

7,14-Bis(5-bromothiophen-2-yl)diindolo[3,2,1-*de*:3',2',1'-*ij*][1,5]naphthyridine-6,13-dione (276 mg, 0.42 mmol), 4,8-bis((2-octyldodecyl)oxy)-2,6-bis(trimethylstannyl)-benzo[1,2-*b*:4,5-*b*']dithiophene (468 mg, 0.42 mmol), tri-*o*-tolylphosphine (161 mg, 0.05 mmol), and tris(dibenzylideneacetone)dipalladium(0) (15 mg, 0.02 mmol) were dissolved in toluene (72 mL) under inert conditions. The reaction mixture was heated to 100°C for 6 days. Next, the reaction mixture was poured into cold methanol to precipitate the polymer, which was filtered off and washed with methanol and acetone

by Soxhlet. For Soxhlet extraction of the polymer, hexane and chloroform were used. After precipitating into methanol, the solid was dried and hexane (149 mg, 28.1%) and chloroform (226 mg, 42.6%) fractions were obtained.

^{1}H NMR (600 MHz, $C_2D_2Cl_4$) δ [ppm] = 8.77-8.50 (m, 2H, Ar-H), 8.45-8.19 (m, 2H, Ar-H), 8.00-7.72 (m, 2H, Ar-H), 7.66-7.53 (m, 2H, Ar-H), 7.45-7.21 (m, 6H, Ar-H), 4.23-4.00 (m, 4H, O-CH_2), 1.43-1.29 (m, 66H, CH_2), 1.04-0.67 (m, 12H, CH_3). **^{13}C NMR** (151 MHz, $C_2D_2Cl_4$) δ [ppm] = 158.4 (C=O), 144.2 (Ar-R), 142.7 (Ar-R), 136.9 (Ar-R), 123.2 (Ar-H), 131.8 (Ar-R), 131.3 (Ar-H), 130.2 (Ar-R), 128.8 (Ar-R), 126.1 (Ar-H), 125.3 (Ar-H), 124.9 (Ar-H), 124.5 (Ar-R), 120.6 (Ar-H), 118.0 (Ar-H), 76.9 (O-CH_2), 39.8 (CH), 32.1 (CH_2), 31.9 (CH_2), 30.4 (CH_2), 30.3 (CH_2), 29.9 (CH_2), 29.8 (CH_2), 29.8 (CH_2), 29.4 (CH_2), 27.3 (CH_2), 22.7 (CH_2), 14.1 (CH_3). **GPC**: hexane fraction in THF detected at 760 nm: M_n = 8,400 g/mol, M_w = 11,200 g/mol, PDI: 1.33, chloroform fraction in THF detected at 760 nm: M_n = 3,900 g/mol, M_w = 9,000 g/mol, PDI: 2.31. **UV-Vis** (chloroform fraction in $CHCl_3$): $\lambda_{max,abs}$ = 766 nm, (solid): $\lambda_{max,abs}$ = 799 nm. **HOMO**: -5.52 eV. **LUMO**: -3.98 eV. **TGA**: onset of decomposing: 280°C. **FT-IR** (ATR): υ [cm^{-1}] = 3066, 2919, 2849, 1629, 1601, 1454, 1415, 1358, 1080, 1030, 960, 799, 754, 721.

PIC-1

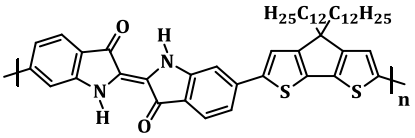

A mixture of (*E*)-6,6'-dibromo-[2,2'-biindolinylidene]-3,3'-dione (121 mg, 0.29 mmol), 4,4-didodecyl-2,6-bis(trimethylstannyl)-4*H*-cyclopenta[1,2-*b*:5,4-*b*']-dithiophene (253 mg, 0.29 mmol), 4,4-didodecyl-2-(trimethylstannyl)-4*H*-cyclopenta[1,2-*b*:5,4-*b*']dithiophene (41 mg, 0.05 mmol) as end capper, and tetrakis(triphenylphosphane)palladium(0) (36 mg, 0.03 mmol) were dissolved in tetrahydrofuran (15 mL) under argon atmosphere. The reaction mixture was heated up for 15 minutes to 125°C in a microwave reactor, followed by stirring at 90°C for 72 hours. After diluting with chloroform, the polymer was extracted with 1M hydrochloric acid. The precipitate from methanol was purified by Soxhlet extraction

with methanol, acetone, methylene chloride, and chloroform. A blue coloured polymer with a yield of 48.1% (112 mg) for the methylene chloride fraction was isolated.

^{1}H NMR (600 MHz, $C_2D_2Cl_4$) δ [ppm] = 8.91 (bs, 2H, NH), 7.75-7.61 (m, 2H, Ar-H), 7.40-7.26 (m, 2H, Ar-H), 7.21-7.12 (m, 2H, Ar-H), 7.00-6.86 (m, 2H, Ar-H), 2.02-1.76 (m, 4H, CH_2), 1.65-0.93 (m, 36H, CH_2), 0.93-0.84 (m, 10H, CH_2, CH_3). **^{13}C NMR** (151 MHz, $C_2D_2Cl_4$) δ [ppm] = 187.1 (Ar-R), 159.6 (Ar-R), 152.8 (Ar-R), 143.6 (Ar-R), 138.9 (Ar-R), 128.8 (Ar-H), 125.2 (Ar-H), 126.7 (Ar-H), 122.0 (Ar-H), 120.6 (Ar-H), 118.2 (Ar-H), 107.8 (Ar-H), 54.3 (C-$(CH_2)_2$), 37.9 (CH_2), 32.1 (CH_2), 30.2 (CH_2), 29.8 (CH_2), 29.8 (CH_2), 29.8 (CH_2), 29.7 (CH_2), 29.5 (CH_2), 29.4 (CH_2), 24.9 (CH_2), 22.8 (CH_2), 14.1 (CH_3). **GPC**: methylene chloride fraction in TCB: M_n = 7,400 g/mol, M_w = 49,400 g/mol, PDI: 6.68. **UV-Vis** (methylene chloride fraction in $CHCl_3$): $\lambda_{max,abs}$ = 658 nm, (solid): $\lambda_{max,abs}$ = 662 nm. **PL** (methylene chloride fraction in $CHCl_3$, 660 nm): $\lambda_{max,em}$ = 724 nm. **HOMO**: -5.52 eV. **LUMO**: -3.58 eV. **TGA**: onset of decomposing: 270°C. **FT-IR** (ATR): υ [cm^{-1}] = 3294, 2918, 2848, 1598, 1441, 1391, 1133, 1101, 1068, 696.

Procedure for the following polycondensations in a Stille-type coupling

Tetrakis(triphenylphosphane)palladium(0) (0.1 eq.), dibromoaryl monomer (1 eq.), and bis(trialkylstannyl)aryl monomer (1 eq.) were evacuated for 1 hour at 1x10^{-3} mbar in a microwave tube. The solids were dissolved in tetrahydrofuran (15 mL) and the reaction was carried out in the microwave reactor at 125°C for 25 minutes, followed by stirring for 72 hours at 90°C. The polymer solution was poured into cold methanol resulting in polymer precipitation. The polymer was filtered off and Soxhlet extracted with methanol and acetone. For extraction of the soluble polymer fractions the Soxhlet tube was rinsed with ethyl acetate, methylene chloride, and chloroform. After drying under high vacuum the polymers were characterised and used.

PIC-3

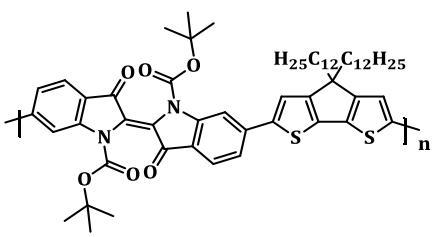

According to the general procedure, 4,4-didodecyl-2,6-bis(trimethylstannyl)-4*H*-cyclopenta[1,2-*b*:5,4-*b*']dithiophene (600 mg, 0.71 mmol), (*E*)-di-*tert*-butyl-6,6'-dibromo-3,3'-dioxo-[2,2'-biindolinylidene]-1,1'-dicarboxylate (443 mg, 0.71 mmol), and tetrakis(triphenylphosphane)palladium(0) (84 mg, 0.07 mmol) were reacted for 15 minutes in the microwave reactor followed by stirring for 3 days at 90°C. After Soxhlet extraction, ethyl acetate (181 mg, 26.1%), methylene chloride (2 mg, 0.3%), and chloroform (3 mg, 0.4%) fractions (brown solids) were obtained.

^{1}H NMR (600 MHz, $C_2D_2Cl_4$) δ [ppm] = 8.30-8.26 (m, 2H, Ar-H), 7.77-7.69 (m, 2H, Ar-H), 7.44-7.36 (m, 4H, Ar-H), 1.93-1.88 (m, 4H, CH_2), 1.66 (s, 18H, CH_3), 1.32-1.08 (m, 40H, CH_2), 0.86-0.82 (m, 6H, CH_3). **^{13}C NMR** (151 MHz, $C_2D_2Cl_4$) δ [ppm] = 182.2 (C=O), 160.7 (Ar-R), 150.2 (Ar-R), 150.0 (Ar-R), 145.1 (Ar-R), 142.7 (Ar-R), 139.0 (Ar-R), 126.1 (Ar-R), 124.9 (Ar-H), 122.0 (Ar-R), 121.2 (Ar-H), 120.5 (Ar-H), 120.6 (Ar-R), 112.8 (Ar-H), 84.9 (C-$(CH_3)_3$), 54.9 (C-$(CH_2)_2$), 38.0 (CH_2), 32.1 (CH_2), 30.3 (CH_2), 29.9 (CH_2), 29.8 (CH_2), 29.8 (CH_2), 29.7 (CH_2), 29.6 (CH_2), 29.4 (CH_2), 28.6 (CH_3), 25.0 (CH_2), 22.8 (CH_2), 14.2 (CH_3). **GPC**: ethyl acetate fraction in THF detected at 600 nm: M_n = 10,100 g/mol, M_w = 13,800 g/mol, PDI: 1.36, methylene chloride fraction in THF detected at 600 nm: M_n = 19,300 g/mol, M_w = 103,000 g/mol, PDI: 5.33, chloroform fraction in THF detected at 600 nm: M_n = 18,900 g/mol, M_w = 167,000 g/mol, PDI: 8.85. **UV-Vis** (ethyl acetate fraction in $CHCl_3$): $\lambda_{max,abs}$ = 600 nm, (solid): $\lambda_{max,abs}$ = 590 nm. **HOMO**: -5.40 eV. **LUMO**: -3.35 eV. **TGA**: onset of decomposing: 150°C. **FT-IR** (ATR): υ [cm^{-1}] = 2920, 2847, 1716, 1598, 1148, 1107, 1079, 774.

PIC-2

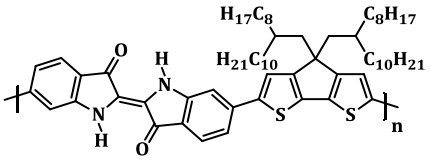

According to the general procedure, 4,4-(2-octyldodecyl)-2,6-bis(trimethylstannyl)-4*H*-cyclopenta[1,2-*b*:5,4-*b*']dithiophene (606 mg, 0.57 mmol), (*E*)-6,6'-dibromo-[2,2'-biindolinylidene]-3,3'-dione (237 mg, 0.57 mmol), and tetrakis-(triphenylphosphane)palladium(0) (68 mg, 0.06 mmol) were reacted. After Soxhlet

extraction, methylene chloride (233 mg, 41.3%) and chloroform (21 mg, 3.8%) fractions (brown solids) were obtained.

^{1}H NMR (600 MHz, $C_2D_2Cl_4$) δ [ppm] = 8.90 (s, 2H, NH), 7.80-7.58 (m, 2H, Ar-H), 7.51-7.27 (m, 2H, Ar-H), 7.21-7.08 (m, 2H, Ar-H), 6.91-9.71 (m, 2H, Ar-H), 2.33-1.91 (m, 4H, CH_2), 1.42-1.00 (m, 66H, CH_2, CH), 0.84-0.78 (m, 12H, CH_3). **^{13}C NMR** (151 MHz, $C_2D_2Cl_4$) δ [ppm] = 187.0 (C=O), 160.1 (Ar-R), 152.7 (Ar-R), 144.6 (Ar-R), 142.7 (Ar-R), 139.2 (Ar-R), 125.3 (Ar-H), 121.1 (Ar-H), 118.3 (Ar-H), 107.9 (Ar-H), 54.9 (C-$(CH_2)_2$), 44.4 (CH_2), 35.7 (CH_2), 35.6 (CH_2), 34.6 (CH), 32.1 (CH_2), 32.0 (CH_2), 30.1 (CH_2), 30.0 (CH_2), 29.9 (CH_2), 29.8 (CH_2), 29.5 (CH_2), 26.9 (CH_2), 26.8 (CH_2), 22.8 (CH_2), 14.2 (CH_3). **GPC**: ethyl acetate fraction in THF detected at 600 nm: M_n = 10,100 g/mol, M_w = 13,800 g/mol, PDI: 1.36, methylene chloride fraction in THF detected at 650 nm: M_n = 15,100 g/mol, M_w = 44,800 g/mol, PDI: 2.97, chloroform fraction in THF detected at 650 nm: M_n = 29,000 g/mol, M_w = 120,000 g/mol, PDI: 4.13. **UV-Vis** (chloroform fraction in $CHCl_3$): $\lambda_{max,abs}$ = 674 nm, (solid): $\lambda_{max,abs}$ = 654 nm. **HOMO**: -5.52 eV. **LUMO**: -3.54 eV. **TGA**: onset of decomposing: 250°C. **FT-IR** (ATR): υ [cm^{-1}] = 3293, 2919, 2849, 1602, 1442, 1135, 1104, 1070, 773.

PIC-4

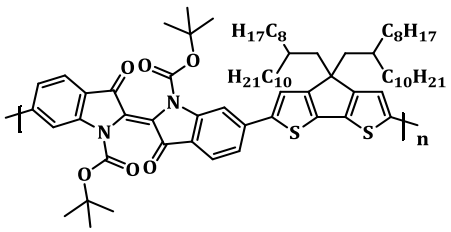

According to the general procedure, 4,4-(2-octyldodecyl)-2,6-bis(trimethylstannyl)-4*H*-cyclopenta[1,2-*b*:5,4-*b*']dithiophene (615 mg, 0.58 mmol), (*E*)-di-*tert*-butyl-6,6'-dibromo-3,3'-dioxo-[2,2'-biindolinylidene]-1,1'-dicarboxylate (359 mg, 0.58 mmol), and tetrakis(triphenylphosphane)palladium(0) (66 mg, 0.06 mmol) were reacted. After Soxhlet extraction, ethyl acetate (427 mg, 61.5%) and methylene chloride (50 mg, 7.2%) fractions (dark green solids) were obtained.

^{1}H NMR (600 MHz, $C_2D_2Cl_4$) δ [ppm] = 8.28-8.21 (m, 2H, Ar-H), 7.70-7.62 (m, 2H, Ar-H), 7.41-7.35 (m, 4H, Ar-H), 2.05-1.96 (m, 4H, CH_2), 1.65 (s, 18H, CH_3), 1.57-1.39 (m, 8H, CH_2, CH), 1.15-0.99 (m, 58H, CH_2), 0.84-0.77 (m, 12H, CH_3). **^{13}C NMR** (151 MHz,

$C_2D_2Cl_4$) δ [ppm] = 182.2 (C=O), 160.2 (Ar-R), 150.1 (Ar-R), 149.6 (Ar-R), 144.7 (Ar-R), 142.6 (Ar-R), 139.3 (Ar-R), 126.0 (Ar-R), 124.8 (Ar-H), 122.0 (Ar-R), 121.1 (Ar-H), 121.1 (Ar-H), 120.6 (Ar-R), 112.7 (Ar-H), 84.7 (C-$(CH_3)_3$), 54.9 (C-$(CH_2)_2$), 44.4 (CH_2), 35.6 (CH_2), 34.6 (CH), 32.1 (CH_2), 32.0 (CH_2), 32.0 (CH_2), 30.0 (CH_2), 29.9 (CH_2), 29.8 (CH_2), 29.7 (CH_2), 29.7 (CH_2), 29.5 (CH_2), 29.4 (CH_2), 28.5 (CH_3), 26.9 (CH_2), 26.8 (CH_2), 22.9 (CH_2), 22.8 (CH_2), 22.7 (CH_2), 14.2 (CH_3). **GPC**: ethyl acetate fraction in THF detected at 590 nm: M_n = 10,200 g/mol, M_w = 31,500 g/mol, PDI: 3.10. **UV-Vis** (ethyl acetate fraction in $CHCl_3$): $\lambda_{max,abs}$ = 590 nm, (solid): $\lambda_{max,abs}$ = 582 nm. **PL** (ethyl acetate fraction in $CHCl_3$, 590 nm): $\lambda_{max,em}$ = 750 nm, (solid, 590 nm): $\lambda_{max,em}$ = 746 nm. **HOMO**: -5.30 eV. **LUMO**: -3.21 eV. **TGA**: onset of decomposing: 150°C. **FT-IR** (ATR): υ [cm^{-1}] = 2919, 2850, 1717, 1675, 1596, 1106, 1147, 1078.

PIB-1

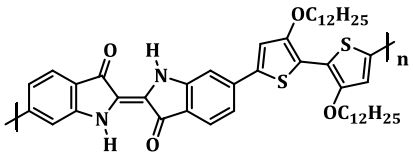

According to the general procedure, tetrakis(triphenylphosphane)palladium(0) (75 mg, 0.07 mmol), 3,3'-bis(dodecyloxy)-5,5'-bis(tributylstannyl)-2,2'-bithiophene (716 mg, 0.65 mmol), and (*E*)-6,6'-dibromo-[2,2'-biindolinylidene]-3,3'-dione (277 mg, 0.66 mmol) were reacted. After Soxhlet extraction, chloroform (8 mg, 1.7%) and trichlorobenzene (143 mg, 27.8%) fractions (black solids) were obtained.

^{1}H NMR and **^{13}C NMR** could not be recorded due to the limited solubility. **GPC**: chloroform fraction in THF detected at 640 nm: M_n = 4,300 g/mol, M_w = 97,900 g/mol, PDI: 22.82, trichlorobenzene fraction in TCB: M_n = 1,800 g/mol, M_w = 3,200 g/mol, PDI: 1.78. **UV-Vis** (chloroform fraction in $CHCl_3$): $\lambda_{max,abs}$ = 644 nm. **TGA**: onset of decomposing: 250°C. **FT-IR** (ATR): υ [cm^{-1}] = 3280, 2920, 2850, 1726, 1625, 1603, 1435, 1137, 1105, 1068, 721, 692.

PIB-2

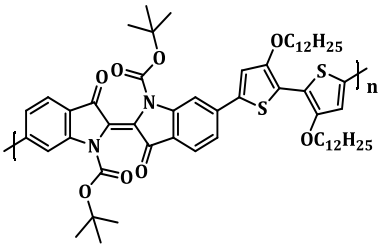

According to the general procedure, tetrakis(triphenylphosphane)palladium(0) (75 mg, 0.07 mmol), 3,3'-bis(dodecyloxy)-5,5'-bis(tributylstannyl)-2,2'-bithiophene (719 mg, 0.65 mmol), and (*E*)-di-*tert*-butyl-6,6'-dibromo-3,3'-dioxo-[2,2'-biindolinylidene]-1,1'-dicarboxylate (400 mg, 0.65 mmol) were reacted. After Soxhlet extraction, chloroform (60 mg, 9.1%), toluene (41 mg, 6.2%), and tetrahydrofuran (188 mg, 28.4%) fractions (brown solids) were obtained.

^{1}H NMR (600 MHz, $C_2D_2Cl_4$) δ [ppm] = 8.23-8.21 (m, 2H, Ar-H), 7.86-7.49 (m, 3H, Ar-H), 7.33-7.32 (m, 1H, Ar-H), 7.27-7.21 (m, 2H, Ar-H), 4.26-4.05 (m, 4H, OCH_2), 2.02-1.77 (m, 4H, CH_2), 1.65-1.22 (m, 48H, CH_3, CH_2), 0.93-0.64 (m, 12H, CH_3). **^{13}C NMR** (151 MHz, $C_2D_2Cl_4$) δ [ppm] = 193.3 (C=O), 154.8 (Ar-R), 153.8 (Ar-R), 151.2 (Ar-R), 151.1 (Ar-R), 143.1 (Ar-R), 138.9 (Ar-R), 124.8 (Ar-H), 124.6 (Ar-H), 123.2 (Ar-R), 120.6 (Ar-R), 120.3 (Ar-H), 114.7 (Ar-H), 112.8 (Ar-H), 83.9 (C-$(CH_3)_3$), 54.9 (C-$(CH_2)_2$), 72.8 (O-CH_2), 32.1 (CH_2), 30.0 (CH), 29.9 (CH_2), 29.8 (CH_2), 29.8 (CH_2), 29.5 (CH_2), 29.4 (CH_2), 28.5 (CH_3), 26.3 (CH_2), 22.8 (CH_2), 14.2 (CH_3). **GPC**: chloroform fraction in THF detected at 480 nm: M_n = 11,600 g/mol, M_w = 134,000 g/mol, PDI: 11.56, toluene fraction in THF detected at 480 nm: M_n = 11,200 g/mol, M_w = 176,000 g/mol, PDI: 15.64, tetrahydrofuran fraction in THF detected at 480 nm: M_n = 11,500 g/mol, M_w = 169,000 g/mol, PDI: 14.74. **UV-Vis** (chloroform fraction in THF): $\lambda_{max,abs}$ = 482 nm, (solid): $\lambda_{max,abs}$ = 504 nm, (toluene fraction in THF): $\lambda_{max,abs}$ = 488 nm, (solid): $\lambda_{max,abs}$ = 499 nm, (tetrahydrofuran fraction in THF): $\lambda_{max,abs}$ = 486 nm, (solid): $\lambda_{max,abs}$ = 504 nm. **HOMO**: -5.01 eV. **LUMO**: -3.22 eV. **TGA**: onset of decomposing: 150°C. **FT-IR** (ATR): υ [cm^{-1}] = 2921, 2850, 1714, 1597, 1366, 1324, 1150, 1109, 1065, 758.

PBAIC-1

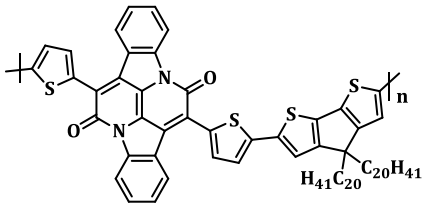

According to the general procedure, tetrakis(triphenylphosphane)palladium(0) (69 mg, 0.06 mmol), 7,14-bis(5-bromothiophen-2-yl)diindolo[3,2,1-*de*:3',2',1'-*ij*][1,5]-naphthyridine-6,13-dione (376 mg, 0.59 mmol), and 4,4-bis(2-octyldodecyl)-2,6-bis(trimethylstannyl)-4*H*-cyclopenta[1,2-*b*:5,4-*b*']dithiophene (633 mg, 0.59 mmol) were reacted. After Soxhlet extraction, methylene chloride (204 mg, 28.3%) and chloroform (20 mg, 2.7%) fractions (black solids) were obtained.

^{1}H NMR (600 MHz, $C_2D_2Cl_4$) δ [ppm] = 8.70-8.53 (m, 2H, Ar-H), 8.40-8.24 (m, 2H, Ar-H), 7.85-7.69 (m, 2H, Ar-H), 7.64-7.49 (m, 2H, Ar-H), 7.42-7.17 (m, 4H, Ar-H), 7.10-6.86 (m, 2H, Ar-H), 1.97-1.87 (m, 4H, C-$(CH_2)_2$), 1.37-0.55 (m, 78H, CH_3, CH_2). **^{13}C NMR** (151 MHz, $C_2D_2Cl_4$) δ [ppm] = 159.7 (C=O), 144.1 (Ar-R), 137.8 (Ar-R), 137.5 (Ar-R), 131.9 (Ar-H), 131.6 (Ar-H), 126.5 (Ar-H), 126.3 (Ar-R), 125.6 (Ar-R), 125.1 (Ar-H), 124.4 (Ar-R), 122.8 (Ar-H), 122.5 (Ar-H), 120.3 (Ar-H), 118.1 (Ar-H), 54.7 (C-$(CH_2)_2$), 44.5 (CH_2), 35.6 (CH_2), 34.6 (CH), 32.1 (CH_2), 29.9 (CH_2), 29.9 (CH_2), 29.8 (CH_2), 29.8 (CH_2), 29.8 (CH_2), 29.7 (CH_2), 29.5 (CH_2), 26.8 (CH_2), 26.7 (CH_2), 22.8 (CH_2), 22.8 (CH_2), 14.2 (CH_3). **GPC**: methylene chloride fraction in THF detected at 800 nm: M_n = 10,900 g/mol, M_w = 22,100 g/mol, PDI: 2.04, chloroform fraction in THF detected at 800 nm: M_n = 16,600 g/mol, M_w = 203,000 g/mol, PDI: 12.24, chloroform fraction in TCB M_n = 8,300 g/mol, M_w = 11,500 g/mol, PDI: 1.39. **UV-Vis** (methylene chloride fraction in $CHCl_3$): $\lambda_{max,abs}$ = 819 nm, (solid): $\lambda_{max,abs}$ = 835 nm, (chloroform fraction in $CHCl_3$): $\lambda_{max,abs}$ = 794 nm, (solid): $\lambda_{max,abs}$ = 803 nm. **HOMO**: -5.03 eV. **LUMO**: -3.55 eV. **TGA**: onset of decomposing: 350°C. **FT-IR** (ATR): υ [cm^{-1}] = 3058, 2919, 2849, 1630, 1602, 1439, 1406, 1318, 1080, 754, 692.

PBAIC-2

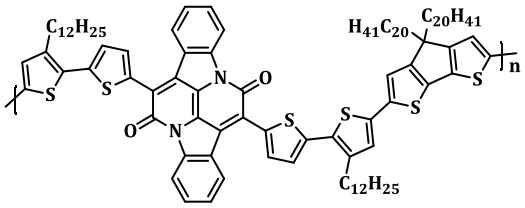

According to the general procedure, tetrakis(triphenylphosphane)palladium(0) (37 mg, 0.03 mmol), 7,14-bis(5'-bromo-3'-dodecyl-[2.2'-bithiophene]-5-yl)diindolo[3,2,1-*de*:3',2',1'-*ij*][1,5]naphthyridine-6,13-dione (242 mg, 0.21 mmol), and 4,4-bis(2-octyldodecyl)-2,6-bis(trimethylstannyl)-4*H*-cyclopenta[1,2-*b*:5,4-*b*']dithiophene (227 mg, 0.21 mmol) were reacted. After Soxhlet extraction, methylene chloride (206 mg, 56.2%) and chloroform (94 mg, 25.6%) fractions (black solids) were obtained.

^{1}H NMR (600 MHz, $C_2D_2Cl_4$) δ [ppm] = 8.69-8.55 (m, 2H, Ar-H), 8.36-8.19 (m, 2H, Ar-H), 7.83-7.68 (m, 2H, Ar-H), 7.65-7.52 (m, 2H, Ar-H), 7.41-7.16 (m, 5H, Ar-H), 7.11-6.94 (m, 3H, Ar-H), 2.99-2.73 (m, 4H, C-$(CH_2)_2$), 2.07-1.87 (m, 4H, C-$(CH_2CH_2)_2$), 1.77-1.68 (m, 4H, CH_2), 1.37-0.55 (m, 120H, CH_3, CH_2, CH). **^{13}C NMR** (151 MHz, $C_2D_2Cl_4$) δ [ppm] = 158.8 (C=O), 144.4 (Ar-R), 141.7 (Ar-R), 140.6 (Ar-R), 137.4 (Ar-R), 135.0 (Ar-R), 132.1 (Ar-H), 131.5 (Ar-R), 131.1 (Ar-H), 129.8 (Ar-R), 129.5 (Ar-R), 127.8 (Ar-H), 126.4 (Ar-H), 126.2 (Ar-H), 125.2 (Ar-H), 124.5 (Ar-R), 123.2 (Ar-H), 122.4 (Ar-H), 118.1 (Ar-H), 54.7 (C-$(CH_2)_2$), 44.5 (CH_2), 35.8 (CH_2), 35.7 (CH_2), 34.7 (CH), 32.1 (CH_2), 32.0 (CH_2), 30.7 (CH_2), 30.6 (CH_2), 30.5 (CH_2), 30.1 (CH_2), 29.9 (CH_2), 29.9 (CH_2), 29.8 (CH_2), 29.8 (CH_2), 29.7 (CH_2), 29.5 (CH_2), 29.4 (CH_2), 22.8 (CH_2), 22.8 (CH_2), 14.1 (CH_3). **GPC**: methylene chloride fraction in THF detected at 740 nm: M_n = 17,900 g/mol, M_w = 24,400 g/mol, PDI: 1.36, chloroform fraction in THF detected at 740 nm: M_n = 47,400 g/mol, M_w = 61,300 g/mol, PDI: 1.29. **UV-Vis** (methylene chloride fraction in $CHCl_3$): $\lambda_{max,abs}$ = 726 nm, (solid): $\lambda_{max,abs}$ = 928 nm, (chloroform fraction in $CHCl_3$): $\lambda_{max,abs}$ = 741 nm, (solid): $\lambda_{max,abs}$ = 875 nm. **HOMO**: -5.07 eV. **LUMO**: -3.78 eV. **TGA**: onset of decomposing: 360°C. **FT-IR** (ATR): υ [cm^{-1}] = 3058, 2920, 2849, 1630, 1415, 1318, 1080, 961, 772, 754.

General procedure for polycondensations in a Suzuki-type coupling

2,2'-(9,9-Didodecyl-9*H*-fluorene-2,7-diyl)bis(4,4,5,5-tetramethyl-1,3,2-dioxaborolane) (1 eq.), (*E*)-6,6'-dibromo-[2,2'-biindolinylidene]-3,3'-dione (1 eq.) or (*E*)-di-*tert*-butyl-6,6'-dibromo-3,3'-dioxo-[2,2'-biindolinylidene]-1,1'-dicarboxylate (1 eq.), sodium carbonate (1.3 eq.), and tetrakis(triphenylphosphane)palladium(0) (0.05 eq.) were evacuated for 1 hour at $1x10^{-3}$ mbar. The solids were dissolved in a degassed solvent mixture of water and butan-1-ol. The catalyst was dissolved in toluene (1/3/3) and added to the monomer solution. The reaction mixture was heated up to 120°C for 3 days. The polymer solution was washed with 2N hydrochloric acid, saturated sodium bicarbonate solution, ethylenediaminetetraacetic acid solution and brine. After concentrating the polymer solution, it was poured into methanol to precipitate the polymer. The polymer was filtered off, dissolved in chloroform and washed with a sodium diethyldithiocarbamate trihydrate solution overnight and 2 hours with water. Again, concentration of the polymer solution was followed by precipitation into cold methanol. After filtration, the polymer was Soxhlet extracted with methanol and acetone. For extraction of the soluble polymer fractions, the Soxhlet tube was rinsed with ethyl acetate, methylene chloride, and chloroform. After drying under high vacuum the polymers were characterised and used.

PIF-1

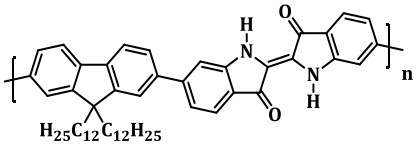

According to the general procedure, 2,2'-(9,9-didodecyl-9*H*-fluorene-2,7-diyl)bis(4,4,5,5-tetramethyl-1,3,2-dioxaborolane) (1.98 g, 2.62 mmol), (*E*)-6,6'-dibromo-[2,2'-biindolinylidene]-3,3'-dione (1.00 g, 2.45 mmol), and sodium carbonate (0.345 g, 3.21 mmol) were dissolved in butan-1-ol (70 mL) and water (24 mL). The catalyst (0.34 g, 3.21 mmol) was dissolved in toluene (70 mL), added to the monomer solution. After Soxhlet extraction, methylene chloride (247 mg, 13.1%), and chloroform (81 mg, 4.1%) fractions (dark green solids) were obtained.

^{1}H NMR (600 MHz, $C_2D_2Cl_4$) δ [ppm] = 8.98 (bs, 2H, NH), 7.78-7.59 (m, 8H, Ar-H), 7.39-7.18 (m, 4H, Ar-H), 2.18-1.93 (m, 4H, CH_2), 1.35-1.06 (m, 40H, CH_3), 0.90-0.74 (m, 6H, CH_3). **^{13}C NMR** (151 MHz, $C_2D_2Cl_4$) δ [ppm] = 188.0 (C=O), 152.8 (Ar-R), 152.6 (Ar-R), 152.5 (Ar-R), 150.7 (Ar-R), 150.3 (Ar-R), 150.1 (Ar-R), 143.3 (Ar-R), 142.1 (Ar-R), 141.5 (Ar-R), 139.6 (Ar-R), 139.5 (Ar-R), 134.1 (Ar-H), 129.5 (Ar-H), 126.8 (Ar-H), 126.6 (Ar-H), 125.0 (Ar-H), 122.6 (Ar-R), 122.6 (Ar-R), 122.2 (Ar-H), 120.7 (Ar-H), 119.4 (Ar-H), 110.8 (Ar-H), 55.6 (C-$(CH_2)_2$), 40.2 (CH_2), 32.1 (CH_2), 30.4 (CH_2), 30.2 (CH_2), 30.0 (CH_2), 29.7 (CH_2), 29.5 (CH_2), 29.4 (CH_2), 25.4 (CH_2), 24.4 (CH_2), 24.2 (CH_2), 22.8 (CH_2), 14.2 (CH_3). **GPC**: methylene chloride fraction in THF detected at 600 nm: M_n = 5,000 g/mol, M_w = 6,000 g/mol, PDI: 1.21, chloroform fraction in THF detected at 600 nm: M_n = 7,200 g/mol, M_w = 8,900 g/mol, PDI: 1.23. **UV-Vis** (methylene chloride fraction in THF): $\lambda_{max,abs}$ = 333 nm, (solid): $\lambda_{max,abs}$ = 334 nm, (chloroform fraction in $CHCl_3$): $\lambda_{max,abs}$ = 335 nm, (solid): $\lambda_{max,\ abs}$ = 335 nm. **HOMO**: -5.67 eV. **LUMO**: -3.72 eV. **TGA**: onset of decomposing: 310°C. **FT-IR** (ATR): υ [cm^{-1}] = 3293, 2920, 2849, 1633, 1605, 1441, 1135, 1110, 1071, 815, 702.

PIF-2

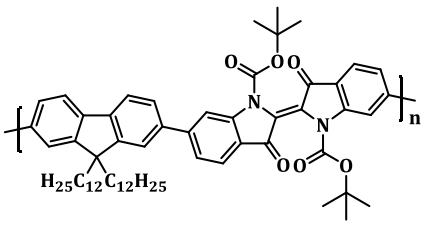

According to the general procedure, 2,2'-(9,9-didodecyl-9*H*-fluorene-2,7-diyl)bis(4,4,5,5-tetramethyl-1,3,2-dioxaborolane) (510 mg, 0.68 mmol), (*E*)-di-*tert*-butyl-6,6'-dibromo-3,3'-dioxo-[2,2'-biindolinylidene]-1,1'-dicarboxylate (410 mg, 0.66 mmol) and sodium carbonate (98 mg, 0.93 mmol) were dissolved in butan-1-ol (30 mL) and water (10 mL). The catalyst (45 mg, 0.04 mmol) was dissolved in toluene (30 mL) and added to the monomer solution. After Soxhlet extraction, ethyl acetate (280 mg, 44.1%), methylene chloride (10 mg, 1.6%), and chloroform (3 mg, 0.5%) fractions (brown solids) were obtained.

^{1}H NMR (600 MHz, $C_2D_2Cl_4$) δ [ppm] = 8.33-8.27 (m, Ar-H), 7.96-7.54 (m, Ar-H), 7.41-7.29 (m, Ar-H), 2.18-1.89 (m, CH_2), 1.66-1.42 (m, CH_3), 1.22-1.07 (m, CH_2), 0.88-

0.82 (m, CH_3). **GPC**: ethyl acetate fraction in THF detected at 360 nm: M_n = 5,200 g/mol, M_w = 11,100 g/mol, PDI: 2.12, methylene chloride fraction in THF detected at 360 nm: M_n = 5,700 g/mol, M_w = 23,000 g/mol, PDI: 4.06. **UV-Vis** (methylene chloride fraction in $CHCl_3$): $\lambda_{max,abs}$ = 366 nm, (ethyl acetate fraction in $CHCl_3$): $\lambda_{max,abs}$ = 366 nm, (solid): $\lambda_{max,abs}$ = 362 nm. **HOMO**: -5.80 eV. **LUMO**: -3.13 eV. **TGA**: onset of decomposing: 150°C. **FT-IR** (ATR): υ [cm^{-1}] = 2922, 2851, 1717, 1603, 1366, 1146, 1108, 1075, 816.

6.4. Polymer-Analogous Reactions

General procedure for cleavage of the boc-protecting groups with 2,2,2-trifluoroacetic acid

The boc-protected polymer (50 mg, 0.05 mmol) was dissolved in methylene chloride. 2,2,2-Trifluoroacetic acid (5 mL, 65.31 mmol) was added and the reaction mixture was heated up to 60°C for 30 minutes. After addition of water (25 mL), methylene chloride was removed and potassium carbonate solution was used to neutralise the aqueous phase. The polymer was washed with water and Soxhlet extracted with ethyl acetate, methylene chloride, chloroform, chlorobenzene, and dichlorobenzene.

Acid cleavage of PIF-2

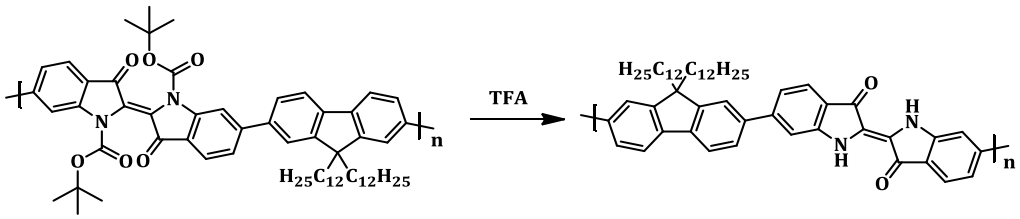

According to the general procedure, poly-(*E*)-di-*tert*-butyl-6-(9,9-didodecyl-9*H*-fluoren-2-yl)-3,3'-dioxo-[2,2'-biindolinylidene]-1,1'-dicarboxylate, and 2,2,2-trifluoroacetic acid were reacted. After Soxhlet extraction methylene chloride (2 mg, 4.5%), chloroform (3 mg, 6.7%), and chlorobenzene (7 mg, 18.6%) fractions (green solids) were obtained.

GPC: methylene chloride fraction in THF detected at 350 nm: M_n = 4,400 g/mol, M_w = 9,800 g/mol, PDI: 2.23, chloroform fraction in THF detected at 350 nm: M_n = 14,600 g/mol, M_w = 27,800 g/mol, PDI: 1.91, chlorobenzene fraction in TCB:

M_n = 7,500 g/mol, M_w = 18,800g/mol, PDI: 2.50. **UV-Vis** (methylene chloride fraction in THF): $\lambda_{max,abs}$ = 363 nm, (chloroform fraction in THF): $\lambda_{max,abs}$ = 359 nm. **FT-IR** (ATR): υ [cm^{-1}] = 3316, 2920, 2849, 1734, 1604, 1440, 1132, 1108, 1069, 815, 701.

Acid cleavage of PIC-3

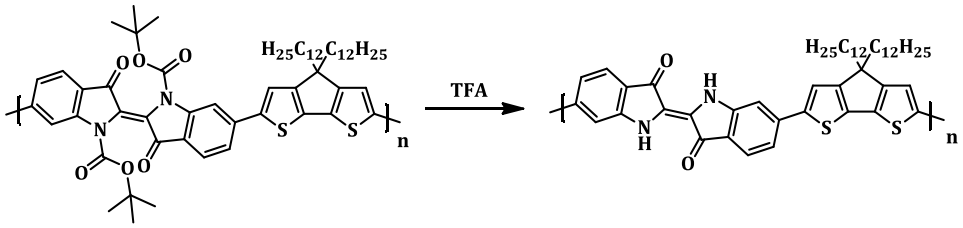

Poly-(*E*)-di-*tert*-butyl-6-(4,4-didodecyl-4*H*-cyclopenta[1,2-*b*:5,4-*b*']dithiophen-2-yl)-3,3'-dioxo-[2,2'-biindolinylidene]-1,1'-dicarboxylate and 2,2,2-trifluoroacetic acid were reacted. After Soxhlet extraction methylene chloride (2 mg, 5.5%), chloroform (4 mg, 10.2%), chlorobenzene (8 mg, 19.0%), and dichlorobenzene (7 mg, 17.5%) fractions (blue solids) were obtained.

GPC: methylene chloride fraction in THF detected at 600 nm: M_n = 6,400 g/mol, M_w = 11,800 g/mol, PDI: 1.86, chloroform fraction in THF detected at 600 nm: M_n = 13,000 g/mol, M_w = 29,400 g/mol, PDI: 2.26, chlorobenzene fraction in TCB: M_n = 6,200 g/mol, M_w = 44,000g/mol, PDI: 7.13, dichlorobenzene fraction in TCB: M_n = 6,000 g/mol, M_w = 51,000g/mol, PDI: 8.38. **UV-Vis** (methylene chloride fraction in THF): $\lambda_{max,abs}$ = 434 nm, (chloroform fraction in THF): $\lambda_{max,abs}$ = 645 nm. **FT-IR** (ATR): υ [cm^{-1}] = 3326, 2919, 2849, 1699, 1598, 1440, 1389, 1132, 1101, 1068, 839, 694.

General procedure for the reduction of indigo-containing polymers

A stock solution ($1.4*10^{-3}$ mol/L) of sodium dithionite (5.01 g, 0.03 mmol) in water (20 mL) was prepared. In a self-assembled glovebox, an absorption cuvette was evacuated and purged with argon. 0.3 mL of the polymer solution in tetrahydrofuran was added into the cuvette and diluted with tetrahydrofuran (2.5 mL), followed by adding 0.1 mL of the sodium dithionite solution. An immediately change of colour was obtained. After diluting the reaction solution one to one with tetrahydrofuran, an

absorption spectrum was recorded. By adding oxygen to the solution, the re-oxidation was investigated by recording an absorption spectrum.

Reduction of PIF-2

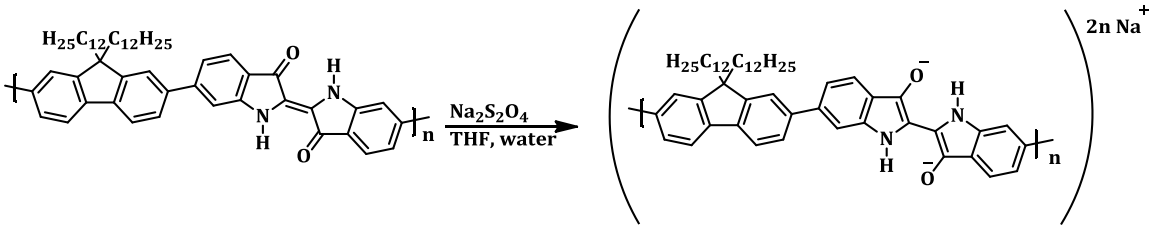

0.5 mg ($6.55*10^{-5}$ mol/L) of poly-(*E*)-6-(9,9-didodecyl-9*H*-fluoren-2-yl)-[2,2'-biindolinylidene]-3,3'-dione were dissolved in tetrahydrofuran (10 mL). $1.96*10^{-8}$ mol of the polymer and $1.4*10^{-4}$ mol of the reducing reagent were reacted. The green polymer solution turned yellow instantly. By adding oxygen, no change of colour was observed. Precipitation into cold methanol leads to a green polymer.

UV-Vis (reduced form in THF): $\lambda_{max,abs}$ = 280 nm, (re-oxidized form (new band) in THF): $\lambda_{max,abs}$ = 613 nm.

Reduction of PIC-3

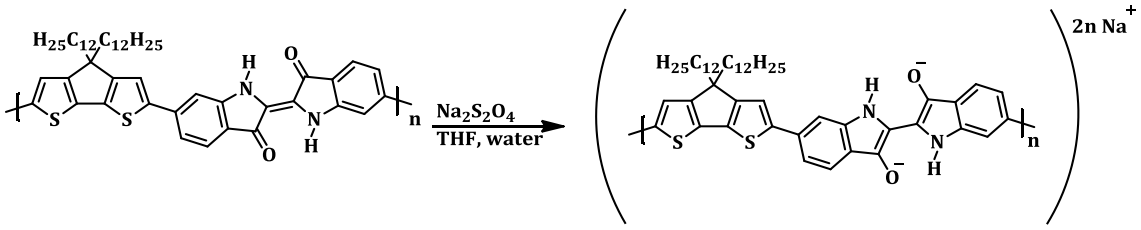

0.9 mg ($1.16*10^{-4}$ mol/L) of poly(4,4-didodecyl-4*H*-cyclopenta[1,2-*b*:5,4-*b*']dithiophen-2-yl)-[2,2'-biindolinylidene-]3,3'-dione were dissolved in tetrahydrofuran (10 mL). $3.48*10^{-8}$ mol of the polymer and $1.4*10^{-4}$ mol of the reducing reagent were reacted. The green polymer solution turned yellow, instantly. By adding oxygen no change of colour was observed.

UV-Vis (reduced form in THF): $\lambda_{max,abs}$ = 280 nm, no re-oxidation observed.

Directories

List of Figures

Figure 1: Chemical structures of the chromophores of indigo, madder, and saffron[1,3] 1

Figure 2 left: Chemical structure of 6,6'-dibromoindigo (Tyrian purple); right: Murex trunculus, also known as Hexaplex trunculus © Hans Hillewaert 2

Figure 3: Structure of mauveine with acetate as counter ions, investigated by Meth-Cohn et al.[18] 4

Figure 4: H-chromophore unit of indigo[7] 6

Figure 5: Excited state of indigo by either single or double proton transfer[38] 7

Figure 6: Selection of five indigoids based on the indigo core 8

Figure 7: Selection of two indigoids related to indigo 9

Figure 8: Copolymer synthesised by Andersson and co-workers, R=hexyldecyl[50,51] 10

Figure 9: Indigo-containing polymers synthesised by Voss et al., m=0-1[53] 11

Figure 10 left: Polymer by Sariciftci (PS-1)[54]; right: Polymer by Li (PL-1)[55], R=2-decyltetradecyl 11

Figure 11: Target structures of indigo-containing polymers 12

Figure 12: Target structures of BAI-containing polymers 13

Figure 13: Solid ^{13}C NMR spectrum of indigo and dibromoindigo I5 19

Figure 14: IR spectrum of dibromoindigo I5 20

Figure 15: IR spectrum of the boc-substituted dibromoindigo I6 21

Figure 16 top: ^{1}H NMR spectrum of model compound IC-1; bottom: ^{13}C NMR of model compound IC-1; in $C_2D_2Cl_4$ (5.91 and 74.2 ppm) 34

Figure 17: IR spectrum of the CPDT model compound IC-1 34

Figure 18: ^{1}H NMR of model compound IF-1; in $C_2D_2Cl_4$ (5.91 ppm) 36

Figure 19: IR spectrum of the fluorene model compound IF-1 36

Figure 20: ^{1}H NMR spectra of indigo-CPDT polymers recorded in $C_2D_2Cl_4$ (5.91 ppm); left: Magnified section of the aromatic region, amine protons green highlighted; right: Aliphatic region, methyl groups of the boc-protecting groups blue highlighted 39

Figure 21: IR spectra of PIC-1 and PIC-3 40

Figure 22: ^{1}H NMR spectra of B3 (top), recorded in $CDCl_3$ (7.26 ppm), and PIB-2 (bottom), recorded in $C_2D_2Cl_4$ (5.91 ppm), ether methylene groups green highlighted, methyl groups of the boc-protecting groups blue highlighted 41

Figure 23: IR spectra of PIB-1 and PIB-2 42

Figure 24: ^{1}H NMR spectra of PIF-1 (top) and PIF-2 (bottom) recorded in $C_2D_2Cl_4$ (5.91 ppm), amine protons red highlighted, methyl groups of the boc-protecting groups green highlighted 43

Figure 25: IR spectra of PIF-1 and PIF-2 44

Figure 26: Absorption spectra of the indigo-CPDT polymers measured in chloroform and as thin films 45

Figure 27: Time-dependent change of the absorption spectrum of PIC-2 in toluene, and of PIC-1 in toluene as reference 46
Figure 28: Absorption spectra of indigo-bithiophene polymers measured in tetrahydrofuran and as thin films 47
Figure 29: Absorption spectra of PIF-1 and PIF-2 measured in chloroform and as thin films 47
Figure 30: Absorption spectra of PIF-1 (methylene chloride and chloroform fraction), IF-1 (top); indigo and didodecylfluorene (bottom) measured in dioxane 49
Figure 31: Absorption spectra of PIC-1 (methylene chloride fraction) and IC-1 measured in toluene (top); indigo and didodecyl-CPDT (bottom) measured in dioxane 50
Figure 32: Fluorescence emission spectra of PIF-1 (methylene chloride and chloroform fraction) and IF-1 in dioxane excited at different wavelengths; the sharp peaks at 560 nm (blue line) and 660 nm (green line) result from frequency doubling of the excitation wavelength 50
Figure 33: Fluorescence emission spectra of PIC-1 (methylene chloride fraction) and IC-1 in toluene excited at different wavelengths; the spectrum of pure toluene was measured for comparison 51
Figure 34: Phosphorescence emission spectra for PIF-1 (methylene chloride and chloroform fraction), didodecylfluorene, and IF-1 in methylcyclohexane at 77K 52
Figure 35: Phosphorescence emission spectra of CPDT and didodecyl-CPDT in methylcyclohexane at 77K 52
Figure 36: Thin film in the solid state absorption spectrum of PIC-1 and tangent for E_g calculations 53
Figure 37: Overview of the chemical structures 54
Figure 38: Cleavage of the boc-protecting groups monitored by IR spectroscopy for PIC-3 56
Figure 39: Cleavage of the boc-protecting groups monitored by absorption spectroscopy for PIF-2 57
Figure 40: Absorption spectra of unprotected PIF-1, boc-protected PIF-2, and acid-treated PIF-2 in tetrahydrofuran 59
Figure 41: Absorption spectra of unprotected PIC-1, boc-protected PIC-3, and acid-treated PIC-3 in tetrahydrofuran 59
Figure 42: Absorption spectra of PIF-1, after reduction, and after oxygen treatment, all in tetrahydrofuran 60
Figure 43: Absorption spectra of PIC-1, after reduction, and after oxygen treatment, all in tetrahydrofuran 60
Figure 44 top: Indigo-containing polymers synthesised in this work; bottom left: Indigo-containing polymer of Yamamoto and co-workers[89]; bottom right: Indigo-containing polymers of Li and co-workers[88] 61
Figure 45: IR spectra of indigo (blue line) and BAI1 (red line) 68
Figure 46: IR spectrum of BAI3 70
Figure 47: ^{1}H NMR of 4,8-bis((2octyldodecyl)oxy)-2,6-bis(trimethylstannyl)benzo[1,2-b:4,5-b']dithiophene (BD5); $CDCl_3$ (7.26 ppm) 75
Figure 48: ^{1}H NMR spectra of PBAIBD-1 (top), PBAIC-1 (middle), and PBAIC-2 (bottom) recorded in $C_2D_2Cl_4$ (5.91 ppm); phenyl protons of the BAI unit green highlighted, protons of the thiophene spacer blue highlighted, and ether methylene protons red highlighted 77
Figure 49: IR spectra of the BAI-containing polymers; PBAIC-1 (black), PBAIC-2 (red), and PBAIBD-1 (green) 78
Figure 50: Absorption spectra of PBAIC-1 and PBAIC-2 in chloroform and as thin films 80

Figure 51: Absorption spectra of PBAIBD-1 in chloroform and as thin films *80*

Figure 52 top: Chemical structure of the three BAI-containing polymers; bottom: Chemical structure of PH-1 by He et al.[90] *82*

Figure 53: Device structure of the three used solar cell architectures *86*

Figure 54: Chemical structure of the indigo-containing polymers by Liu et al.[101] *87*

Figure 55 left: OFET structures; top: top-gate/bottom-contact (TGBC); down left: bottom-gate/top-contact (BGTC); bottom right: bottom-gate/bottom-contact (BGBC);[107] *right: Chemical structure of PBAIC-2* *88*

Figure 56 a: Output (I_{DS}-V_{DS}); b: Transfer (I_{DS}-V_{GS}) characteristics of an OFET based on polymer PBAIC-2 *89*

Figure 57: Structure of PBT-1 synthesised by Bronstein and co-workers [48] *90*

Figure 58: Alkylated BAI derivatives *93*

Figure 59: Section of ^{1}H NMR spectrum recorded in $C_2D_2Cl_4$ (5.91 ppm) of the mixture including calculation of the ratio of di-stannylated C8, mono-stannylated, and non-stannylated C6 *103*

List of Schemes

Scheme 1: Chemistry behind the indigo extraction, the dashed square demonstrates the side reaction[14,15] 3
Scheme 2: Synthesis of indigo investigated by Adolf von Baeyer and Viggo Drewsen 4
Scheme 3: Synthesis of indigo by Heumann (top) and Pfleger (bottom)[7] 5
Scheme 4: Keto and leuco form of indigo 5
Scheme 5: Synthesis of 6,6'-dibromoisoindigo and (E)-6,6'-bis(5'-hexyl-[2,2'-bithiophene]-5-yl)-[3,3'-biindolinylidene]-2,2'-dione[49] 10
Scheme 6: Synthesis plan of 6,6'-dibromoindigo[56] 15
Scheme 7: Synthesis of 4-methyl-3-nitroaniline (I1), via I1a 15
Scheme 8: Synthesis of 4-bromo-2-nitromethylbenzene (I2) 16
Scheme 9: Synthesis of 4-bromo-2-nitrobenzylidene diacetate (I3) 17
Scheme 10: Synthesis of 4-bromo-2-nitrobenzaldehyde (I4) 17
Scheme 11 top: Synthesis of dibromoindigo I5; bottom: Baeyer-Drewson reaction mechanism[19,57] 18
Scheme 12: Synthesis of (E)-6,6'-dibromo-3,3'-dioxo-[2,2'-biindolinylidene]-1,1-dicarboxylate (I6) 20
Scheme 13: Synthesis plan of 2,2'-(9,9-didodecyl-9H-fluorene-2,7-diyl)bis(4,4,5,5-tetramethyl-1,3,2-dioxaborolane) (F2) via 2,7-dibromo-9,9-didodecyl-9H-fluorene (F1) 22
Scheme 14: Synthesis of 2-bromo-9,9-didodecyl-9H-fluorene (F3) 22
Scheme 15: Synthesis of 2-(9,9-didodecyl-9H-fluoren-2-yl)-4,4,5,5-tetramethyl-1,3,2-dioxaborolane (F4) 22
Scheme 16: Synthesis plan of 3,3'-bis(dodecyloxy)-5,5'-bis(tributylstannyl)-2,2'-bithiophene (B4) 23
Scheme 17: Synthesis of 3-dodecyloxythiophene (B1) 24
Scheme 18: Synthesis of 2-bromo-3-dodecyloxythiophene (B2) 24
Scheme 19: Proposed mechanism of the autopolymerisation[62] 25
Scheme 20: Synthesis of 3,3'-bis(dodecyloxy)-2,2'-bithiophene (B3) 26
Scheme 21: Synthesis of 3,3'-bis(dodecyloxy)-5,5'-bis(tributylstannyl)-2,2'-bithiophene (B4) 26
Scheme 22: Synthesis plan of CPDT; $C_{20}H_{41}$= octyldodecyl side chain 28
Scheme 23: Synthetic route to the CPDT core[68] 29
Scheme 24: Alkylation of CPDT; a: Using a bromide alkyl chain;[67] *b: Using an iodide alkyl chain*[69],[70] 29
Scheme 25: Stannylation of the didodecyl-CPDT[71] 30
Scheme 26: Synthesis of the di-stannylated C10[72],[73] 31
Scheme 27: Synthesis of the mono-stannylated C11 and C12[74] 31
Scheme 28: Synthesis of (E)-6,6'-bis(4,4-didodecyl-4H-cyclopenta[1,2-b:5,4-b']dithiophen-2-yl)-[2,2'-biindolinylidene]-3,3'-dione (IC-1) 32
Scheme 29: Synthesis of (E)-6,6'-bis(9,9-didodecyl-9H-fluoren-2-yl)-[2,2'-biindolinylidene]-3,3'-dione (IF-1) 35
Scheme 30: Overview of the polymers synthesised by Stille cross-coupling 37
Scheme 31: Overview of the polymers synthesised by Suzuki cross-coupling 38
Scheme 32: Cleaving the boc-protecting groups using thermal exposure 56
Scheme 33: Cleavage of the boc-protecting groups using TFA 57

Scheme 34: Reduction of PIC-1 and PIF-1 using sodium dithionite 59

Scheme 35: Synthesis plan of 7,14-bis(5'-bromo-3'-dodecyl-[2,2'-bithiophene]-5-yl)diindolo[3,2,1-de:3',2',1'-ij][1,5]naphthyridine-6,13-dione (BAI4)[90] 65

Scheme 36: Synthesis plan of 2-(trimethylstannyl)-3-dodecylthiophene (T3) 66

Scheme 37: Synthesis of 2-(trimethylstannyl)-3-dodecylthiophene (T3) 66

Scheme 38 top: Synthesis of BAI1; bottom: Mechanism of the annulation[47,90,92] 67

Scheme 39: Bromination of BAI1 to 7,14-bis(5-bromothiophen-2-yl)diindolo[3,2,1-de:3',2',1'-ij][1,5]naphthyridine-6,13-dione (BAI2) 68

Scheme 40: Stille-type coupling to 7,14-bis(3'-dodecyl-[2,2'-bithiophene]-5-yl)diindolo[3,2,1-de:3',2',1'-ij][1,5]naphthyridine-6,13-dione (BAI3) 69

Scheme 41: Synthesis of the monomer 7,14-bis(5'-bromo-3'-dodecyl-[2,2'-bithiophene]-5-yl)diindolo[3,2,1-de:3',2',1'-ij][1,5]naphthyridine-6,13-dione (BAI4) 70

Scheme 42: Synthesis plan of 4,8-bis((2-octyldodecyl)oxy)-2,6-bis(trimethylstannyl)-benzo[1,2-b:4,5-b']dithiophene (BD5)[95] 71

Scheme 43: Synthesis of N,N-diethylthiophene-3-carboxamide BD1 71

Scheme 44 top: Synthesis of benzo[1,2-b:4,5-b']dithiophene-4,8-dione (BD2); bottom: Formation of benzodithiophene BD2[96] 72

Scheme 45: Synthesis of 4,8-bis((2-octyldodecyl)oxy)benzo[1,2-b:4,5-b']dithiophene (BD4) 73

Scheme 46: Synthesis of 4,8-bis((2-octyldodecyl)oxy)-2,6-bis(trimethylstannyl)benzo[1,2-b:4,5-b']-dithiophene (BD5) 74

Scheme 47: Synthesis of the polymers PBAIC-1 and PBAIC-2 75

Scheme 48: Synthesis of PBAIBD-1 76

Scheme 49: PIB-2, PIC-1, and PBAIC-1 used for solar cell investigations 85

Scheme 50: Synthesis route for thioindigo[112] 93

List of Tables

Table 1: Absorption maxima of indigo and derivatives recorded in 1,2-dichloroethane; taken from ref.[7] 7

*Table 2: GPC results measured in tetrahydrofuran; * measured in trichlorobenzene* 41

*Table 3: GPC results measured in tetrahydrofuran; * measured in trichlorobenzene* 43

Table 4: GPC results measured in tetrahydrofuran 44

Table 5: Absorption maxima of PIC-1, PIC-2, PIC-3, and PIC-4 in chloroform and as thin films in the solid state; the underlined values are the most intense absorption maxima 45

Table 6: Absorption maxima of the indigo-bithiophene polymers in tetrahydrofuran and as thin films 46

Table 7: Absorption maxima of PIF-1 and PIF-2 in chloroform and as thin films; the underlined values are the most intense absorption maxima 47

Table 8: Molar extinction coefficients measured in chloroform 48

Table 9: Fluorescence emission decay values (monoexponential decay); fluorene compounds measured in dioxane and CPDT compounds measured in toluene 51

Table 10: HOMO- and LUMO-energy levels of the indigo-containing polymers 54

Table 11: TGA results of the indigo-containing polymers 55

Table 12: GPC results for the acid treated polymers PIC-3 and PIF-2, measured in tetrahydrofuran; bold values: used fractions of PIC-3 and PIF-2 for cleavage; measured in trichlorobenzene* 58

*Table 13: GPC measurements recorded in tetrahydrofuran; * measured in trichlorobenzene at 160°C* 79

Table 14: Absorption maxima of the three BAI-containing polymers, measured in chloroform and as thin films in the solid state, the underlined values are the most intense absorption maxima 80

Table 15: Molar extinction coefficients measured in chloroform 81

Table 16: Energy levels of the BAI-containing polymers 81

Table 17: Solar cell results; DIO: diiodooctane 86

Table 18: Overview of the absorption bands of the synthesised polymers; the underlined values are the most intense absorption maxima 91

References

[1] M. Zarkogianni, E. Mikropoulou, E. Varella, E. Tsatsaroni, *Coloration Technol.* **2011**, *127*, 18.

[2] P. Morris, A. S. Travis, *Am. Dyest. Repo.* **1992**, *81*,1.

[3] J. Escribano, G.-L. Alonso, M. Coca-Prados, J.-A. Fernández, *Cancer Lett.* **1996**, *100*, 23.

[4] H. van Olphen, *Science* **1966**, *154*, 645.

[5] *The Temple of the Warriors: Chichen Itzá, Yuncatan*, ed.: E. H. Morris, J. Charlot, A. A. Morris, 1.ed., Carnegie institutio of Washington, Washington **1931**.

[6] D. E. Arnold, J. R. Branden, P. R. Williams, G. M. Feinman, J. P. Brown, *Antiquity* **2008**, *82*, 151.

[7] R. M. Christie, *Colour Chemistry*, Royal Society of Chemistry, Cambridge **2001**.

[8] S. Ovarlez, A.-M. Chaze, F. Giulieri, F. Delamare, *C. R. Chim.* **2006**, *9*, 1243.

[9] S. Ovarlez, F. Giulieri, A.-M. Chaze, F. Delamare, J. Raya, J. Hirschinger, *Chemistry* **2009**, *15*, 11326.

[10] M. Sánchez Del Río, P. Martinetto, C. Reyes-Valerio, E. Dooryhée, M. Suárez, *Archaeometry* **2006**, *48*, 115.

[11] J. Balfour-Paul, *Indigo*, British Museum pr, London **2000**.

[12] G. Chiari, R. Giustetto, J. Druzik, E. Doehne, G. Ricchiardi, *Appl. Phys. A* **2007**, *90*, 3.

[13] R. J. Clark, C. J. Cooksey, M. A. Daniels, R. Withnall, *Endeavour* **1993**, *17*, 191.

[14] J.-Y. Lee, Y.-S. Shin, H.-J. Shin, G.-J. Kim, *Bioresource technol.* **2011**, *102*, 9193.

[15] T. Kokubun, J. Edmonds, P. John, *Phytochemistry* **1998**, *49*, 79.

[16] G. Eisenbrand, F. Hippe, S. Jakobs, S. Muehlbeyer, *J. Cancer Res. Clin.* **2004**, *130*, 627.

[17] W. H. Perkin, *J. Chem. Soc., Trans.* **1896**, *69*, 596.

[18] O. Meth-Cohn, M. Smith, *J. Chem. Soc., Perkin Trans. 1* **1994**, *1*, 5.

[19] A. Baeyer, V. Drewsen, *Ber. Dtsch. Chem. Ges.* **1882**, *15*, 2856.

[20] M. Bender, *J. Chem. Educ.* **1947**, *24*, 2.

[21] A. de Meijere, *Angew. Chem. Int. Ed. Engl.* **2005**, *44*, 7836.

[22] J. Seixas de Melo, A. P. Moura, M. J. Melo, *J. Phys. Chem. A* **2004**, *108*, 6975.

[23] R. Rondao, J. S. Seixas de Melo, G. Voss, *Chemphyschem* **2010**, *11*, 1903.

[24] R. S. Blackburn, T. Bechtold, P. John, *Color. Technol.* **2009**, *125*, 193.

[25] H. Zollinger, *Color chemistry: Syntheses, properties, and applications of organic dyes and pigments*, 3.ed., Verl. Helvetica Chimica Acta; Wiley-VCH, Zürich, Weinheim **2003**.

[26] A. Reis, W. Sehneider, *Z. Kristallogr. Cryst. Mater.* **1928**, *68*, 543.

[27] P. W. Sadler, *J. Org. Chem.* **1956**, *21*, 316.

[28] S. Yamazaki, A. L. Sobolewski, W. Domcke, *Phys. Chem. Chem. Phys.* **2011**, *13*, 1618.

[29] D. Jacquemin, J. Preat, V. Wathelet, E. A. Perpete, *J. Chem. Phys.* **2006**, *124*, 74104.

[30] G. M. Wyman, B. M. Zarnegar, *J. Phys. Chem.* **1973**, *77*, 831.

[31] G. M. Wyman, B. M. Zarnegar, *J. Phys. Chem.* **1973**, *77*, 1204.

[32] E. A. Perpete, J. Preat, J.-M. Andre, D. Jacquemin, *J. Phys. Chem. A* **2006**, *110*, 5629.

[33] W. Dilthey, Wizinger R., R. Wizinger, *J. Prak. Chem.-Leip.* **1928**, *118*, 321.

[34] H. Bauer, K. Kowski, H. Kuhn, W. Lüttke, P. Rademacher, *J. Mol. Struct.* **1998**, *445*, 277.

[35] W. Lüttke, H. Hermann, M. Klessinger, *Angew. Chem. Int. Ed. Engl.* **1966**, *5*, 598.

[36] M. Klessinger, *Dyes Pigments* **1982**, *3*, 235.

[37] R. M. Christie, *Biotech. Histochem.* **2007**, *82*, 51.

[38] E. D. Głowacki, G. Voss, N. S. Sariciftci, *Adv. Mater.* **2013**, *25*, 6783.

[39] J. S. Seixas de Melo, H. D. Burrows, C. Serpa, L. G. Arnaut, *Angw. Chem. Int. Ed. Engl.* **2007**, *46*, 2094.

[40] M. M. Sousa, C. Miguel, I. Rodrigues, A. J. Parola, F. Pina, J. S. Seixas de Melo, M. J. Melo, *Photoch. Photobio. Sciences* **2008**, *7*, 1353.

[41] H. E. Fierz-David, *Grundlegende Operationen der Farbenchemie*, 3.ed., Springer Berlin Heidelberg, Berlin, Heidelberg **1924**.

[42] G. Boice, B. O. Patrick, R. McDonald, C. Bohne, R. Hicks, *J.Org. Chem.* **2014**, *79*, 9196.

[43] D. Jacquemin, J. Preat, V. Wathelet, M. Fontaine, E. A. Perpete, *J. Am. Chem. Soc.* **2006**, *128*, 2072.

[44] H. Güsten, *J. Chem. Soc. D* **1969**, *3*, 133.

[45] D. L. Ross, J. Blanc, F. J. Matticoli, *J. Am. Chem. Soc.* **1970**, *92*, 5750.

[46] A. D. Ainley, R. Robinson, *J. Chem. Soc.* **1934**, 1508.

[47] G. Engi, *Z. Angew. Chem.* **1914**, *27*, 144.

[48] K. J. Fallon, N. Wijeyasinghe, N. Yaacobi-Gross, R. S. Ashraf, D. M. E. Freeman, R. G. Palgrave, M. Al-Hashimi, T. J. Marks, I. McCulloch, T. D. Anthopoulos, H. Bronstein, *Macromolecules* **2015**, *48*, 5148.

[49] J. Mei, K. R. Graham, R. Stalder, J. R. Reynolds, *Org. Lett.* **2010**, *12*, 660.

[50] Z. Ma, E. Wang, M. E. Jarvid, P. Henriksson, O. Inganäs, F. Zhang, M. R. Andersson, *J. Mater. Chem.* **2012**, *22*, 2306.

[51] E. Wang, Z. Ma, Z. Zhang, K. Vandewal, P. Henriksson, O. Inganäs, F. Zhang, M. R. Andersson, *J. Am. Chem. Soc.* **2011**, *133*, 14244.

[52] H. Tanaka, K. Tokuyama, T. Sato, T. Ota, *Chem. Lett.* **1990**, *19*, 1813.

[53] G. Voss, M. Drechsler, S. Eller, M. Gradzielski, D. Gunzelmann, S. Mondal, S. van Smaalen, C. S. Voertler, *Helv. Chim. Acta* **2009**, *92*, 2675.

[54] E. D. Głowacki, D. H. Apaydin, Z. Bozkurt, U. Monkowius, K. Demirak, E. Tordin, M. Himmelsbach, C. Schwarzinger, M. Burian, R. T. Lechner, N. Demitri, G. Voss, N. S. Sariciftci, *J. Mater. Chem. C* **2014**, *2*, 8089.

[55] C. Guo, J. Quinn, B. Sun, Y. Li, *J. Mater. Chem. C* **2015**, *3*, 5226.

[56] P. Imming, I. Imhof, M. Zentgraf, *Synth. Commun.* **2001**, *31*, 3721.

[57] *Die Praxis des organischen Chemikers* ed.: L. Gattermann, T. Wieland, W. Sucrow, de Gruyter, 1.ed., Berlin, New York **1982**.

[58] E. D. Głowacki, G. Voss, K. Demirak, M. Havlicek, N. Sünger, A. C. Okur, U. Monkowius, J. Gąsiorowski, L. Leonat, N. S. Sariciftci, *Chem. Commun.* **2013**, *49*, 6063.

[59] *Hydrocarbons*, ed.: K. Griesbaum, A. Behr, D. Biedenkapp, H.-W. Voges, D. Garbe, C. Paetz, G. Collin, D. Mayer, H. Höke, 1.ed., Wiley-VCH Verlag GmbH & Co. KGaA, Weinheim **2012**.

[60] T. Ishiyama, M. Murata, N. Miyaura, *J. Org. Chem.* **1995**, *60*, 7508.

[61] X. Guo, M. D. Watson, *Org. Lett.* **2008**, *10*, 5333.

[62] P. Wagner, K. W. Jolley, D. L. Officer, *Aust. J. Chem.* **2011**, *64*, 335.

[63] T. Yamamoto, S. Wakabayashi, K. Osakada, *J.Organomet. Chem.* **1992**, *428*, 223.

[64] Takakazu Yamamoto, T. Yamamoto, *Prog. Polym. Sci.* **1992**, *17*, 1153.

[65] A. R. Bassindale, C. Eaborn, R. Taylor, A. R. Thompson, D. R. M. Walton, J. Cretney, G. J. Wright, *J. Chem. Soc., B:* **1971**, 1155.

[66] A. Kraak, Wiersema, A. K. Wiersema, P. Jordens, H. Wynberg, *Tetrahedron* **1968**, *24*, 3381.

[67] C.-H. Chen, C.-H. Hsieh, M. Dubosc, Y.-J. Cheng, C.-S. Hsu, *Macromolecules* **2010**, *43*, 697.

[68] Udom Asawapirom, *Dissertation*, Bergische Universität Wuppertal **2003**.

[69] I. Mancini, M. Cavazza, G. Guella, F. Pietra, *J. Chem. Soc., Perkin Trans. 1* **1994**, *15*, 2181

[70] J. W. Rumer, S. Rossbauer, M. Planells, S. E. Watkins, T. D. Anthopoulos, I. McCulloch, *J. Mater. Chem. C* **2014**, *2*, 8822.

[71] Z. Zhu, D. Waller, R. Gaudiana, M. Morana, D. Mühlbacher, M. Scharber, C. Brabec, *Macromolecules* **2007**, *40*, 1981.

[72] A. Lange, H. Krueger, B. Ecker, A. V. Tunc, E. von Hauff, M. Morana, *J. Polym. Sci. A Polym. Chem.* **2012**, *50*, 1622.

[73] E. Ahmed, S. Subramaniyan, F. S. Kim, H. Xin, S. A. Jenekhe, *Macromolecules* **2011**, *44*, 7207.

[74] B. P. Karsten, J. C. Bijleveld, L. Viani, J. Cornil, J. Gierschner, R. A. J. Janssen, *J. Mater. Chem.* **2009**, *19*, 5343.

[75] V. Dehlinger, F. Cordier, C. P. Dell, N. Dreyfus, N. Jenkins, A. J. Sanderson, C. W. Smith, *Tetrahedron Lett.* **2006**, *47*, 8973.

[76] G. B. Consiglio, F. Gaggini, A. Mordini, G. Reginato, *Amino acids* **2010**, *39*, 175.

[77] A. Suzuki, *J. Organomet. Chem.* **1999**, *576*, 147.

[78] G. Wilke, H. Schott, P. Heimbach, *Angew. Chem.* **1967**, *79*, 62.

[79] D. J. Ashworth, C.-J. Chang, S. E. Unger, R. G. Cooks, *J. Org. Chem.* **1981**, *46*, 4770.

[80] F. Bovey, *High Resolution NMR of Macromolecules*, 1.ed., Elsevier Science, Oxford **1972**.

[81] R. C. Coffin, C. M. MacNeill, E. D. Peterson, J. W. Ward, J. W. Owen, C. A. McLellan, G. M. Smith, R. E. Noftle, O. D. Jurchescu, D. L. Carroll, *Journal of Nanotechnology* **2011**, 572329.

[82] Z. Bao, W. K. Chan, L. Yu, *J. Am. Chem. Soc.* **1995**, *117*, 12426.

[83] D. I. James, S. Wang, W. Ma, S. Hedström, X. Meng, P. Persson, S. Fabiano, X. Crispin, M. R. Andersson, M. Berggren, E. Wang, *Adv. Electron. Mater.* **2016**, *2*, 1500313.

[84] J. Pina, Seixas de Melo, J. Sérgio, A. Eckert, U. Scherf, *J. Mater. Chem. A* **2015**, *3*, 6373.

[85] *Polyfluorenes*, ed.: U. Scherf, D. Neher, K. Becker, 1.ed., Springer, Berlin, Heidelberg **2008**.

[86] *Handbook of Photochemistry*, ed.: M. Montalti, A. Credi, L. Prodi, M. T. Gandolfi, 3.ed., CRC Press, Hoboken **2006**.

[87] Benjamin Souharce, *Dissertation*, Bergische Universität Wuppertal **2008**.

[88] C. Guo, B. Sun, J. Quinn, Z. Yan, Y. Li, *J. Mater. Chem. C* **2014**, *2*, 4289.

[89] H. Fukumoto, H. Nakajima, T. Kojima, T. Yamamoto, *Materials* **2014**, *7*, 2030.

[90] B. He, A. B. Pun, D. Zherebetskyy, Y. Liu, F. Liu, L. M. Klivansky, A. M. McGough, B. A. Zhang, K. Lo, T. P. Russell, L. Wang, Y. Liu, *J. Am. Chem. Soc.* **2014**, *136*, 15093.

[91] X. Guo, R. P. Ortiz, Y. Zheng, Y. Hu, Y.-Y. Noh, K.-J. Baeg, A. Facchetti, T. J. Marks, *J. Am. Chem. Soc.* **2011**, *133*, 1405.

[92] R. Tobler, *Helv. Chim. Acta* **1945**, *28*, 901.

[93] H. Pan, Y. Li, Y. Wu, P. Liu, B. S. Ong, S. Zhu, G. Xu, *J. Am. Chem. Soc.* **2007**, *129*, 4112.

[94] J. Hou, M.-H. Park, S. Zhang, Y. Yao, L.-M. Chen, J.-H. Li, Y. Yang, *Macromolecules* **2008**, *41*, 6012.

[95] P. Beimling, G. Koßmehl, *Chem. Ber.* **1986**, *119*, 3198.

[96] D. W. Slocum, P. L. Gierer, *J. Org. Chem.* **1976**, *41*, 3668.

[97] C. Gege, R. R. Schmidt, *Carbohydr. Res.* **2002**, *337*, 1089.

[98] D. W. H. MacDowell, J. C. Wisowaty, *J. Org. Chem.* **1972**, *37*, 1712.

[99] W. Yue, R. S. Ashraf, C. B. Nielsen, E. Collado-Fregoso, M. R. Niazi, S. A. Yousaf, M. Kirkus, H.-Y. Chen, A. Amassian, J. R. Durrant, I. McCulloch, *Adv. Mater.* **2015**, *27*, 4702.

[100] L. Fang, Y. Zhou, Y.-X. Yao, Y. Diao, W.-Y. Lee, A. L. Appleton, R. Allen, J. Reinspach, S. C. B. Mannsfeld, Z. Bao, *Chem. Mater.* **2013**, *25*, 4874.

[101] C. Liu, S. Dong, P. Cai, P. Liu, S. Liu, J. Chen, F. Liu, L. Ying, T. P. Russell, F. Huang, Y. Cao, *ACS Appl. Mater. Inter.* **2015**, *7*, 9038.

[102] G.-M. Ng, E. L. Kietzke, T. Kietzke, L.-W. Tan, P.-K. Liew, F. Zhu, *Appl. Phys. Lett.* **2007**, *90*, 103505.

[103] Q. Tao, Y. Xia, X. Xu, S. Hedström, O. Bäcke, D. I. James, P. Persson, E. Olsson, O. Inganäs, L. Hou, W. Zhu, E. Wang, *Macromolecules* **2015**, *48*, 1009.

[104] Y. Huang, E. J. Kramer, A. J. Heeger, G. C. Bazan, *Chem. Rev.* **2014**, *114*, 7006.

[105] A. A. Bakulin, J. C. Hummelen, M. S. Pshenichnikov, van Loosdrecht, Paul H. M., *Adv. Funct. Mater.* **2010**, *20*, 1653.

[106] J. Yan, B. R. Saunders, *RSC Adv.* **2014**, *4*, 43286.

[107] X. Guo, A. Facchetti, T. J. Marks, *Chem. Rev.* **2014**, *114*, 8943.

[108] A. R. Murphy, J. M. J. Frechet, *Chem. Rev.* **2007**, *107*, 1066.

[109] S. Allard, M. Forster, B. Souharce, H. Thiem, U. Scherf, *Angew. Chem. Int. Ed. Engl.* **2008**, *47*, 4070.

[110] C. R. Newman, C. D. Frisbie, D. A. da Silva Filho, J.-L. Brédas, P. C. Ewbank, K. R. Mann, *Chem. Mater.* **2004**, *16*, 4436.

[111] C. D. Dimitrakopoulos, P. Malenfant, *Adv. Mater.* **2002**, *14*, 99.

[112] *Grundlegende Operationen der Farbenchemie*, ed.: H. E. Fierz-David, L. Blangey, 8.ed., Springer Vienna, Vienna **1943**.

[113] Jakob W. Lüthy, *Dissertation*, Eidgenössische Technische Hochschule Zürich **1974**.

Acknowledgements

First of all, I would like to sincerely thank my supervisor *Prof. Dr. Ullrich Scherf* for the possibility to work on this challenging topic. As well, I would like to thank him for the financial support and the opportunities to present my work at national and international conferences. I am very thankful for the motivation and the always open door as well as sharing his knowledge.

I am very thankful to *Prof. PhD J. Sérgio Seixas de Melo* for reviewing this thesis as referee.

Dipl.-Ing. Sylwia Adamczyk, Dr. Sybille Allard, Dr. Michael Forster, Ina Hallbauer, Dipl.-Ing. Anke Helfer and *Kerstin Müller* are rewarding my special thanks for the support and motivation to continue in difficult situations.

I would like to thank *Dr. Michael Forster, Dr. Sebastian Kowalski, Dr. Venkata Suresh Mothika, Dr. Eduard Preis, and Dr. Christian Widling* for revision of this thesis.

My special thanks go to *Dipl.-Ing. Anke Helfer* for measuring like thousands of GPC, LC-MS, APCI-MS, APLI-MS, and HPCL measurements. *Dipl.-Ing. Anke Helfer* and *Dipl.-Ing. Sylwia Adamczyk* are rewarding my thanks for TGA and DSC measurements. I would like to thank them as well for all the discussions of the results and the common development of new purification processes.

Andreas Siebert, Ilka Polanz, and *Simone Bettinger* of the organic chemistry department are giving thanks for the NMR, GC-MS, APCI-MS, and APLI-MS measurements.

Dr. Gunther Brunklaus from the Westfälische Wilhelms-Universität Münster is giving thanks for measuring the solid state MNR measurements.

I would like to thank the Max Plank Institute for Polymer Research in Mainz for measuring the high temperature GPC, MALDI-MS, and FD-MS.

PhD João Pina, co-worker in the group of *Prof. PhD J. Sérgio Seixas de Melo* in Portugal is giving special thanks for investigating the photophysical properties of the indigo-containing polymers as well as for welcoming me during my research stay in Portugal.

The groups of *Prof. Dr. Thomas Riedl* from Bergische Universität Wuppertal and *Prof. Dr. Ergang Wang* from Chalmers University of Technology are giving thanks for the investigations of the solar cells. The group of *Prof. PhD Franco Cacialli* from the London

Centre for Nanotechnology, UCL is giving thanks for the investigations of the organic thin layer transistors.

B.Sc. Marie-Claire Ockfen, M.Sc. Christine Polaczek, B.Sc. Stefania Petarra, and all the remaining students who were working with me are giving thanks. Especially, my Bachelor student 'Schleifchen', thank you so much.

Furthermore, I would like to thank all the preceding and to come PhD students of the macromolecular chemistry group since 2011. Especially, *Dr. Wenyue Dong, Dr. Mario Kraft, Dr. Alex Palma-Cando, Dr. Eduard Preis, Dr. Sebastian Kowalski, Dr. Christian Widling, M.Sc. Şebnem Bayseç, M.Sc. Kim-Julia Kass, M.Sc. Tina Keller*, and the fellas of the current group.

Last but not least I want to thank my *family, friends*, and my *boyfriend Christian* for the support and treating with all my emotions during the last years. Words are not enough to describe the things you did to me. So just: Thanks a Mill! ;-)